Neurone and astrocyte response to Aβ25-35: Role of glutathione in neuroprotection

By

Mary Clare Hughes

A thesis submitted in partial fulfilment for the degree of Doctor of Philosophy in the Faculty of Science at the University of London

January 2007

I, Mary Hughes, confirm that the work presented in this thesis is my own. Where information has been derived from other sources I confirm that this has been indicated in the thesis

Division of Neurochemistry
Department of Molecular Neurosciences
Institute of Neurology
University College London
Queens Square
London WC1N 3BG
United Kingdom

ProQuest LLC
789 East Eisenhower Parkway
P.O. Box 1346
Ann Arbor, MI 48106-1346

ABSTRACT

Amyloid beta (Aβ) is strongly implicated in the pathogenesis of Alzheimer's disease and has been shown to cause oxidative stress and neurone death *in vivo* and in cell culture models. Astrocytes in cell culture conditions and *in vivo* appear to be more resistant to Aβ mediated toxicity, but do undergo morphological changes to adopt a stellate "activated" morphology.

The experiments presented in this thesis have used the aggregating Aβ fragment Aβ25-35 to model Aβ toxicity to study why neurones are more vulnerable than astrocytes. Neurones and astrocytes were both shown to generate reactive oxygen species (ROS) in the presence of Aβ25-35 although astrocytes contained higher levels of the antioxidant glutathione (GSH). It was shown that both astrocyte conditioned medium, and the GSH precursor γ-glutamylcysteine raised neurone intracellular GSH levels and protected against Aβ25-35 mediated neurotoxicity to the same degree. In the brain, astrocytes provide neurones with the precursors needed for GSH synthesis. To test whether astrocyte support of neurone GSH synthesis was maintained in the presence of Aβ25-35, intracellular [GSH] was measured in both cell types after Aβ25-35 treatment. It was shown that intracellular [GSH] was lowered in neurones but was maintained in astrocytes. The ability of astrocytes to maintain their GSH levels appeared to be dependent on an increase in the activity of glutathione reductase, the enzyme that recycles oxidised glutathione (GSSG) to its reduced form GSH. Furthermore, the amount of GSH released by astrocytes was increased after treatment with Aβ25-35. Conditioned medium from Aβ25-35 treated astrocytes raised neurone intracellular GSH to the same degree, and gave similar neuroprotection as conditioned medium from control astrocytes.

A co-culture protocol was developed in which neurones could be treated with Aβ25-35 and then transferred to co-culture with astrocytes. Astrocytes co-cultured with Aβ25-35 treated neurones showed a decrease in intracellular GSH. This suggests that although Aβ25-35 does not affect the ability of astrocytes to protect neurones by releasing GSH, signals from damaged neurones could limit the amount of antioxidant support neurone populations receive from astrocytes.

ACKNOWLEDGEMENTS

I would firstly like to thank my supervisors, Dr Laura Canevari and Prof John Clark for their excellent advice and support during the last 3 years. I feel very privileged to have worked with them.

I would also like to thank the members of the Neurochemistry department, past and present, particularly Dr Susan Griffin for her tutorage in cell culture techniques, Dr Simon Heales, Dr Lee Stanyer, Dr Simon Pope, Dr Nasi Mian both for their advice on this thesis and on the various presentations given throughout the duration of my PhD. I must thank Prof Michael Duchen both for the use of his confocal microscope and for a mock viva mid-way through this project. I would also like to thank Elizabeth Beech whose efficient running of the lab made our lives much easier than we probably deserved!

I am very appreciative of the British Council and Dr Maria Vincenza Catania for the wonderful opportunity to work in her laboratory in Sicily for two months.

I would like to thank my parents for their overwhelming support throughout my PhD.

Lastly I would like to thank The Brain Research Trust for their generous funding of this research.

CONTENTS

List of Figures and tables

Tables

ABBREVIATIONS

Aβ	Amyloid β
Aβ25-35	Amyloid β 25-35 fragment
ACM	Astrocyte conditioned medium
AD	Alzheimer's disease
ADAM	A disintegrin and metalloprotease
ADE	Angiotensin degrading enzyme
AGE	Advanced glycation end products
AICD	APP intracellular domain
APN	Amino peptidase N
ApoE	Apolipoprotein E
APP	Amyloid precursor protein
AraC	Cytosine arabinoside
ATP	Adenosine triphosphate
BACE	beta-site APP-cleaving enzyme
BBB	Blood brain barrier
BDGF	Brain derived growth factor
BSA	Bovine serum albumin
CTF	C terminal fragment
CSF	Cerebral spinal fluid
CysGly	Cysteinyl glycine
Cys-SS-Cys	Cystine
DAPI	4'-6-Diamidino-2-phenylindole
DCF	Dichlorofluroscein
DEA NONOate	Diethylammonium (Z)-1-(N,N-diethylamino) diazen-1-ium-1, 2-diolate
DIV	Day *in vitro*
DMSO	Dimethyl sulphoxide
DS	Down's syndrome
EAAT	Excitatory amino acid transporter
EBSS	Earle's balanced saline solution
ECD	Electrochemical detector
EDTA	Ethylene diamine tetra acetic acid

FAD	Familial Alzheimer's disease
FBS	Foetal bovine serum
FGF	Fibroblast growth factor
FITC	Fluorescein isothiocyanate
6PGD	6-phosphogluconate dehydrogenase
G6PD	glucose-6-phosphate dehydrogenase
γ-GC	γ-Glutamyl cysteine
γ-GT	γ-Glutamyl transpeptidase
GCL	Glutamate cysteine ligase
GFAP	Glial fibrillary acidic protein
Glu	Glutamate
Gln	Glutamine
GPx	Glutathione peroxidise
GR	Glutathione reductase
GS	Glutathione synthetase
GS·	Thiyl radical
GSH	Glutathione
GSHEE	Glutathione ethyl ester
GSSG	Glutathione disulphide
H_2O_2	Hydrogen peroxide
HBSS	Hank's buffered saline solution
HEK	Human endothelial kidney cell
HNE	Hydroxynonenal
HPLC	High performance liquid chromatography
IDE	Insulin degrading enzyme
IL	Interleukin
L-BSO	L- buthionine sulfoximine
LDH	Lactate dehydrogenase
LDL	Low density lipoprotein
LPS	Lipopolysaccharide
LRP	Low density lipoprotein receptor related protein
MCB	Monochlorobimane
MCP-1	Monocyte chemoattractant protein
MAPT	Microtubule associated tau

MDA	Malondialdehyde
MEM	Minimal essential medium
MRI	Magnetic resonance imaging
MRP-1	Multidrug resistance protein-1
MTT	(4,5-dimethylthiazol-2-yl)-2,5 diphenyltetrazolium bromide
NADPH	Nicotinamide adenine dinucleotide phosphate (reduced form)
NCM	Neurone conditioned medium
NEP	Neprilysin
NGF	Nerve growth factor
NMDA	N-methyl-D-aspartic acid
NO	Nitric oxide
NOS	Nitric oxide synthase
NSAID	Non steroidal anti- inflammatory drugs
$O_2^{-\cdot}$	Superoxide radical
$OH^{\cdot}$	Hydroxl radical
$ONOO^-$	Peroxynitrite
OPA	Orthanophosphoric acid
PDL	Poly-D-Lysine
PET	Positron emission tomography
PI	Propidium iodide
PPP	Pentose phosphate pathway
PS	Presenilin
PLO	Poly-L-Ornithine
RAGE	Receptor for advanced glycosylation end products
RNA	Ribonucleic acid
RNS	Reactive nitrogen species
ROS	Reactive oxygen species
sAPP	Soluble APP
SOD	Super oxide dismutase
TACE	Tumour necrosis factor-α converting enzyme
TBARS	Thiobarbituric acid reactive substances
TCA	Tricarboxylic acid cycle

TNF-α	Tumour necrosis factor-α

Chapter 1: Introduction

1. Introduction

In 1907 Alois Alzheimer described the case of a 51 year-old female patient exhibiting cognitive and language deficits, as well as psychiatric disturbances. On autopsy it was revealed that she had brain atrophy, neuritic plaques (described at the time as miliary foci), neurofibrillary tangles, gliosis and arteriosclerotic changes in her brain (Alzheimer, 1907, English translation Alzheimer, Stelzmann *et al.* (1995)). These pathological features were grouped as pathological hallmarks of a progressive age linked dementia that took his name. Alzheimer's disease (AD) is the most common form of adult dementia (Franks *et al.*, 1998).

Until 20 years ago, the progress in the understanding of the basic mechanisms involved in the pathogenesis of AD was relatively slow. AD follows a stereotyped progression of cognitive impairment from short-term memory loss, language impairment, increased cognitive decline, psychiatric disturbances to disturbed gait. This stereotyped progression was explained by the selective vulnerability of the hippocampus and temporo-parietal lobes to plaque and tangle deposition, synapse and neurite loss and cell death. The cerebellum shows less plaque and tangle pathology and is spared from atrophy until the latter stages of the disease (Braak and Braak, 1991).

However, at the molecular level, it was only in the last two decades that the main protein components of neuritic plaques and neurofibrillary tangles were elucidated: Amyloid β (Aβ) and tau respectively (Glenner and Wong, 1984; Masters *et al.*, 1985; Grundke-Iqbal *et al.*,1986).

In their study Glenner and Wong had shown that the amyloid protein found in AD and Down's syndrome (DS) was homologous (Glenner and Wong, 1984). DS sufferers exhibit AD-like neuritic plaque and neurofibrillary tangle pathology. The Aβ deposition increases with age and predominates in the same areas that are principally affected in AD (Leverenz *et al.*,1998). Some people with DS exhibit a progressive cognitive impairment in their later years, and brain atrophy that parallels that seen in AD (Aylward *et al.*, 1999).

The similarities between DS and AD suggested the gene encoding Aβ could be on chromosome 21. Using a complementary DNA probe targeted to the Aβ sequence, the gene for a larger amyloid precursor protein (APP), from which Aβ is cleaved, was located on chromosome 21 (Kang *et al.*, 1987).

A key finding was that Aβ is generated constitutively from APP throughout life (Haass *et al.*,1992; Seubert *et al.*,1992). Furthermore, as Down's syndrome arises from a trisomy of chromosome 21, it was proposed that abnormally high Aβ production and subsequent accumulation was a key event in neurodegeneration. The hypothesis that Aβ might be involved in the pathogenesis of AD provided a kick-start for accelerated research into AD.

In the centenary of Alois Alzheimer's description of AD, there has been an explosion of research activity into the biology of Aβ and its effects on the brain. The first part of this introduction presents an overview of Aβ biology and the evidence implicating Aβ in the pathogenesis of AD. The second part of the introduction describes the biochemical changes that occur in aging neurones and in neurones in the presence of Aβ and the hypothesis that cell death occurs as a consequence of oxidative stress mediated mechanisms.

Much work has focussed on the effects of Aβ on neurones but clearly neurones are not the only cells affected by Aβ. Even 100 years ago "activated" astrocytes, or astrocytes that had undergone a structural change were noted to surround neuritic plaques (Alzheimer, 1907). Astrocytes migrate to the periphery of neuritic plaques (Wyss Corey *et al.*, 2003), where in addition to their structural changes, they undergo functional changes collectively referred to as astrogliosis.

The precise role of astrocytes on the periphery of neuritic plaques is yet to be elucidated. Astrocytes could be protective to neurones as in the normal brain neurones and astrocytes have an exceedingly close cellular partnership and where it is appropriate to think of them as a functional unit. Neurones rely on astrocytes for metabolic and antioxidant support and to maintain the homeostasis of their extracellular environment. It is not yet known to what extent these supportive functions are maintained in the AD

brain. Activated astrocytes have also been attributed additional roles in the AD brain, but their overall effect on the pathogenesis of AD is yet to be determined. On the one hand astrocytes have been attributed a role in Aβ clearance (Wyss Corey *et al.*,2003; Apelt *et al.*, 2003), suggesting they are protective. However, the inflammatory response of astrocytes surrounding neuritic plaques has been proposed to be neurotoxic (McGeer *et al.*, 1996; Hu *et al.*, 1998; Sastre *et al.*, 2006). Astrocytes have furthermore been implicated in promoting Aβ accumulation in the brain (Nagele *et al.*, 2004).

Research into the interactions between astrocytes and neurones in the presence of Aβ is very much in its infancy. The third part of this introduction gives an overview of what is known about the interactions between neurones and astrocytes in the normal and AD brain. As oxidative stress is strongly implicated as a mechanism underlying neurone death in AD (Martins *et al.*,1986; Mattson *et al.*, 1999), this thesis has focussed on the astrocyte derived glutathione antioxidant support of neurones and how this is affected in the presence of Aβ.

Part 1: The role of Aβ in the pathogenesis of AD

1.1.1 Amyloid pathology in AD

Neuritic plaques are extracellular proteinaceous structures 50-200μm in diameter (Benveniste *et al.*, 1999). The protein component of the plaque is predominantly fibrillar amyloid β (Aβ). Aβ is a cleavage product of the amyloid precursor protein (APP) and is 39-42 amino acids in length. In amyloid plaques, this soluble peptide forms insoluble fibrillar aggregates. It is proposed that deposits of Aβ first appear in the brain parenchyma as loose accumulations, which are referred to as diffuse plaques (Yamaguchi *et al.*, 1990). These plaques are thought to mature into dense core plaques. Dense core plaques, unlike the diffuse plaques, contain dystrophic neurites, and are surrounded by activated astrocytes and microglia (Yamaguchi *et al.*, 1990). Dense core plaques also contain proteins such as apolipoprotein E (ApoE) (Shao *et al.*, 1997), heparin sulfate glycosaminoglycan (Su *et al.*, 1992), transition metal ions Cu^{2+} and Zn^{2+} (Dong *et al.*, 2003), and RNA (Ginsberg *et al.*, 1998). It has been suggested by some groups that as plaques mature, the Aβ peptides can become racemized and truncated (Naslund *et al.*, 1994; Kaneko *et al.*, 2001).

1.1.2 Aβ cleavage from the amyloid precursor protein

The APP gene has 19 exons and codes for a type I integral membrane protein. APP is ubiquitous and can exist in a number of different isoforms generated by the alternate splicing of exons 7,8 and 15. The most abundant isoforms are APP-695, APP 714, APP-751 and APP-770. The isoforms differ in their N terminal domains. The shortest isoform APP-695 predominates in brain tissue (Kang *et al.*, 1987; Kitaguchi *et al.*, 1988; Ponte *et al.*, 1988; Sandbrink *et al.*, 1994).

All of the spliced isoforms of APP encode for multi-domain proteins with a small cytosolic C-terminal domain, a large N-terminal domain and a transmembrane spanning domain (Beyreuther and Masters, 1991). The role of full length APP is unknown but has been implicated in neurite outgrowth (Qiu *et al.*, 1995), cell adhesion (Breen *et al.*,

1991), catalysis of the reduction of Cu^{2+} to Cu^{+} (Multhaup *et al.*, 1996) and protection from oxidative stress by maintaining copper homeostasis (Barnham *et al.*, 2003).

In cultured neuronal cells it has been shown that APP matures through the constitutive secretory pathway and is modified by the addition of N- and O-linked oligosaccharides and tyrosine sulphation (Weidemann *et al.*, 1989). APP has 3 principle cleavage sites for the α, β, and γ secretases (Figure 1.1). There are two pathways of Aβ cleavage: the α, γ pathway which is non-amyloidgenic and the β, γ pathway that generates Aβ. As α-secretase cleaves in the middle of the Aβ sequence, in this case the fragments obtained are soluble APP (sAPPα), which is secreted, and the membrane bound C terminal fragment α (CTFα). CTFα is further processed by γ secretase to generate the P3 fragment and the APP intracellular domain (AICD), which is released into the cytosol. β-secretase cleaves APP at the N terminal end of the Aβ sequence. The following γ-secretase cleavage generates Aβ, which is released into the lumen, and AICD, which is released into the cytosol (Golde and Younkin, 2001; Gu *et al.*, 2001). The exact cellular location of these cleavages along the secretory pathway is yet to be elucidated.

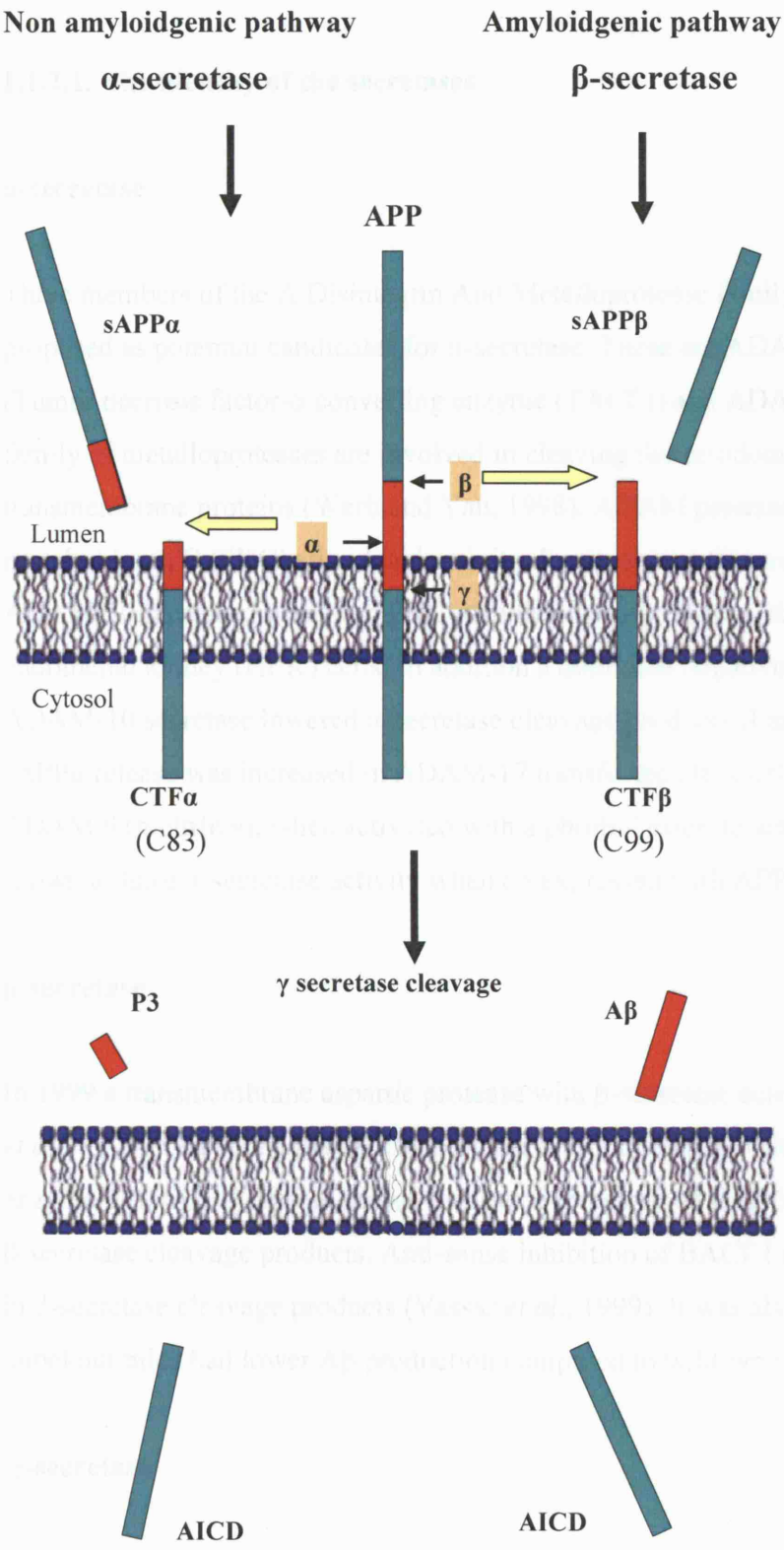

Figure 1.1: APP cleavage: There are two pathways of Aβ cleavage the α, γ pathway which is non-amyloidgenic and the β, γ pathway that generates Aβ. APP = amyloid precursor protein, s-APP = soluble APP, CTF = c terminal fragment, AICD = APP intracellular domain, Aβ = amyloid β

1.1.2.1. The identity of the secretases

α-secretase

Three members of the A Disintegrin And Metalloprotease family (ADAM) have been proposed as potential candidates for α-secretase. These are ADAM-10, ADAM 17 (Tumor necrosis factor-α converting enzyme (TACE)) and ADAM 9. The ADAM family of metalloproteases are involved in cleaving the ectodomain of various transmembrane proteins (Werb and Yan, 1998). ADAM proteinases have basal and protein kinase C (PKC) stimulated activity. It was shown that overexpression of ADAM-10 increased basal and PKC stimulated α- secretase activity in human endothelial kidney (HEK) cells. In addition a dominant negative mutant form of ADAM-10 secretase lowered α-secretase cleavage products (Lammich *et al.*, 1999). sAPPα release was increased in ADAM-17 transfected HEK cells (Slack *et al.*, 2001). ADAM 9 (meltrin γ), when activated with a phorbol ester, to activate PKC, was also shown to have α-secretase activity when co-expressed with APP (Koike *et al.*, 1999).

β-secretase

In 1999 a transmembrane aspartic protease with β-secretase activity was cloned (Sinha *et al.*, 1999; Yan *et al.*, 1999). The protease was named beta –site APP –cleaving enzyme 1 (BACE1). It was shown that overexpression of BACE1 leads to an increase in β-secretase cleavage products. Anti-sense inhibition of BACE1 mRNA led to a decrease in β-secretase cleavage products (Vassar *et al.*, 1999). It was also observed that BACE1 knockout mice had lower Aβ production compared to wild type mice (Luo *et al.*, 2001).

γ-secretase

The cleavage site for γ-secretase is an intramembrane site, which is an unusual site of protease activity. The γ-secretase activity is proposed to be due to the activity of a complex of proteins rather than the activity of one protease. The first proposed component of this complex, presenilin, was investigated as mutations in the genes

encoding two homologues (PS1 and PS2) of this family of transmembrane proteins were identified through genetic linkage analysis of families with autosomal –dominant forms of AD (see section 1.1.4.1). Patients with these mutations have greater levels of plasma Aβ than controls (Scheuner *et al.*, 1996). Yu and colleagues (2000) used immunoextraction to remove presenilin1 and tightly associated proteins from intracellular membrane fractions of HEK cells. The transmembrane glycoprotein nicastrin was separated from presenilin and identified using mass spectroscopy. Genetic linkage studies of *c. elegans* APP γ secretase activity showed that two more genes, APH1 and PEN2, might code for proteins involved in γ secretase cleavage (Francis *et al.*, 2002). It was later shown that expressing PS, Nct (the gene encoding nicastrin), PEN2 and APH-1 in the yeast, *Saccharomyces cerevisiae*, which has no known homologues for these genes, caused the appearance of γ secretase activity. The study showed that it was necessary for all four of these genes to be expressed for this secretase activity to be observed (Edbauer *et al.*, 2003).

1.1.3. Aβ clearance mechanisms

As Aβ is found in the cerebral spinal fluid (CSF) of non-demented individuals throughout life (Tamaoka *et al.*, 1997), it is likely to have a physiological function in normal central nervous systems. Plant and colleagues (2003) showed that inhibition of the amyloidgenic APP processing pathways by inhibition of β and γ secretase activity caused a decrease in the viability of neurones in culture, which could be prevented if low concentrations of Aβ1-40 (pico- to nanomolar) were added at the same time. They also showed an increase in neurone cell death if an Aβ1-40 specific antibody was added to neuronal cell culture media. The physiologic role of Aβ is yet to be elucidated, but it has been suggested to be involved in protection against copper mediated generation of reactive oxygen species, physiological control of synaptic activity and a response to hypoxia (Kontush *et al.*, 2003; Pearson and Pears, 2006).

Under normal circumstances Aβ is thought to be cleared from the brain by two main mechanisms, though transport across the blood brain barrier (BBB), and by degradation by proteases. Soluble Aβ is postulated to be transported from the brain through the BBB by the low-density lipoprotein (LDL)- receptor related protein (LRP). LRP expression

declines with age and is further lowered in AD patients compared to controls. Mutations in the gene encoding LRP are associated with increased risk of AD. LRP has been shown to clear both soluble Aβ1-40 and Aβ1-42 in APP and LRP transfected fibroblasts (Kang *et al.*, 2000). Shibata *et al.,* 2000 demonstrated that clearance of soluble Aβ1-40 through the blood brain barrier, after injections of Aβ1-40 into the cerebral cortex of mice, was also mediated by LRP. Deane *et al.*, 2004 showed that LRP transports Aβ1-40 more efficiently than Aβ1-42, and that accumulated Aβ promotes proteosome-dependent LRP degradation.

Clearance of fibrillar Aβ from neuritic plaques has been shown in transgenic mice overexpressing APP and with plaque pathology, after immunization with Aβ (Schenk *et al.,* 1999) and treatment with the Cu^{2+} chelator clioquinol (Cherny *et al.*, 2001). These two studies prompted further investigations into finding mechanisms by which fibrillar amyloid could be degraded in the brain. Recent studies have identified several candidate proteases that may contribute to Aβ catabolism. These include the zinc metalloproteases neprilysin, insulysin (Insulin Degrading Enzyme (IDE)), Angiotensin Converting Enzyme (ACE), endothelin converting enzyme and matrix metalloproteases (White *et al.*, 2006; reviewed in Carson and Turner 2002).

The strongest evidence has been found implicating neprilysin and IDE in fibrillar Aβ clearance. Neprilysin was implicated after studies showed that degradation of radiolabelled Aβ1-42, injected into rat cerebral cortex was inhibited by the neprilysin inhibitor thiorphan (Iwata *et al.*, 2000), it was also shown by the same group in neprilysin knockout animals that exogenously applied Aβ1-42 was not cleared (Iwata *et al.*, 2002). Insulin degrading enzyme knockout mice have higher levels of Aβ1-40 and Aβ1-42 (Miller *et al.*, 2003)). Interestingly, White *et al.*, 2006 showed that clioquinol treatment leads to an upregulation of matrix metalloprotease 2 and 3.This suggests a mechanism by which this antibiotic metal chelator can clear Aβ in plaques.

1.1.4. Genetic mutations associated with Alzheimer's disease.

Accumulations of Aβ in AD are proposed to occur as a consequence of an imbalance between its production and clearance. Supportive evidence has been provided by genetic studies.

Alzheimer's disease can be grouped as familial or sporadic. Familial Alzheimer's disease (FAD) is characterised in most cases by an early age of onset compared with sporadic AD, generally around 50 years of age. However, the progression of clinical symptoms and neuropathology of the disease is the same as that seen in later onset sporadic AD. Mutations in three genes are thought to have a causative link to FAD. Mutations in these genes have an autosomal dominant inheritance and 100% penetrance, however the proportion of people with these mutations that develop FAD is much less as in most cases AD has a complex aetiology, where environmental and other genetic susceptibility factors play a role. The genetic mutations associated with familial AD appear to promote Aβ production, particularly the Aβ1-42 isoform, which is more predisposed to aggregate (Jarrett *et al.*, 1993).

Mis-sense mutations in the APP gene are thought to account for 5% of FAD cases (see table 1.1). Mutations have been found at codons 670,692,693,694,714,715,716,717 and 723. APP mutations associated with FAD are thought to increase the risk of AD as they are located near to the APP cleavage sites and promote APP cleavage through the β secretase pathway (De Jonghe *et al.*, 2001; Selkoe and Podlisny, 2002).

Presenilin gene mutations (PSEN1 and PSEN2) are thought to cause 80% of FAD cases. They code for presenilins 1 and 2, multi-spanning transmembrane proteins that, as described in section 1.2.2, are hypothesised to have γ-secretase activity or be a co-factor for γ-secretase.

Dominantly inherited familial AD only contributes ~3% of all AD cases (Ott *et al.*, 1995) so the search is on to find genes associated with late onset Alzheimer's disease, which affects a greater proportion of the population. The Apolipoprotein E (ApoE) ε4 allele is the only confirmed risk factor for both early and late onset AD identified to date (Strittmatter *et al.*, 1993). The ApoE gene has three alleles, ε2, ε3 and ε4. 5-10% of the general population have an ε2 allele, 60-70% have an ε3 and 15-20% have an ε4 allele (Mahley *et al.*, 2006). 40-60% of patients with AD possess at least one ApoE ε4 allele (Farrer *et al.*, 1997).

ApoE can bind lipids, including cholesterol, and Aβ. ApoE mediated transport of lipids is important for the repair, growth and maintenance of myelin and neuronal membranes during development or after injury (reviewed in Sjögren *et al.*, 2006). The transport of cholesterol is essential for maintaining lipid homeostasis and determining the fluidity of the membrane. Cholesterol has been implicated in the pathogenesis of AD after the observation that patients receiving cholesterol-lowering statin treatment had a lowered risk for AD (Jick *et al.*, 2003). ApoE4 is proposed to promote the production of Aβ from APP by altering the cholesterol content of the plasma membrane containing the region of APP from which Aβ is cleaved (reviewed in Puglielli *et al.*, 2003). Cholesterol homeostasis in lipid membranes may be governed by ApoE phenotype (Poirier *et al.*, 2005).

Lipid free ApoE4 has been reported to have a strong binding affinity for Aβ compared to ApoE3 and ApoE2 (Strittmater *et al.*, 1993), and binding of ApoE to soluble Aβ has been suggested to directly promote Aβ fibrillogenesis (Ma *et al.*, 1994).

ApoE has also been shown to mediate uptake of Aβ in astrocytes, neurones, and microglia by a LRP mediated mechanism (Koistinaho *et al.*, 2004; Beffert *et al.*, 1998; Chung *et al.*, 1999 Permanne *et al.*, 2001). Astrocytes and microglia are proposed to internalise soluble and fibrillar Aβ as part of a degradation pathway (Chung *et al.*, 1999; Nagele *et al.*, 2003; Kostinaho *et al.*, 2004). However, it has been shown that only about 20% of fibrillar Aβ is degraded by microglia and that fibrillar Aβ can be released from these cells (Chung *et al.*, 1999). Some authors also suggest a model in which soluble Aβ is taken up by an ApoE dependent mechanism into endosomes where it

aggregates into fibrillar Aβ, which is then released (Puglielli *et al.*, 2003) or that glial cells become overburderned with fibrillar Aβ then lyse to generate glial derived extracellular deposits (Nagele *et al.*, 2003).

Through further genetic linkage and association studies, polymorphisms in many genes have been implicated as risk factors for AD. Two of the stronger candidates are α2-macroglobulin and Insulin degrading enzyme (IDE). α2 macroglobulin interacts with LRP, and is proposed to play a role in the binding, clearance or degradation of Aβ, while IDE, as discussed in section 1.1.3, is implicated in Aβ degradation (Selkoe and Podlisny, 2002).

Gene	Location	Biochemical consequence of mutation	Hypothesised mechanism	Age of onset
APP missense mutation i) K/M670/1NL ii) E693G (Arctic) iii) V717F (Indiana) iv) V717G	21q21.3-q22.05	i) ↑ Aβ ii) ↑ AβProtofibrils Aβ ↓ iii +iv) ↑ Aβ42:40	Altered cleavage of APP	Early 40+
Presenilins i) Presenilin1 ii) Presenilin2	i)14q24.3 ii)1q31q42	↑ Aβ42 ↑ Oligomerisation	Altered γ secretase activity	Early 50+
Apolipoprotein E (ApoE), ε4 allele	19q32.2	↑ Plaque burden	↑ Aβ aggregation in blood vessels and brain OR decrease in Aβ clearance	Late 60+
PROPOSED RISK FACTORS				
ApoE promoter	19q32.2		Affected ApoE function	Late
α 2-macroglobulin + lipoprotein related protein	12		Can bind ApoE and other proteins implicated in AD, Clearance mechanisms affected	Late
Insulin degrading enzyme (IDE)	10q23q25		Aβ degradation	Late
Tumour necrosis factor α (TNFα)	6		Chronic astrocyte and microglial response	Late

Table 1.1 A summary of the genetic risk factors for AD. Summarises (Selkoe and Podlisny , 2002; Rocchi *et al.*, 2003).

1.1.5. Cell culture models of AD: Evidence for a direct toxic effect of Aβ on neurones.

Although initial studies did not show a correlation between the number of plaques and the degree of cognitive decline, when total Aβ load was measured using biochemical techniques there was a correlation between levels of Aβ and cognitive impairment. (Naslund *et al.*, 2000). The amount of brain atrophy measured by MRI correlates with cognitive decline measured by the mini mental state examination (Fox *et al.*, 1999). However, it has also been shown that prior to cell death, loss of neurites and synaptic connections can also correlate with impaired cognitive performance (Scheff *et al.*, 2005).

Synthetic Aβ peptides and fragments have been shown to be toxic to neurones and neuronal cell lines grown in culture (Yankner *et al.*, 1989; Pike *et al.*, 1993). Initial studies using synthetic Aβ1-42 peptides showed that freshly dissolved peptides were not toxic to cells and needed to be incubated for 3-7 days for toxicity to be observed. This toxicity correlated with increased presence of aggregated Aβ (Pike *et al.*, 1991). Some groups suggest that Aβ must be in an aggregated state in order to be toxic (Pike *et al.*, 1993). It has been shown by analysis of the aggregation of different fragments of the Aβ peptide that residues 17-20 and 30-35 are necessary for aggregation and that it is only the aggregating Aβ fragments that are neurotoxic in cell culture conditions (Liu *et al.*, 2003). Therefore aggregating Aβ fragments are often used in Aβ toxicity models. The most commonly used fragment is Aβ25-35 (Pike *et al.*, 1995). The properties and use of this fragment will be discussed in detail in section 3.1.2.

Astrocytes under cell culture conditions appear to be more resistant to Aβ toxicity than neurones (Pike *et al.*, 1996). However, astrocytes in culture conditions do undergo a morphological change and upregulation of glial fibrillary acidic protein (GFAP) in the presence of exogenously added Aβ (See section 1.3).

Depending on the conditions, solutions of Aβ1-40 and Aβ1-42 can be heterogeneous, consisting of monomeric peptides, oligomers and fibrillar peptides (Walsh *et al.*, 1997).

Oligomeric protofibrils isolated from solutions of Aβ1-40 using size exclusion chromatography were shown to be neurotoxic (Hartley *et al.*, 1999; Walsh *et al.,* 1999). Chinese hamster ovary cells expressing APP release Aβ1-40. The oligomeric form of Aβ1-40 has been identified in the conditioned medium of these cells (Podlisny *et al.*, 1998). Aβ oligomers have also been shown to be present in the brain (Walsh *et al.*, 2002). It has been suggested that as the total amount of Aβ correlates better with cognitive decline than plaque load (Naslund *et al.*, 2000) and that neurotoxicity is associated with the maturation of soluble Aβ in diffuse plaques to fibrillar Aβ in dense core plaques, therefore protofibrils may be the toxic species. However, it is only dense core plaques containing fibrillar Aβ, which are associated with activated astrocytes and microglia, and neurones with dystrophic neurites (Nagele *et al.*, 2004). It is likely that there are toxic mechanisms involving Aβ in both oligomeric and in aggregated forms.

1.1.6 Animal models of Aβ toxicity: Evidence for Aβ being key to a cascade of pathological events in Alzheimer's disease

Transgenic animal models have been generated to attempt to model AD pathology. In accordance with the hypothesis that Aβ overproduction is key to the pathogenesis of AD, models expressing human APP mutations from patients with FAD, which are more liable to β-secretase cleavage (Suzuki *et al.,* 1994) (see 1.1.4.1), generally show amyloid deposition. Transgenic animals expressing more Aβ1-42 than Aβ1-40, as expected, also show more amyloid deposition. However, despite showing Aβ deposition, two transgenic mice expressing mutant APP isoforms found in FAD, the PDAPP mouse and the Tg2576 mouse, did not show increased neurone death (see Table 1.2) (reviewed in McGowen *et al.*, 2006)

However, accumulation of mutant Microtubule Associated Protein Tau (MAPT) appears to correlate better with neurone loss. Tau is responsible for microtubule assembly and stabilisation. Microtubules serve as tracks for motor proteins such as kinesin to transport organelles from the soma to the synapse of neurone processes. Tau in its normal state is a globular protein (Mandlekow *et al.*, 2003), containing multiple phosphorylation sites. In the neurofibrillary tangles accumulations observed in the AD

brain, hyperphosphorylated tau is observed. The hyperphosphorylated tau is unable to bind to microtubules (Bramblett *et al.*, 1998) and forms insoluble paired helical filaments. There are numerous protein kinases that could phosphorylate tau, but the tau phosphorylation pathway is yet to be elucidated (Billingsley and Kincaid, 1997).

Neurones containing hyperphosphorylated tau are unable to transport mitochondria, peroxisomes and endoplasmic reticulum to the periphery of their processes. Therefore the neurites of neurones with tau inclusions are more vulnerable to damage by hydrogen peroxide (see section (1.2.1.) as they do not have peroxisome derived catalase. As mitochondria and endoplasmic reticulum transport to the periphery is impaired, neurones are likely to be limited in their ability to perform ATP-dependent processes and perform local protein synthesis in their neurites (Mandelkow *et al.*, 2003).

The loss of synapses and neurite degeneration is a characteristic early stage phenomenon of Alzheimer's disease. Synapse and neurite loss correlates with loss of memory and brain functions (Callahan *et al.*, 1995). It has been shown *in vitro* that overexpression of tau can cause neurite degeneration, but this is due to impaired organelle transport rather than a direct toxic effect of tau (Mendelkow *et al.*, 2003).

Evidence from transgenic animal models suggests that Aβ accumulation may precede and promote tau deposition. Mice expressing mutant APP and mutant tau exhibit more tangles than mice expressing mutant tau alone (Lewis *et al.*, 2001). Mice solely expressing tau never exhibit Aβ pathology, and tauopathies such as frontotemporal dementia show tau pathology without any Aβ deposition. This suggests that Aβ may promote tau accumulation but that tau does not lead to amyloid deposition. It has been proposed that Aβ triggers altered kinase and phosphatase activity, leading to the hyperphosphorylation and fibrillization of tau (Litersky *et al.*, 1996). However tau deposition is not observed in all transgenic models, which exhibit Aβ deposition (Schwab *et al.*, 2004).

Transgenic models expressing mutant isoforms of APP, where Aβ is deposited show evidence of astrocytosis. Activated astrocytes surrounded neuritic plaques in some transgenic models (Terai *et al.*, 2004; Schmitz *et al.*, 2004; Schwab *et al.*, 2004),

however in some models astrocytosis is not localised but is found over the whole cerebral cortex (Ozmen *et al.*, 2005).

A complete mouse model of AD has proven elusive. Although amyloid deposition appears to be a key event in AD, APP mutant and PSAPP mice generate accumulations of Aβ but do not show brain atrophy. The transgenic model that generates the closest approximation of AD pathology is the triple transgenic animal of Oddo *et al.*, 2003. This mouse contains transgenes for mutant APP, MAPT and PS1 and shows amyloid and tangle pathology and also synapse dysfunction.

Alzheimer's disease has a complex aetiology. There are limitations in the development of a murine model of AD as the lifespan of mice is relatively short and brain anatomy differs. Age is the greatest risk factor for AD, and other environmental factors are likely to contribute to the initiation of the disease.

NAME	TRANSGENE	Plaque pathology	Tangle pathology	Synapse loss/dysfunction	Neurone loss	Cognitive impairment
APP						
PDAPP	APP_{v717F}	YES. 6-9 months Increase in Aβ1-42 Diffuse plaques	NO	YES	NO	N/A
Tg2576	APP_{SWE} + Hamster prion promoter	YES 9 months Dense core	NO	N/A	NO	N/A
APP_{23}	APP_{SWE} + Thy 1 promoter	YES 6 months	N/A	N/A	YES In hippocampus	N/A
TgCRND8	APP_{SWE} + $APP_{INDIANA}$	YES 3 months	N/A	N/A	N/A	YES
Bri Aβ1-40	Fusion between Aβ1-40 and a protein (BRI) involved in amyloid deposition in some familial AD cases. Aβ1-40 is cleaved from BRI so Aβ1-40 increased without increasing APP expression	NO				
Bri Aβ1-42	Aβ1-42 fused to BRI	YES Diffuse and compact plaques.				
Presenilin						
PSEN1m146v/l	PSEN1m146v/l	NO but increase in amount of Aβ1-42	N/A	N/A	N/A	N/A
Microtubule associated protein Tau (MAPT)						
JNPL3	4R0N MAPT with P301L mutation	NO	YES	YES	YES	Motor neurone loss in spinal cord
Tau_{p3015}	Shortest isoform 4R MAPT with P301S	NO	YES	N/A	YES	N/A

Cont…

NAME	TRANSGENE	Plaque pathology	Tangle pathology	Synapse loss/dysfunction	Neurone loss	Cognitive impairment
Tau_{v337M}	Decreased 4R MAPT with v337M mutation PDGF promoter	NO	YES	N/A	N/A	YES
RTg4510	Inducible MAPT transgene FTDP-17 mutation.	NO	YES	N/A	YES	YES
APP + Presenilin						
PSAPP	PSEN1 M146L x Tg2576	N/A	N/A	N/A	YES Earlier than Tg2575	N/A
APP + MAPT						
TAPP	JNPL3 x Tg2576	YES	YES Increased compared to JNPL3	YES	YES	N/A
APP + Presenilin + MAPT						
3xTgAD	APP_{SWE} $MAPT_{p301L}$ PSEN1	YES 6 months	YES 12 months	YES	N/A	N/A

Table 1.2 : Summary of commonly used transgenic mouse models of AD and their phenotypes.

Summarises McGowan *et al.*, 2006 (N/A = data not available)

Part 2: Biochemical changes associated with aging and AD

1.2.1 Oxidative stress in the aging brain

Old age is the greatest risk factor for AD. The incidence of AD in the population increases with age (Finkel, 2005). APP is expressed constitutively throughout our lifetime, yet neuritic plaques only develop in later years. It is important to understand the changes in the brain associated with age and how these may increase vulnerability to Aβ deposition and toxicity. One change is increased incidence of oxidative stress in the aged brain (Floyd , 1999; Lu *et al.*, 2004; Finkel, 2005). Oxidative stress can be defined as a production of reactive oxygen species (ROS) that exceeds the tissue's antioxidant capability.

The brain is particularly vulnerable to oxidative stress as it is a highly metabolically active organ. Mitochondria are a primary source of reactive oxygen species (ROS). Superoxide ($O_2^{-\bullet}$) is generated when molecular oxygen is reduced during respiration (see figure (1.2)). $O_2^{-\bullet}$ is converted to hydrogen peroxide (H_2O_2) by superoxide dismutase (SOD). H_2O_2 can be broken down to H_2O and O_2 by the enzymes catalase or glutathione peroxidase.

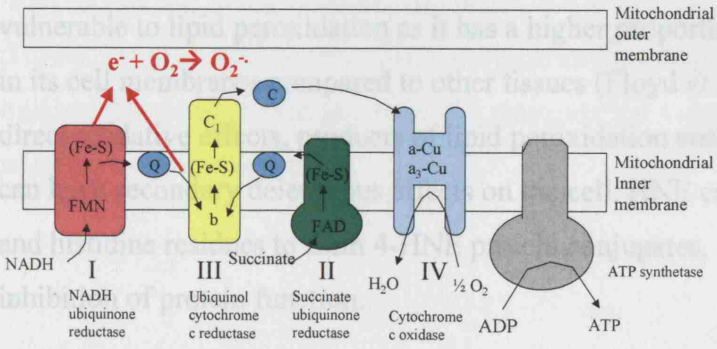

Figure 1.2: The mitochondrial electron transport chain. The superoxide radical is generated during electron transfer through the electron transport chain during normal respiration.

The brain has high levels of $Fe^{2+/3+}$ compared to other organs. In the presence of Fe^{2+} or Cu^{+}, H_2O_2 can undergo the Fenton reaction (equation 1.1) and, in the presence of Fe^{3+}, the Haber Weiss reaction (Equation 1.2 and 1.3) to generate the highly reactive hydroxyl radical $^{\bullet}OH$ (Shaw, 1998).

$$H_2O_2 + Fe^{2+} \text{ (or } Cu^{+}) \longrightarrow OH^{-} + {}^{\bullet}OH + Fe^{3+} \text{ (or } Cu^{2+}) \quad \textbf{(1.1)}$$

i) $$Fe^{3+} + {}^{\bullet}O_2 \rightleftharpoons Fe^{2+} + O_2 \quad \textbf{(1.2)}$$

Fe Catalyst

ii) $$H_2O_2 + O_2^{\bullet -} \longrightarrow O_2 + OH^{-} + {}^{\bullet}OH \text{ (Haber Weiss reaction)} \quad \textbf{(1.3)}$$

In the brain ROS and reactive nitrogen species (RNS) can also be generated enzymatically: $O_2^{-\bullet}$ for example through the activity of NADPH oxidase, and nitric oxide (NO) by nitric oxide synthase (NOS). NO and $O_2^{-\bullet}$ can react to form peroxynitrite (ONOO–) which is extremely reactive.

ROS and RNS can damage proteins, lipids and nucleic acids. The brain is particularly vulnerable to lipid peroxidation as it has a higher proportion of unsaturated fatty acids in its cell membranes compared to other tissues (Floyd *et al.*, 1999). Alongside the direct oxidative effects, products of lipid peroxidation such as hydroxynonenal (HNE) can have secondary deleterious effects on the cell. HNE can react with cysteine, lysine and histidine residues to form 4-HNE protein conjugates, which can result in an inhibition of protein function.

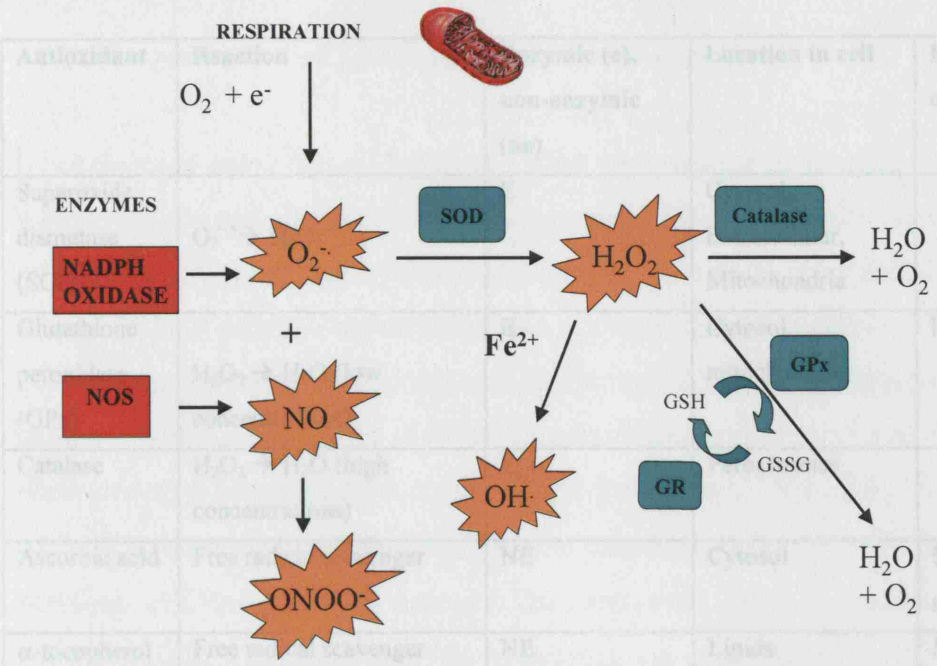

Figure 1.3: Pathways of ROS and RNS generation in the brain, and the main enzymic antioxidant defences. SOD = superoxide dismutase; GPx = Glutathione peroxidase; GR = Glutathione reductase; NOS = Nitric oxide synthase; NADPH = nicotinamide adenine dinucleotide phosphate, $O_2^{-\cdot}$ = superoxide radical; NO = nitric oxide; $ONOO^-$ = peroxynitrite; H_2O_2 = hydrogen peroxide; $OH^{\cdot}$ = Hydroxyl radical; GSH = Glutathione; GSSG = Glutathione di-sulphide.

To limit ROS and RNS mediated damage the brain contains the antioxidant enzymes catalase, glutathione peroxidase (GPx), superoxide dismutase (SOD) and the free radical scavengers glutathione (GSH), α-tocopherol and ascorbic acid (see Table 1.3). It has been shown that SOD, catalase, GPx and GSH are increased in the aging mouse brain (Hussain *et al.*, 1995). Antioxidant upregulation is a response to increased antioxidant demand. However, in the longterm, the upregulation is not sufficient to prevent age related oxidative damage.

Antioxidant	Reaction	Enzymic (e), non-enzymic (ne)	Location in cell	Interaction of GSH
Superoxide dismutase (SOD)	$O_2^{-\bullet} \rightarrow H_2O_2$	E	Cytosol, Extracellular, Mitochondria	
Glutathione peroxidase (GPx)	$H_2O_2 \rightarrow H_2O$ (low concentrations)	E	Cytosol, mitochondria	Proton donor
Catalase	$H_2O_2 \rightarrow H_2O$ (high concentrations)	E	Peroxisomes	
Ascorbic acid	Free radical scavenger	NE	Cytosol	Synergistic antioxidant
α-tocopherol	Free radical scavenger	NE	Lipids	Synergistic antioxidant
GSH	Free radical scavenger	NE	Cytosol, mitochondria, extracellular	

Table 1.3: The major brain antioxidants.

Oxidative stress is normally evaluated by the following markers in the brain 1) Oxidative modification of proteins, marked by higher levels of nitrated tyrosine residues and higher levels of protein carbonyl, 2) Lipid peroxidation marked by increased levels of 4-hydroxynonenal (HNE), thiobarbituric acid reactive substances (TBARS) and malondialdehyde (MDA), 3) Modification of sugars marked by increased amounts of advanced glycation end products (AGE) and 4) DNA and RNA oxidation shown by increased 8-hydroxyl-2-deoxyguanosine (8OHdG), and DNA fragmentation (reviewed in Zhu *et al.*, 2004).

In the aged human brain there is evidence for increased lipid peroxidation (Yoritaka *et al.*, 1996; Reich *et al.*, 2001) oxidative damage to DNA (Lu *et al.*, 2004) and oxidative damage to proteins (Smith *et al.*, 1991).

1.2.2. The promotion of Aβ accumulation in the aging brain

It has been suggested that the highly oxidative environment of the aging brain promotes Aβ aggregation and accumulation. Non-aggregated Aβ, in low concentrations has been proposed to have antioxidant properties, owing to the transition metal binding sites located in the N terminal region being able to chelate transition metal ions (Kontush, 2001). Some oxidative insults such as H_2O_2 increase Aβ secretion from neurones in culture conditions (Olivieri *et al.*, 2001). An oxidative environment may promote Aβ fibril formation as antioxidants decrease fibril formation in vitro (Naiki *et al.*, 1998). In addition levels of the Aβ degrading enzymes Insulin degrading enzyme (IDE) and neprilysin (NEP) are lowered with age (Caccamo *et al.*, 2005). Vascular transport systems are also a potential target of the aging process. A reduction in Aβ clearance through the blood brain barrier (BBB) with age may also lead to Aβ accumulation in the brain (Deane *et al.*, 2005).

1.2.3. Oxidative stress in AD

Over and above the increased incidence of oxidative stress markers in the aging brain, there is abundant evidence for a greater levels of oxidative stress markers in people with AD compared with age-matched controls as shown by an increased incidence of oxidised proteins and lipid peroxidation (Markesbery and Lovell, 1998; Butterfield and Lauderback, 2002), oxidized mitochondrial and nuclear DNA (Wang *et al.*, 2005) and advanced glycation endproducts in neuritic plaque fractions (Vitek *et al.*, 1994).

Fibrillar Aβ has been shown to induce ROS production in astrocyte and neurone cell cultures, as shown by the non-specific marker of ROS production the fluorescent probe dichlorofluorescein, DCF (Alvarez *et al.*, 2003). The antioxidants catalase and α tocopherol, protect from Aβ mediated toxicity in cell culture conditions (Behl *et al.*, 1992; Behl *et al*, 1994). Likewise, neurones supplemented with GSH precursors to up-regulate their intracellular GSH also show decreased cell death when treated with Aβ (Abramov *et al.*, 2004; Boyd Kimball *et al.*, 2005).

1.2.4. Sources of ROS and RNS in the presence of Aβ

The proposed mechanisms by which fibrillar Aβ can generate ROS and RNS can be mostly grouped into 4 categories: 1) chemical interactions between Aβ peptides and ions and molecules in the brain, 2) activation of ROS and RNS producing enzymes, 3) impairment of energy metabolism and 4) disruption of Ca^{2+} homeostasis.

1.2.4.1. Chemical interactions between the Aβ and ions and molecules in the brain

The amino acid methionine in position 35 of Aβ has been implicated in the generation of ROS, and Aβ toxicity. Aβ fragments in which this methionine is substituted for norleucine or valine, or removed, are non-toxic to cultured neurones and do not generate ROS (Varadarajan *et al.*, 1999). The oxidation of the sulphur in methionine to produce a sulphur radical cation, has been implicated as mediating toxicity (Varadarajan *et al.*, 2001). In cell culture systems where a metal chelator has been added to the cell culture media before treatment with Aβ, lowered toxicity is observed (Rottkamp *et al.*, 2001). The generation of free radicals by Aβ in cell free solutions is reported to be dependent on the presence of metal ions in solution (Dikalov *et al.*, 1999). It is proposed that the oxidation of methionine can reduce transition metals. Reduced transition metals are potent oxidants.

1.2.4.2. Activation of ROS and RNS producing enzymes or binding to receptors initiating ROS generating cascades

NADPH Oxidase

NADPH is an enzyme expressed in neutrophils, microglia and astrocytes. In the presence of Aβ it is activated in all three cell-types (Bianca *et al.*, 1999; Abramov *et al.*, 2005). NADPH oxidase transfers electrons donated from NADPH to O_2, generating the superoxide radical.

Nitric oxide synthase (NOS)

Nitric oxide is a free radical that has been implicated in many physiological roles including neurotransmission, neuromodulation and vasodilation (Dawson and Snyder, 1994). In a cell NO can react with transition metals, thiol groups and other parts of proteins, therefore it has many potential targets. As NO is gaseous it can pass quickly through the cell and across cell membranes to react with its target. As NO is so reactive, the action of NO is limited spatiotemporally by potential targets around its source.

NO is synthesised by three isoforms of nitric oxide synthase (NOS). Neuronal NOS (nNOS) and endothelial NOS (eNOS) are constitutive enzymes; these require the cofactor calmodulin to be present. In order for calmodulin to bind to NOS Ca^{2+} must be present. The third isoform of NOS, inducible NOS (iNOS), is not normally expressed in cells. Its expression may be induced in some cells by cytokine activation as part of the inflammatory response.

Total levels of nitrite and nitrate, the stable end products of NO metabolism, are comparable in the cerebral spinal fluid of AD patients and age-matched controls (Milstien *et all.*, 1994). However, increased NO production in AD brains on a local level has been suggested by the increase in nitro tyrosine residues in the AD brain. NO reacts with $O_2^{-\bullet}$ to form peroxynitrite ($ONOO^-$). Nitrotyrosine is thought to arise as a consequence of the reaction between $ONOO^-$ and tyrosine residues in proteins (Smith *et al.*, 1997).

The source of NO in AD has been largely attributed to the inflammatory response of astrocytes and microglia surrounding neuritic plaques. Aβ has been shown to upregulate iNOS expression in cultured cortical astrocytes and has been suggested to cause NO release (Hu *et al.*, 1998). Aβ can cause NO release in microglial cultures (Li et al., 1996). Astrocyte NO release in the presence of Aβ may be modulated by various cytokines, neurotrophic factors and transcription factors. Astrocytes release the neurotrophic factor S100β in the presence of Aβ (Pena *et al.*, 1995) and the presence of S100β may consequently induce astrocytes to release NO (Hu *et al.*, 1997). Akama *et*

al., 1998 have shown that astrocyte NO production is likely to be secondary to the Aβ induced inflammatory response (see section 1.3.5.2).

Receptor for advanced glycation end products-RAGE

The RAGE receptor has been proposed to provide a mechanism by which Aβ can bind to endothelial cells, astrocytes and neurones in the AD brain (Yan *et al.*, 1994) The RAGE receptor is suggested to be the route by which advanced glycation end products can be taken into macrophages and degraded in the lysosome system (Araki *et al.*, 1995). Astrocytes may also be able to internalise Aβ through this receptor (Sasaki *et al.*, 2001). However, it is also suggested that the RAGE receptor provides a transport mechanism to carry systemic Aβ, generated by platelets in the blood into the brain (Donahue *et al.*, 2006). In addition, when Aβ binds to RAGE oxidative species are generated (Yan *et al.*, 1994).

1.2.4.3. Impairment of energy metabolism

There is evidence for impaired metabolism in AD from brain imaging studies using positron emission tomography (PET). These studies suggest a decrease in cerebral glucose utilization that appears before neuronal loss in AD patients (Ibanez *et al.*, 1998) and worsens as dementia becomes more severe (Duara *et al.*, 1986; Alexander *et al.*, 2002)

The mitochondria are a major source of ROS. There is a strong reciprocal relationship between metabolic impairment and ROS generation. It has been shown that mitochondrial function is impaired in the AD brain. Cytochrome oxidase catalyses the final step of the respiratory chain, the oxidation of cytochrome c and the reduction of oxygen to water. This reaction is coupled with the pumping of protons across the inner mitochondrial membrane, to form a gradient which in turn drives the ATP synthetase (see Figure 1.2). The activity of cytochrome oxidase is decreased in post mortem brain tissue and in platelets from AD patients (Parker *et al.*, 1990; Kish *et al.*, 1992). Impaired mitochondrial function can lead to increased generation of ROS. Studies using cybrids obtained by inserting mitochondria from the platelets of AD patients into mitochondria-

free rho0 cells (Human neuroblastoma SH-SY5Y cells depleted of mitochondria) demonstrated elevated ROS production in these cybrid cells (Sheehan *et al.*, 1997), consistent with the mitochondria of AD patients being sufficient to elevate ROS.

Addition of Aβ to primary neurone cell cultures causes inhibition of cytochrome oxidase (Casley *et al.*, 2002). This inhibition could be a direct effect of the peptide as Aβ can impair cytochrome oxidase activity in isolated mitochondria (Canevari *et al.*, 1999). Aβ could also impair mitochondrial function though the action of RNS generated in its presence. Nitric oxide (Bolanos *et al.*, 1994) or its metabolic product peroxynitrite (Sharp and Cooper, 1998) can inhibit cytochrome oxidase.

Studies have shown that cytochrome oxidase purified from the AD brain lacks the high affinity binding site for cytochrome c (Parker and Parks, 1995). However, it could be the case that the membrane environment is the target of the effect of Aβ on cytochrome oxidase activity. Cytochrome oxidase requires the phospholipid cardiolipin for full activity. Cardiolipin may be particularly vulnerable to oxidation as it is high in unsaturated fatty acids. It has been shown that there is a close correlation between cardiolipin peroxidation and a reduction in cytochrome oxidase activity, and that replenishing cardiolipin in mitochondria treated with peroxidation agents can restore cytochrome oxidase activity (Paradies *et al.*, 1998).

The activity of the tri carboxylic acid (TCA) cycle enzyme α- ketoglutarate dehydrogenase, and the metabolic enzyme pyruvate dehydrogenase are inhibited in post mortem tissue from AD patients (Gibson *et al.*, 1998). The activities of these enzymes are also inhibited in neuronal cell culture models treated with Aβ (Casley *et al.*, 2002). The reciprocal relationship between oxidative stress and metabolic impairment is again demonstrated in an interesting study where it was shown that in the absence of its substrate, NAD+, α-ketoglutarate dehydrogenase complex can produce H_2O_2 (Tretter *et al.*, 2004).

1.2.4.4 Disruption of calcium homeostasis

Altered Ca^{2+} homeostasis is a consequence of oxidative stress. Hydroxynonenal (HNE), a product of lipid peroxidation, can bind to membrane ion motive ATPases (Na^{+}/K^{+} and Ca^{2+} ATPases, glucose and glutamate transporters), which can lead to membrane depolarisation, lowered ATP levels and an increase in cytosolic Ca^{2+} (Mattson, 1997). If HNE is added to neurones in culture conditions it causes a delayed elevation of cytosolic Ca^{2+} (Mark *et al.*, 1997).

Aβ may also have a direct effect on Ca^{2+} homeostasis in the AD brain. Aβ25-35 and Aβ1-42 have been shown to induce calcium oscillations in cortical astrocytes resulting from an influx of extracellular Ca^{2+} (Abramov *et al.*, 2004). In cerebellar neurones Aβ1-42 causes an increase in calcium influx into the cell by modulating N-type Ca^{2+} channels (Price *et al.*, 1999)).Calcium permeable pores can be formed by Aβ25-35 and Aβ1-42 in artificial lipid bilayers (Mirabekov *et al.*, 1994; Hirakura *et al.*, 1999; Arisbe *et al.*, 1993) and by Aβ1-40 in an immortalised hypothalamic murine cell line (Kawahara and Kuroda, 2000). However, no evidence of calcium pore formation has been found *in vivo* to date.

Disrupted Ca^{2+} homeostasis can contribute to oxidative damage. Increased intracellular Ca^{2+} levels can lead to increased ROS or RNS by three routes. Firstly Ca^{2+} alongside calmodulin is an essential cofactor for endothelial and neuronal nitric oxide synthase activity (Dawsen and Snyder, 1994). Secondly, Ca^{2+} promotes activation of phospholipase A_2 which leads to the release of arachidonic acid which is a substrate for lipoxygenases and cycloxygenases to form ROS. Thirdly, increased Ca^{2+} can lead to altered mitochondrial activity and increased $O_2^{\bullet -}$ release (Reviewed in Mattson, 1997).

Disrupted Ca^{2+} homeostasis may lead to increased oxidative stress but can also have many ROS independent effects on neurones that may contribute to their death. Calcium is involved in an abundant array of signalling cascades. Many kinases and phosphatases have Ca^{2+} as a cofactor. It has been proposed that Ca^{2+}/ calmodulin dependent protein kinase II, contributes to tau phosphorylation (Litersky *et al.*, 1996). It has been shown that hippocampal neurones that are particularly vulnerable in AD have particularly high

concentrations of Ca^{2+}/ calmodulin dependent protein kinase II (McKee *et al.*, 1990). A disruption to calcium homeostasis is reported to make human cortical neurones more vulnerable to glutamate-mediated excitotoxicity (Mattson *et al.*, 1992).

Part 3: Neurone and astrocyte interactions in the normal and AD brain

It is interesting to observe that as the mammalian brain has evolved and increased in size and complexity the proportion of astrocytes relative to neurones has increased (Nedergaard *et al.*, 2003). The hypothesised role of astrocytes in the brain has been promoted in the last two decades from that of an ancillary structural support cell to a dynamic regulator of neurone development, phenotype and functional activity. In the mature brain neurones and astrocytes form a functional unit. Astrocytes extend processes to envelop neurone synaptic connections. They also form direct connections between each other governed by gap junctions. They can therefore be considered a glial syncytium in intimate contact with synapses, and with wide reaching signalling capabilities (Benarroch., 2005). Astrocytes also have a close relationship with the endothelial cells of the blood brain barrier and regulate the transfer of blood-derived factors to neurones. Most neuronal cell culture models have strived to achieve high purity from astrocyte contamination. However, neuronal culture models closest to their physiology *in vivo* are those that aim to reproduce the functional unit to some extent.

In addition to their normal supportive functions, astrocytes have the ability to respond to a number of pathological situations where they engage in a series of structural and functional changes collectively termed astrogliosis. These activated astrocytes are usually characterised by an upregulation of glial fibrillary acidic protein (GFAP) and a morphological change from a flat polygonal morphology to a more stellate shape. In Alzheimer's disease these activated astrocytes are found surrounding dense core neuritic plaques.

This section gives an overview of the supportive functions of astrocytes, the changes that arise when astrocytes undergo their reactive response, and discusses the role of the astrocytes surrounding neuritic plaques in neurotoxicity and neuroprotection.

1.3.1. The supportive functions of astrocytes.

The supportive functions of astrocytes include regulating synaptic transmission, maintaining extracellular homeostasis, providing metabolic and antioxidant support to neurones (figure 1.4.). Here, the main focus is the antioxidant support from astrocytes; however, their role in metabolic support and glutamate clearance will be introduced briefly for their relevance to AD.

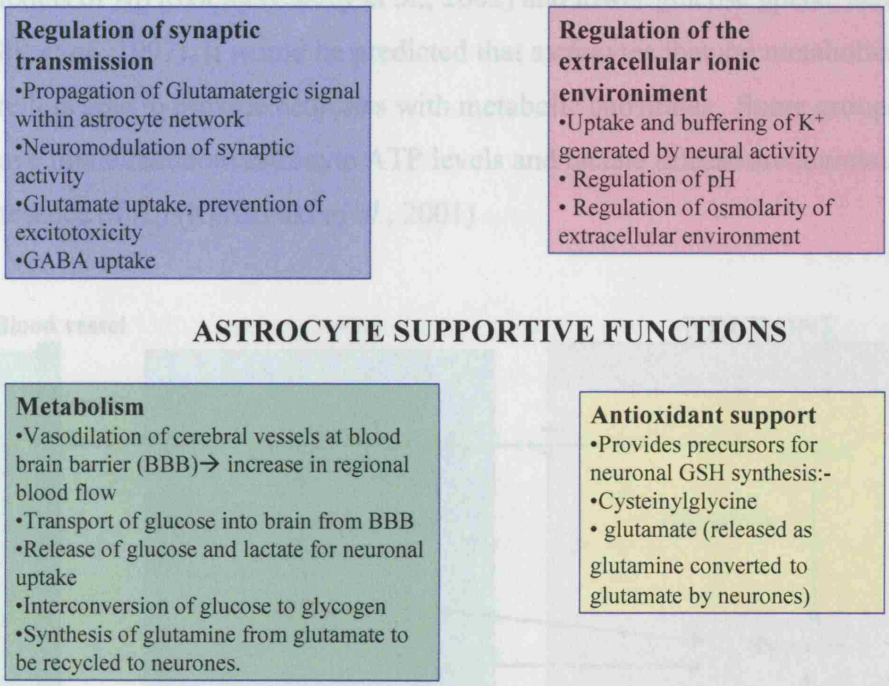

Figure 1.4: A summary of astrocyte supportive functions to neurones in the normal brain. Summarises (Benarroch 2005)

1.3.2. Metabolic support of neurones by astrocytes.

As discussed in the last section, neurones in the AD brain are metabolically impaired. The cytoarchitecture of the brain is such that the astrocytes form the bridge between the endothelial cells of blood vessels in the brain and neurones. Glucose from blood is taken up by astrocytes and a small amount can be stored as glycogen. Astrocytes form the predominant storage site for glycogen in the brain (Wiesinger *et al.*, 1997) Astrocytes

can regulate the amount of glucose released to neighbouring neurones (see figure 1.5). Astrocytes also release lactate and pyruvate (Wang and Cynader, 2001; Pellerin and Magistretti, 2004) although it is a contentious issue as to which astrocyte derived metabolic substrate neurones preferentially use for their metabolism. It has been shown that ATP is released by astrocytes treated with exogenously applied NO and LPS/IFNγ (Bal-price *et al.*, 2002). ATP is involved in inter-astrocyte signalling, but may also be utilised by neighbouring neurones (Fellin *et al.*, 2006). Metabolic support from astrocytes may be neuroprotective as supplementation of neurones with malate or pyruvate can protect neurones against Aβ25-35 mediated neurone death (Alvarez *et al.*, 2003). Some groups have shown a lowering of ATP levels in astrocyte cell culture models of Aβ toxicity (Casley *et al.*, 2002) and lower glucose uptake activity (Parpura Gill *et al.*, 1997). It would be predicted that astrocytes that are metabolically impaired are less able to provide neurones with metabolic substrates. Some groups, however, have found that both astrocyte ATP levels and lactate release are maintained in the presence of Aβ (Kerokoski *et al.*, 2001)

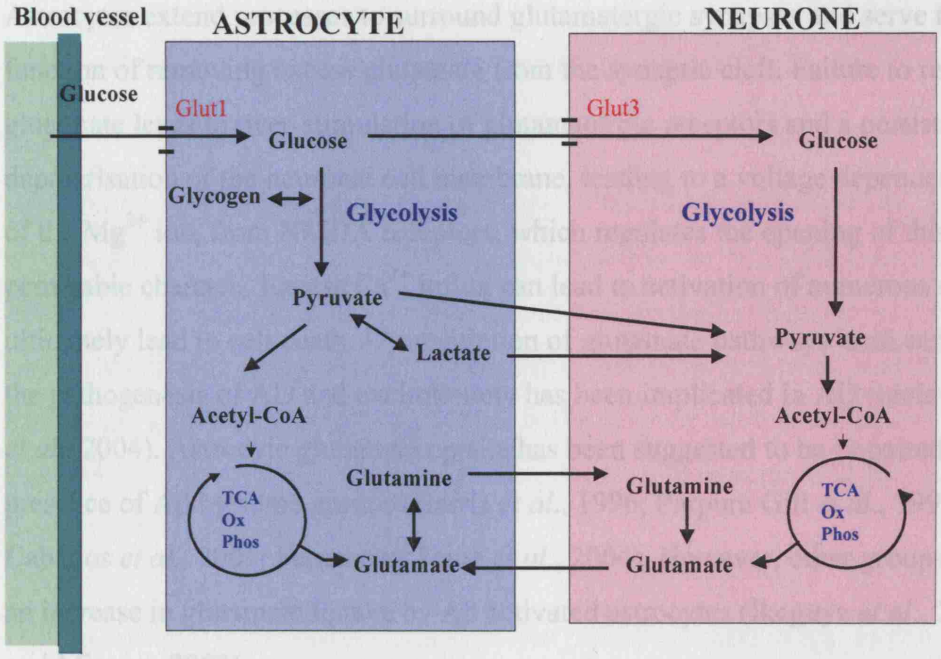

Figure 1.5: Metabolic coupling of neurones and astrocytes. Astrocytes provide glucose pyruvate and lactate for neurone energy metabolism. They also replenish neurone glutamate stores, and remove excess glutamate.

1.3.3. Regulation of glutamate

The amino acid glutamate is synthesised from the TCA cycle intermediate α-ketoglutarate, in a reaction catalysed by glutamate dehydrogenase. As glutamate is a common amino acid and the principle excitatory neurotransmitter its provision to glutamatergic neurones needs to be tightly regulated. In a series of experiments (reviewed in Hertz *et al.*, 1999) neurone glutamate levels were shown to be dependent on the astrocyte TCA cycle. In these studies, fluoroacetate, which is selectively taken up by astrocytes, but not by neurones, was converted inside astrocytes to fluorocitrate. Fluorocitrate inhibits the metabolism of citrate to isocitrate, a step in the TCA cycle that procedes the formation of α-ketoglutarate. In hippocampal slices addition of fluroacetate inhibited neurone gluatmatergic transmission.

Astrocytes extend processes to surround glutamatergic synapses and serve the vital function of removing excess glutamate from the synaptic cleft. Failure to remove excess glutamate leads to over-stimulation of glutamatergic receptors and a persistent depolarisation of the neuronal cell membrane, leading to a voltage dependent removal of the Mg^{2+} ion, from NMDA receptors, which regulates the opening of this Ca^{2+} permeable channel. Excess Ca^{2+} influx can lead to activation of numerous cascades that ultimately lead to cell death. Dysregulation of glutamate pathways is an early event in the pathogenesis of AD and excitotoxicty has been implicated in AD (reviewed in Hynd *et al.*, 2004). Astrocyte glutamate uptake has been suggested to be impaired in the presence of Aβ by some groups (Harris *et al.*, 1996; Parpura Gill *et al.*, 1997; De Caballos *et al.*, 2001; Fernandez Tome *et al.*, 2004). However, other groups have found an increase in glutamate uptake by Aβ activated astrocytes (Ikeguya *et al.*, 2002; Abe and Misawa, 2003).

Astrocytes, but not neurones, contain the enzyme glutamine synthetase, which catalyses the amidation of glutamate to glutamine by the addition of an ammonium group. Both neurones and astrocytes can hydrolyse glutamine to glutamate in a reaction catalysed by

phosphate-activated glutaminase. As glutamine has no neurotransmitter activity this serves a mechanism by which astrocytes can replenish neuronal glutamate without stimulating glutamatergic receptors (Reviewed in Hertz *et al.*, 1999).

1.3.4. Astrocyte derived antioxidant support

As introduced in part 2, as humans age their brains become more susceptible to oxidative damage. Aβ causes further increases in the production of ROS and RNS. There is a reciprocal interaction between production of oxidative species, metabolic impairment and inappropriate Ca^{2+} signalling which is a pathogenic spiral leading to cell death. Antioxidant treatment can protect neurones in culture from Aβ toxicity. However, it is important to investigate how the brain's intrinsic antioxidant systems respond to Aβ, and how the biochemical changes induced by Aβ may lead to these systems being overburdened.

1.3.4.1. Structure and antioxidant properties of glutathione

Glutathione (GSH) is a tri-peptide consisting of the amino acids cysteine, glutamate and glycine, and is the most abundant non-protein thiol in the brain (Meister and Anderson, 1983). GSH is found in milli molar concentrations in the brain and it has been implicated directly and indirectly in numerous biological processes, such as scavenging free radicals, maintaining redox potential in the cell and modulating neural signalling (reviewed in Shaw, 1998). Here, the focus is on its role in protecting cells against free radicals and other toxic species.

GSH is involved in the detoxification of free radicals in three ways: 1) as a free radical scavenger, 2) as a co-factor for glutathione peroxidase and 3) as a substrate for glutathione S transferases.

1.3.4.1.1 GSH as a free radical scavenger

The brain's enzymic antioxidants can only break down $O_2^{-\bullet}$ and H_2O_2, therefore it relies on free radical scavengers to detoxify $^{\bullet}OH$, NO and radical products of lipid peroxidation. The free radical scavenging properties of GSH arise from the thiol group of its cysteine. GSH can react with free radicals to form a thiyl radical ($GS^{\bullet}$). The thiyl radical can then react with other thiyl radicals to form glutathione disulphide (GSSG) (Halliwell and Gutteridge, 1989). As a free radical scavenger, GSH acts synergistically with other free radical scavengers such as ascorbic acid (Meister, 1994) and α-tocopherol (Chen *et al.*, 1994)

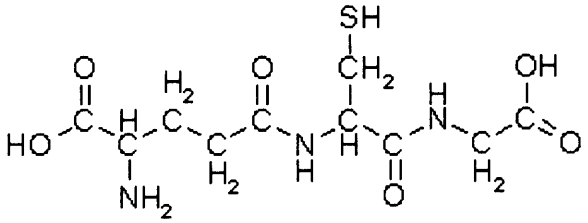

Reduced Glutathione (GSH)

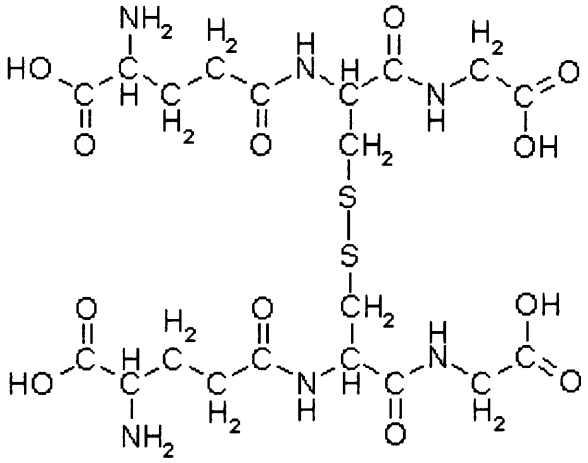

Glutathione Di-sulphide (GSSG)

Figure 1.6: The molecular structure of reduced glutathione and glutathione disulphide.

1.3.4.1.2 GSH as a cofactor for glutathione peroxidase

GSH also acts as a proton donor for glutathione peroxidase (GPx), which breaks down hydrogen peroxide. The brain contains proportionally more GPx than catalase therefore is thought to rely more on the GSH/GPx system to break down H_2O_2. Mitochondria do not contain catalase so the mitochondrial GSH/ GPx system detoxifies the small amount of H_2O_2 generated by these organelles (Martensson *et al.*, 1990). In this reaction two GSH molecules are oxidised and form a di-sulphide bond between their cysteine residues to form glutathione disulphide GSSG (see equation 1.4).

$$H_2O_2 + 2GSH \xrightarrow{GPx} GSSG + 2H_2O \qquad \textbf{(1.4)}$$

1.3.4.1.3 GSH as a substrate for glutathione s-transferase

Glutathione s-transferases are a family of enzymes that catalyse the reaction of various molecules with GSH to form a sulphur-substituted GSH conjugate. In this way, GSH can be conjugated to NO to form nitrosoglutathione in the presence of glutathione S transferase. Glutathione s-transferases also provide a route by which toxic products generated by oxidative stress can be removed via the Multidrug Resistance Protein 1 (see section 1.3.4.6). Importantly the glutathione s-transferase system is important for the removal of hydroxynonenal from the cell which is a highly toxic lipid peroxidation product found to be elevated in the AD brain (Sultana and Butterfield, 2004).

1.3.4.2. Reduction of oxidised glutathione (GSSG) to replenish GSH stores

The GSH:GSSG ratio is important in maintaining a cell viability. Normally this ratio is around 98: 2 GSH: GSSG (Hirrlinger *et al.*, 2002). To maintain the ratio, GSSG is either transported from the cell (Hirrlinger *et al.*, 2001) or reduced to GSH by the

enzyme glutathione reductase (GR). This reaction requires NADPH (Meister and Anderson, 1983) (see equation 1.5)

$$GSSG + NADPH + H^+ \xrightarrow{GR} 2\,GSH + NADP^+ \qquad \textbf{(1.5)}$$

1.3.4.3. GSH levels in the aged brain and in AD

As there is increased oxidative stress in aged and AD brains, some groups have investigated whether or not GSH levels are affected. These studies have produced conflicting results.

It has been reported that there is an age-related decline in GSH levels in the human brain (Benzi and Moretti, 1995). However, in the AD brain it has been reported, by some groups, that there are increased levels of GSH (Makar *et al.*, 1995), whereas others report that total brain levels are unaffected (Balazs and Leon, 1994). In contrast, glutathione is lowered in lymphoblasts from patients with familial AD (Cecchi *et al.*, 1999). It is difficult to make deductions about the involvement of GSH in the pathogenesis of AD from these studies. Firstly the GSH content varies between brain areas (Kang *et al.*, 1999). Secondly, the method of measuring glutathione is important, particularly whether it measures total GSH and GSSG or solely GSH. Thirdly, an increase in GSH may suggest compensatory mechanisms: for example, glutathione reductase activity is increased in some areas in the amygdala and hippocampus (Lovell *et al.*, 1995).

1.3.4.4. GSH and Aβ mediated toxicity

There are however compelling reasons to further study the GSH system in relation to Aβ toxicity.

1) The GSH antioxidant systems can detoxify the free radicals generated in the presence of Aβ.

2) GSH is present in, and is essential for, normal mitochondrial function, and may serve to limit damage caused by Aβ. Mitochondrial GSH is not synthesised within the mitochondria, rather it is transported from the cytosol (Martensson *et al.*, 1990). Under normal conditions mitochondrial GSH is required to maintain mitochondrial thiols in their reduced state. Mitochondrial thiols are necessary to maintain selective membrane permeability to Ca^{2+} (Bains and Shaw, 1997). In addition mitochondria rely on the GSH/ GPx system to detoxify the small amount of H_2O_2 they produce (Martensson *et al.*, 1990). It has been shown that loss of GSH can cause mitochondrial damage (Heales *et al.*, 1995), and depletion of mitochondrial GSH, using ethacrynic acid, can cause cell death (Muyderman *et al.*, 2004).

3) In metabolically compromised cells, GSH levels may be affected, as GSH synthesis requires ATP (see section 1.3.4.4.). The mitochondrial impairment observed in the presence of Aβ, in addition to generating ROS, could lead to a decrease in GSH levels by limiting GSH synthesis (Mitopher *et al.*, 1992).

4) The difference in neurone and astrocyte susceptibility to Aβ toxicity may be a direct consequence of differences in astrocyte and neurone GSH levels. Neurones in the adult rat cerebral cortex (Langeveld *et al.*, 1996), and grown from an embryonic source in cell culture (Bolanos *et al.*, 1995; Hirrlinger *et al.*, 2002) contain lower GSH levels than astrocytes in the same conditions. Neurones rely on astrocytes to provide the precursors needed for their GSH synthesis (Sagara *et al.*, 1993). Neurones are more vulnerable to Aβ and a variety of oxidative insults than astrocytes (Pike *et al.*, 1993; Pike *et al* 1994., Gegg *et al.*, 2003; Watts *et al.*, 2005; Rathinam *et al.*, 2006). A contributing factor to this may be that they have lower GSH levels than astrocytes.

1.3.4.5. Synthesis of GSH in astrocytes and neurones

GSH synthesis requires the provision of the component amino acids, glutamate, cysteine and glycine. Availability and uptake of cysteine is thought to limit the rate of GSH synthesis in neurones (Sagara *et al.,* 1993). Neurones and astrocytes differ in their mechanisms of cysteine uptake. Astrocytes can take up cysteine and also the di-peptides Cysteinylglycine (CysGly) or Glutamylcysteine (γ- GC) (Dringen *et al.*, 1997). Although astrocytes take up the reduced form of cysteine (Cys), they have a higher affinity for the uptake of the oxidised disulphide form, cystine (Cys-SS-Cys) (Kranich *et al.,* 1998). Neurones on the other hand preferentially uptake cysteine (Kranich *et al* (1996)). Neurones do not appear to be able to take up di-peptides, but contain a membrane bound enzyme, aminopeptidase N, which cleaves γ-GluCys to its component amino acids, which can be taken up by neurones (Dringen *et al.*, 2001).

Cystine is proposed to be taken into astrocytes by the X_c^- Na^+ dependent antiporter (Mahar, 2005). Cysteine is thought to be taken up by neurones via the excitatory amino acid transporters, EAAT2 and EAAT3 (Chen *et al.*, 2003). The mechanism by which CysGly is taken up as a di-peptide by astrocytes has not been elucidated (Dringen *et al.*, 1997)

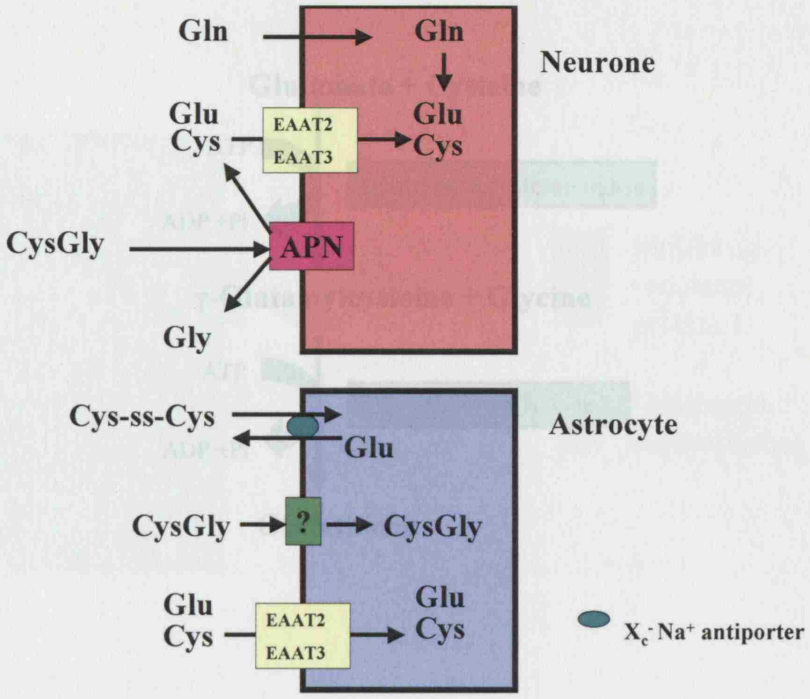

Figure 1.6: GSH precursor amino acid transport into neurones and astrocytes. Gln = Glutamine, Cys = cysteine, Glu = glutamate, CysGly = cysteinylglycine, Cys-ss-cys = cystine. EAAT = excitatory amino acid transorter, APN = amino peptidase N.

Glutathione is synthesised by the sequential action of two enzymes. The first is glutamate cysteine ligase (GCL), which catalyses the formation of γ-glutamylcysteine (γGluCys) from glutamate and cysteine. The bond between these amino acids is unusual as it is between the γ-carbon of glutamate rather than the α-carbon of the carboxyl group. This unusual peptide bond has been suggested to protect the GSH from degradation by aminopeptidases (Sies, 1999). The second enzyme in GSH synthesis is glutathione synthetase, which catalyses the addition of glycine to γ-glutamylcysteine to generate GSH (Meister and Anderson, 1983) (see figure 1.7). Both enzymatic steps require ATP. GCL is proposed to be the rate limiting enyme of GSH synthesis (Meister and Anderson, 1983). GCL undergoes feedback inhibition by GSH (Huang *et al.*, 1993). GCL can also be modulated by protein kinase C, protein kinase A and calcium calmodulin kinase type II (Sun *et al.*, 1996).

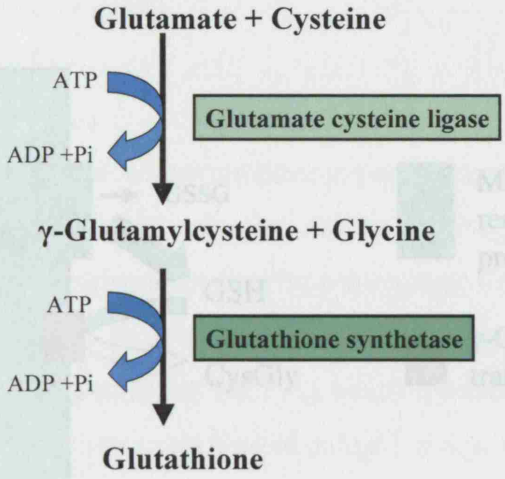

Figure 1.7: The two enzymatic steps of GSH synthesis

1.3.4.6. Release of GSH from astrocytes

Astrocytes, unlike microglia, oligodendrocytes and neurones, release GSH (Hirrlinger *et al*., 2002). GSH and GSSG release is mediated by the multi-drug resistance protein1 (MRP1) (Hirrlinger *et al*., 2001; Hirrlinger *et al*., 2002). In two separate studies the MRP1 inhibitors MK571 and Verapamil have been shown to promote GSH efflux when presented to astrocytes in low concentrations, but lower the rate of GSH efflux when presented in high concentrations (Hirrlinger *et al*., 2002; Loe *et al*., 2000). A proposed mechanism for GSH efflux from the cell depends on two binding sites on MRP1, when one of these sites is occupied by an inhibitor and the other by GSH, typically at low inhibitor concentrations, GSH efflux is enhanced. When there is a high concentration of inhibitor, both sites are occupied with inhibitor therefore GSH efflux is impaired. (Hirrlinger *et al*., 2002). Sagara *et al*., 1996 suggest that GSH efflux is dependent on the intracellular concentration of GSH. GSH-S- conjugates are also transported out of the cell via this system (see Figure 1.8).

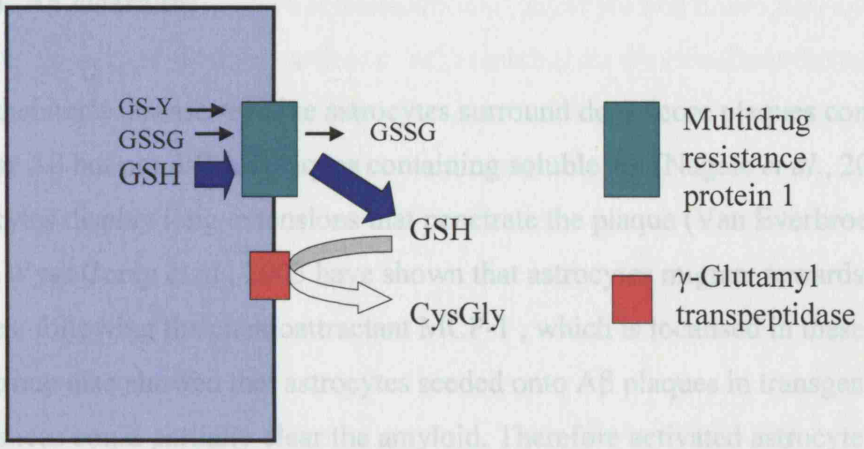

Figure 1.8: GSH efflux from astrocytes. GSH, GSSG and Glutathione S conjugates (GS-Y) are transported through the multidrug resistance protein 1. GSH can be further cleaved by the astrocyte membrane bound enzyme γ glutamyl transpeptidase.

Astrocytes express a membrane bound enzyme γ glutamyl transpeptidase. This enzyme cleaves GSH and glutathione-S conjugates to generate CysGly. Astrocytes can use this to replenish their intracellular GSH (Dringen and Hamprecht, 1998). Neurones can also break down CysGly to Cys and Gly by aminopeptidase N catalysed reaction. Cys and Gly can then be taken up by neurones (Dringen *et al.*, 1997).

It has recently been shown that astrocytes release other factors, which preserve GSH in its reduced form (Stewart *et al.*, 2002). One of the proposed factors is extracellular SOD (EcSOD).

1.3.5. Additional roles for activated astrocytes

1.3.5.1. Aβ clearance

In Alzheimer's disease reactive astrocytes surround dense core plaques containing fibrillar Aβ but not diffuse plaques containing soluble Aβ (Nagale *et al.*, 2004) Astrocytes display long extensions that penetrate the plaque (Van Everbroeck *et al.*, 2004).Wyss Corey *et al.*, 2003 have shown that astrocytes migrate towards neuritic plaques, following the chemoattractant MCP-1 , which is localised in these plaques. This group also showed that astrocytes seeded onto Aβ plaques in transgenic murine brain slices could partially clear the amyloid. Therefore activated astrocytes surrounding plaques may be involved in amyloid clearance. However, Nagele *et al.*, 2004 propose as AD progresses astrocytes become overburdened with Aβ, lyse and release Aβ to form astrocyte derived, GFAP-rich neuritic plaques. Reactive astrocytes have also been implicated in Aβ clearance, by a mechanism mediated by metalloproteases (see section 1.3).One of these, neprilysin, is upregulated in activated astrocytes (Apelt *et al.*, 2003).

1.3.5.2. The inflammatory response of astrocytes

Astrocytes when activated upregulate numerous soluble factors (Eddleston and Mucke, 1993). These are summarised in Figure 1.9. It is not known whether these factors have a neuroprotective effect or are indeed contributing to the pathogenesis of disease. The increase in production of the ROS, NO and $O_2^{\bullet -}$, is proposed to be toxic to neurones. However, as described above, astrocytes also release antioxidants, which may be able to buffer this effect. Nonetheless astrocyte derived NO has been shown to inhibit neurone mitochondrial function *in vitro*, and prolonged mitochondrial inhibition can lead to cell death (Stewart *et al.*, 2000).

Activated astrocytes release inflammatory cytokines and chemokines, as do activated microglia that also surround neuritic plaques. Epidemiological studies have suggested that there may be a beneficiary effect of non-steroidal anti-inflammatory drugs (NSAID) in AD (McGeer *et al.*, 1996). The inflammatory response of astrocytes and microglia in AD has been suggested to increase amyloid deposition, increase the

transcription of BACE1 or increase APP mRNA levels (reviewed in Sastre *et al.*, 2006). However the direct effects of these inflammatory modulators on neurones are far from being elucidated. The reciprocal modulation of astrocyte and microglia –inflammation make the dissection of how particular inflammatory mediators affect the neurones in the vicinity very complex (Mrak and Griffin, 2001). It has been proposed that the astrocyte immune response to Aβ may serve to modulate microglial neurotoxicity by modulating the amount of pro-apoptotic factors released by microglia (Von Bernhardi and Eugenín, 2004).

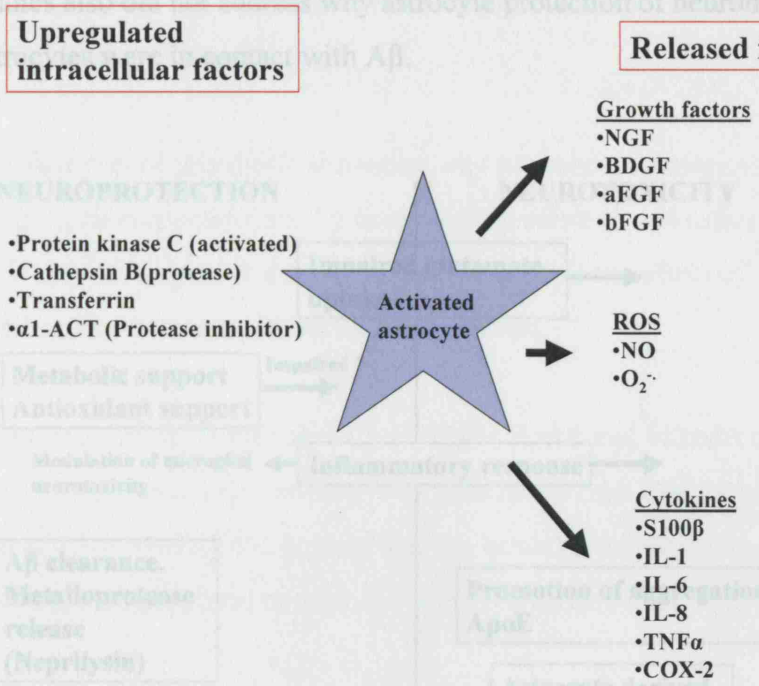

Figure 1.9: Factors upregulated and released by Aβ – activated astrocytes. Summary of Eddleston and Mucke , 1993; Tuppo and Arias, 2005.

1.3.6 The role of astrocytes in neurotoxicity and neuroprotection

It is unknown whether the astrocytes surrounding neuritic plaques have an overall protective effect or are contributing to the pathogenesis of AD either by loss of function or a toxic gain of function (Figure 1.10). Although much work has been done to elucidate the effects of Aβ on separate neurone and astrocyte cultures there is only one group to date that has addressed whether astrocytes are protective or toxic to neurones using a co-culture system. In three studies using primary hippocampal astrocytes and

neurone co-cultures and mixed cultures, the group showed neuroprotection from Aβ mediated neurotoxicity by Aβ untreated astrocytes but no protection by Aβ-treated astrocytes (Paradisi *et al.*, 2004), a pro-apoptotic effect of Aβ treated astrocytes on neurones (Malchiodi-Albedi *et al.*, 2001), and enhanced neuritic tree degradation in neurone-astrocyte mixed cultures treated with Aβ (Domenici *et al.*, 2002). However, as these studies were performed by the same group, the culture conditions were the same in all three experiments. The group used neurones and astrocytes that had matured in culture after dissociation from their embryonic source for three to four days which is a relatively short time of maturation for neuronal cells in culture (See chapter 3). The studies also did not address why astrocyte protection of neurones was impaired when astrocytes were in contact with Aβ.

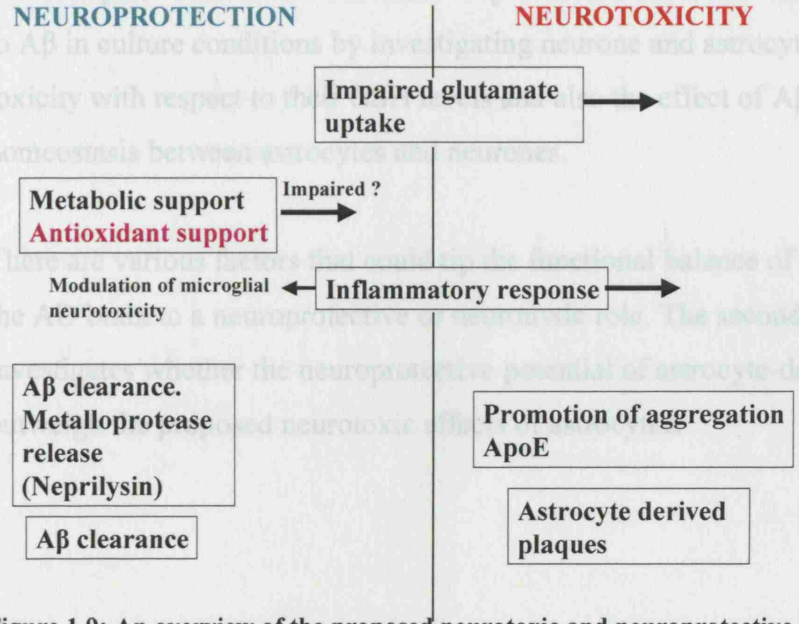

Figure 1.9: An overview of the proposed neurotoxic and neuroprotective activity of activated astrocytes. Columns show roles of astrocytes, which are potentially neuroprotective or neurotoxic. Normal support functions of astrocytes such as taking up glutamate, giving metabolic support or antioxidant support should be neuroprotective, but these may be impaired in AD. Astrocytes release metalloproteases and have been attributed a role in Aβ clearance which would be neuroprotective. However they have also been implicated in taking up Aβ and promoting aggregation leading to the generation of glial derived plaques. The neuroprotective or neurotoxic consequence of the astrocyte inflammatory response on neurones is not known.

1.4. Aim of thesis.

Current cell culture models of Aβ toxicity demonstrate that neurones are more vulnerable to Aβ toxicity than astrocytes. Neurones in these conditions are deprived of the astrocyte-derived support that they receive *in vivo*. Oxidative stress has been implicated in AD and is thought to underlie neurone death in cell culture models of Alzheimer's disease. Exogenously applied antioxidants can halt the pathway to oxidative stress and cell death in these models. Targeting antioxidant support to neurones in the Alzheimer's disease brain is a potential therapeutic target, however, it is not known how the astrocyte-neurone antioxidant GSH system responds to the presence of Aβ in the AD brain.

The first part of this thesis addresses why neurones are more vulnerable than astrocytes to Aβ in culture conditions by investigating neurone and astrocyte susceptibility to Aβ toxicity with respect to their GSH levels and also the effect of Aβ on the glutathione homeostasis between astrocytes and neurones.

There are various factors that could tip the functional balance of activated astrocytes in the AD brain to a neuroprotective or neurotoxic role. The second part of this thesis investigates whether the neuroprotective potential of astrocyte-derived glutathione can outweigh the proposed neurotoxic effects of astrocytes.

Chapter 2: Materials and methods

2 Materials and methods

2.1 Materials

Cell culture

Earle's balanced salt solution (EBSS), Hanks buffered salt solution (HBSS), antibiotic-antimyotic solution (10,000 units/ml penicillin 10mg/ml streptomycin, 25μg/ml amphotericin B) (αM), L-Glutamine, bovine serum albumin (BSA) deoxyribonuclease type 1 (DNAse, EC 3.1.21.1; from bovine pancreas), trypsin (EC 3.4.21.4, from bovine pancreas), trypsin/EDTA (5g porcine trypsin and 2g EDTA/L), cytosine arabinoside (AraC), trypan blue, poly-L-ornithine (PLO, molecular mass 30,000 – 70,000 g/mol), poly-D-lysine (P/L, molecular mass 300,000 g/mol), and monosodium glutamate were purchased from Sigma-Alrich Chemical Co. (poole UK). Coverslips were purchased from VWR (Poole UK). B-27 supplement (with and without antioxidants), Neurobasal medium (NB) (with and without phenol red), minimal essential medium (MEM, L-valine based), goat serum, horse serum and foetal bovine serum (FBS) were purchased from Gibco BRL (Renfrewshire, UK) flasks and 6 well plates for astrocytes were purchased from Nagle Nunc International (Naperville, IL, USA). Six well plates for neurone use were purchased from Costar (Corning Costar, High Wycombe, UK). Beads were purchased from The Bead shop (London, UK).

Immunocytochemistry and fluorescent microscopy

Propidium iodide was purchased from Sigma-Aldrich, Hoechst 33342 was from Molecular Probes Europe BV (Leiden, The Netherlands). Mouse anti beta III tubulin antibody and donkey anti-mouse fluorescein isothiocyanate (FITC) conjugated antibody were purchased from Abcam (Cambridge, UK). Rabbit anti GFAP antibody and Cy5 conjugated goat anti rabbit antibody were purchased from Chemicon (Hampshire, UK). Mouse anti CD11b antibody was purchased from Serotec (Oxford, UK). Citifluor was purchased from Citifluor Ltd (London, UK).

HPLC

Techsphere octodecasilyl 5μM HPLC columns and guard columns were from HPLC technologies (Macclesfield, UK). Chromacol HPLC vials and caps were purchased from VWR international. High performance liquid chromatography grade orthophosphoric

acid was purchased from Fisher Scientific (Loughbrough, UK). Glutathione, both oxidised and reduced forms, were purchased from Sigma-Aldrich.

Miscellaneous

Diethylammonium (Z)-1-(N, N-diethylamino) diazen-1-ium-1, 2-diolate (DEA NONO ate) was purchased from Alexis Biochemicals (Nottingham, UK), Aβ25-35 and Aβ35-25 peptides were from Bachem (Basel, Switzerland), 2, 7, Dichlorofluorescin diacetate, β nicotinamide adenine dinucleotide (β NADPH), Nicotinamide adenine dinucleotide (NADH), sodium pyruvate, γ-glutamyl cysteine (γ GluCys), Cysteinyl Glycine (CysGly), Glutathione ethyl ester (GSHEE), Acivicin and L-Buthionine sulfoximine (L-BSO) were purchased from Sigma Aldrich.

Solutions and Media

Name	**Base**	**Supplements**
Neurone medium	Neurobasal (NB) + Phenol red (PR)	2mM Glutamine (Gln) 2% B27 with antioxidants (+AO)
Astrocyte medium	Minimal essential medium (MEM) + PR	2mM Gln, 10% Foetal bovine serum (FBS)
Treatment medium	NB - PR	2mM Gln, 2% B27 - AO
Astrocyte conditioned medium	NB + PR	2mM Gln, 2% B27 + AO, incubated with confluent astrocytes for 24 hours.
Dissection solutions		
Astrocyte solution A	Earle's buffered saline solution (EBSS) +PR	3mg/ml Bovine serum albumin (BSA), 20μg/ml DNAse
Astrocyte solution B	EBSS + PR	3mg/ml BSA, 0.25 mg/ml trypsin, 0.1mg/ml DNAse
Neurone solution A	NB + PR	3mg/ml BSA, 24μg/ml DNAse.
Neurone solution B	NB + PR	3.25 mg/ml BSA, 24μg/ml DNAse, 0.25mg/ml trypsin
Coating solution	NB + PR	5% FBS, 5% foetal horse serum, 2mM Gln, 62.5μM Glutamate (Glu), 2% B27 +AO
Seeding solution	NB + PR	2% B27 + AO, 2mM Gln, 2.5mM Glu.

Table 2.1.

2.2 Tissue culture

2.2.1 Animals

Sprague Dawley rats were procured from colonies maintained at the University College London Biological Services unit. The animals were used in accordance with Home Office guidelines.

2.2.2 Cortical astrocyte culture from neonatal rat brain.

2.2.2.1. Preparation of cortical astrocyte suspensions from postnatal day 1 rat brains

Postnatal day 1 rats were sacrificed by cervical dislocation followed by decapitation. The top section of the skull was cut away and the cerebellum removed and discarded. The cortices and midbrains were placed in Hank's Buffered Saline solution (HBSS) on ice. Under a dissecting microscope inside a hood, the hemispheres were separated and the midbrain removed. The hippocampi were cut away from the cortex and also discarded. The meninges were removed from the brain hemispheres (see Figure 2.1). The cortices were placed in 10 ml **Astrocyte Solution A** (Earle's balanced salt solution (EBSS) containing 20μg/ml DNAse and 3mg/ml BSA) and chopped finely using scissors, then triturated with a 1 ml Gilson pipette. The suspension was centrifuged at 2000 rpm for 5 minutes at 4°C (Universal 32R (Hettich Zentrifugen)).

The pellet was resuspended in 3ml **Astrocyte Solution B** (EBSS containing 3mg/ml BSA, 0.25mg/ml trypsin and 0.1mg/ml DNase), transferred to a 90mm Petri dish with 17ml solution B, and triturated briefly before incubating at 37°C for 15 minutes. The trypsinisation was stopped by the addition of 1ml, foetal bovine serum (FBS) at 4°C. The suspension was centrifuged at 2000rpm for 5 minutes at 4°C. The pellet was resuspended in 10 ml **Astrocyte solution A**. The cell suspension was allowed to settle for 2 minutes to allow large debris and groups of cells to settle to the bottom and for single cells to remain in suspension. The supernatant was removed and kept. This

process was repeated three times and the supernatants were pooled and centrifuged at 2000 rpm for 5 minutes at 4˚C.

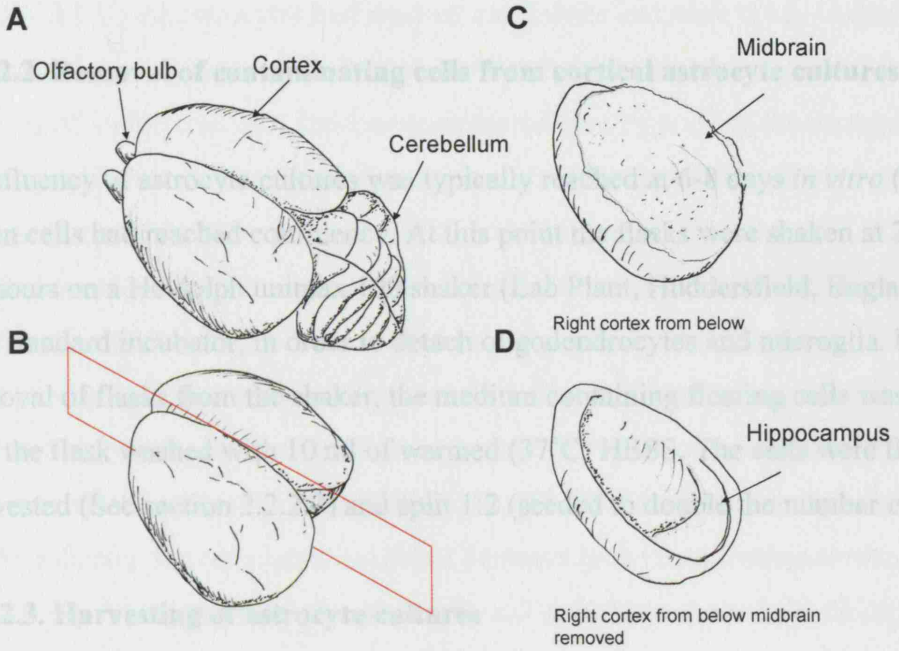

Figure 2.1: Isolation of cortex from rat brain. The whole rat brain was removed from the skull (A), the cerebellum and olfactory bulbs were removed and the cortical hemispheres split in two (B). Each cortical hemisphere was inverted and the midbrain removed (C), revealing the hippocampus (D). The hippocampus was cut away. The cortex was inverted again and the meninges peeled away.

After centrifugation, the supernatant was discarded and the pellet resuspended in **astrocyte medium** (Minimal Essential Medium (MEM) containing 10% FBS and 2mM glutamine). The suspension was filtered through a nylon mesh of 100µm pore size. The cell suspensions were plated onto 80cm^2 tissue culture flasks, one flask per starting cortex. The flasks were incubated at 37°C in an atmosphere 5% CO_2/95% air, with a humidity of >90%. Within 24 hours of plating the medium was replaced and subsequently changed every 3 days.

2.2.2.2. Removal of contaminating cells from cortical astrocyte cultures

Confluency of astrocyte cultures was typically reached at 6-8 days *in vitro* (DIV6-8) when cells had reached confluency. At this point the flasks were shaken at 200 rpm for 18 hours on a Heidolph unimax 100 shaker (Lab Plant, Huddersfield, England) housed in a standard incubator, in order to detach oligodendrocytes and microglia. Upon removal of flasks from the shaker, the medium containing floating cells was removed and the flask washed with 10 ml of warmed (37°C) HBSS. The cells were then harvested (See section 2.2.2.3) and split 1:2 (seeded to double the number of flasks).

2.2.2.3. Harvesting of astrocyte cultures

Medium was removed from the flasks and cells were washed with 10 ml HBSS at 37°C. The cells were incubated for 5 minutes at 37°C with 10ml of 1% trypsin ethylene diamine tetra acetic acid (trypsin/EDTA) diluted 1:1 with HBSS. The trypsinisation reaction was stopped by the addition of 1ml cold FBS. The cell suspensions were transferred to centrifuge tubes, and the flasks washed with 5ml HBSS, this was added to the centrifuge tubes and the cell suspensions were centrifuged at 2000 rpm for 5 minutes at 4°C. Cells were resuspended in 1ml astrocyte media. The cell suspensions were then diluted in MEM to split in a 1:2 ratio between flasks.

2.2.2.4. Coating of surfaces for astrocyte seeding

Plastic 6 well plates were coated with 1ml of 0.01% poly-L-ornithine (PLO) for 30 minutes at 37°C. Glass coverslips were coated with 300µl of 0.1mg/ml poly-D-lysine (PDL) for 1 hour at room temperature. The PLO or PDL was aspirated and the wells were washed 3 times with sterile H_2O. Plates were then allowed to dry in the hood and were placed in front of a UV lamp for 20 minutes to ensure sterility.

2.2.2.5. Seeding of astrocytes for experimentation

At DIV 11-12 the astrocytes had reached confluence and were ready to seed onto 6 well plates for experimentation. Cells were harvested as described in section 2.2.2.3. The number of viable cells in a 7ml suspension produced by pooling the resuspended pellets from centrifugation were counted using the vital dye trypan blue. A 10µl aliquot of cell suspension was mixed with 30 µl HBSS, and 40µl trypan blue (0.4mM). 10 µl of this mixture was loaded onto a haemocytomer and viable single cells (excluding trypan blue) were counted from 4 units of the haemocytometer, using a phase contrast inverted microscope, and the average cell count taken. The cell density was subsequently adjusted to 75,000 cells/2ml media and 2 ml of this suspension was added to each well of 6 well plate coated with Poly-L-Ornithine (PLO) (0.01%) see section 2.2.2.5. At this seeding density the cells were confluent 24 hours later when treatment was commenced. At seeding densities greater than this, after a 2-day treatment and conditioning period there was a slight increase in the number of floating dead astrocytes. For 2-day astrocyte conditioned medium protocols (see chapter 5), astrocytes were seeded at 50,000 cell/ well.

2.2.3 Primary neurone cultures from foetal rat brain.

2.2.3.1 Preparation of neurone suspension from foetal rat brains

Pregnant Sprague Dawley rats were culled by cervical dislocation at 17 days of gestation. Foetuses were carefully removed and placed in a Petri dish containing EBSS. Cutting the skull along each side and lifting it with forceps exposed the brain. The early cerebella were removed; the cortex was removed from the mid brain and rolled on sterile Whatman filter paper to remove the meninges. The cortices were transferred to a Petri dish containing Neurobasal media containing 3mg/ml BSA and 24μg/ml DNAse (**Neurone solution A**) and the cortices were tritrated 2 times using a 10 ml pipette and transferred to a new 50ml centrifuge tube. The Petri dish was washed with 10 ml **Neurone solution A**. This was added to the tube and the suspension was allowed 2 minutes to settle. At this point the supernatant was carefully removed and 10 ml of **Neurone solution B** (Neurobasal media containing 3.25 mg/ml BSA, 24μg/ml DNAse and 0.25mg/ml trypsin) was added. The cell suspension was incubated at 37 °C for 15 minutes, mixing midway through incubation. The addition of 1 ml of cold FBS stopped the trypsin reaction. The suspension was allowed to settle for 2 minutes. In order to aid cell dissociation and to remove any debris, cells were resuspended in 12 ml **Neurone solution A**, resuspended 5 times with a 1ml Gilson pipette, then 5 times with a 0.2 ml Gilson pipette. After 4 minutes any larger groups of cells had settled to the bottom of the tube, but the supernatant contained single cells. The supernatant was collected and transferred to a fresh Falcon tube. The trituration process was repeated 2 times and the supernatants pooled.

The pooled suspension was centrifuged at 2000 rpm for 5 minutes at 4°C. The supernatant was discarded and the pellet carefully resuspended in 1 ml **Seeding solution** (Neurobasal media containing 2% B27 supplement (containing antioxidants (+AO)), 2mM glutamine and 2.5 mM glutamate). The resuspended cells were passed through a mesh of 100μm pore size. Neurones were seeded at a density of 1 million cells/ml media onto coverslips coated with 0.01% (w/v) PDL (see section 2.2.2.4). 100μl of cell suspension was added to a 100μl **coating solution**, which was incubated on the coverslip for at least 1 hour prior to seeding. The **coating solution** was nutrient

rich (5% foetal horse serum, 5% foetal bovine solution, 2mM glutamine, 62.5 μM glutamate, 2% B27 supplement). 2 hours after seeding, when healthy neurones had adhered to the coverslips, the neurones were topped up with 2 ml **Seeding solution**. Neurones seeded on PLO coated wells (see section 2.2.2.5.) were seeded 1 million cells per well in **seeding solution**.

2.2.3.2. Preparation and coating of glass coverslips for neurone seeding

For fluorescence imaging neurones were required to be seeded on glass coverslips. In order for the neurones to adhere, the coverslips needed to be coated with a basic amino acid polymer, to provide a charged surface for the neurones to anchor onto, and to provide a surface suitable for neurite outgrowth. This was necessary, as the neurones had been sheared of axons and dendrites during preparation and dissociation procedures. Neurones were particularly difficult to grow on glass. Coverslips were coated with 300μl of 0.1mg/ml PDL for 1 hour at room temperature. 3 brands of coverslip, Deckglasser, Chance Propper and Marienfield were used. Differences in the manufacture of these brands led to different composition of residues on the surface of the coverslips, although Marienfield coverslips could be coated without treatment, Deckglasser and Chance Propper required washing for 24 hours in 30% nitric acid to remove any residues. They were then washed three times in water and dried using acetone. All coverslips were baked for two hours at 200°C to sterilise before coating. Although a basic step in the neurone preparation, it was vital to ensure that the coverslips had been coated sufficiently, before the neurone preparation was commenced. After washing, the coverslips were tested by applying a drop of water. If the coverslip was sufficiently clean for coating the surface tension would be low and the water droplet would spread; if it required further washing then the water would form a high droplet in the centre of the coverslip. PDL was always applied at room temperature after being thawed at 37°C from frozen aliquots, as the application of warm PDL resulted in crystal formation on the surface of the coverslips. PDL was re-used but was not used after 4 freeze-thaw cycles.

After coating for 1 hour the coverslips were washed three times with sterile water, air dried in a sterile class II hood and placed in front of a UV lamp for 20 minutes to sterilise.

2.2.3.3. Preparation of tissue culture plates for neurone seeding

Polystyrene tissue culture plates for neurones also required coating. In contrast to glass, where neurones grew better on PDL, on plastic surfaces neurones preferred PLO and plates of a particular brand, CoStar. Plates were coated with 1 ml 0.01% PLO for 30 minutes at 37°C. The PLO was removed and wells washed 3 times with sterile water. The plates were then placed in front of a UV lamp for 20 minutes to sterilise in a sterile class II hood.

2.2.3.4. Care of neurone cultures

Highly pure neurone cultures require supplementation with **astrocyte conditioned medium** on Day *in Vitro* (DIV) 3 and DIV 7 to maintain to DIV9 for experimentation. On DIV 3 half the medium in the wells was removed, and replaced with 1 ml of **astrocyte-conditioned medium** containing cytosine arabinofuranoside (AraC), with a final concentration of 10μM. AraC was added to prevent glial cell proliferation. The medium was half changed again on DIV 7 with **astrocyte conditioned medium**, which was generated by incubating confluent flasks of DIV11 to DIV14 astrocytes with 12ml NB containing 2% B27 and 2mM glutamine for 24 hours. The medium was removed and centrifuged at 2000 rpm for 5 mins at 4˚C to remove cell debris. Each flask was used to condition 3 x 12 ml media. **Astrocyte conditioned medium** was stored at -80˚C and used within 2 weeks.

2.2.4. Harvesting of astrocytes and neurones after experiments

Both the astrocytes and neurones seeded onto 6 well plates for experiments were harvested in the same way. The medium was removed from the well and the cells washed with 1 ml warm HBSS. The HBSS was removed and replaced with 700μls trypsin/EDTA, after incubation the reaction was stopped with 70μl FBS and the wells

were scraped gently with a cell scraper to aid total removal of the astrocytes or neurones. The cells were transferred to a 1.5 ml Eppendorf tube; the wells were washed with a further 700µl HBSS, which was also transferred to the tube. The cells were centrifuged at 17,000 x g for 5 minutes at 4°C. The cell pellet was resuspended thoroughly in 200µl HBSS and snap frozen in liquid nitrogen. Samples were stored at -70°C.

2.3 Immunocytochemistry

2.3.1. Antibodies

To check the purity from contaminating cell types the cultures were stained for specific markers of astrocytes, neurones and microglia. Primary antibodies raised against rabbit Glial Fibrillary Acid Protein (GFAP) ((a cytoskeletal protein specific to astrocytes), mouse beta III Tubulin subunit (a cytoskeletal protein subunit specific to neurones) and mouse CD11b (an integrin specific to microglia) were used. Two different fluorescent secondary antibodies were used: anti-mouse Fluorescein-isothiocyanate (FITC)-conjugated, raised in donkey, and anti-rabbit CY5-conjugated raised in goat. All slides were also stained with a fluorescent nuclear stain 4'6-Diamidino-2-phenylindole (DAPI).

	Primary antibody	Secondary antibody
Astrocyte	GFAP (1:1000)	CY5 (1:500)
Neurone	Beta tubulin III (1:500)	FITC (1:500)
Microglia	Cd11b (1:1000)	FITC (1:500)

Table 2.2: The primary and secondary antibodies used to stain for astrocytes, neurones and microglia. The dilution factor of the antibody is given in brackets.

2.3.2 Application of antibodies

Cells seeded on coverslips were taken on DIV 14 for astrocytes and DIV10 for neurones and washed with Tris buffered saline (40mM TRIS HCL, 10mM TRIS base, 0.15M NaCl, pH 7.6-7.8 (TBS)). The cells were then fixed by adding 2ml ice-cold methanol to each well containing a coverslip and put on ice for 10 minutes. The methanol was removed and the cells were rinsed twice with TBS for 5 minutes. 2ml of sodium deoxycholate was then added for 10 minutes at room temperature. This was removed and cells were rinsed with 0.025%Triton X-100 in TBS (TBS/Triton) to permeabilise membranes. A blocking solution of 2ml TBS containing 10% normal serum (the serum

in which the secondary antibody was raised) and 1% bovine serum albumin (BSA) was added to the cells for 2 hours at room temperature. The blocking solution was completely removed and 2ml of the primary antibody solution were added and incubated at 4°C overnight. The coverslips were then washed twice for 5 minutes with TBS/Triton. 2ml of the secondary antibody were added for 1 hour at room temperature. The coverslips were then rinsed twice with TBS for 5 minutes. 2ml of DAPI (0.1μg/ml) were then added for 10 minutes at room temperature in the dark. The cells were rinsed with TBS for 5 minutes. To mount the cells on slides, 10μl of the mounting medium citifluor were placed on the slide; coverslips were removed from the TBS and inverted onto the citifluor. The coverslips were held in position using colourless nail varnish (Mavala, Switzerland).

In order to check for non-specific binding the following blanks were run in each experiment.

Condition	Primary antibody	Secondary antibody
No antibodies	-	-
No primary antibody	-	FITC/ CY5
Neurone and astrocyte primary no secondary antibody	Tub, GFAP	-
Microglia primary no secondary antibody	Cd11b	-

Table 2.3: Control blanks used in immunocytochemical staining.

2.3.3. Imaging immunocytochemical stains

Immunocytochemical stains were imaged using fluorescence confocal microscopy, (see section 2.6.2.) using a Zeiss 510 laser scanning confocal microscope using a 40x oil immersion-quartz objective (NA 1.3)

DAPI was excited at the 405nm using a diode laser. FITC was excited by 488nm line of an argon laser. The 633nm helium neon laser excited CY5. A photmultiplier tube detected the emitted light. The emission of DAPI (blue light), FITC (green light) and Cy5 (red light) were collected on three separate channels using appropriate filters and dichroic mirrors.

2.3.4. Quantifying immunocytochemical stain and assessing purity of cultures

10 fields of view were randomly selected from each duplicate slide. Images were generated and analysed using the Zeiss LSM image browser. The number of DAPI positive nuclei was taken as the total number of cells. Positive cells were cells that had the appropriate fluorescent staining around a nucleus. Purity of cell populations was determined as total number of positive cells as a percentage of total number of nuclei present.

2.4 Experimental treatment of cells

2.4.1. Determination of aggregation properties of Aβ25-35

2.4.1.1. Principle.

The aggregation properties of Aβ25-35 were assessed using the fluorescent dye thioflavin T. Thioflavin dye is excited at 355nm and shows peak emission at 445nm. Thioflavin T associates rapidly with aggregated β sheets of synthetic amyloid peptides (LeVine 1993), which causes a shift to a new excitation maximum of 450nm and an enhanced emission at 482nm. The change is dependent on the Aβ25-35 aggregated state, as monomeric or dimeric peptides do not react (LeVine, 1993) (see Figure 2.2).

2.4.1.2. Protocol

A solution of 5μM thioflavin T was made in 50mM potassium phosphate buffer pH6.0. Using a Perkin Elmer luminescence spectrophotometer LS50B, and FlwinLab software, with the excitation slit set at 5.0nm, the emission slit set at 5.0 nm and the integration time set at 6.0 seconds, the wavelengths of maximal excitation and emission for the thioflavin free dye were calibrated. To calibrate, the expected peak excitation wavelength was set and an emission spectrum generated. From this spectrum, the wavelength at which the dye gave peak emission was set, and the excitation spectrum generated. Again, from this spectrum, the wavelength giving peak excitation could be determined. This process was repeated to fine tune the optimal excitation and emission wavelengths. For the free dye maximal excitation was at 355nm, maximal emmision was at 445nm.

From a 5mM stock of Aβ25-35, dissolved in H_2O, a 50μM solution of Aβ25-35 was made in thioflavin T solution. As described above the new peak excitation and emission wavelengths were generated. The new maximal excitation wavelength was 450nm and the maximal emission peak was 482 nm.

The excitation and emission spectra of 50μM Aβ25-35 and 50μM Aβ35-25 diluted from 5mM stock diluted in H_2O were compared. The spectrum of 50μM Aβ25-35 from a

5mM stock of Aβ25-35 that had been dissolved in dimethyl sulfoxide (DMSO) was also compared (see figure 2.2)

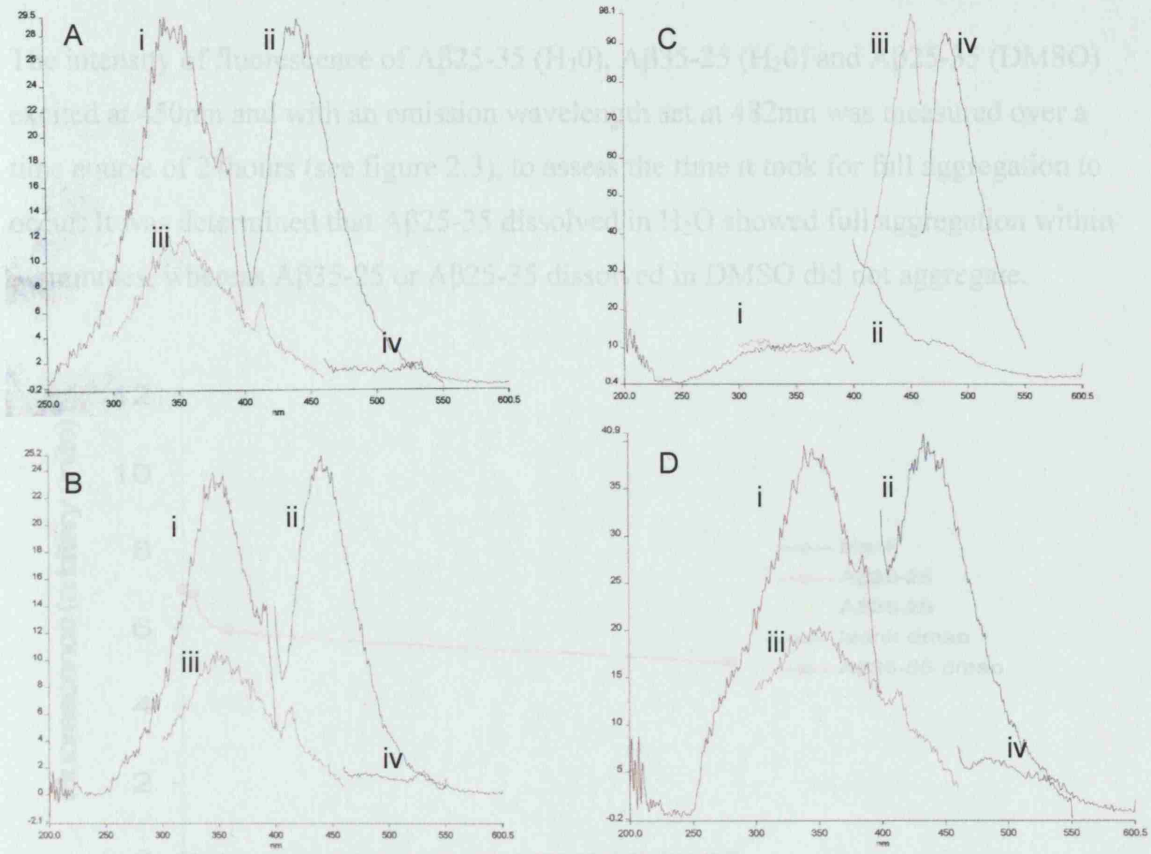

i) Excitation spectrum. Emission set at 450nm.

ii) Emission spectrum. Excitation set at 350 nm.

iii) Excitation spectrum. Emission set at 480nm.

iv) Emission spectrum. Excitation set at 450nm.

Figure 2.2: Excitation and emission spectra of Thioflavin T dye. A) Blank, B) Aβ35-25 dissolved in H_2O, C) Aβ25-35 dissolved in H_2O, D) Aβ25-35 dissolved in DMSO. Only Aβ25-35 dissolved in H_2O caused a shift in the excitation and emission spectrum to 450 nm (excitation) and 480 nm (emission).

The intensity of fluorescence of Aβ25-35 (H_20), Aβ35-25 (H_20) and Aβ25-35 (DMSO) excited at 450nm and with an emission wavelength set at 482nm was measured over a time course of 24hours (see figure 2.3), to assess the time it took for full aggregation to occur. It was determined that Aβ25-35 dissolved in H_2O showed full aggregation within 30 minutes, whereas Aβ35-25 or Aβ25-35 dissolved in DMSO did not aggregate.

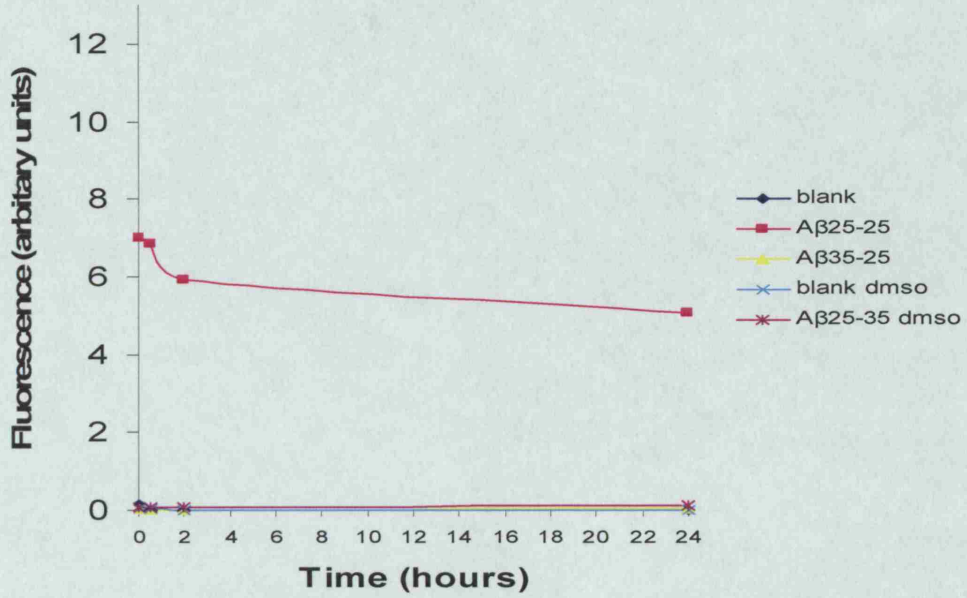

Figure 2.3. Aggregation of Aβ25-35. The fluorescence intensity of solutions of 50μM Aβ25-35 and Aβ35-25 dissolved in H_2O, Aβ25-35 dissolved in DMSO and a H_2O and DMSO blank were measured over a 24-hour time course with the excitation wavelength set at 450nm and the emission wavelength set at 482nm. Only Aβ25-35 dissolved in water aggregated over this period.

It was a matter of concern that as Aβ25-35 forms aggregates, which may be heterogeneous in size, the concentration of Aβ25-35 in aliquots made from a stock solution may vary between aliquots. To assess for the linearity of the assay, and to determine that it would be possible to generate diluted aliquots from the Aβ25-35 stock that would contain the same concentration of peptide, the fluorescence intensity of serial dilutions of Aβ25-35, at excitation 450nm and emission 482nm, was measured. Serial dilutions of Aβ25-35 were made from 5mM stock peptide solution using thioflavin T solution, from 50μM to 12.5nM (see figure 2.4). The intensity of fluorescence showed a linear relationship up to the concentration of peptide diluted in this way.

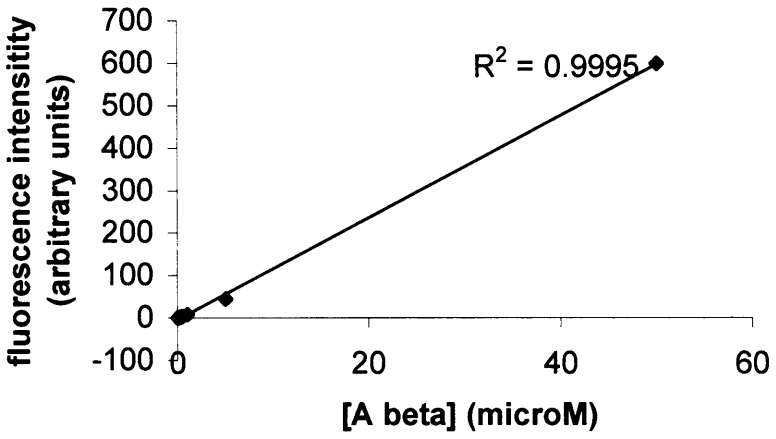

Figure 2.4: Fluorescence of Thioflavin T in relation to Aβ25-35 concentration. Serial dilutions of Aβ25-35 in thioflavin T solution were made from 50μM to 12.5 nM.

2.4.2. Preparation and storage of peptides

5mM stocks of Aβ25-35 and Aβ35-25 were made up in ultra pure water purified to an electrochemical resistance of 18.2 Mohms.cm^{-1} (Purelab Maxima, Elga, Derbyshire). These were vortexed and divided into 20μl aliquots and frozen at –70°C within 10 minutes of preparation.

2.4.3. Treatment media and treatment of cells with Aβ25-35 and Aβ35-25

All experiments on astrocytes and neurones were carried out in **Treatment medium** (Neurobasal medium without phenol red, supplemented with 2% B27 supplement (without antioxidants (-AO)) and 2 mm glutamine. This medium and supplement are designed for neurone growth (Brewer *et al.,1996*). Before treatment astrocytes were always washed 2 times with HBSS to remove cell debris and, importantly, traces of FBS. Neurones were not washed to limit stress on cells. Aβ25-35 and Aβ35-25 peptide solutions were thawed at room temperature and left at room temperature for 15 minutes. The peptide solutions were then vortexed to mix, diluted 1:100 in the media and incubated for 15 minutes at 37°C to ensure full aggregation of Aβ25-35. 2 ml of treatment medium were added to each well of neurones or astrocytes.

2.4.4. Supplementation of neurone medium with glutathione precursors

In this study, neurones were supplemented with cysteinylglycine (CysGly), γ-glutamyl cysteine (γ-glucys) and GSH ethyl ester (GSHee). Both di-peptides and GSHee were prepared in distilled H_2O, and then filtered through 0.2μm sterile filters. Stocks of cysgly (100μM), γ-glucys (100mM), and GSHee (2.5mM) were stored at -30°C.

2.4.5. Inhibition of astrocyte γ-glutamyl transpeptidase with Acivicin

γ-Glutamyl transpeptidase cleaves GSH to produce CysGly that can be taken up by neurones for GSH synthesis. Acivicin was made up to 50mM stock dissolved in 1M hydrochloric acid. This was then sterile filtered and stored at -30˚C. To find the optimal concentration of acivicin needed to inhibit γ-glutamyl transpeptidase in the astrocyte cultures, wells of astrocytes were treated with 5-100μM acivicin in treatment media for 24hours, compared to a control (treatment medium + HCl). The spent medium was collected from the astrocytes and the GSH concentration measured using HPLC (see section 2.7.3). Acivicin was used at 5μM concentrations to treat astrocytes.

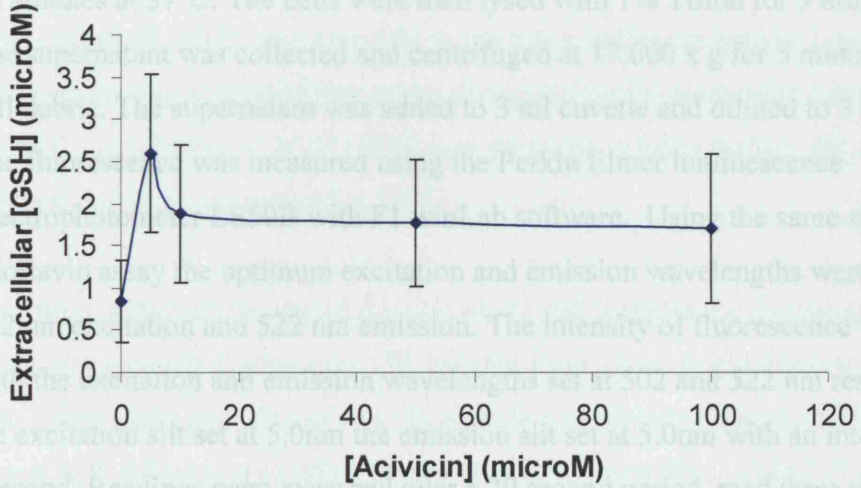

Figure 2.5: Inhibition of astrocyte γ-glutamyl transpeptidase with acivicin caused an increase in GSH in the extracellular medium. Astrocytes were treated for 24 hours with concentrations of acivicin in the range 5-100μM or a control containing vehicle (HCl). n=3 Error bars = SEM.

2.5. Measurement of reactive oxygen species (ROS) using the fluorescent probe 2′, 7′-dichlorofluorescin diacetate.

2.5.1 Principle

2′, 7′-Dichlorofluorescin diacetate is non-fluorescent. When dissolved in DMSO it is permeable to cells. It undergoes deacetylation by intracellular esterases. On exposure to oxidising species it is oxidised to 2′, 7′-dichlorofluorescein that is a fluorescent compound with optimal excitation at 502nm and optimal emission at 522nm.

2.5.2 Protocol

ROS production in neuronal and astrocyte cultures was determined according to Alvarez *et al.,* 2003, with modifications. A 2mM stock of 2′, 7′-Dichlorofluorescin diacetate (DCF) in DMSO was prepared in the dark under N_2. The stock was immediately aliquotted and stored at -30°C. To measure ROS production from cells the medium was removed from neurones and astrocytes that had been treated with Aβ25-35 at the same time. The cells were washed with 1ml HBSS. 1ml of HBSS containing 10μM DCF was added to the cells in the dark. The cells were incubated with DCF for 10 minutes at 37°C. The cells were then lysed with 1% Triton for 5 minutes at 37°C. The supernatant was collected and centrifuged at 17,000 x g for 5 minutes to remove cell debris. The supernatant was added to 3 ml cuvette and diluted to 3 ml using HBSS. The fluorescence was measured using the Perkin Elmer luminescence spectrophotometer LS50B with F1 winLab software. Using the same approach as in the thioflavin assay the optimum excitation and emission wavelengths were determined as 502 nm excitation and 522 nm emission. The intensity of fluorescence was measured with the excitation and emission wavelengths set at 502 and 522 nm respectively and the excitation slit set at 5.0nm the emission slit set at 5.0nm with an integration time of 1second. Readings were averaged over a 20 second period, read three times and the mean value taken.

2.6. Measurement of glutathione reductase activity

2.6.1. Principle

Glutathione reductase (GR) reduces GSSG to GSH in the presence of NADPH.

$$GSSG + NADPH + H^{+} \xrightarrow{GR} 2\,GSH + NADP^{+} \qquad (2.1)$$

In the presence of GSSG and GR the oxidation of NADPH to NADP was measured spectrophotometrically, by measuring the decrease in absorbance of NADPH at 340 nm as it was oxidised. The activity of GR was measured by the rate of oxidation of NADPH.

2.6.2. Protocol

The protocol of this assay was based on the protocol from the Sigma glutathione reductase assay kit. The assay was linear from 0.003 to 0.012 units/ml GR. One unit (U) of GR will cause the oxidation of 1.0μM of NADPH per minute at 25°C at pH 7.5. A 100 U/ml stock of GR was prepared in the assay buffer containing 1mg/ml BSA. The assay buffer was a 100mM potassium phosphate buffer containing 1mM EDTA, pH 7.5 @ 25°C. A solution of 2mM GSSG was prepared in assay buffer. All assay components were maintained at 25°C.

In order to establish the useful dilution of the cell samples for this assay, a standard curve was generated using pure GR isolated from yeast. Serial dilutions of the 100U/ml stock were made and 10μl of this GR sample was added to 500μl of GSSG solution, mixed with 440μl assay buffer. To initiate the reaction 50μl of NADPH was added and the change in absorbance at 340 nm over a 2 minute period was measured relative to a blank (containing all of the components except sample).

The activity of the enzyme was calculated by the following formula where one Unit (U) caused oxidation of 1μM of NADPH per minute.

$$\text{Units/ml} = \frac{(\Delta A_{sample} - \Delta A \text{ blank}) \times (\text{dilution factor})}{\varepsilon^{mM} \times (\text{volume of sample in ml})}$$

For NADPH $\varepsilon^{mM} = 6.22\ mM^{-1}cm^{-1}$.

ΔA = absorbance change per minute

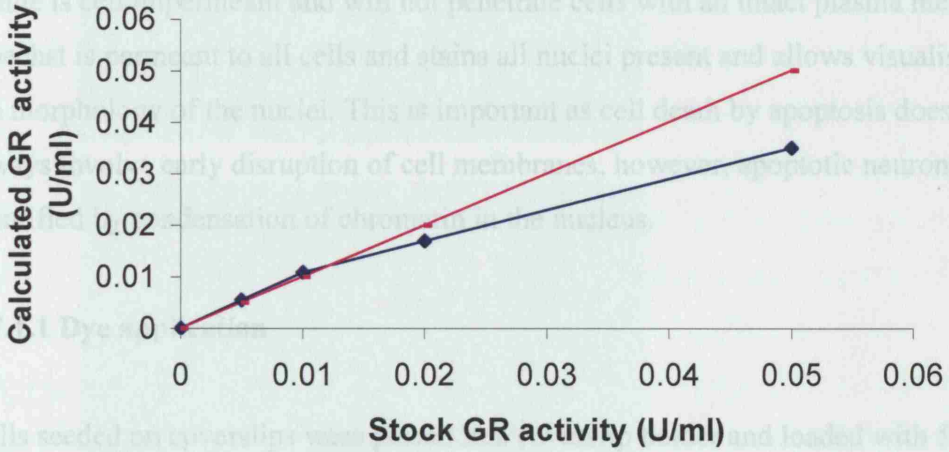

Figure 2.6: Standard curve of glutathione reductase (GR) Units/ml with increasing concentrations of GR. The curve is linear at concentrations < 0.012 U/ml over a 2-minute measurement period. Pink line shows X=Y to illustrate region of the curve that is linear.

The standard curve was demonstrated to be linear at concentrations < 0.012 U/ml over a 2-minute period (Figure 2.6). The dilution factor by which to dilute astrocyte and neurone samples to give GR activity within this range was determined. GR activity of astrocyte and neurone samples was detectable if 0.05-0.1 mgs of cellular protein were added to the reaction medium. For measurement of GR activity, astrocyte and neurone pellets harvested from a 30mm diameter well were resuspended in 150μl HBSS. The GR activity in 100μl of this cell suspension could be measured using this assay. The GR activity in cell samples was related to the cellular protein content to express the GR activity as nmol of NADPH oxidised per minute per mg of protein.

2.7 Assessment of cell viability

2.7.1. Fluorescent nuclear dye exclusion assay

Fluorescence microscopy (see section 2.6.2) was used to quantify neurone viability, by assessing nuclear morphology and cell membrane integrity. Two fluorescent dyes, which target nuclear DNA, propidium iodide and Hoechst 33342, were used. Propidium iodide is cell impermeant and will not penetrate cells with an intact plasma membrane. Hoechst is permeant to all cells and stains all nuclei present and allows visualisation of the morphology of the nuclei. This is important as cell death by apoptosis does not always involve early disruption of cell membranes, however, apoptotic neurones can be identified by condensation of chromatin in the nucleus.

2.7.1.1 Dye application

Cells seeded on coverslips were placed in a coverslip holder and loaded with 500µl 10µM propidium iodide, 4.5µM Hoechst 33342 (stock in DMSO) in HBSS at 37°C for 10 minutes in the dark.

2.7.1.2. Dye visualisation

Nuclei were observed using fluorescent microscopy (see section 2.6.2). The Hoechst dye was excited at 360nm and the emission measured at 460nm (green). The propidium iodide was excited at 530nm and measured at 615 nm (red).

2.7.1.3. Nuclear morphology classification

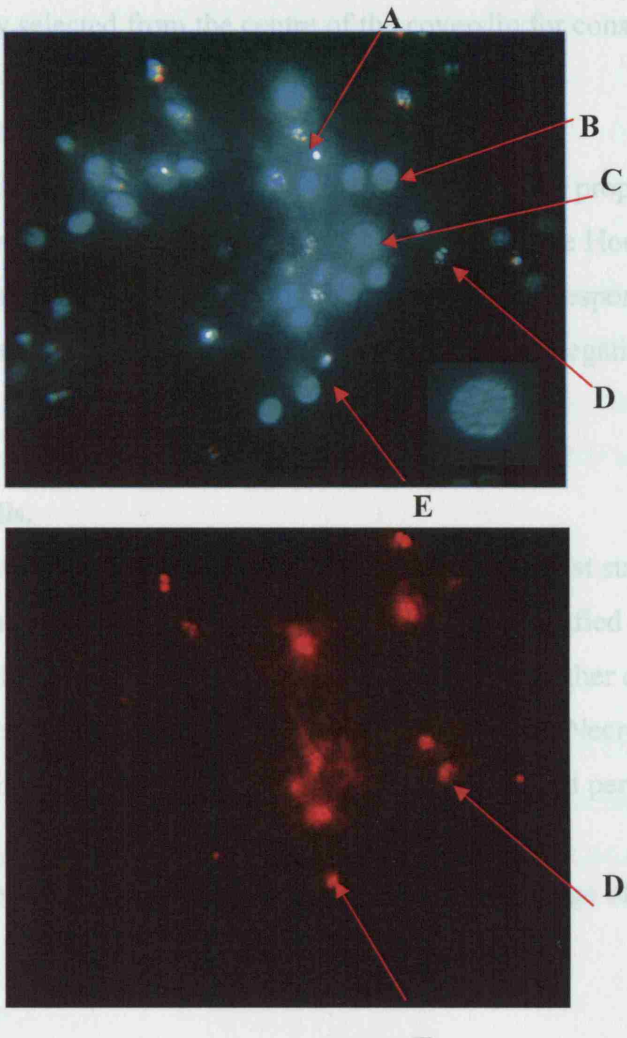

Hoechst	Propidium iodide	Nuclear condensation	Dead/alive	Cell
Yes	No	No	Alive	B
Yes	No	Early	Alive	C
Yes	No	Yes	Dead	A
Yes	Yes	Yes	Dead	E
Yes	Yes	Fragmented	Dead	D
Yes	Yes	No	Dead	-

Figure 2.7: Classification of Hoechst and propidium iodide stained control neurones. The top panel shows Hoechst stained cells with emission at 460nm, the bottom panel shows propidium iodide stained cells with emission at 615nm. The table shows classification of cells as dead or alive. Cells B + C are alive, cells A, D and E are dead. Insert shows cell like C at higher magnification.

The cells from 10 fields of view were counted from each duplicate slide. Fields were randomly selected from the centre of the coverslip for consistent density of cells.

Live cells.

These cells were positive for Hoechst but negative for propidium iodide. The staining of the cell was homogeneous see cell B. In some cells the Hoechst staining was not homogenous and had patches of brighter staining corresponding to early chromatin condensation (C), these cells were propidium iodide negative and were classified as living at the time of measurement

Dead cells.

Cells that were small with bright homogeneous Hoechst staining either like cell (A) or with a fragmented appearance like cell (D) were classified as late apoptotic. Some of these cells like (A) were propidium iodide negative, other cells like (D) and (E) were both Hoechst positive and propidium iodide positive. Necrotic cells showed no chromatin condensation and generally were larger, and permeable to propidium iodide.

Cell viability was expressed as live cells as a percentage of total number of nuclei present.

2.7.2. 3-(4,5-dimethylthiazol-2-yl)-2,5 diphenyltetrazolium bromide (MTT) assay

MTT is a redox dye. It is converted to a purple formazan by the redox activity of living cells. Intracellularly formed formazan crystals are exocytosed from the cells and appear as purple crystals on the cell surface. It is not known where in the cell the reduction reaction occurs. However, it is commonly used as an index as cellular redox capability (Shearman *et al.*, 1994, Liu *et al.*, 1997). A 1mg/ml solution of MTT was made in HBSS. Cells were washed and 1ml of this solution were added to the wells for 30 minutes at 37°C in the dark. The supernatant was carefully removed and the formazan crystals were dissolved in 1 ml of dimethyl sulphoxide (DMSO). Three 200µl aliquots of this formazan solution were taken from each well and read on a SpectraMax Plus spectrophotometric plate reader (Molecular Devices, Wokingham, UK) at 540nM. MTT

reduction, as measured by formazan absorbance, was expressed in treated cells as a percentage relative to control cells.

2.7.3 Lactate dehydrogenase (LDH) assay.

2.7.3.1. Principle

Membrane integrity was used as a means of assessing cell viability. Membrane integrity was measured by measuring lactate dehydrogenase (LDH) release (Vassault, 1983; Dringen *et al.,* 1990). Lactate dehydrogenase is a predominantly cytosolic enzyme which catalyses the reversible dehydrogenation of lactate to form pyruvate.

$$\text{Lactate} + NAD^+ \xrightleftharpoons{\text{LDH}} \text{Pyruvate} + NADH + H^+ \qquad \textbf{(2.2)}$$

LDH activity was measured in the extracellular medium and total LDH activity was measured after lysing the cells. LDH was measured spectrophotometrically, measuring the oxidation of NADH in the presence of pyruvate. LDH release was then expressed as a percentage of total cellular LDH activity.

2.7.3.2 Protocol

50µl of medium were removed from each well of neurones and astrocytes treated in a six well plate and placed on ice (extracellular LDH). 10µl of 10% Triton X-100 was then added to each well to solubilise the cell membranes allowing the total LDH inside the cell to be released. A 50µl sample was than collected from the well (total LDH). The 50µl aliquots were spun at 17,000 x g to remove cell debris

5µl of the extracellular or total sample was added to each well of a glass 96 well plate. This was diluted to 100µl with buffer (containing 80mM Tris/HCL, 200mM NaCl buffered at pH 7.2). To initiate the reaction 100µl of buffer containing 3.2mM pyruvate and 0.4mM NADH was added (final concentration of NADH: 0.2mM). The absorbance was read at 340nm immediately on a SpectraMax plus spectrophotometric plate reader.

The absorbance was read every 5 minutes for 30 minutes. During this period the absorbance of NADH had approximately halved. The decrease in absorbance at 340nm was due to oxidation of NADH in the process of reduction of pyruvate to lactate by LDH. The decrease in absorbance (Δ_{abs}) over 30 minutes was calculated for the extracellular LDH and total LDH aliquot for each treatment. The Δ_{abs} extracellular LDH was expressed as a percentage of the Δ_{abs} of the total LDH sample after the cells had been lysed.

2.8. Microscopy

2.8.1 Phase-contrast light microscopy

Cells were photographed using a Nikon coolpix950 camera mounted on a Nikon TMS phase contrast microscope using a 20x objective. The phase contrast microscope had a 10x magnification eyepiece. The camera was mounted on top of this eyepiece, giving a total magnification of 200x.

2.8.2 Fluorescence microscopy

Fluorescent molecules absorb photons from high-energy light; this increases the energy of the molecules to an excited state. The molecule returns to basal state emitting a photon with less energy (see figure 2.8). Fluorescence microscopes use dichroic mirrors; a dichroic mirror is a wavelength selective mirror that reflects light of a wavelength shorter than the cut-off and transmits light at higher wavelength (see figure 2.9).

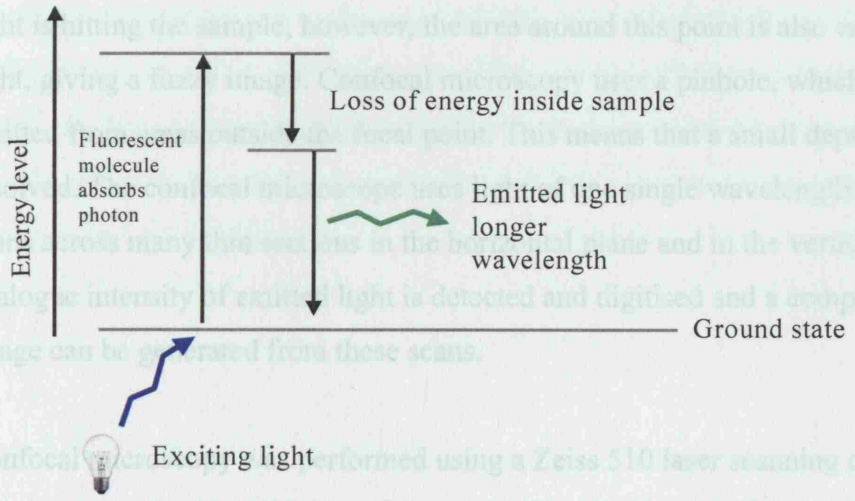

Figure 2.8 Principle of fluorescence.

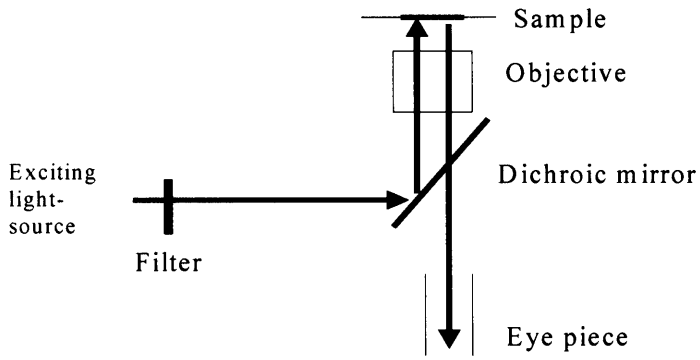

Figure 2.9: Principle of fluorescence microscopy.

Fluorescence microscopy was performed using a Leitz Fluovert FU inverted microscope (Leica, Wetzlar, Germany) with an XBO75w/2 light source. Cells were observed through a 10x magnification eyepiece using a 40x oil immersion objective.

2.8.3 Confocal microscopy

In fluorescence microscopy there is a focal point where the highest intensity of exciting light is hitting the sample, however, the area around this point is also excited and emits light, giving a fuzzy image. Confocal microscopy uses a pinhole, which blocks light emitted from areas outside the focal point. This means that a small depth of field can be resolved. The confocal microscope uses light of one single wavelength from a laser, and scans across many thin sections in the horizontal plane and in the vertical plane. The analogue intensity of emitted light is detected and digitised and a composite 2d or 3d image can be generated from these scans.

Confocal microscopy was performed using a Zeiss 510 laser scanning confocal microscope and a 40x oil immersion quartz objective lens. A photomultiplier tube detected the emitted light. Images were generated and analysed using the Zeiss LSM image browser.

2.9. Quantification of cellular protein

The protein content of freeze thawed cell suspensions were measured either using a modification of the method of Lowry, 1951 or by the method of Bradford, 1976.

2.9.1.1 Principle of Lowry assay

For measurement of protein concentrations by the Lowry method the Bio-Rad protein assay kit (Bio-Rad, Buckinghamshire, UK) was used. This kit consists of two reagents, A and B. Reagent A is an alkaline copper tartrate solution. Reagent B is a Folin-Ciocalteau reagent (consisting of sodium tungstate, molybdate and phosphate). Proteins in solution form a complex with Cu^{2+} in the alkaline copper tartrate solution. The protein complex reduces Cu^{2+} to Cu^{+}. Folins phenol reagent is reduced leading to an enhancement of the blue colour of this complex. The intensity of colour correlates to the protein concentration (Chou and Goldstein, 1958).

2.9.1.2. Protocol of Lowry assay.

A standard curve of bovine serum albumin (BSA) diluted in H_2O was carried out in duplicate, using standards in the range 20-200µg/ml. 10µl of cell sample was diluted to 200µl with H_2O. 100µl of solution A and 800µl solution B were added to sample and standards. The samples were incubated for 20 minutes at room temperature. The absorbance of the samples was read using an Uvikon spectrophotometer (BioTeck Instruments Ltd) at 750nM.

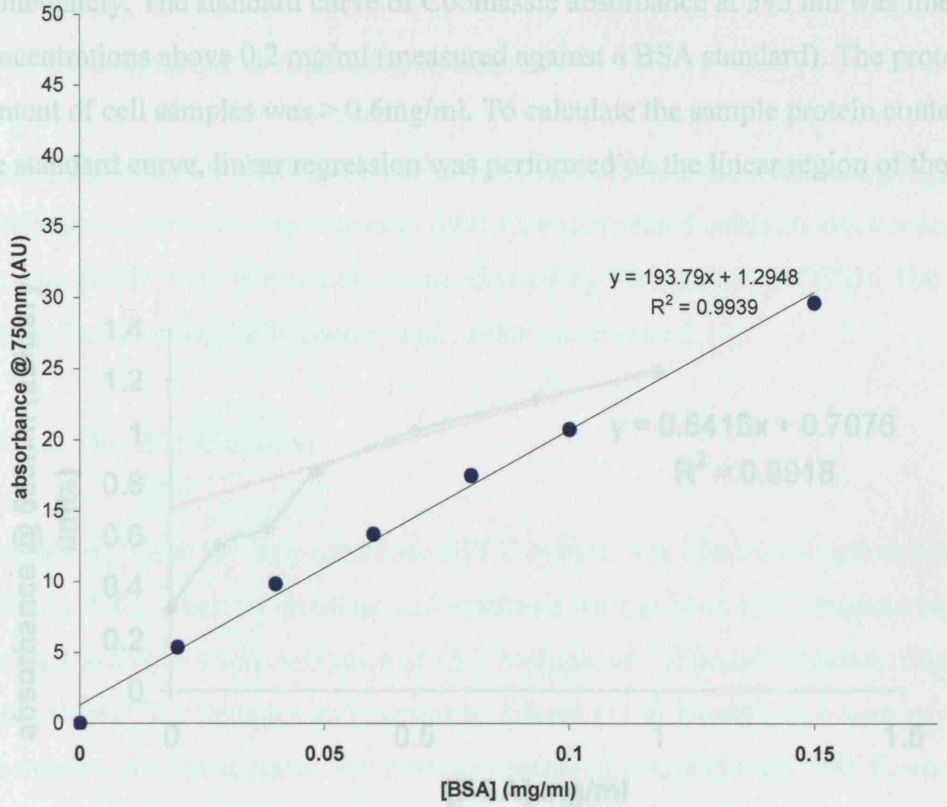

Figure 2.10: Standard curve of BSA standard measured by the Lowry assay.

2.9.2.1. Principle of Bradford assay

For measurement of protein concentrations by the Bradford method the Bio-Rad preparation of Coomassie dye in an acidified solution (phosphoric acid and methanol) (Bio-Rad, Buckinghamshire, UK) was used. The Bradford assay, detects protein based on the interaction of the Coomassie dye primarily with basic and aromatic amino acid residues. This interaction causes a shift in maximal absorbance from 470nm to 595nm. The assay is particularly sensitive to arginine and lysine and is preferentially used to detect larger proteins > 3,000 kDa (Bradford, 1976).

2.9.2.2. Protocol of Bradford assay.

A standard curve of bovine serum albumin (BSA) diluted in HBSS was carried out in duplicate, with standards in the range 0.1-1 mg/ml. 40 µl of Coomassie dye was added to 20 µl of sample. 140 µl of H_2O was added and the absorbance was read at 595 nm

immediately. The standard curve of Coomassie absorbance at 595 nm was linear at concentrations above 0.2 mg/ml (measured against a BSA standard). The protein content of cell samples was > 0.6mg/ml. To calculate the sample protein content from the standard curve, linear regression was performed on the linear region of the curve.

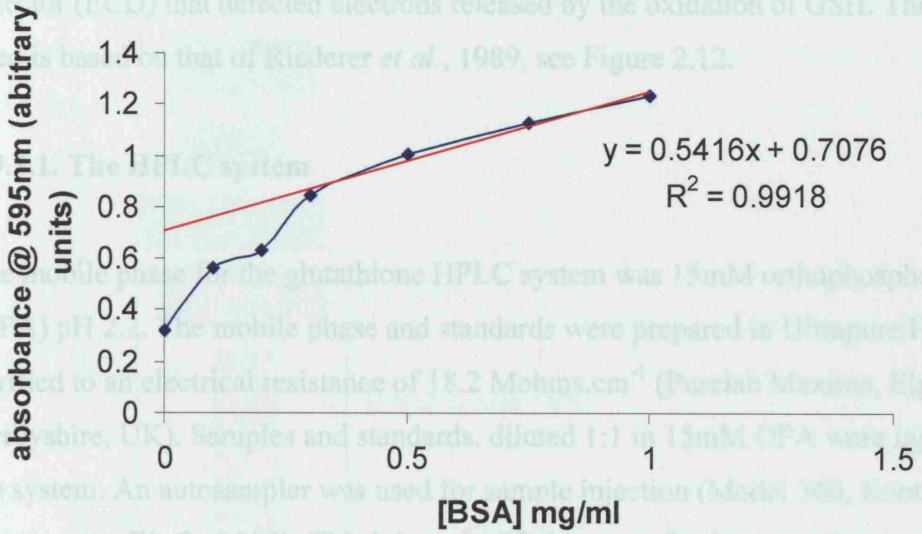

Figure 2.11: Standard curve of BSA standard measured by the Bradford assay. The assay is linear at protein concentrations > 0.2 mg/ml. Red line shows points over which linear regression was conducted. Linear regression was performed using Microsoft Excel.

2.9.3. Measurement of reduced Glutathione

Reduced glutathione (GSH) was extracted from cells, and separated using high performance liquid chromatography (HPLC) and detected using an electrochemical detector (ECD) that detected electrons released by the oxidation of GSH. The method used is based on that of Riederer *et al.*, 1989, see Figure 2.12.

2.9.3.1. The HPLC system

The mobile phase for the glutathione HPLC system was 15mM orthophosphoric acid (OPA) pH 2.2. The mobile phase and standards were prepared in Ultrapure H_2O purified to an electrical resistance of 18.2 Mohms.cm^{-1} (Purelab Maxima, Elga, Derbyshire, UK). Samples and standards, diluted 1:1 in 15mM OPA were injected onto the system. An autosampler was used for sample injection (Model 360, Kontron instruments, Watford UK). This injected a 20µl sample firstly onto a 3mm x 10mm guard column (to protect the main HPLC column from possible contamination). After the guard column the sample components were resolved by passing through the analytical column (dimensions 4.6mm x 250mm). Both columns were packed with 5µM octadecasilyl (Techsphere, HPLC technology, Macclesfield, UK). The column separated sample components based on the hydrophobic or hydrophilic nature of the molecules (more hydrophobic molecules have higher affinity for the octadecasilyl therefore pass through the column more slowly than hydrophilic ones that have a higher affinity for the mobile phase). The main HPLC column was housed in a block heater (Model 7970, Jones Chromatography, Mid Glamorgan, UK) that maintained the column at 30°C. The GSH concentration was measured using an electrochemical detector. The coulometric electrochemical detector consisted of two electrodes in series in a porous graphite analytical cell (Model 5010, ESA Analytical, Aylesbury, UK). The upstream electrode 1 potential was set at +250mV. This was used to screen out molecules with an oxidation potential lower than GSH. The GSH was oxidised at the downstream electrode 2 and the current (electrons released by GSH oxidation) was measured. The current was proportional to the amount of GSH in the sample. The potential of the downstream electrode needed to be set each time HPLC system was re-started after shut down, and

was checked regularly during use to ensure the appropriate oxidising potential for complete oxidation of the glutathione in the sample (see section 2.9.3.3). During this project the downstream electrode potential was in the range of +525mV and +750mV.

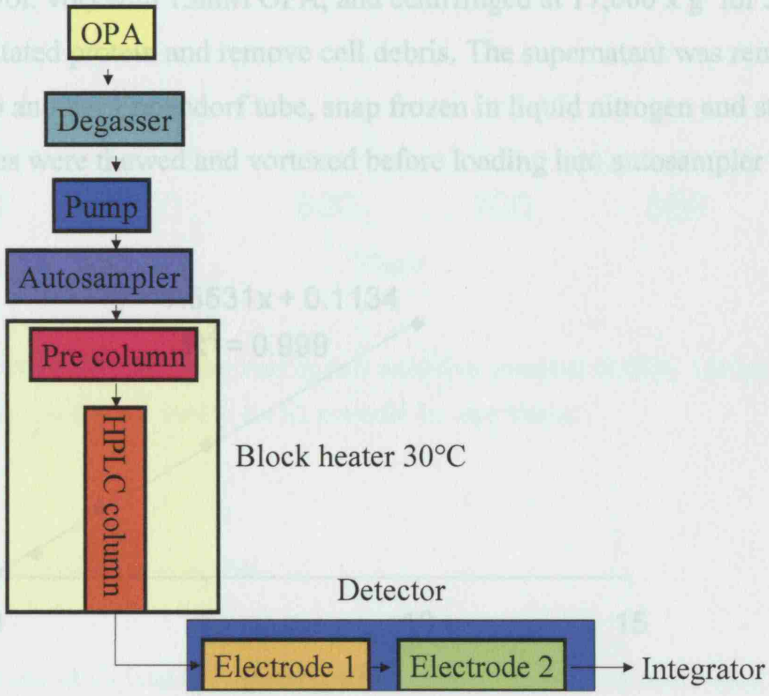

Figure 2.12: Flow diagram showing flow of mobile phase and sample through the components of the HPLC system.

2.9.3.2. Sample and standard preparation

GSH standards were prepared in 15mM OPA (prepared as mobile phase see section 2.9.3.1) at a 10mM stock concentration and stored at -70°C (the high concentration of the stock was used to increase stability of standards) Standards were then serially diluted between 0- 10µM (Figure 2.13)

Cell pellets were resuspended in 200µl HBSS and stored at -80°C. Glutathione measurements were taken within one month of freezing cells. Cells were thawed, and vortexed. 100µl of the suspension was frozen for protein analysis. 100µl of the cell suspension was taken and diluted 1:1 (vol:vol) with 15mM OPA, to extract and stabilise GSH in its reduced form. The suspension was then centrifuged at 17,000 x g for 5

minutes to pellet the precipitated protein. The supernatant was removed and immediately transferred to autosampler vials for loading onto the HPLC system.

To measure extracellular GSH, cell media was collected from samples and immediately diluted 1:1 (vol: vol) with 15mM OPA, and centrifuged at 17,000 x g for 5 minutes to pellet precipitated protein and remove cell debris. The supernatant was removed and transferred to another Eppendorf tube, snap frozen in liquid nitrogen and stored at -70°C. Samples were thawed and vortexed before loading into autosampler vials.

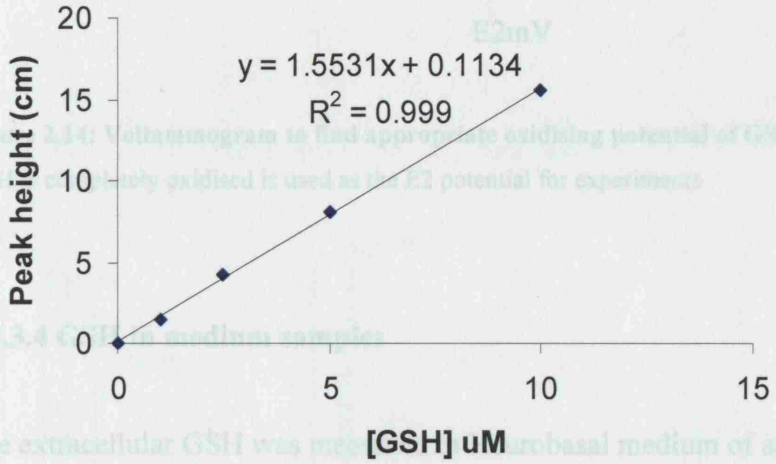

Figure 2.13: GSH standard curve. Glutathione standards of 1,2.5, 5 and 10µM as well as a blank (OPA only) were injected onto the HPLC column. Linear regression was performed using Microsoft Excel.

2.9.3.3. Determination of a potential for GSH detection

In order to ascertain optimal potential for GSH detection where all GSH would be oxidised 10µM standards were injected onto the column at various downstream electrode potentials. Between each change of electrode potential the electrochemical detector was allowed to settle for 30 minutes before injecting the next standard. Plotting the peak heights of the GSH peak against voltage generated a Voltammogram. The electrode potential at the point at just before the peak heights reached a plateau was used for GSH detection. In the voltammogram shown (figure 2.14), this point was reached at +680mV.

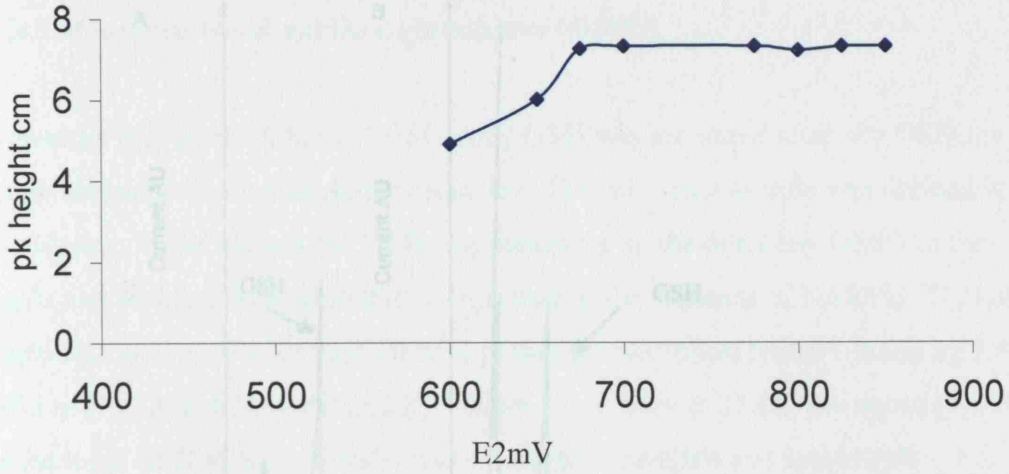

Figure 2.14: Voltammogram to find appropriate oxidising potential of GSH. The potential where GSH is completely oxidised is used as the E2 potential for experiments

2.9.3.4 GSH in medium samples

The extracellular GSH was measured in Neurobasal medium of astrocytes after 24 hours. Before starting these experiments, deproteinated Neurobasal medium was run through the column to determine late eluting peaks. As there was a peak at 70 minutes the flow rate was increased to 0.75ml/min to reduce run time. GSH and CysGly standards were run in OPA and Neurobasal medium before each sample run. The CysGly eluted at the end of the solvent front therefore could not be quantified accurately in samples although its presence in conditioned medium of astrocytes was verified by spiking the sample with a CysGly standard. Astrocyte conditioned medium samples had a noisier baseline than astrocyte cell samples. In astrocyte conditioned medium samples there was a consistent peak that eluted just before the GSH peak. This peak did not vary in size between control and Aβ25-35 treated samples. There was also a peak that eluted immediately after the GSH peak, which was present in Neurobasal blanks. This did not vary in size between control and Aβ25-35 treated samples. The GSH in the sample was measured from the baseline indicated in Figure 2.15.

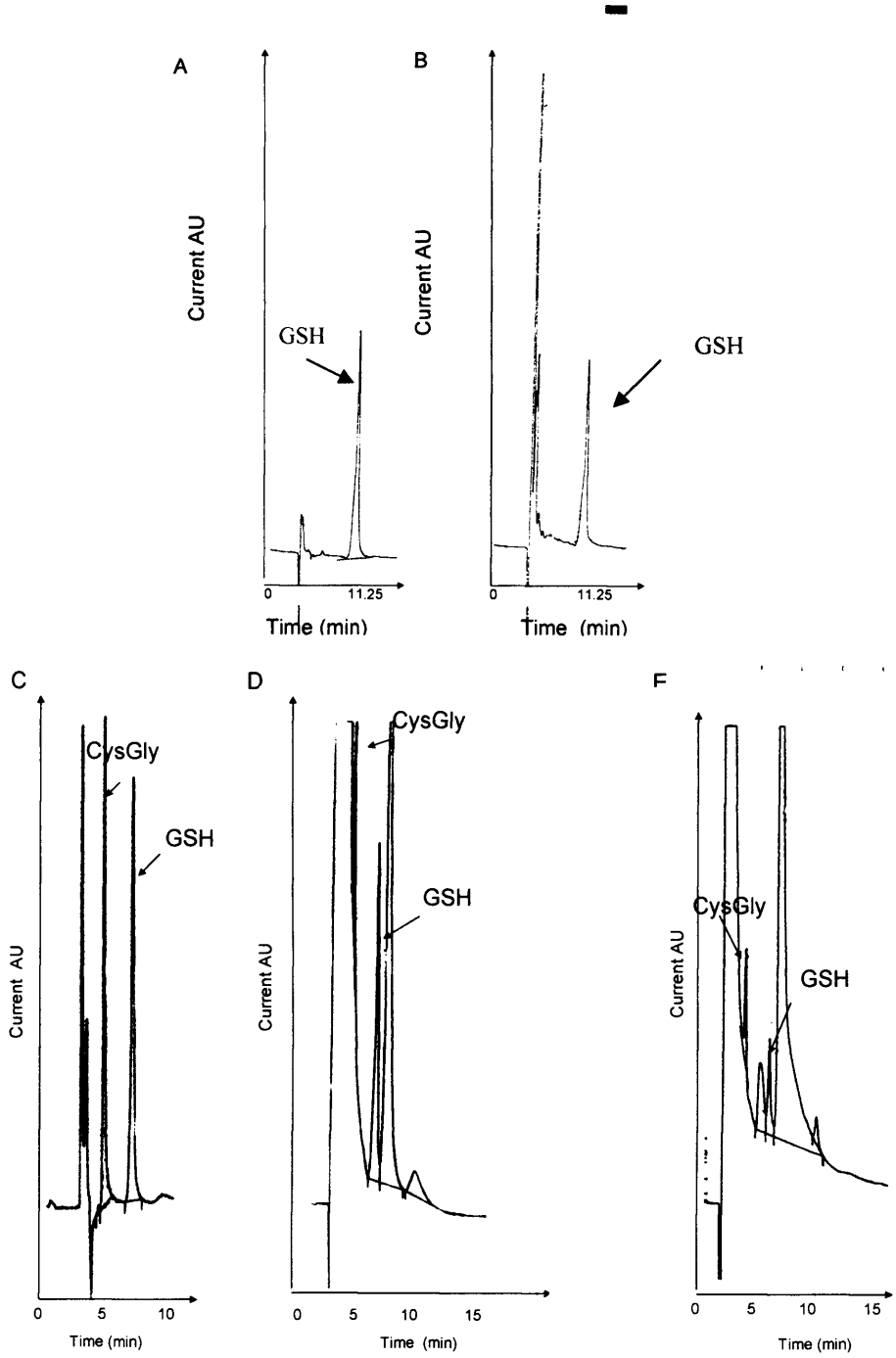

Figure 2.15: HPLC chromatograms. A) 5μM standard in OPA B) Astrocyte pellet sample C) 5μM CysGly and GSH standards in OPA D) 5μM CysGly and GSH standards in deproteinated neurobasal medium E) Astrocyte conditoned medium chromatogram.

2.9.3.5 Measurement of oxidised glutathione (GSSG)

To measure the ratio of GSH to GSSG, total GSH was measured after any GSSG in the sample was reduced by glutathione reductase. The cell pellet sample was divided into two aliquots. In one aliquot the **GSH** was measured. In the other any GSSG in the sample was reduced using glutathione reductase in the presence of NADPH (50µl of sample was incubated with 50µl 100mM potassium phosphate buffer containing 3.4mM EDTA pH7.6, 80µM NADPH and 2U GR for 10 minutes at 37°C) (see equation 2.1) and the **total GSH** (GSH + GSSG) was measured. The **GSH** and **total GSH** concentrations were adjusted for their dilution factors. The concentration of GSSG was calculated by subtracting **GSH** from **total GSH** and dividing this value by 2 (see Figure 2.16).

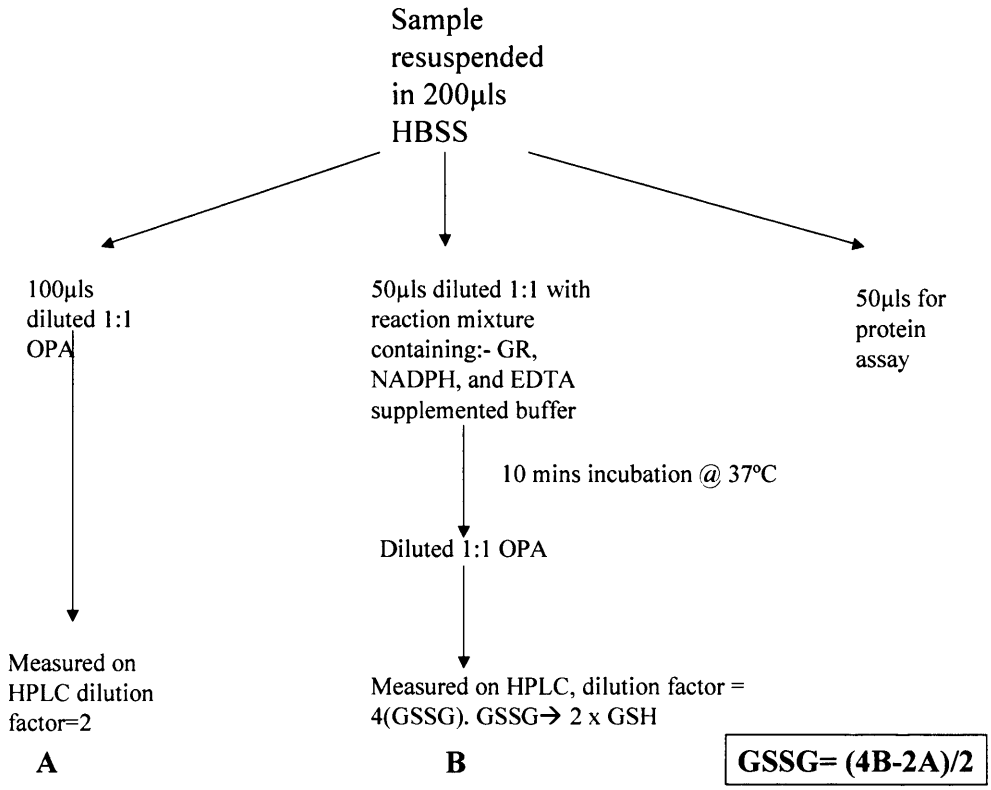

Figure 2.16: Protocol to measure ratio of GSH: GSSG.

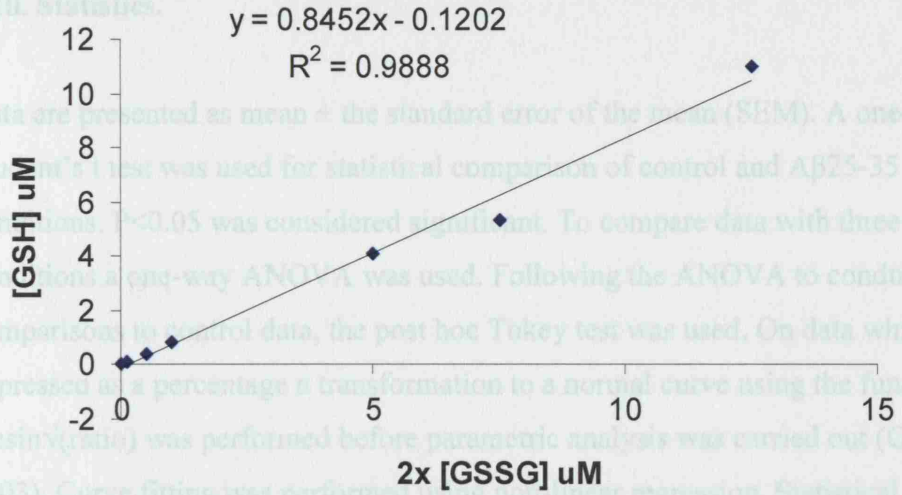

Figure 2.17. Standard curve of GSSG reduced by GR to GSH, and then measured by HPLC.

Linear regression conducted using Microsoft Excel.

2.10. Statistics.

Data are presented as mean ± the standard error of the mean (SEM). A one-way paired Student's t test was used for statistical comparison of control and Aβ25-35 treatment conditions. $P<0.05$ was considered significant. To compare data with three or more conditions a one-way ANOVA was used. Following the ANOVA to conduct multiple comparisons to control data, the post hoc Tukey test was used. On data which were expressed as a percentage a transformation to a normal curve using the function $\arcsin\sqrt{(\text{ratio})}$ was performed before parametric analysis was carried out (Gegg *et al.*, 2003). Curve fitting was performed using non-linear regression. Statistical analysis was carried out using Microsoft Excel.

Chapter 3: Development of a standard treatment protocol with Aβ25-35

3 Development of a standard treatment protocol with Aβ25-35.

3.1. Introduction

The initial aim of this project was to compare the response of highly pure astrocyte and neurone primary cultures to Aβ25-35. Based on the findings from the above experiments it was intended to investigate interactions between the two cell types using co-culture or conditioned medium protocols.

Therefore, it was necessary to develop a standard treatment protocol in suitable culture conditions to model Aβ toxicity in separate neurone and astrocyte monocultures which could also be used in co-culture paradigms.

3.1.1 Neurone and astrocyte cell culture conditions

The development of cultured neurones and astrocytes, and their response to stimuli can be highly influenced by their cell culture conditions. Therefore it is important to choose the most appropriate cell culture conditions as possible to model Aβ toxicity.

In this project primary cortical cell cultures were used. Both neurones and astrocytes were dissociated from the cortex. The cortex, alongside the hippocampus, is the most vulnerable brain structure to neurodegeneration in AD (Braak and Braak, 1991).

Primary neurone cultures require development to a mature state before they can be used for experiments. This is firstly because the neurones are dissociated from a foetal tissue source, where many of the cells are still in an immature or undifferentiated state, and secondly because of the dissociation process neurones are sheared of their neurites. The neurones need to re-grow their neurites and express the proteins needed to form synaptic connections. Within the studies of the effects of Aβ on primary neurone cultures presented in the literature there is some degree of variation in the age at which neurones are treated from 3 to 7 days *in vitro* (DIV). As glutamate receptor signalling and excitotoxicity have been implicated in Aβ-mediated toxicity (see section 1.3.3.) it was considered important to have as close to full glutamate receptor subunit expression

as possible. It has been estimated that primary cortical neurones from an embryonic source require at least 8 days *in vitro* to exhibit mature NMDA receptor expression (Janssens and Lesage, 2001). It was therefore decided for the standard treatment protocol that neurones should be treated on the 9 DIV.
It had been shown previously by our laboratory that comparable neurones to those used in this study have a healthy rise in intracellular Ca^{2+} after stimulation with glutamate at DIV9 (Dr Susan Griffin, personal communication).

Astrocytes also need time in culture for mature protein expression. Astrocytes generated from 1 day-old rat pups are used as standard at DIV 14 in the majority of cell culture treatment paradigms. To promote proliferation, astrocytes are typically grown in medium containing foetal bovine serum (FBS)(Brewer *et al.*, 1993). Foetal bovine serum, which contains various growth factors and hormones, can influence the development and receptor expression of astrocytes in culture conditions. For example, astrocytes grown in foetal bovine serum express a greater number of metabotropic glutamate receptors subtypes than astrocytes grown in chemically defined medium (Janssens and Lesage, 2001).

Neurobasal medium has been developed to promote neurone growth, and to limit glial cell proliferation, as it has a lower osmolarity, which is preferable for neurone growth. The medium is used with the supplementation of the supplement B27 a chemically defined serum substitute (Brewer *et al.*, 1993). For this project it is necessary to treat both cell types in the same treatment medium. This was in order to be able to compare the response of the two cell types to Aβ25-35 and to develop co-culture and conditioned medium paradigms. It has been a standard procedure, to treat astrocytes with Aβ in the absence of serum (Pike *et al.,* 1994). This is firstly because serum contains a high protein content that could affect cell- Aβ interactions, for example by binding to Aβ. Secondly as components of serum, which vary in concentration from batch to batch, such as the serine protease thrombin, or various growth factors, can affect astrocyte response to Aβ (Ogino *et al.*, 1992, Pike *et al.*, 1996). As neurones are a more delicate cell to culture, neurones and astrocytes were treated in the preferable medium for neurones, Neurobasal. This treatment medium was supplemented with B27 supplement and glutamine.

3.1.2. A cell culture model of aggregated Aβ toxicity: use of the Aβ25-35 fragment.

The Aβ25-35 fragment is not a naturally occurring APP cleavage product, yet is widely used to investigate Aβ toxicity in cell culture models. The 11 amino acid peptide has been demonstrated to show most of the toxic properties of the full length Aβ peptide (Pike *et al.*, 1995). The 25-35 region of the Aβ peptide spans part of the region of the Aβ1-40 and Aβ1-42 peptides that form a β pleated sheet. It has been suggested, based on NMR studies, that Aβ1-42 peptides form a β- strand-turn-β-strand motif with the β-sheets formed by residues 18-26 and 31-42 and that protofibrils form unidirectionally as side chain interactions occur between the β- motifs of peptides in close proximity (Luhrs *et al.*, 2005). It has been shown, by analysis of the aggregation of different fragments of the Aβ peptide, that residues 17-20 and 30-35 are necessary for aggregation and that it is only the aggregating Aβ fragments that are neuro-toxic in cell culture conditions (Liu *et al.*, 2003).

Despite the difference in length between the two peptides, when added to neurones and astrocyte cultures aggregated Aβ25-35 and aggregated Aβ1-42 peptides elicit similar responses. Both Aβ25-35 and Aβ1-42 cause similar amounts of cell death to neuronal cell cultures (Pike *et al.,* 1995), cause an influx of Ca^{2+} into neuronal cells in culture (Blanchard *et al.,* 1997), and damage neurones by the generation of ROS (Richardson *et al.,* 1996). In astrocyte cultures, Aβ25-35 and Aβ1-42 also induce stellation (Pike *et al.*, 1996) and similar intracellular Ca^{2+} oscillations (Abramov *et al.,* 2004). As discussed in section (1.2.4.4.) Aβ1-42 is thought to insert into lipid membranes and Aβ25-35 has been shown to also insert into lipid bi-layers (Dante *et al.,* 2003). Aβ25-35, like Aβ1-42 also causes the activation of NADPH oxidase in astrocytes (Abramov *et al.*, 2004).

The appealing property of Aβ25-35 is that it completely aggregates almost instantly in water, therefore it does not require the aging process that is needed to form Aβ1-40/42 aggregates before treatment of cultured cells. As discussed in section 1.1.5 Aβ1-40/42 form oligomer intermediates in the process of the formation of their aggregates and therefore without the aging process can form heterogeneous solutions of aggregates and

oligomers, which may vary from batch to batch. Therefore Aβ25-35 is considered a useful tool to model the effects of Aβ aggregates in cell culture conditions.

The problems with using a peptide fragment to model the effects of a longer peptide on cells, are that 1) secondary and aggregate structures of that peptide may be different for the given region, 2) absent regions of the peptide may have independent or synergistic effects on the cell. For example, Aβ25-35 lacks the region needed for binding to the C1q receptor, that Aβ1-40/42 contain, which is part of the complement immunological pathway (Meda *et al.*, 2001). It also lacks the transition metal binding sites in the N terminal region, which have been proposed to chelate metal proteins, inhibiting metal – catalysed oxidation of molecules (Kontush, 2001) As introduced in section (1.2.4.1) the amino acid methionine in the 35 position has been implicated in Aβ mediated toxicity by causing the generation of ROS in cell culture. In the Aβ25-35 fragment, this methionine is the terminal amino acid at the C terminus and it has been suggested by Varadarajan *et al.*, 2004 that a terminal methionine is more likely to undergo oxidative reactions than a methionine flanked by other amino acids on both sides.

As it is likely that multiple regions of the Aβ1-40/42 peptides have effects on the neurones and astrocytes in and surrounding neuritic plaques, by understanding the toxic mechanisms of Aβ25-35 and by comparing and contrasting the effects of Aβ25-35 and longer Aβ fragments specific effects can be attributed to particular peptide regions and structures. In this project Aβ25-35 has been used to model aggregated Aβ toxicity, as a tool to set up and test novel co-culture and conditioned medium paradigms to be compatable for use with the full length Aβ1-40/42 peptides.

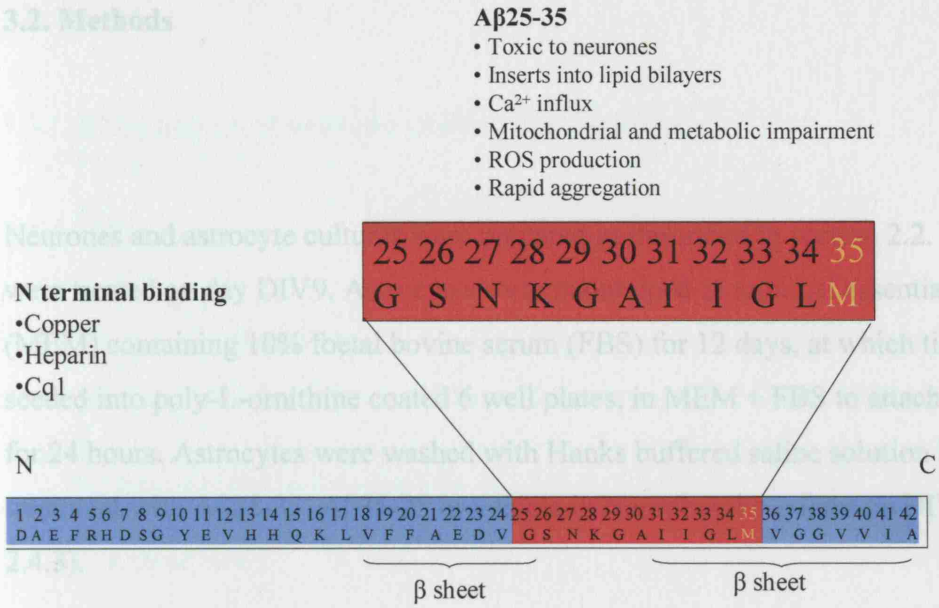

Figure 3.1 The Aβ25-35 fragment: Aβ25-35 contains part of the two β sheet segments of Aβ1-42, it aggregates rapidly and shows similar toxicity to neurones in culture conditions as Aβ1-42. However, as it lacks the N terminal domain of Aβ1-42, it does not have a binding site for copper, heparin or the complement 1 receptor (Cq1) of the classical complement immunological pathway.

3.1.3. The standard protocol for treatment of astrocytes and neurones with Aβ25-35.

The basic criteria for the standard treatment protocol were 1) treatment of the two cell types in the same medium 2) a concentration of Aβ25-35 sufficient to cause a significant amount of neurone cell death over a 24 hour period and 3) appropriate controls for the Aβ25-35 treatment.

In this chapter, the neurone and astrocyte cultures were characterised, and the toxicity of Aβ25-35 to neurones and astrocytes was assessed. The intricacies in producing appropriate controls for treatment with an aggregating peptide were also investigated.

3.2. Methods

Neurones and astrocyte cultures were prepared as described in section 2.2. Neurones were treated on day DIV9. Astrocytes were maintained in minimal essential medium (MEM) containing 10% foetal bovine serum (FBS) for 12 days, at which time they were seeded into poly-L-ornithine coated 6 well plates, in MEM + FBS to attach and recover for 24 hours. Astrocytes were washed with Hanks buffered saline solution before treatment with Aβ25-35, Aβ35-25 or vehicle in Neurobasal medium on DIV13 (section 2.4.3).

Immunocytochemical assessment of the purity of neurone and astrocyte cell cultures was performed as described in section 2.3.

The degree of cell death following Aβ25-35 treatment was measured in neurones and astrocytes, by assessing nuclear morphology and the permeability of the membrane to propidium iodide (section 2.7.1)

The reducing potential of neurones and astrocytes following Aβ25-35 treatment was assessed by the ability of both cell types to reduce 3-(4,5-dimethylthiazol-2-yl)-2,5-diphenyltetrazolium bromide (MTT) as described in section 2.7.2.

The cells were harvested as described in section 2.2.4 . The protein content was assessed by the Lowry assay (section 2.9.1.1) and the Bradford assay (section 2.9.1.4)

3.3. Results.

3.3.1. Morphology of neurone and astrocyte cultures.

3.3.1.1. Neurones

At DIV9 neurones had formed extensive synaptic connections. Neurone cell bodies were generally dark and round with thin axonal processes and dendritic branches (Figure 3.2a).

3.3.1.2. Astrocytes

Astocytes at DIV13, grown in MEM medium containing serum, had a flat polygonal morphology (Figure 3.3 a). DIV14 astrocytes incubated in Neurobasal medium for 24 hours, had a slight alteration in morphology, with a darkening of cell bodies and appearance of a few distinct processes (figure 3.3b).

3.3.2. Immunocytochemical assessment of neurone and astrocyte preparations

3.3.2.1. Neurones

Neurones were isolated from embryonic day 17 foetuses. At DIV 3 the cells were treated with cytosine arabinoside to inhibit division of proliferating cells. Immunocytochemical staining using the neurone specific anti beta tubulin III antibody , the astrocyte specific anti GFAP antibody and the microglial specific anti cd11b antibody, showed that the cell preparation consisted of 98.1 % neurones. 1.05 % of cells were GFAP positive. There were no cd11b positive cells, indicating an absence of microglia. 0.85% of cells were negative for beta tubulin III, GFAP and cd11b. These were classified as contaminating cells of unknown type.

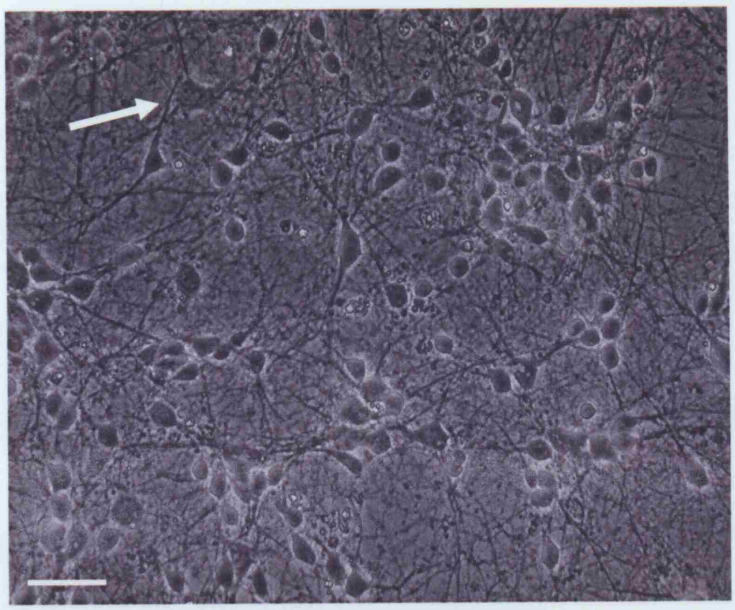

A

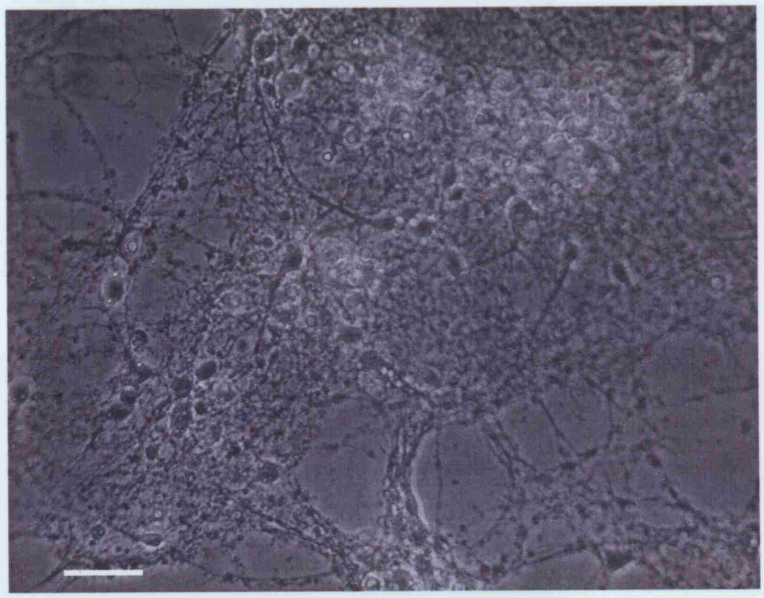

B

Figure 3.2: Phase contrast images of neurone morphology.

A) Neurone DIV9 in control conditions. B) Neurone DIV9, 24 hr treatment with 50μM Aβ25-35. Images as observed through phase contrast microscope, 20X objective lens, total magnification 200X. Scale bar represents 40μm. Arrow in A points to contaminating astrocyte.

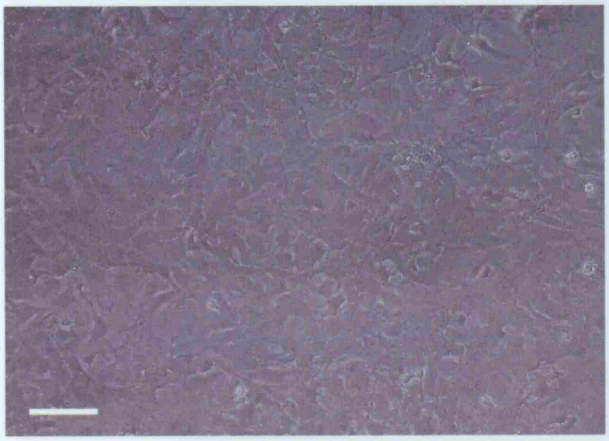

A

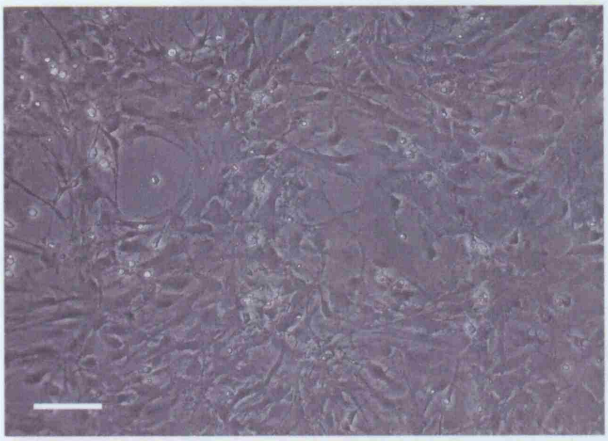

B

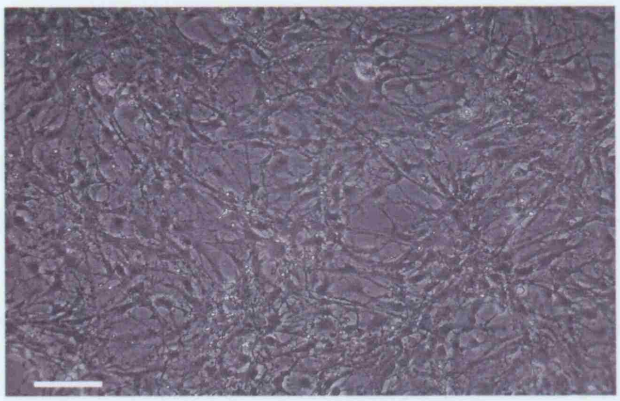

C

Figure 3.3: Phase Contrast Images of Astrocyte Morphology.

A)Astrocyte DIV13 in MEM + FBS B) Astrocyte DIV14, in control conditions (Neurobasal medium) C) Astrocyte DIV14, 24 hr treatment with 50 μM Aβ25-35 in Neurobasal medium. All images as observed through phase contrast microscope, 20X objective lens, total magnification 200X. Scale bar represents 80μm.

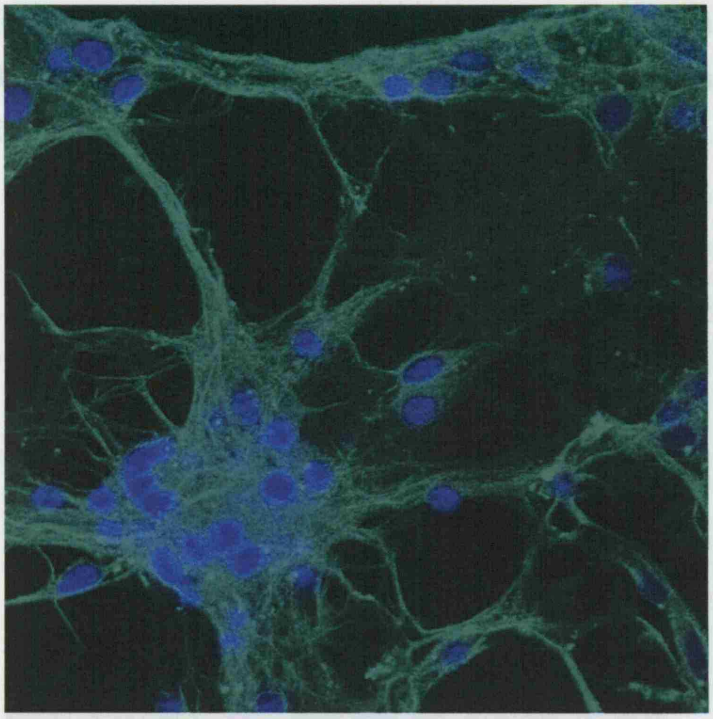

Figure 3.4 Immunocytochemical staining of DIV 10 cortical neurones. Image taken using confocal microscopy. Green colour is the anti-beta III tubulin stain, the blue colour is the DAPI stained nuclear DNA. Image taken using 40x objective, total magnification 400x.

3.3.2.2. Astrocytes

To generate high purity cortical astrocyte cultures, the mid brain and hippocampus of newborn rats were removed by careful dissection, and contamination by fibroblasts was prevented by removal of the meninges by dissection. The astrocyte cultures were shaken for 18 hours on DIV 6 to remove contaminating microglia and oligodendrocytes.

The purity of astrocyte cultures was assessed by immuncytochemical staining using specific antibodies as described in the previous section. 97.8% of the total number of cells (DAPI positive) stained for GFAP. In all immunocytochemistry experiments, the specificity of the FITC and CY5 conjugated secondary antibodies was verified by the absence of fluorescence in the absence of primary antibody. The standard procedure includes an incubation of methanol-fixed cells with detergents, to allow antibodies into

the cell during the immunocytochemistry protocol. However, this step could damage cell surface antigens such as the microglial marker cd11b, which is a membrane spanning integrin. The immunocytochemical procedure was repeated in the absence of detergent to allow for false negatives microglial screening, but there was still no evidence of microglial contamination.

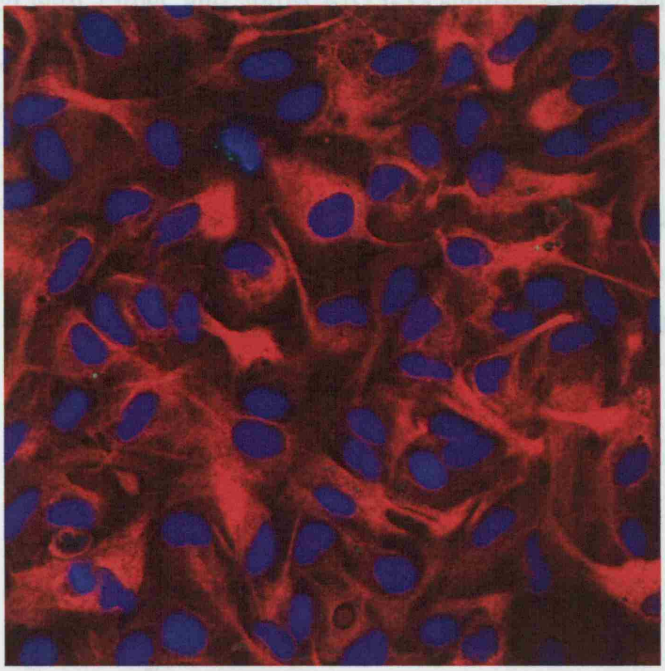

Figure 3.5 Immunocytochemical staining of DIV 14 non-stellate cortical astrocytes. Image taken using confocal microscopy. The red colour is anti-GFAP stain, the blue colour is the DAPI stained nuclear DNA. Image taken using 40x objective, total magnification 400x.

3.3.3. Neurone death following Aβ25-35 treatment.

As described in the Introduction (section 1.1), Aβ accumulations in AD is thought to arise from an imbalance of production and clearance. The amount of Aβ generated and the local Aβ aggregate concentrations in the extracellular matrix are very difficult to estimate *in vivo*. However Harper and Lansbury have estimated that Aβ must reach concentrations of 10-40μM in order to aggregate (Harper and Lansbury, 1997) In a cell culture model of Aβ toxicity the short life of cells determines that Aβ treatment time has to be kept relatively short. The majority of Aβ toxicity experiments use a 24-hour

treatment period. Therefore, the approach was adopted to use concentrations of Aβ which cause neurone death as is seen *in vivo* but within this time scale.

In the literature, Aβ25-35 concentrations used to measure toxicity in neurone primary cultures range from 10 μM to 50μM. Aβ25-35 shows concentration-dependent toxicity within this range (Weiss *et al.*, 1994). In this study, in three independent preparations, neurones treated with 25μM, and 50μM Aβ25-35 showed significant increase in cell death ($p < 0.05$, one way ANOVA, followed by Tukey test comparing each concentration to vehicle treated control). 50 μM Aβ25-35 was used as this concentration gave maximal cell death in 24 hours. In addition, this project followed on from previous studies carried out within this laboratory, which showed metabolic and mitochondrial electron transport chain complex inhibition in comparable cell cultures, using a 24-hour treatment with 50μM Aβ25-35 (Casley *et al.*, 2002a; Casley *et al.*, 2002b).

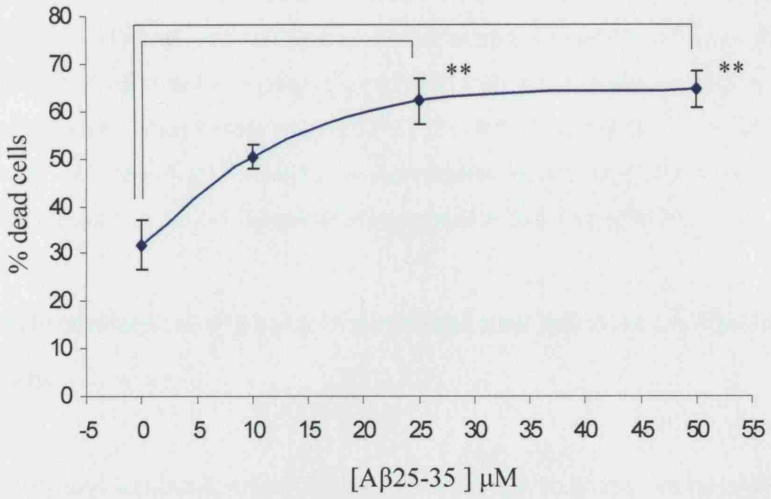

Figure 3.6: Concentration dependence of Aβ25-35 toxicity in neurones. Cell death was calculated as the number of propidium iodide permeable and cells with condensed nuclei (dead cells, see section 2.7) as a percentage of the total number of cells present (both dead and alive) (% dead cells: Vehicle = 31.8 ± 5.2%, 10μM = 50.3 ± 2.56%, 25μM = 62.0 ± 3.8%, 50μM = 64.5 ± 3.8%). 25 and 50μM treatments result in a significant increase in cell death (one way ANOVA followed by Tukey comparison test ** = $P < 0.01$). n=3 independent experiments. Error bars = SEM.

3.3.4 Comparison of neurone and astrocyte viability following a 50μM Aβ25-35 treatment

The degree of cell death following exposure to 50μM Aβ25-35, with vehicle (H_2O) or with the control reverse peptide Aβ35-25 , was measured in neurones and astrocytes, grown on glass coverslips, by assessing nuclear morphology and membrane permeability (section 2.7.1.3). Neurones showed the same basal amount of cell death when treated with vehicle or Aβ35-25 (Vehicle = 30.3 ± 7.1.1%, Aβ35-25 = 34.2 ± 6.76%). Neurones treated with Aβ25-35 showed increased cell death (Aβ25-35 = 57.5± 11.3%) ($P < 0.05$, one way ANOVA, followed by multiple comparison test (Tukey), n=3).

There was no increase in the amount of cell death in astrocytes following, Aβ35-25 or Aβ25-35 treatments compared to vehicle (Vehicle = 10.5 ± 2.0%, Aβ35-25 = 9.1 ± 3.8 %, Aβ25-35 = 8.4 ± 1.2 %).

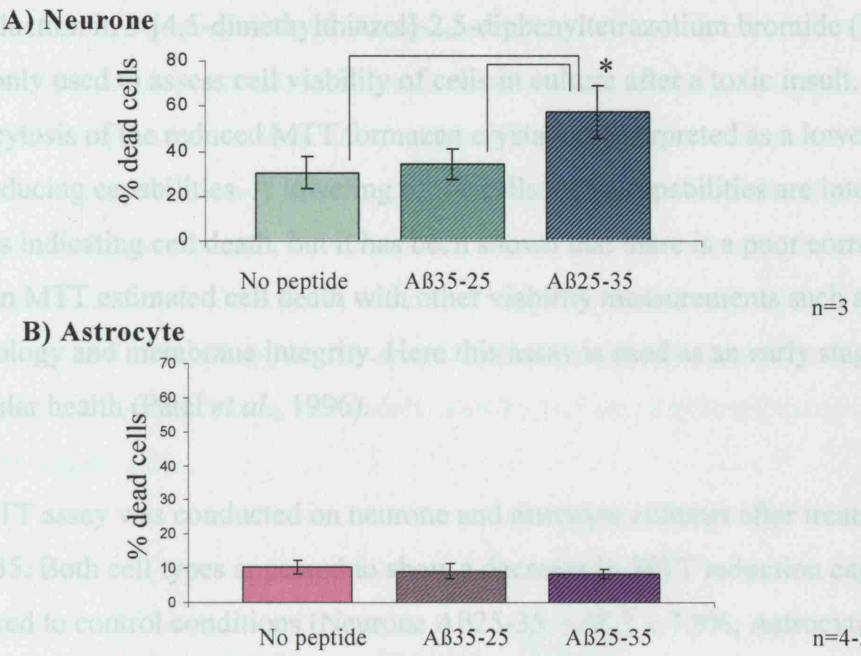

Figure 3. 7: Neurone and astrocyte cell death following Aβ25-35, Aβ35-25 or vehicle treatment. Neurones and astrocyte cell cultures were treated for 24 hours with 50μM Aβ25-35, 50μM Aβ35-25 or vehicle (H_2O). Cell death was assessed by nuclear morphological characterisation and membrane permeability and expressed as a percentage of dead cells out of total cells present. Neurones show increased cell death when treated with Aβ25-35 ($P < 0.05$, one way ANOVA, followed by multiple comparison test (Tukey), n=3 independent experiments. Astrocytes showed the same degree of cell death in all three treatments. n= 4-5 independent experiments. Error bars=SEM.

3.3.5. Morphological changes in neurones and astrocytes following Aβ25-35 treatment

Morphological analysis, using phase contrast microscopy, of neurones after Aβ25-35 treatment showed clear evidence of neurite degeneration compared to the two control conditions (figure 3.2 B).

Astrocytes adopted an increased stellate morphology after Aβ25-35 peptide treatment compared to the two control conditions, with a higher proportion of cells showing distinct cell bodies and processes (figure 3.2 C).

3.3.6. Neurone and astrocyte reducing potential after Aβ25-35 treatment

The reduction in 3-[4,5-dimethylthiazol]-2,5-diphenyltetrazolium bromide (MTT) is commonly used to assess cell viability of cells in culture after a toxic insult. A lowering of exocytosis of the reduced MTT formazan crystals is interpreted as a lowering of a cells reducing capabilities. A lowering of the cells redox capabilities are interpreted by some as indicating cell death, but it has been shown that there is a poor correlation between MTT estimated cell death with other viability measurements such as nuclear morphology and membrane integrity. Here this assay is used as an early stage indicator of cellular health (Patel *et al.*, 1996).

The MTT assay was conducted on neurone and astrocyte cultures after treatment with Aβ25-35. Both cell types appeared to show a decrease in MTT reduction capability compared to control conditions (Neurone Aβ25-35 = 48.2 ± 7.9%, Astrocyte Aβ25-35 = 57.3 ± 8.5%).

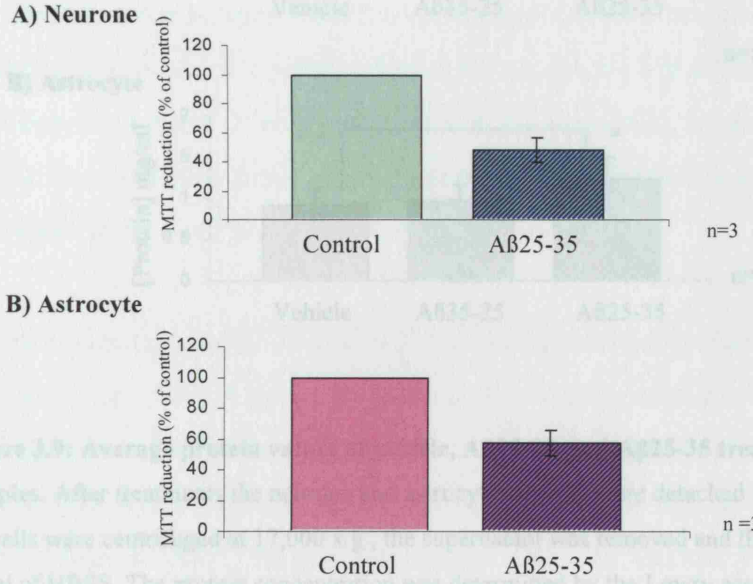

Figure 3.8 MTT reduction capability of neurones and astrocytes after Aβ25-35 treatment. Both neurone and astrocytes appeared to show a lowering in their ability to reduce MTT after Aβ25-35 treatment. (Neurone Aβ25-35 = 48.2 ± 7.9% of control neurones , Astrocyte Aβ25-35 = 57.3 ± 8.5% of control astrocytes). n=3.

3.3.7. Appropriate controls for Aβ25-35 treatment

Biochemical comparisons were performed normalised to protein content. As treatment with Aβ25-35 involves addition of protein to cells it was initially thought that treatment with Aβ35-25 should be an appropriate control for increased protein content via addition of peptide. However, after systematic measurements of the total protein in cell suspensions after treatment with Aβ25-35, Aβ35-25 or vehicle it was observed that the protein content of cells (both neurones and astrocytes) treated with Aβ25-35 had significantly and consistently higher protein content than those treated with Aβ35-25 or vehicle, when measured using the widely used Folin's reagent based assay of Lowry *et al.*, 1951 (figure 3.9).

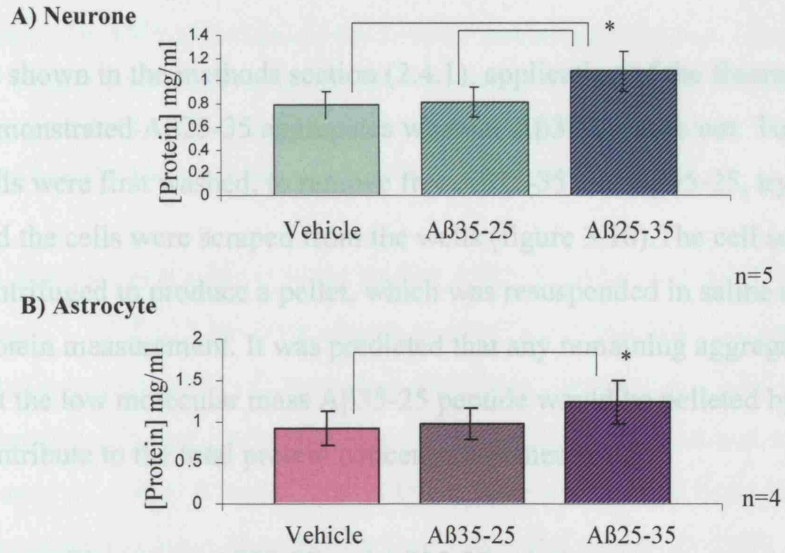

Figure 3.9: Average protein values of vehicle, Aβ35-25, and Aβ25-35 treated astrocytes and neurone samples. After treatments the neurone and astrocyte samples were detached from the wells using trypsin, the cells were centrifuged at 17,000 x g , the supernatant was removed and the cells were resuspended in 200µl of HBSS. The protein concentration was determined by the Lowry assay. For each cell type the protein concentration of vehicle, Aβ35-25 or Aβ25-35 treated cells was compared. In the neurone samples the concentration of Aβ25-35 treated neurones was greater than Aβ35-25 or vehicle treated neurones. (control = 0.79 ± 0.12mg/ml, Aβ35-25 = 0.81± 0.13mg/ml, Aβ25-35 = 1.086 ± 0.17mg/ml) $p< 0.05$ paired t-test n=5. In the astrocyte samples the Aβ25-35 treated astrocytes had a greater protein concentration than vehicle treated astrocytes. $p<0.05$ paired t test n=4. (control = 0.92± 0.208 mg/ml, Aβ35-25 = 0.817 ± 0.13 mg/ml, Aβ25-35 = 1.086 ± 0.17 mg/ml). Error bars = SEM.

Folin's phenol reagent contains molybdate, tungstate and phosphoric acid. In the first step of the Lowry assay used in this study proteins forms a complex around Cu^{2+} in an alkaline copper tartrate solution. The protein complex reduces Cu^{2+} to Cu^{+}. Folin's phenol reagent is reduced leading to an enhancement of the blue colour of this complex. The intensity of colour correlates to the number of peptide bonds. However, some amino acids such as tryptophan and tyrosine (not present in Aβ25-35) can reduce the phenol reagent directly (Chou and Goldstein, 1958).

Both Aβ25-35 and Aβ35-25 were detected by the Lowry assay. It was proposed that the discrepancy in protein content between Aβ25-35 and Aβ35-25 treated cells occurred as Aβ35-25 was removed during the harvesting of cells, whereas Aβ25-35 was not (figure 3.10).

As shown in the methods section (2.4.1), application of the fluorescent dye thioflavin T demonstrated Aβ25-35 aggregates whereas Aβ35-25 does not. To harvest the cells, the cells were first washed, to remove free Aβ25-35 and Aβ35-25, trypsin was then added and the cells were scraped from the wells (figure 3.10).The cell suspension was centrifuged to produce a pellet, which was resuspended in saline solution prior to protein measurement. It was predicted that any remaining aggregates of Aβ25-35 but not the low molecular mass Aβ35-25 peptide would be pelleted by centrifugation to contribute to the total protein concentration measured.

To test this notion, Aβ25-35 and Aβ35-25 solutions were prepared in HBSS, and allowed to age over 24 hours, to give a similar aggregation state to that achieved over the treatment period. These solutions were centrifuged, the pellet resuspended and a Lowry protein assay conducted. In accordance with the notion, aggregated Aβ25-35 was pelleted from solution, but non- aggregated Aβ35-25 was not. With increasing centrifugation speed a greater amount of Aβ25-35 was pelleted from solution (figure 3.10).

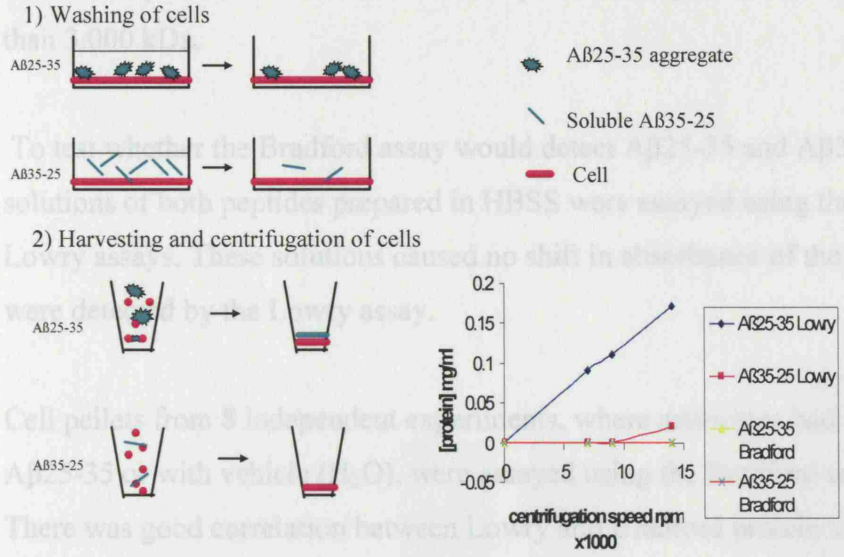

Figure 3.10: Aβ35-25 is removed but Aβ25-35 remains after the harvesting process of cells. Aβ25-35, if bound to the cell could remain after the washing stage of the harvesting process (1), or as shown aggregated Aβ25-35, but not Aβ35-25 can be pelleted from solution (2). With increasing centrifugation speed a greater amount of Aβ25-35 is pelleted from solution.

An alternate explanation could be that Aβ25-35 associated with the cell, but Aβ35-25 does not. Aβ25-35 has been shown to insert into lipid bilayers, and might insert into the plasma membrane of neurones and astrocytes (Dante *et al.*, 2003). Aβ has been shown to bind to cell surface receptors such as the RAGE receptor and scavenger receptors (Yan *et al.,* 1994; Alcaron *et al.*, 2005). Aβ peptides have been proposed to be internalised by both neurones and astrocytes (Nagele *et al.,* 2003; Pugielli *et al.*, 2003). These Aβ cell interactions may be dependent on conformational state. For this study, in order to eliminate the possibility of generating false positives by normalising to non-controlled protein levels it was attempted to selectively measure total cellular protein levels without measuring Aβ25-35.

The amino acid sequence of Aβ25-35 is GSNKGAIIGLM . The amino acids of this sequence are neutral with the exception of Lysine (K), which is basic. The Coomassie dye based Bradford assay, detects protein based on the interaction of the Coomassie dye selectively with basic amino acid residues. This interaction causes a shift in maximal absorbance from 470nm to 595nm. The assay is particularly sensitive to Arginine and

less so to Lysine (Bradford ,1976) and is preferentially used to detect proteins larger than 3,000 kDa.

To test whether the Bradford assay would detect Aβ25-35 and Aβ35-25 0.2mg/ml solutions of both peptides prepared in HBSS were assayed using the Bradford and Lowry assays. These solutions caused no shift in absorbance of the Coomassie dye, but were detected by the Lowry assay.

Cell pellets from 8 independent experiments, where astrocytes had been treated with Aβ25-35 or with vehicle (H_2O), were assayed using the Bradford and Lowry assays. There was good correlation between Lowry and Bradford protein values for control astrocytes (although the Lowry assay tended to measure a slightly higher protein content against a bovine serum albumin standard). In each experiment the average control protein concentration was compared to the average Aβ25-35-treated protein content by a paired t-test. The Lowry assay showed a significant difference at the 5% level between the two cell treatments, whereas the Bradford did not (Figure 3.11). It was concluded that the Bradford assay was more appropriate for measuring the cellular protein concentrations since it would not be affected by the addition of the Aβ25-35 peptide.

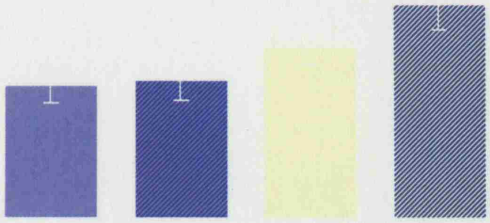

Chapter 4: Effect of Aβ25-35 on neurone and astrocyte glutathione homeostasis

4. Effect of Aβ25-35 on neurone and astrocyte glutathione homeostasis

4.1 Introduction

Neurones and astrocytes form a functional unit in the brain (see section 1.3). Astrocytes produce and compartmentalise various energy substrates, amino acids and antioxidants, which are provided to neurones in a regulated manner. Neurones grown in culture conditions in the absence of astrocytes have limited access to the substrates, which they require for normal metabolism and survival.

One well-established biochemical difference between the two cell types is their glutathione (GSH) levels. Cortical astrocytes have higher levels of GSH than neurones both in the brain *in vivo*, and in cell culture conditions *in vitro* (Bolanos *et al.*, 1995; Langeveld *et al.*, 1996; Hirrlinger *et al.*, 2002). Aβ25-35 has been shown to induce an increase in reactive oxygen species (ROS) when added to neurones and astrocytes in cell culture conditions. It was proposed that neurones are less capable to defend themselves against ROS, which leads to mitochondrial and metabolic impairment, initiation of apoptotic processes and cellular damage such as membrane perturbations. Supplementation of neurones with GSH precursors has been reported to provide protection against Aβ25-35 mediated toxicity (Boyd Kimball *et al.*, 2005; Abramov *et al.*, 2003).

It was postulated that if neurones *in vitro* receive astrocyte derived GSH, as they would under normal physiological conditions in the brain, they would show greater resistance to Aβ25-35 toxicity. However, in the presence of Aβ, astrocytes, despite remaining viable, may still be affected. For example, it has not been elucidated as yet whether or not astrocytes in contact with Aβ retain their ability to release GSH to maintain neurone GSH levels.

Previous studies have shown an Aβ25-35 induced decrease in the level of intracellular GSH in both neurones and astrocytes (Casley *et al.*, 2002; Abramov *et al.*, 2004). The levels of GSH within a cell depend on the balance between the rate of GSH synthesis, and reduction of glutathione disulphide (GSSG), with the utilisation of GSH (reactions

directly with ROS, GPx and glutathione transferase mediated reactions), its efflux from the cell (in astrocytes), and leakage from the cells, if membrane integrity is compromised (Figure 4.1). The exact mechanisms resulting in an imbalance and leading to glutathione depletion after treatment with Aβ25-35 have not been fully elucidated as yet.

It has been shown that if astrocyte intracellular GSH levels are compromised then the astrocyte to neurone GSH support was affected and neighbouring neurones could not upregulate their intracellular GSH (Gegg *et al.*, 2005). To date the effect of Aβ25-35 on astrocyte GSH release and its subsequent effect on neuron GSH homeostasis has not been fully elucidated.

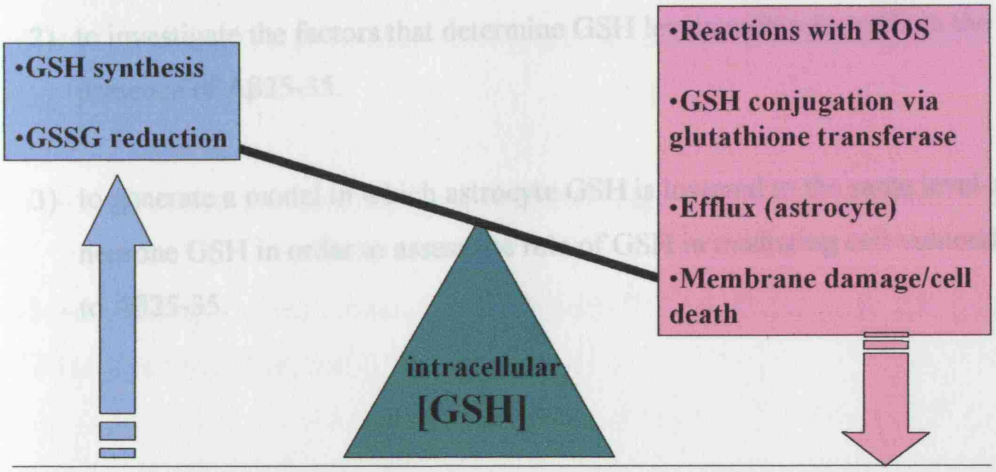

Figure 4.1 Factors affecting the balance of GSH within a cell. Intracellular GSH levels are governed by a balance of its synthesis and recycling capabilities and its utilisation in reactions with ROS and other species, its efflux from the cell (in astrocytes) and leakage through disrupted membranes.

In addition to the anomalies described above it is not clear whether intracellular GSH levels can dictate a cells vulnerability to Aβ25-35 mediated toxicity. It could be predicted that astrocytes are more able to defend themselves against Aβ25-35 generated ROS as they have higher glutathione levels than neurones. However, there could be ROS independent or synergistic effects of Aβ25-35 on neurones that contribute to their higher vulnerability than of astrocytes to Aβ25-35 mediated toxicity. In this chapter an attempt has been made to develop a model to assess the effect of Aβ25-35 on astrocytes depleted of their glutathione defences to the same extent as neurones in culture conditions.

The aims of the experiments presented in this chapter were:

1) to measure GSH levels after Aβ25-35 treatment in the two cell types under the cell culture conditions outlined in the previous chapter.

2) to investigate the factors that determine GSH levels within the cells in the presence of Aβ25-35.

3) to generate a model in which astrocyte GSH is lowered to the same level as neurone GSH in order to assess the role of GSH in mediating cell vulnerability to Aβ25-35.

4.2. Methods

Cultures of rat cortical neurones and astrocytes were prepared and maintained as described in section 2.2.

Astrocytes and neurones were treated for 24 hours with 50μM Aβ25-35 in neurobasal medium containing 2mM glutamine and supplemented with 2% anti-oxidant free B27 as described in chapter 3. Control treatments were vehicle (H_2O), or 50μM of the reverse peptide Aβ35-25 for the same period.

GSH was measured in cell pellets harvested as described in 2.2.4, using reverse phase HPLC coupled to an electro-chemical detector as described in section 2.9.
GSH was measured in deproteinated astrocyte conditioned medium as described in section 2.9.3.4.

Protein content was measured using the Bradford assay described in section 2.9.2.2.

ROS were measured using the fluorescent probe 2',7'-Dichorofluerescin diacetate (DCF) as described in section 2.5.

Lactate dehydrogenase (LDH) release was measured spectrophotometrically, measuring LDH activity in the spent medium of neurones and astrocytes. This was related to the total LDH levels measured after cell lysis, as described in section 2.7.3.

Glutathione reductase activity was measured spectrophotometrically in neurone and astrocyte cell lysates as described in section 2.6.

4.3. Results

4.3.1. Neurone and astrocyte intracellular GSH levels after Aβ25-35 treatment

The neurone and astrocyte intracellular GSH levels were measured after Aβ25-35 or vehicle (control) treatment. In experiments conducted prior to changing the method for measuring protein content, where the protein concentration was measured by the Lowry assay it was found that Aβ35-25 treatment had no effect on neurone GSH levels (Vehicle, 1.64 ± 0.36 nmol/mg protein, Aβ35-25 = 1.73 ± 0.41 nmol/mg protein no significant difference at 5% level, paired t test (n=6)). There was also no difference between astrocyte GSH when astrocytes were treated with vehicle or Aβ35-25 (Vehicle 5.22 ± 1.21 nmol/mg protein, Aβ35-25 4.72 ± 1.11 nmol/mg protein, no significant difference at 5% level, paired t test, n=6.

The following data were normalised to protein content as measured by the Bradford assay (see a discussion on this issue in section 3.3.7) and used vehicle (H_2O) treatment as a control. The neurone intracellular GSH was lowered after Aβ25-35 treatment (Control = 1.32 ± 0.17 nmol/ mg protein; Aβ25-35 = 0.6 ± 0.13 nmol/mg protein) $P<0.05$, paired t test n=3). However, in contrast to other studies (Casley *et al.*, 2002; Abramov *et al.*, 2004), under the culture conditions used in this study, the astrocyte intracellular GSH levels were maintained after Aβ25-35 treatment (Control = 23.5 ± 3.5 nmol/mg protein; Aβ25-35 = 21.8 ± 4.0 nmol/mg protein, n=9, see Figure 4.2. It should also be noted that whilst Aβ25-35 treated neurones showed a decrease in their intracellular GSH levels in repeated experiments, astrocytes actually showed an increase in their GSH levels in 5 of the 9 repeats of this experiment.

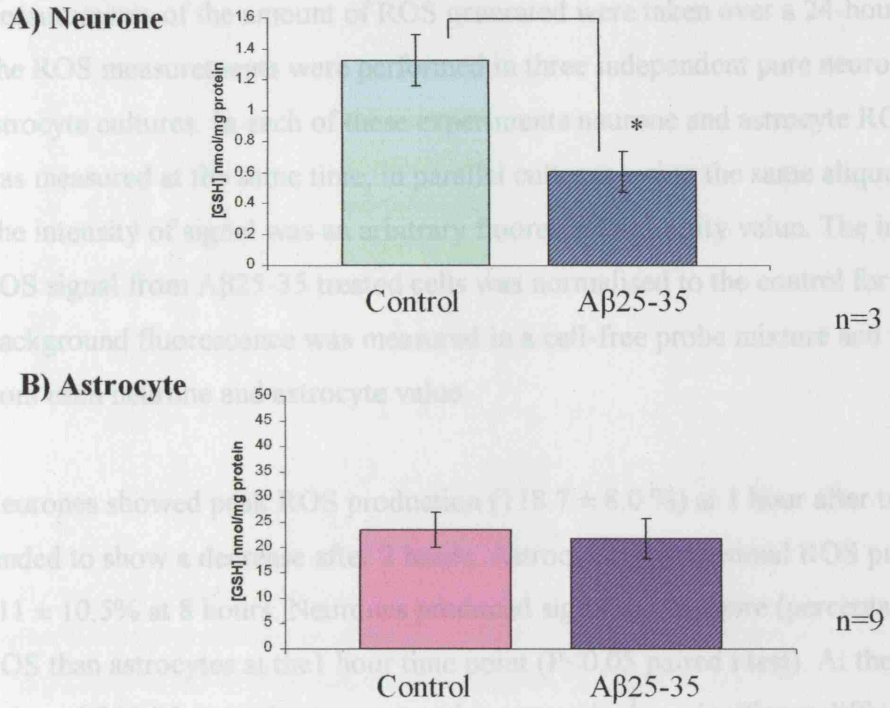

Figure 4.2: Neurone and astrocyte intracellular GSH levels after Aβ25-35 treatment. Neurone GSH is lowered after a 24 hour, 50μM Aβ25-35 treatment but astrocyte GSH levels are maintained. Neurone (Control = 1.32 ± 0.17 nmol/ mg protein; Aβ25-35 = 0.6 ± 0.13 nmol/mg protein) $P < 0.05$, paired t test n=3) Astrocyte (Control = 23.5 ± 3.5 nmol/mg protein; Aβ25-35 = 21.8 ± 4.0 nmol/mg protein n=9). Error bars = SEM

4.3.2. ROS production in neurones and astrocytes in the presence of Aβ25-35

To address the question as to why astrocytes maintained their GSH homeostasis, whereas neurones could not, the ROS generated in the presence of Aβ was measured in the each cell types to assess their "oxidative load". Aβ has been shown to induce ROS production in neurones and astrocytes in culture conditions (Alvarez *et al.*, 2003), however it has not been reported whether there is a difference between the two cell types with regards to the proportional increase in ROS production in the presence of Aβ25-35 compared to their controls. ROS production in neurones and astrocytes was measured using the fluorescent probe 2,7 Dichloroflorescin diacetate (DCF). As this

probe gives a discrete value of the levels of ROS at the time of addition, multiple measurements of the amount of ROS generated were taken over a 24-hour time course. The ROS measurements were performed in three independent pure neurone and pure astrocyte cultures. In each of these experiments neurone and astrocyte ROS production was measured at the same time, in parallel cultures, using the same aliquot of probe. The intensity of signal was an arbitrary fluorescent intensity value. The intensity of the ROS signal from Aβ25-35 treated cells was normalised to the control for each cell type. Background fluorescence was measured in a cell-free probe mixture and subtracted from each neurone and astrocyte value.

Neurones showed peak ROS production (118.7 ± 8.0 %) at 1 hour after treatment, but tended to show a decrease after 2 hours. Astrocytes had maximal ROS production of 111 ± 10.5% at 8 hours. Neurones produced significantly more (percentage of control) ROS than astrocytes at the1 hour time point ($P<0.05$ paired t test). At the other time points, Aβ25-35 treated astrocytes and neurones had no significant difference in the percentage increase compared to their controls. In accordance with other studies (Alvarez *et al.*, 2003) there was a large degree of variation in the percentage increase in ROS compared to controls at each time point, see Figure 4.3.

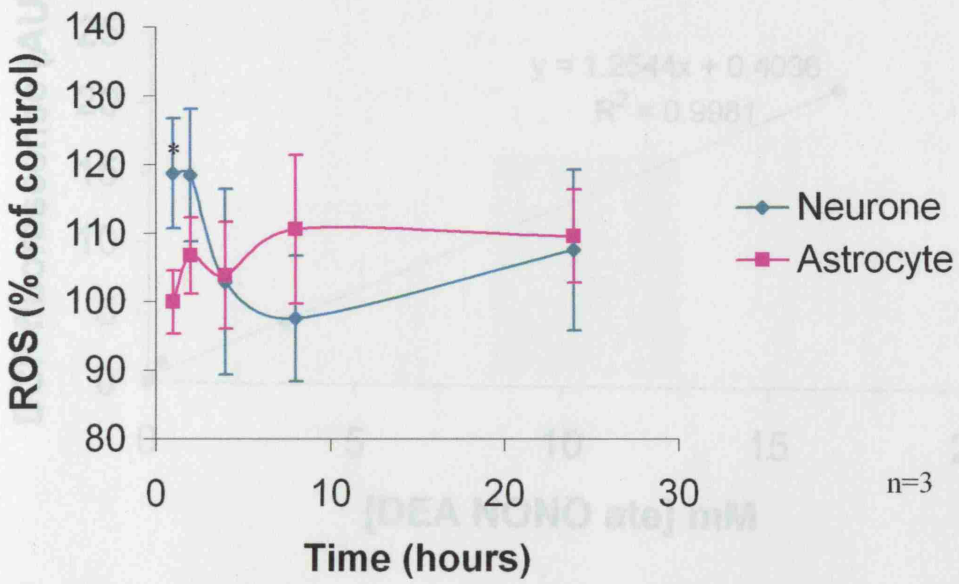

Figure 4.3: ROS production in astrocytes and neurones over a 24 period of Aβ25-35 treatment. Separate neurone and astrocyte cultures were treated with vehicle, H_2O (control) or 50μM Aβ25-35 for 1,2,4,8 or 24 hours. At each time point the cells were incubated with 10μM DCF for 10 minutes, the cells were lysed and the fluorescence intensity was measured at an excitation wavelength set at 502nm and an emission wavelength set at 522 nm. The fluorescence intensities of the Aβ25-35 treated neurones and astrocytes were normalised to their respective vehicle treated controls (The level of ROS in the control cells was expressed as 100%). Neurones showed a higher proportional increase in ROS production than astrocytes 1 hour after treatment relative to their respective controls (* =$P<0.05$ paired t test). At all other time-points there was no significant difference between the ROS generated by neurones and astrocytes relative to controls. n=3 independent experiments.

To ensure that the Aβ25-35 treated neurones and astrocytes were not producing concentrations of ROS capable of saturating the dye, DCF was incubated with a range of concentrations of the NO donor diethylammonium (Z) –1-(N, Ndiethylamino)diazen-1-ium-1,2-diolate (DEA NONO ate) under the same conditions as the cell samples. The intensity of DCF fluorescence maintained linearity, far in excess of the values typically obtained by Aβ25-35 treated neurones and astrocytes (<2.5 arbitrary units AU). See Figure 4.4.

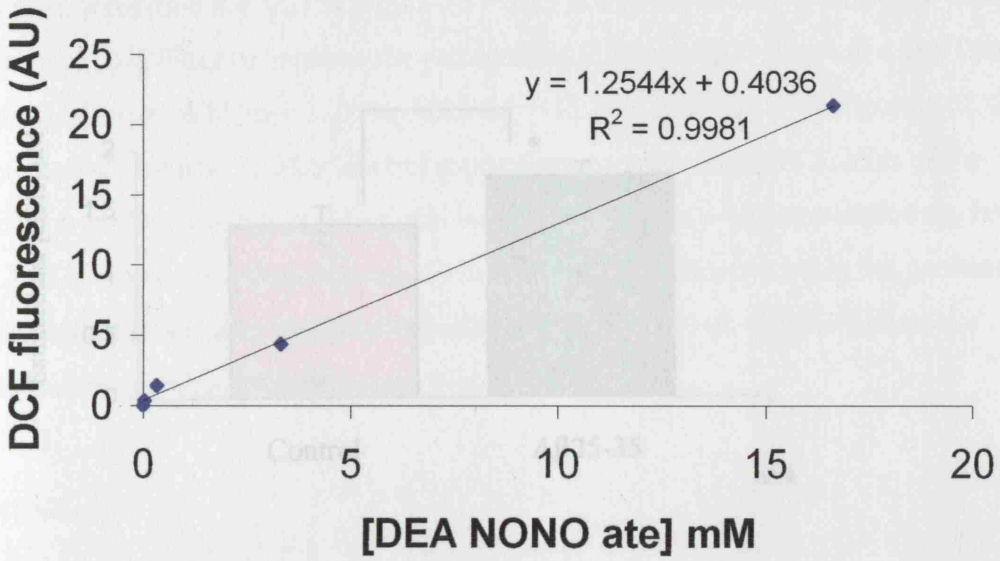

Figure 4.4: DCF fluorescence increases linearly with increasing concentrations of the NO donor DEA NONO ate.

In a 10 μM solution of DCF prepared in HBSS, DEA NONO ate was added to give a final concentration from 0.03 mM to 16 mM. After a 10-minute incubation at 37°C the fluorescence intensity was measured at an excitation wavelength set at 502 nm and an emission wavelength set at 522 nm.

4.3.3. Extracellular GSH after Aβ25-35 treatment

Astrocytes release GSH (Sagara *et al.*, 1993). It was a possibility that to maintain their intracellular GSH levels in the presence of Aβ25-35 astrocytes may release less GSH. Therefore GSH in astrocyte-spent medium, which had been collected from the astrocytes after the 24 hour incubation period with Aβ25-35, was measured by HPLC coupled to electro-chemical detection (section 2.9). The GSH in the medium from Aβ25-35 treated astrocytes was greater than the GSH from the control astrocytes (Control 1.4 ± 0.15 μM, Aβ25-35 = 1.8 ± 0.09 μM, $p < 0.05$ paired t test) see Figure 4.5. It was also possible to detect the glutathione precursor CysGly in both Aβ25-35 treated and control astrocytes, but this could not be accurately quantified because it was eluted too close to the solvent front of Neurobasal medium (see section 2.9.3.4). GSH was not detected in the extracellular medium of neurones.

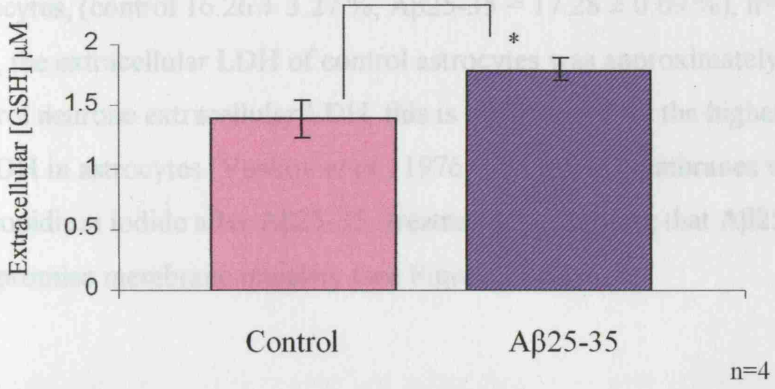

Figure 4. 5: GSH in the extracellular medium of astrocytes after 24 hour Aβ25-35 treatment. Astrocytes were treated with vehicle (Control) or 50µM Aβ25-35 for 24 hours, presented in 1.5ml treatment medium. After treatment the extracellular medium was collected and GSH measured. There was increased GSH in the extracellular medium of astrocytes Aβ25-35 treatment. Control = 1.4 ± 0.15 µM, Aβ25-35 = 1.8 ± 0.09 µM $p<0.05$ paired t test. n=4 independent experiments.

4.3.4. Lactate dehydrogenase (LDH) release from astrocytes and neurones in the presence of Aβ25-35.

A rise in extracellular astrocyte GSH could be due to its leakage through damaged membranes. To test this possibility, the amount of LDH release, a relatively small cytosolic enzyme, was measured from astrocytes. This is widely used as a viability marker, to measure the extent of membrane damage. The LDH assay was also performed on neurone cultures. The data shows the amount of LDH released in the extracellular medium as a percent of the total intracellular LDH.

Fluorescent staining experiments (see Section 3.3.4) had shown that 88 ± 2.7% of dead neurones had propidium iodide permeable membranes. In accordance with this data neurones exhibited increased LDH release into the extracellular medium after Aβ25-35

treatment (control 6.5 ± 3.27 %; Aβ25-35 = 16.7 ± 4.96 %, P<0.05 paired t test n=3). There was no difference between the extracellular LDH of Aβ25-35 treated and control astrocytes, (control 16.26 ± 3.27 %, Aβ25-35 = 17.28 ± 0.69 %), n=9 (Figure 4.6). Of note, the extracellular LDH of control astrocytes was approximately 3 times of the control neurone extracellular LDH, this is likely to reflect the higher intracellular levels of LDH in astrocytes (Venkov *et al.*, 1976). Astrocyte membranes were not permeable to propidium iodide after Aβ25-35 -treatment, confirming that Aβ25-35 did not compromise membrane integrity (see Figure 3.7B).

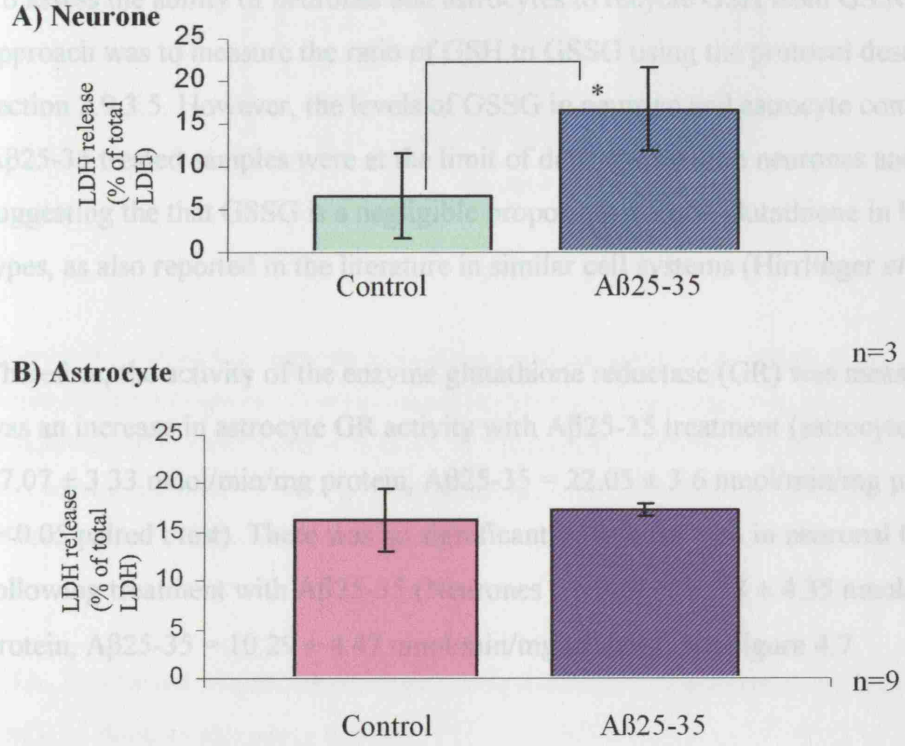

Figure 4.6: LDH release from neurones and astrocytes after 24-hour Aβ25-35 treatment.
Separate neurone and astrocyte cultures were treated with vehicle (control) or 50μM Aβ25-35 for 24 hours. After treatment membrane integrity was assessed by measuring levels of LDH leakage into the extracellular medium from the cells as a percentage of the total LDH in the cell. There was and increase in neurone extracellular LDH after Aβ25-35 treatment but no change in astrocyte extracellular LDH. Neurone control 6.5 ± 3.27 %, Aβ25-35 = 16.7 ± 4.96 % p<0.05 paired t test, n= 3 independent experiments: Astrocyte control 16.26 ± 3.27 %, Aβ25-35 = 17.28 ± 0.69 %, n=9 independent experiments.

4.3.5. Glutathione disulphide (GSSG) reduction in the presence of Aβ25-35.

Both astrocytes and neurones contain glutathione reductase an enzyme which catalyses the reduction of GSSG to GSH.

To assess the ability of neurones and astrocytes to recycle GSH from GSSG, the first approach was to measure the ratio of GSH to GSSG using the protocol described in section 2.9.3.5. However, the levels of GSSG in neurone and astrocyte control and Aβ25-35 treated samples were at the limit of detection in both neurones and astrocytes, suggesting the that GSSG is a negligible proportion of total glutathione in both cell types, as also reported in the literature in similar cell systems (Hirrlinger *et al.*, 2002).

Therefore, the activity of the enzyme glutathione reductase (GR) was measured. There was an increase in astrocyte GR activity with Aβ25-35 treatment (astrocytes control = 17.07 ± 3.33 nmol/min/mg protein, Aβ25-35 = 22.05 ± 3.6 nmol/min/mg protein $p<0.05$ paired t test). There was no significant difference with in neuronal GR activity following treatment with Aβ25-35 (Neurones Control = 12.48 ± 4.35 nmol/min/mg protein, Aβ25-35 = 10.29 ± 4.47 nmol/min/mg protein), see Figure 4.7.

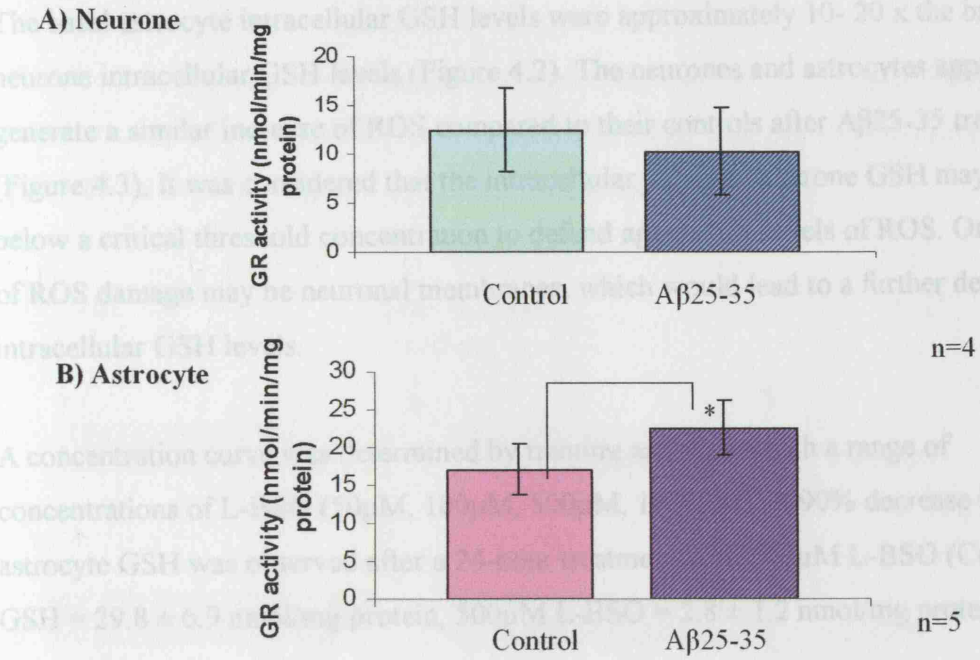

Figure 4.7: Neurone and astrocyte glutathione reductase activity after Aβ25-35 treatment. Astrocytes, but not neurones show an increase in glutathione reductase activity after 24 hour 50μM Aβ25-35 treatment. (Neurones Control = 12.48 ± 4.35 nmol/min/mg, Aβ25-35 = 10.29 ± 4.47 nmol/min/mg n=4; Astrocytes control = 17.07 ± 3.33 nmol/min/mg protein, Aβ25-35 = 22.05 ± 3.6 nmol/min/mg protein * $p < 0.05$ paired t test n=5).

4.3.6. Inhibition of glutamate cysteine ligase with L-buthionine sulfoximine (L-BSO) to deplete astrocyte GSH.

A model was developed in which the astrocyte intracellular GSH was lowered to the same level as basal neurone intracellular GSH, before treatment with Aβ25-35, using the specific glutamate-cysteine ligase inhibitor L-BSO. The model was developed for two reasons, firstly to determine whether *de novo* GSH synthesis was necessary to maintain astrocyte GSH levels in the presence of Aβ25-35 and secondly to test the hypothesis that astrocytes were less vulnerable to Aβ25-35 toxicity than neurones as they could better defend against ROS generated in the presence of Aβ25-35 using their GSH systems.

The basal astrocyte intracellular GSH levels were approximately 10- 20 x the basal neurone intracellular GSH levels (Figure 4.2). The neurones and astrocytes appeared to generate a similar increase of ROS compared to their controls after Aβ25-35 treatment (Figure 4.3). It was considered that the intracellular levels of neurone GSH may be below a critical threshold concentration to defend against the levels of ROS. One target of ROS damage may be neuronal membranes, which would lead to a further decrease in intracellular GSH levels.

A concentration curve was determined by treating astrocytes with a range of concentrations of L-BSO (50μM, 100μM, 500μM, 1000μM). A 90% decrease in astrocyte GSH was observed after a 24-hour treatment with 500μM L-BSO (Control GSH = 29.8 ± 6.9 nmol/mg protein, 500μM L-BSO = 2.8 ± 1.2 nmol/mg protein) See figure 4.8.

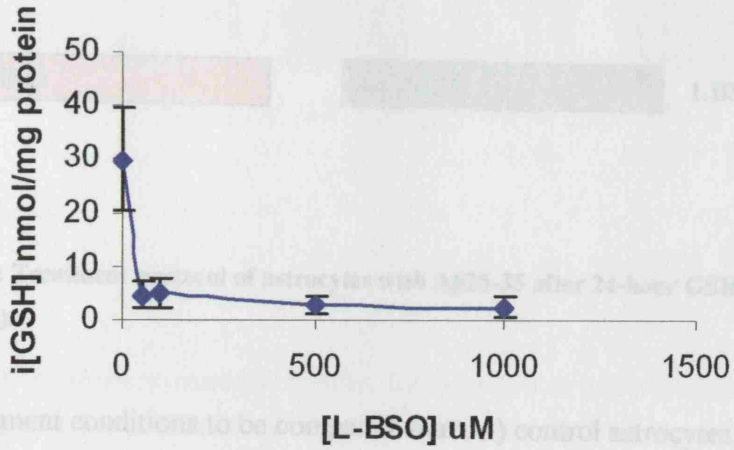

n=3

Figure 4.8: Astrocyte GSH depletion with increasing concentrations of L-BSO.
Astrocytes were treated with 50,100,500 and 1000μM L-BSO presented in treatment medium for 24 hours. After treatments cells were harvested and intracellular GSH was measured. n=3 independent experiments. Error bars= SEM.

4.3.7. Treatment of GSH depleted astrocytes with Aβ25-35

The initial treatment protocol was to treat astrocytes with 500 μM L-BSO for 24 hours, in order to reproduce as closely as possible the neuronal GSH levels, then to treat with Aβ25-35 for 24hours (figure 4.9) **(L-BSO protocol A)**.

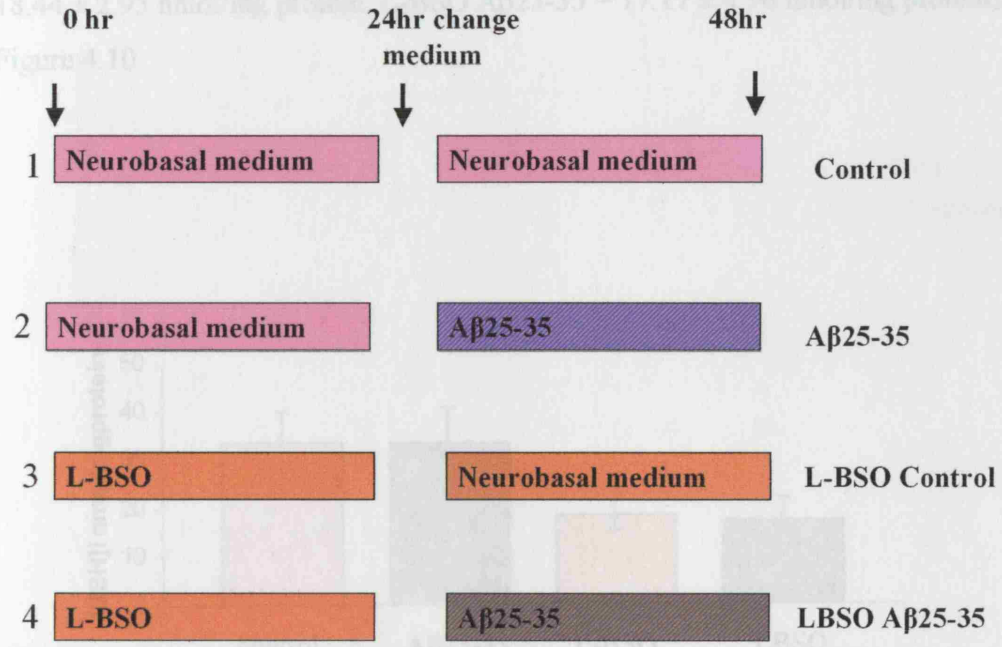

Figure 4.9: Treatment protocol of astrocytes with Aβ25-35 after 24-hour GSH depletion (L-BSO protocol A).

The treatment conditions to be compared were: 1) control astrocytes, vehicle treated (control), 2) Aβ25-35 treated astrocytes (Aβ25-35), 3) L-BSO treated astrocytes (L-BSO control) and 4) L-BSO pre-treated astrocytes followed by Aβ25-35 treatment (L-BSO Aβ25-35).

It was observed at the end of this treatment that the astrocyte GSH levels in L-BSO treated astrocytes were approximately 50% of the control astrocytes (control 33.71 ± 6.31 nmol/mg protein, control L-BSO = 18.44 ± 2.95 nmol/mg protein n=3). It was considered possible that over the second 24-hour period of this protocol, GSH synthesis

had begun to recover after the 90% depletion described in section 4.3.6. This was probably due to GCL turnover (Ali-Osman *et al.*, 1995). In addition, replacement of the L-BSO medium with fresh medium would provide astrocytes with a fresh supply of GSH precursors that would help them to recover their GSH levels. There was no difference in the GSH levels of L-BSO control astrocytes and L-BSO Aβ25-35 astrocytes at the 5% significance level as determined by a paired t test (control L-BSO = 18.44 ± 2.95 nmol/mg protein, L-BSO Aβ25-35 = 17.17 ± 4.96 nmol/mg protein), Figure 4.10.

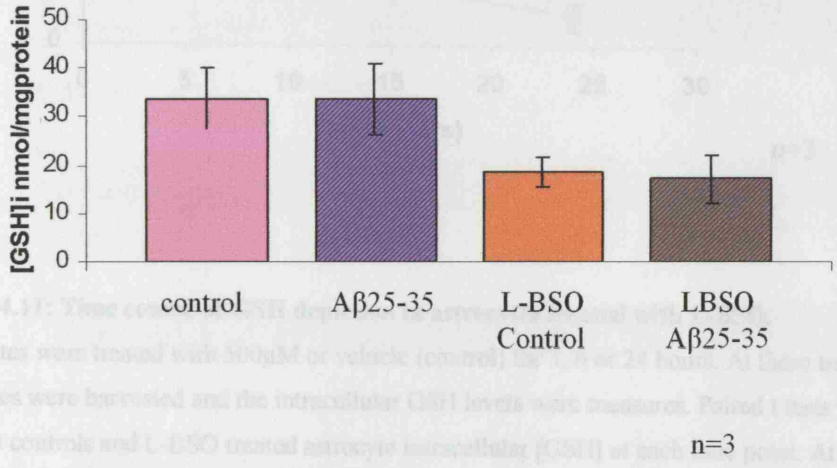

Figure 4.10: Astrocyte intracellular GSH levels after a 24-hour pre-treatment with 500μM L-BSO followed by a 24 hour, 50μM Aβ25-35 treatment. Control = 33.71 ± 6.31 nmol/mg protein, Aβ25-35 + 33.55 ± 7.40 nmol/mg protein, Control L-BSO = 20.87 ± 2.9 nmol/mg protein, L-BSO Aβ25-35 = 21.73 ± 3.3 nmol/mg protein. n=3 independent experiments. Error bars = SEM.

To adjust the treatment protocol a time-course of the GSH depletion induced by L-BSO in astrocytes was conducted. GSH levels in astrocytes at 3, 6 and 24 hours were compared between control and L-BSO treated astrocytes (Figure 4.11). At 3 hours there was a significant difference between control and L-BSO treated astrocyte GSH levels ($p < 0.05$ paired t test). The difference between the GSH levels in L-BSO treated and control astrocytes increased over a 24-hour period.

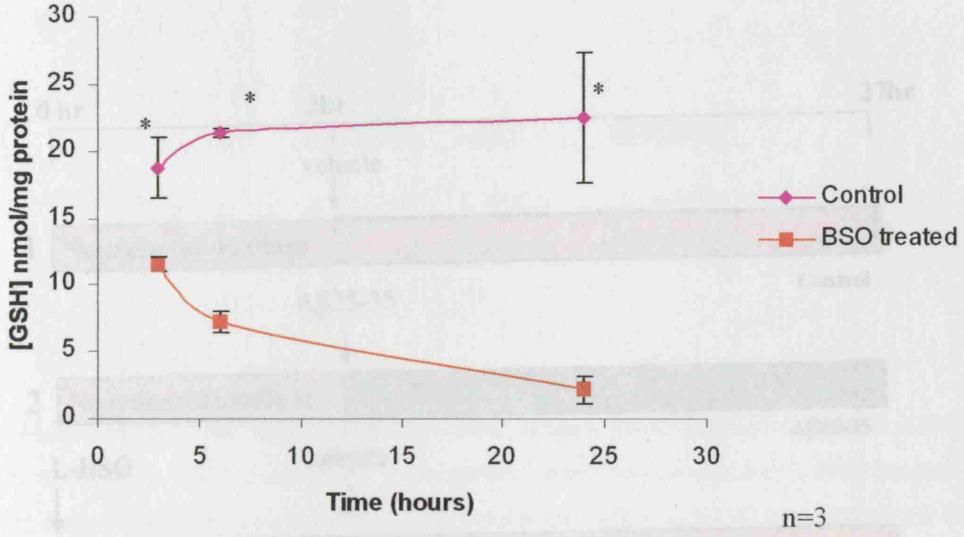

Figure 4.11: Time course of GSH depletion in astrocytes treated with L-BSO.
Astrocytes were treated with 500μM or vehicle (control) for 3, 6 or 24 hours. At these time points the astrocytes were harvested and the intracellular GSH levels were measures. Paired t tests were performed between controls and L-BSO treated astrocyte intracellular [GSH] at each time point. At all time points the L-BSO treated astrocytes contained lower levels of GSH than their corresponding controls $p<0.05$. n=3 independent experiments

To adapt the protocol, a three-hour L-BSO pre-treatment was given to the astrocytes before Aβ25-35 treatment. In this protocol Aβ25-35 or vehicle was added to wells by removing a 500μl aliquot into a sterile Eppendorf, adding the peptide or vehicle, vortexing and returning to the well. In this way L-BSO remained present during the final 24-hour treatment with Aβ25-35 or vehicle (Figure 4.12).

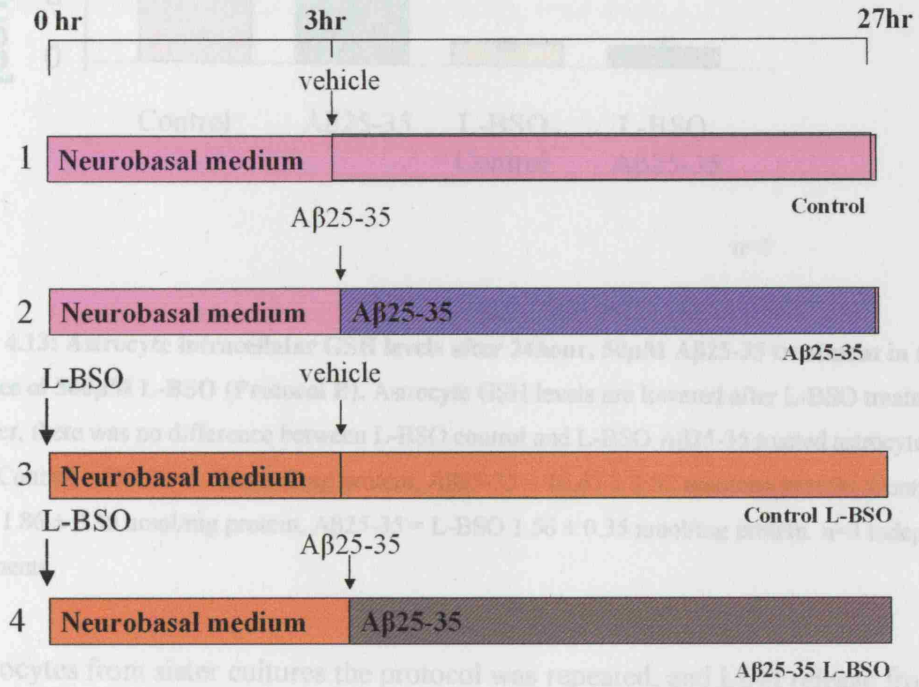

Figure 4. 12: Protocol for treatment of astrocytes with Aβ25-35 in the presence of L-BSO. (L-BSO protocol B).

Using this protocol the GSH levels of the L-BSO treated control astrocytes were found to be lowered to 1.74 ± 0.3 nmol/mg protein (control = 17.1 ± 2.5 nmol/mg protein). There was no significant difference between L-BSO control and L-BSO Aβ25-35 astrocytes, paired t-test at 5% level (L-BSO Aβ25-35 = 1.7 ± 0.5 nmol/mg protein). As with previous experiments there was no difference in the intracellular GSH levels of astrocytes that were treated with GSH in the absence of L- BSO with their controls (control = 17.1 ± 2.5 nmol/mg protein, Aβ25-35 = 16.9 ± 4.9 nmol/mg protein). See Figure 4.13.

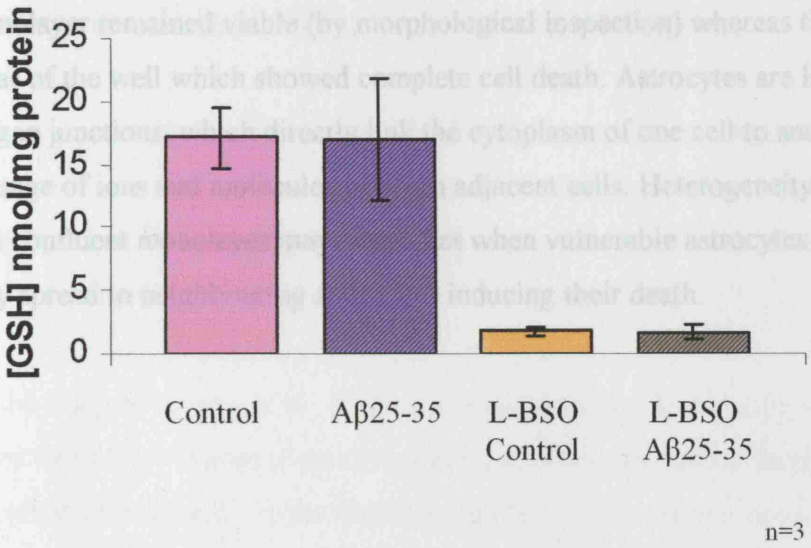

Figure 4.13: Astrocyte intracellular GSH levels after 24hour, 50μM Aβ25-35 treatment in the presence of 500μM L-BSO (Protocol B). Astrocyte GSH levels are lowered after L-BSO treatment. However, there was no difference between L-BSO control and L-BSO Aβ25-35 treated astrocyte GSH levels. Control = 18.12 ± 1.62 nmol/mg protein, Aβ25-35 = 16.67 ± 2.93 nmol/mg protein, Control L-BSO = 1.86 ± 0.39 nmol/mg protein, Aβ25-35 = L-BSO 1.56 ± 0.35 nmol/mg protein. n=3 independent experiments.

In astrocytes from sister cultures the protocol was repeated, and LDH release from the four treatments was measured. In this instance there was no increase in LDH release from L-BSO and L-BSO Aβ25-35 treated astrocytes and in fact there appeared to be a decrease in LDH leakage in Aβ25-35 treated astrocytes (Control = 13.56 ± 2.41%, Aβ25-35 = 5.99 ± 2.3%, BSO control = 14.35 ± 3.19%, BSO Aβ25-35 = 5.01± 0.22% n=3). In previous experiments astrocyte LDH leakage had been the same from Aβ25-35 treated and control astrocytes (see figure 4.6). It was proposed that the lowering of the amount of LDH released from Aβ25-35 treated astrocytes in this series of experiments may be an artefact. The L-BSO protocol B was repeated on astrocytes seeded onto glass coverslips so that cell death could be measured by assessment of nuclear morphology and the permeability of membranes to propidium iodide (see section 2.7.1). However, in repeated experiments using equivalent treatments, both the control L-BSO and Aβ25-35 L-BSO treatments complete cell death was observed at the end of the treatment period, indicating a greater vulnerability of astrocytes seeded on glass coverslips to GSH

depletion. Of note, in populations of astrocytes seeded in wells, after increased treatment time with L-BSO (> 36 hours), it was observed that patches of the astrocyte monolayer remained viable (by morphological inspection) whereas there were other areas of the well which showed complete cell death. Astrocytes are linked to each other by gap junctions, which directly link the cytoplasm of one cell to another allowing free passage of ions and molecules between adjacent cells. Heterogeneity between astrocytes in a confluent monolayer may mean that when vulnerable astrocytes die, noxious factors may spread to neighbouring astrocytes inducing their death.

4.4 Discussion

4.4.1 GSH is maintained in astrocytes but not in neurones.

The present study has demonstrated that after treatment with Aβ25-35 intracellular GSH levels were maintained in astrocytes but not in neurones. The maintenance of astrocyte GSH levels is in contrast with the previous two published studies (Abramov *et al.*, 2003; Casley *et al.*, 2002).

In the study by Casley *et al.*, 2002, astrocyte GSH was lowered by 41%. Astrocytes were treated in medium containing serum, whilst in the present study a serum free supplement was used. As discussed in chapter 3, the culture conditions may affect the astrocyte response to Aβ25-35. Factors in serum maintain astrocytes in a non-activated state, with a flat polygonal morphology (Ogino *et al.*, 1992; Pike *et al.*, 1996). Serum deprivation for 24 hours is a method for inducing stellation in astrocytes (Morrison and De Vellis, 1983). The cells used in the present study were treated in conditions where serum was substituted with B27 supplement, and showed a slight darkening of cell bodies and the appearance of a few distinct processes (see Figure 3. 2b). In a recent study, it has also been shown that cortical astrocyte cultures deprived of serum for 24 - hours, show an increase in intracellular GSH levels after this period. This rise in intracellular GSH did not occur until after 12 hours in the serum free medium, suggesting that serum withdrawal may affect astrocyte GSH metabolism by a mechanism independent of GSH precursor supplementation (Adachi *et al.*, 2006)

However, it is possible that the methods used to measure GSH in the study of Casley *et al.*, 2002 may account for the different outcome on astrocyte GSH levels to the data presented in this study. Prior to the method used for measuring protein was changed to the Bradford assay, astrocyte samples, which had been normalised to Lowry protein values showed a significant lowering of GSH levels after Aβ25-35 treatment (by 22% $p < 0.05$ paired t test $n=6$), but as demonstrated in chapter 3, the data set were not controlled for protein levels. In the study conducted by Casley *et al.*, 2002, the GSH concentration was related to cellular protein measured by the Lowry assay. This may have contributed to the lowered GSH levels in the presence of Aβ25-35.

In the study of Abramov *et al.*, 2003, cortical astrocyte GSH levels were lowered by 55% after Aβ25-35 treatment. Astrocyte GSH levels were measured in individual cells using the fluorescent probe Monochlorobimane (MCB), astrocytes were treated in medium containing serum.

MCB measures GSH-MCB conjugate fluorescence. It is more specific than other bimanes to measure GSH over other thiols as it requires glutathione transferase for conjugation to GSH. To demonstrate specificity it was shown that inhibiting glutathione transferase with ethacrynic acid or lowering GSH levels with L-BSO lowered the fluorescent signal given by the probe in astrocytes (Keelan *et al.*, 2001). However, as discussed in section (1.3.4.1.), glutathione transferase can also conjugate GSH to other substrates generated in the presence of Aβ, for example, NO or hydroxynonenal (HNE). Therefore a decrease in GSH-MCB fluorescence may reflect a functional competitive inhibition of glutathione transferase rather than a decrease of cellular GSH levels.

4.4.2 Upregulation of GSH synthesis and recycling in mild oxidative conditions in astrocytes; a common mechanism

The data acquired in this study seems to fit a pattern found in astrocytes when treated with a mild oxidative insult. GSH levels are increased, or maintained, in astrocytes after a variety of mild oxidative conditions. For example, after treatment with DETA-NO (a nitric oxide donor (Gegg *et al.*, 2003), lipopolysaccharide, (a bacterial cell wall component that induces NO production in astrocytes)(Garcia Nogales *et al.*, 1999), H_2O_2 (Sagara *et al.*, 1996), and ethanol, (which has been shown to increase general ROS production in astrocytes)(Rathinam *et al.*, 2006), GSH levels are maintained or increased (See Figure 4.14).

There is evidence to suggest that GSH synthesis is upregulated under oxidative conditions. Glutamate cysteine ligase (GCL) activity is increased in astrocytes treated with DETA-NO (Gegg *et al.*, 2003). The availability of the GSH precursor cysteine limits GSH synthesis (See section (1.3.4.4.). Astrocytes show increased rate of cysteine uptake in the presence of H_2O_2 (Sagara *et al.*, 1999). However, in this study GSH synthesis did not appear to be crucial for the maintenance of GSH levels as inhibition of

GCL with L-BSO did not impair the astrocytes ability to maintain GSH levels after Aβ25-35 treatment.

		Synthesis		Recycling		Efflux		
Insult	[GSH] intra	GCL/GS activity	Cystine uptake	GR activity	PPP activity	[GSH] extra	γ-GT activity	Ref
DETA-NO (NO) *	↑	GCL ↑	-	-	-	↑	↑	Gegg *et al.*, 2003
EtOH *	↔	GS ↔	-	↑	-	↑	↑	Watts *et al.*, 2005; Rathinam *et al.*, 2006
Glucose/glucose oxidase (H_2O_2)	↑	-	↑	-	-	↑	-	Sagara *et al.*, 1996
LPS (NO)	↑	-	-	-	Expression of G6PD ↑ Activity of G6PD	-	-	Garcia Nogales *et al.*, 1999
$ONOO^-$	-	-	-	-	↑	-	-	Garcia Nogales *et al.*, 2003
Aβ25-35 (Various) *	↔	↔	-	↑	-	↑	-	

Figure 4.14: Effects of oxidative insults on astrocyte GSH homeostasis. A summary of the effects of a variety of oxidative insults on astrocyte intracellular GSH levels. Radical species produced by insult is shown in brackets. * denotes studies in which the same treatment as astrocytes caused significant neurone death.

GSH recycling from GSSG may be enhanced in the presence of a mild oxidative insult. In studies by other groups, where astrocytes were treated with ethanol, glutathione reductase activity was increased (Watts *et al.*, 2005). In the present study glutathione reductase activity was also increased in astrocytes treated with Aβ25-35.

In the current study there was no effect on the GR activity in neurones. Both neurones and astrocytes have a highly efficient GSH recycling system. The ratio of GSH: GSSG has been estimated to be as low as 100:2 in astrocytes and 100:2.5 in neurones (Hirrlinger *et al.*, 2002). In the present study the amount of GSSG in astrocytes and neurones was at the limit of detection, suggesting a very low GSSG:GSH ratio. It has previously been shown that neurones contain relatively higher levels of GR than astrocytes (Gutterer *et al.*, 1999). The observation that neurones did not upregulate their GR activity may be due in part to a proportion of the neurones dying over the treatment period. In the studies by other groups highlighted in table 4.14 (marked with *), the concentration of toxin that generated these changes in astrocytes, caused a significant degree of cell death in neurones, however, Aβ25-35 in sub-lethal doses caused an increase in GR activity in neurones (White *et al.*, 1999). This suggests that some of the pathways required to maintain GSH levels in astrocytes may also be present in neurones, yet neurones have a lower critical threshold for oxidative damage and these mechanisms do not operate in damaged cells.

An upregulation of GR may depend on the availability of its cofactor NADPH which may become rate limiting in conditions of stress. The main source of NADPH within a cell is through the pentose phosphate pathway (PPP) (See figure 4.15). There are two NADPH producing steps in this pathway. The first is the conversion of glucose-6-phosphate to 6–phosphogluconolactone, which is catalysed by the enzyme glucose-6-phosphate dehydrogenase (G6PD) and is rate limiting for the pathway. The second is the conversion of 6-phosphogluconolactone to 6-phoshogluconate, catalysed by the enzyme 6-phosphogluconate dehydrogenase (6PGD). Increased expression and activity of G6PD has been demonstated in astrocytes after treatment with LPS (Garcia- Nogales *et al.*, 1999). This may be a direct oxidative effect on these enzymes, or a response to increased utilisation of NADPH by the cells. It has been shown that decreasing cellular NADPH levels increases neuronal PPP activity in a dose dependent manner (Ben Yoseph *et al.*, 1995). Astrocytes have greater basal PPP activity than neurones but at sub-lethal doses of $ONOO^-$ neurones have been demonstrated to increase their PPP activity and NADPH production (Garcia Nogales *et al.*, 2003).

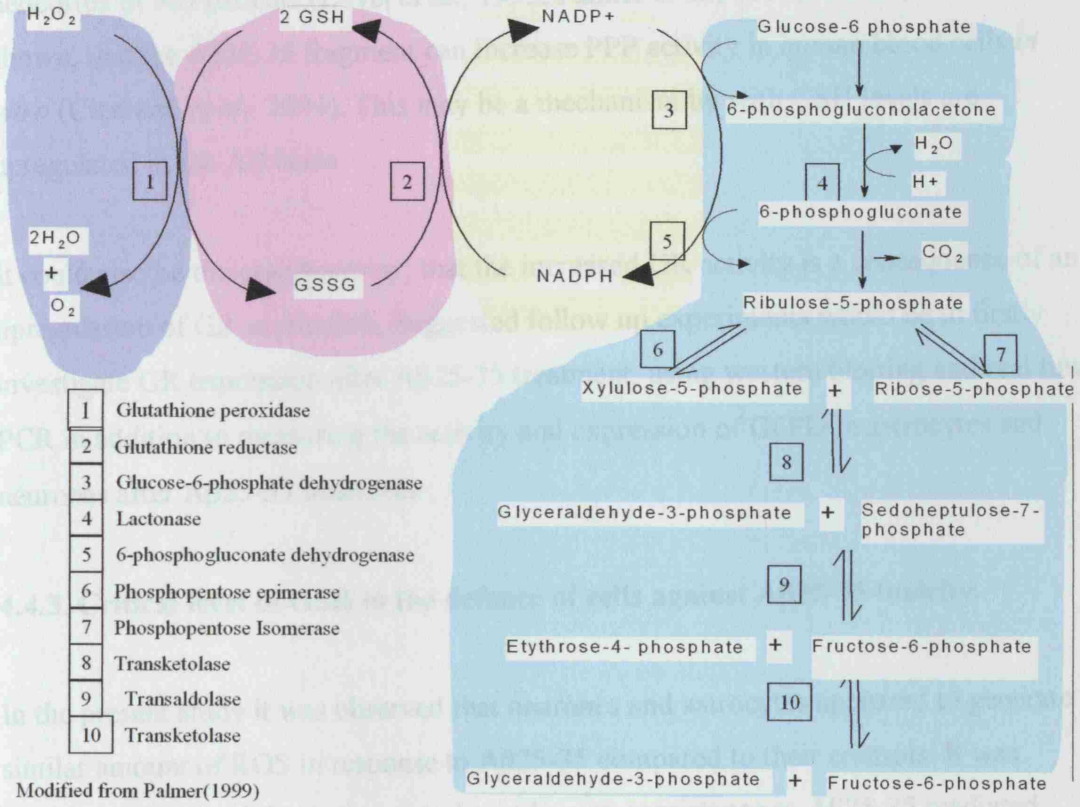

Figure 4.15: The Pentose Phosphate Pathway and GSH, GSSG recycling. The PPP (blue) generates NADPH, which may increase the GSSG to GSH recycling capability of astrocytes. Modified from Palmer, 1999.

Interestingly, increased activity of G6PD was shown in post-mortem samples from the neocortex of AD patients (Lovel *et al.*, 1995; Palmer *et al.*, 1999). It has also been shown, that the Aβ31-35 fragment can increase PPP activity in human blood cells *in vitro* (Clementi *et al.*, 2004). This may be a mechanism by with GSH levels are upregulated in the AD brain.

It could also be the case however, that the increased GR activity is a consequence of an upregulation of GR expression. Suggested follow up experiments would be to firstly investigate GR expression after Aβ25-35 treatment, using western blotting and real time PCR in addition to measuring the activity and expression of G6PD in astrocytes and neurones after Aβ25-35 treatment.

4.4.3. Critical level of GSH in the defence of cells against Aβ25-35 toxicity.

In the present study it was observed that neurones and astrocytes appeared to generate a similar amount of ROS in response to Aβ25-35 compared to their controls. It was therefore postulated that astrocytes showed greater resistance to Aβ25-35 mediated toxicity because they had higher basal GSH levels to defend against ROS. The astrocytes used in the present study had 10 times the amount of GSH as neurones. It was attempted to generate an astrocyte model where the astrocytes were depleted of their GSH stores so that they had the same basal GSH as neurones levels at the point of treatment to investigate whether the astrocytes would still be able to maintain their GSH levels and to test whether astrocytes with lower intracellular GSH levels would be more vulnerable to Aβ25-35 toxicity.

In the initial treatment protocol, astrocyte GSH was lowered to 10% of control levels using the specific inhibitor of GCL, L-BSO. The medium containing L-BSO was removed, the cells washed, and fresh medium was added to the cells. Both Aβ25-35-treated and vehicle-treated astrocytes were able to re-synthesise their GSH to about 50% of control levels within the 24-hour period. This was in agreement with studies conducted on glioma cells that showed a re-synthesis of GSH and increase in γ-

glutamate cysteine ligase synthesis after L-BSO treatment on provision of fresh medium (Ali-Osman *et al.*, 1996). It had previously been shown that ATP levels in astrocytes are significantly decreased after Aβ25-35 treatment (Casley *et al.*, 2002). Both steps of GSH synthesis require ATP (See section 1.3.4.4.). It was predicted that GSH synthesis in metabolically compromised astrocytes would be impaired. However, as the re-synthesis of glutathione was the same in astrocytes recovering from L-BSO treatment in medium containing Aβ25-35 as vehicle, it was concluded that GSH synthesis is not impaired in the presence of Aβ25-35.

The second treatment protocol attempted to prevent GSH re-synthesis during treatment with Aβ25-35 to assess whether GSH synthesis was required to maintain GSH levels in astrocytes in the presence of Aβ25-35. Again astrocytes were pre-treated with L-BSO to lower GSH levels compared to controls, prior to Aβ25-35 treatment, but this time the medium was not replaced, in order to avoid providing astrocytes with fresh GSH precursors and removing the inhibitor. Also in this case there was no significant difference in GSH levels between Aβ25-35 and vehicle treated astrocytes, suggesting that *de novo* GSH synthesis was not essential to maintain GSH levels over this period.

However, the models generated in this study did not fully meet the initial aim, which was test the toxicity of Aβ25-35 on astrocytes that contained comparable GSH levels to neurones. Figure 4.16 gives a schematic representation of the astrocyte GSH levels in the two models that used L-BSO to deplete astrocyte GSH levels over the 24-hour period in which they were treated with Aβ following 1) a 24 hour pretreatment with L-BSO followed by Aβ25-35 treatment in fresh medium and 2) a pre-treatment with L-BSO followed by the 24 hour Aβ25-35 treatment in medium containing L-BSO. It also shows a representation of the neurone GSH levels (relative to astrocyte levels) to highlight the limitations of this model. To lower astrocyte GSH levels to the same level as neurone GSH at the start of treatment and throughout treatment would require a 24-hour pre-treatment with L-BSO followed by a 24-hour treatment with Aβ25-35 in the presence of L-BSO. However 2 times 24-hour treatments with L-BSO lead to extensive astrocyte cell death.

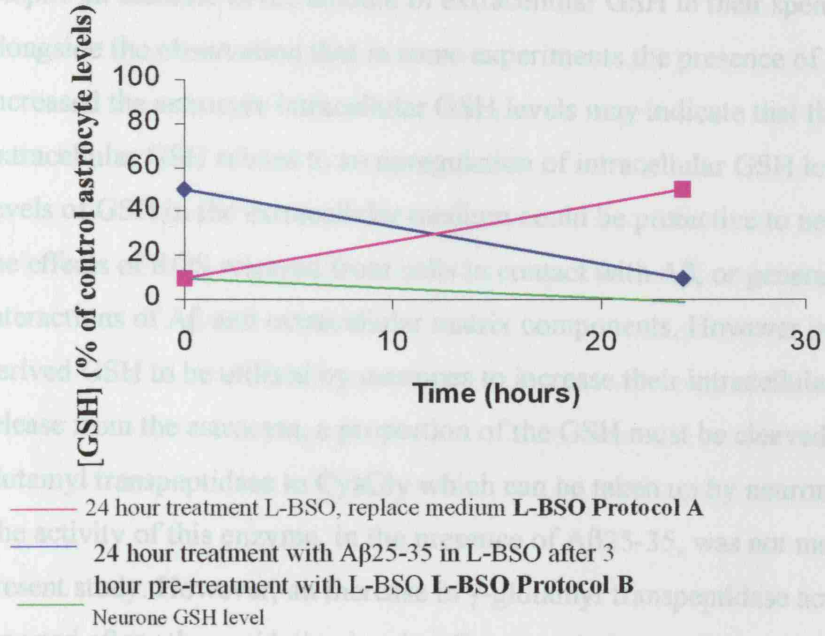

Figure 4.16: Schematic representation of relative levels of GSH in the two protocols using L-BSO to deplete astrocyte GSH. Control neurone GSH levels are represented as a proportion of typical astrocyte GSH levels

4.4.4. GSH Efflux from astrocytes in oxidative conditions

The present study showed higher levels of GSH in the extracellular medium of Aβ25-35 treated astrocytes compared to controls, which is similar to the observation of an increase in extracellular GSH in the medium from astrocytes under other oxidative conditions (Gegg *et al.*, 2003; Sagara *et al.*, 1999; Watts *et al.*, 2005).

Extracellular GSH levels, like intracellular GSH, are determined by a balance of various factors such as 1) the amount of intracellular GSH, 2) the rate of GSH efflux, 3) the rate of GSH cleavage to dipeptides and its component amino acids, 4) the preservation of GSH in its reduced form by complementary antioxidants or metal chelators in the extracellular environment and 5) the amount of ROS in the extracellular environment.

GSH efflux rate has been proposed to relate to the levels of GSH within the cell (Sagara *et al.*, 1999). In the present study astrocyte intracellular GSH levels were maintained despite an increase in the amount of extracellular GSH in their spent medium. This alongside the observation that in some experiments the presence of Aβ25-35 actually increased the astrocyte intracellular GSH levels may indicate that the increase in extracellular GSH relates to an upregulation of intracellular GSH levels. Increased levels of GSH in the extracellular medium could be protective to neurones by buffering the effects of ROS released from cells in contact with Aβ, or generated through interactions of Aβ and extracellular matrix components. However in order for astrocyte derived GSH to be utilised by neurones to increase their intracellular GSH levels, on release from the astrocyte, a proportion of the GSH must be cleaved by the enzyme γ-glutamyl transpeptidase to CysGly which can be taken up by neurones (section 1.3). The activity of this enzyme, in the presence of Aβ25-35, was not measured in the present study. However, an increase in γ-glutamyl transpeptidase activity has been reported after other oxidative insults (Gegg *et al.*, 2003; Watts *et al.*, 2005; Rathinam *et al.*, 2006).

4.5 Conclusions.

In conclusion, astrocytes, but not neurones are capable of maintaining their GSH levels in the presence of Aβ25-35. This appears to be largely due to the great capability of astrocytes to recycle GSH from GSSG and appears to fit a pattern where astrocytes can upregulate their GSH levels in the presence of oxidative insults. This would serve not only to protect the astrocytes, but as it also appears to coincide with an increased level of extracellular GSH, which could protect neurones from ROS in their extracellular environment. Although astrocytes and neurones, when treated with Aβ25-35, appear to show a proportionally similar increase in ROS, neurones in cell culture conditions may have GSH levels below a critical level to defend against these ROS.

Chapter 5: The neuroprotective potential of astrocyte derived glutathione.

5. The neuroprotective potential of astrocyte derived GSH

5.1. Introduction

In the brain neurones and astrocytes receive a continual supply of cysteine, glycine and glutamate from the circulation. Neurones and astrocytes in culture conditions, however, are presented with a limited amount of substrates for GSH synthesis in Neurobasal medium (Cysteine 10μM, glycine 400μM, Glutamine- for glutamate synthesis 500μM (see section (1.3.2.)). As discussed in section 1.3.4.4 cysteine availability is rate limiting for GSH synthesis (Sagara *et al.*, 1993). As the medium used in this study does not contain antioxidants but contains trace levels of ferrous ions, a proportion of cysteine is likely to be present in its oxidised form cystine (Hua Long and Halliwell, 2001). Astrocytes, unlike neurones, can take up cystine as well as cysteine, therefore astrocytes can better utilise the GSH precursors available in cell culture medium for their GSH synthesis. As described in section (1.3.4.5) neurones utilise cysteinylglycine delivered by astrocytes as a source of cysteine. Neurones have been shown to increase intracellular GSH when co-cultured with astrocytes (Bolanos *et al.*, 1995; Dringen *et al.*, 1998). It is postulated here that neuronal GSH synthesis may be limited in culture conditions, where they do not receive astrocyte-derived support, by cysteine availability.

In the experiments described in this chapter the first aim was to provide neurones with the precursors they require for GSH synthesis, in order to raise neuronal intracellular levels to the maximum in culture conditions and so that substrate availability was not a limiting factor for neurones to maintain their GSH homeostasis in the presence of Aβ25-35.

The second aim was to assess the upregulation of neurone GSH by GSH precursors derived from control astrocytes compared to Aβ25-35 treated astrocytes.
In the previous chapter it was demonstrated that there was greater GSH in the extracellular medium of Aβ25-35 treated astrocytes compared than control astrocytes. Neurones cannot take up or directly cleave GSH; rather they rely on a supply of

cysteinylglycine (Dringen *et al.*, 1998). Although cysteinylglycine has electrochemical properties and can be detected by electrochemical detection (Gegg *et al.*, 2002), the amount of cysteinylglycine could not be accurately measured in the Neurobasal medium used in this study by the HPLC techniques used in this project because the cysteinylglycine eluted too closely to the solvent front. Studies by other groups have reported that in astrocytes increased γ glutamyl transpeptidase activity correlates with the increased extracellular GSH release associated with NO or EtOH treatments, as presented in Figure 4.14 (Gegg *et al.*, 2003; Rathinam *et al.*, 2005). Watts *et al.*, 2005 used neurones co-cultured with astrocytes and showed that astrocytes treated with ethanol released greater levels of GSH and had higher γ-glutamyl transpeptidase activity than control astrocytes and the neurones in these conditions had higher intracellular GSH levels than neurones co-cultured with control astrocytes. In this project it is proposed that the intracellular GSH measured in neurones after incubation in astrocyte conditioned medium can be an indicator of "usable" GSH derivatives in astrocyte extracellular medium.

The third aim was to assess whether astrocyte derived GSH could protect neurones from Aβ25-35 toxicity. Astrocyte derived GSH could have a dual protective effect on neurones treated with Aβ25-35. Firstly the GSH released from astrocytes that is not cleaved to cysteinylglycine, could act as an extracellular antioxidant, protecting neurones from extracellularly derived ROS. Secondly, cleaved GSH could be taken up and re-synthesised by neurones in the cytosol to defend against intracellularly generated ROS.

However, as described in section 1.3.5.2 astrocytes in an activated state as observed in the presence of Aβ25-35 show a different spectrum of protein expression and release numerous soluble factors, including some potentially neurotoxic compounds such as NO, $O_2^{-\bullet}$ (Hu *et al.*, 1998; Abramov *et al.*, 2004). The fourth aim of the experiments presented in this chapter was to generate a model in which the overall balance of protection versus neurotoxicity of astrocyte derived factors could be assessed.

There is to date one group that has sought to determine whether astrocytes are protective or neurotoxic to neurones in the presence of Aβ. Two of the three papers produced by

the group have assessed the effect of Aβ25-35 on neurones in the presence of astrocytes by using mixed neurone astrocyte hippocampal cultures that were compared to pure neurone hippocampal cultures (Domenici *et al.*, 2002; Paradisi *et al.*, 2004). In these studies it was found that the presence of astrocytes and Aβ25-35 caused more damage to neurite morphology than Aβ25-35 on pure neurones. However, there are problems comparing mixed cultures to pure cultures, as astrocytes are highly involved in neurone development (Banker *et al.*, 1980). For example, in the study of Paradisi *et al.*, 2004, it was noted that in the absence of Aβ25-35, neurones grown on an astrocyte monolayer exhibited a greater volume of neuritic tree than neurones grown in the absence of astrocytes. In these studies they were effectively comparing non-controlled neurones.

However, also included in the study, Paradisi *et al.*, 2004, compared the response of Aβ25-35 treated hippocampal neurones co-cultured with control astrocytes or Aβ25-35 treated astrocytes in inserts. Using inserts is an appropriate method of co-culture in the presence of Aβ25-35 as it allows the two cell types to be treated separately and for diffusible factors to pass through the pores of the inserts between cell types. This set of experiments suggested that non-treated astrocytes could protect neurones, but Aβ25-35 treated astrocytes could not. The neurones used in the study of Paradisi and colleagues were from a hippocampal source and were treated on DIV3, are relatively immature neurones for use in cell culture models of Aβ25-35 mediated toxicity.

The intercellular signalling pathways between neurones and astrocytes are probably bi-directional *in vivo*. However, in the present study, in the first instance, it was intended to isolate and investigate astrocyte to neurone signalling and to develop an astrocyte conditioned medium protocol, which could be used to assess the neurotoxic/ neuroprotective effect of Aβ25-35 induced-astrocyte derived factors on more developed cortical neurone cultures than those used in the study of Paradisi *et al.*, 2004.

5.2 Methods

Neurones and astrocytes were prepared as described in section 2.2. For GSH experiments neurones were seeded at a density of 10^6 cells per well of a 6-well plate. For cell toxicity experiments neurones were seeded at a density of 10^5 cells per coverslip. Cells were cultured in Neurobasal medium supplemented with B27 and 2mM glutamine.

The degree of cell death following Aβ25-35 treatment was assessed in neurones and astrocytes by examining nuclear morphology and permeability of the membrane to propidium iodide as described in section 2.7.1.

GSH was measured using HPLC coupled to electrochemical detection as described in section 2.9.3.

5.3. Results

5.3.1. Development of an astrocyte conditioned medium (ACM) protocol

Neurones and astrocytes signal bi-directionally between each other. The premise for setting up a conditioned medium protocol was to firstly to specifically study astrocyte to neurone signalling in the absence of neurone to astrocyte signalling. Secondly, this approach allowed astrocytes to receive a different treatment to the neurones on which their conditioned medium was to be placed to compare the effects of control astrocytes (control ACM) with Aβ25-35 treated astrocytes (Aβ25-35 ACM) on neurones.

Astrocytes were incubated with Aβ25-35 for 24hours (treatment period), at the end of this period the cells were washed and the medium replaced with fresh medium for a further 24 hours, to be conditioned by the astrocytes (conditioning period) see Figure 5.1.

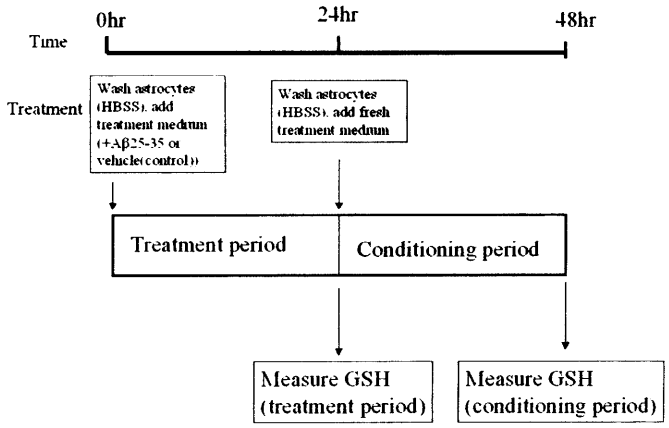

Figure 5.1: Conditioned medium protocol. Astrocytes were treated for 24 hours with Aβ25-35 or vehicle. The treatment medium was then removed, the cells washed and incubated with fresh medium for a further 24 hour conditioning period.

The experiments presented in this study were carried out on astrocytes over a 24-hour period. It was demonstrated that astrocytes extracellular GSH levels were higher in

Aβ25-35 treated astrocytes compared to controls (see Section 4.4.3.) However in this conditioned medium protocol neurones would be incubated in ACM generated in the subsequent 24-hour conditioning period. It was observed that astrocyte stellation was maintained during this conditioning period. To test whether the pattern of increased extracellular GSH was maintained in this conditioning period, the GSH in aliquots of Aβ25-35 and control ACM media were measured at the end of the treatment period and at the end of the conditioning period. There was an increase in extracellular GSH in Aβ25-35ACM compared with control ACM at the end of the conditioning period (conditioning period control 1.8 ± 0.3μM, conditioning period Aβ25-35 = 2.4 ± 0.4μM, $P<0.05$ paired t test n=4) Figure 5.2.

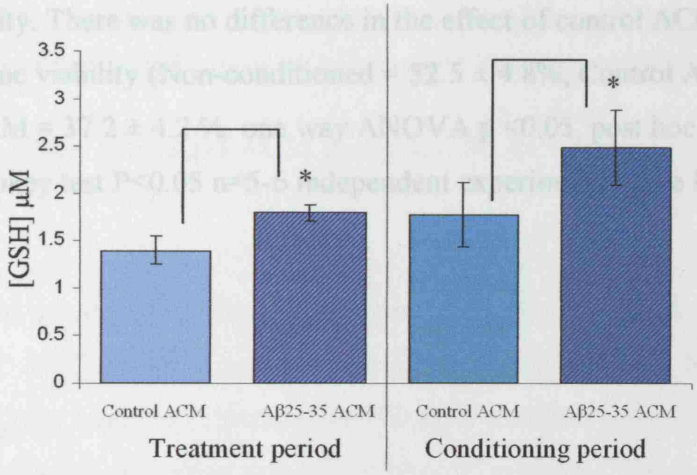

Figure 5.2: Extracellular GSH in astrocyte medium at the end of a 24-hour treatment with 50μM Aβ25-35 and at the end of a subsequent 24-hour conditioning period. There were higher levels of GSH in the extracellular medium of Aβ25-35 treated astrocytes than control astrocytes both at the end of the treatment period and at the end of the conditioning period. Treatment period Control = 1.4 ± 0.2μM, Aβ25-35 = 1.8 ± 0.1μM, Conditioning period control = 1.8 ± 0.3μM, Aβ25-35 = 2.4 ± 0.4μM. $P<0.05$, paired t test between control and Aβ25-35 treated cells, n=5 independent experiments. Error bars= SEM.

5.3.2. Effect of astrocyte conditioned medium from control and Aβ25-35 –treated astrocytes on neurones.

To test the neurotoxicity of astrocyte conditioned medium from astrocytes that had been exposed to Aβ25-35, neurones were incubated in control ACM (ACM from astrocytes that had not received Aβ25-35 treatment), Aβ25-35 ACM (ACM from astrocytes that had received 24 hour Aβ25-35 treatment) or in non-conditioned medium for 24 hours. Before adding to the neurones, non- conditioned medium was incubated in the absence of astrocytes for 24 hours at 37°C to use as an appropriate control (see Figure 5.5). In this experiment neurones were not treated with Aβ25-35.

There was a significantly smaller proportion of cell death of neurones incubated in both control ACM and Aβ25-35 ACM compared to neurones incubated in non-conditioned medium indicating that both Aβ25-35 and control ACM improved basal neurone viability. There was no difference in the effect of control ACM and Aβ25-35 ACM on neurone viability (Non-conditioned = 52.5 ± 4.8%, Control ACM = 37.3 ± 3.8%, Aβ25-35ACM = 37.2 ± 4.2 %. one way ANOVA $p < 0.05$, post hoc analysis was done using the Tukey test $P<0.05$ n=5-6 independent experiments). See Figure 5.3.

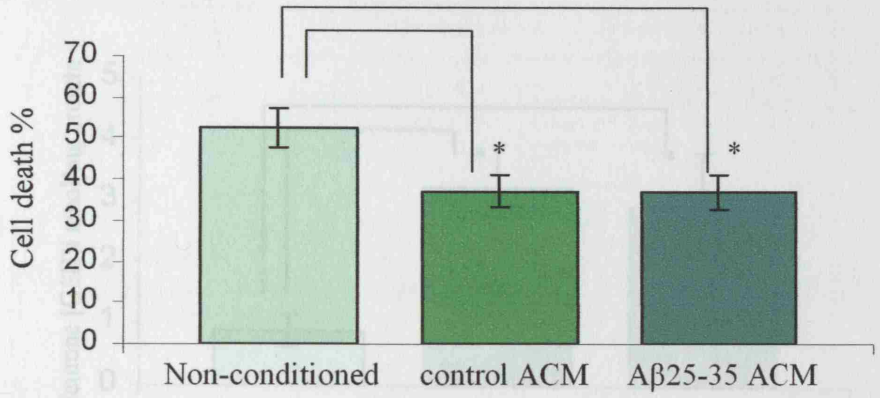

Figure 5.3: Neurone viability after 24-hour incubation in conditioned medium from control astrocytes or Aβ25-35 treated astrocytes or non-conditioned medium. Non-conditioned = 52.5 ± 4.9%, Control ACM = 37.3 ± 3.8%, Aβ25-35 ACM = 37.2 ± 4.2% n=5-6 independent experiments P<0.05 one way ANOVA followed by Tukey test). Error bars= SEM

5.3.3. Effect of control ACM and Aβ25-35 ACM on neurone intracellular GSH levels

The intracellular GSH was measured in neurones that had been incubated in control ACM, Aβ25-35 ACM and non-conditioned medium for 24 hours. There was a significant increase in intracellular GSH of neurones incubated in Aβ25-35 ACM and control ACM compared to non-conditioned medium (Non-conditioned medium = 0.9 ± 0.2 nmol/mg protein, control ACM = 3.2 ± 0.7 nmol/mg protein, Aβ25-35 ACM = 3.0 ± 0.9 nmol/mg protein, data from 6-8 independent experiments P<0.05 by one way ANOVA followed by Tukey post hoc test). Despite the observation that there were higher levels of GSH in Aβ25-35 ACM than control ACM (see Section 5.3.1), there was no difference in the intracellular GSH levels of neurones incubated in each type of ACM, Figure 5.4

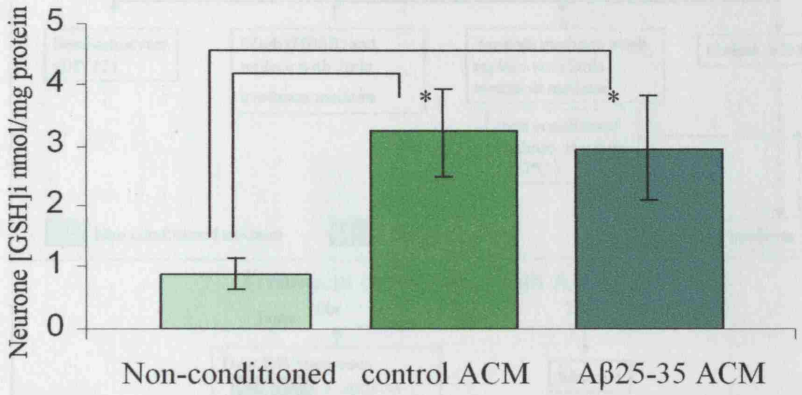

Figure 5.4: Neurone intracellular [GSH] after 24 hour incubation in non-conditioned medium, ACM from control astrocytes or ACM from Aβ25-35 –treated astrocytes. Non-conditioned medium = 0.9 ± 0.2 nmol/mg protein, Control ACM = 3.2 ± 0.7 nmol/mg protein, Aβ25-35 ACM = 3.0 ± 0.9 nmol/ mg protein. Data from 6-8 independent experiments. P< 0.05 ANOVA followed by Tukey post hoc test. Error bars= SEM.

5.3.4. Response of neurones treated with Aβ25-35 in control ACM

To test whether ACM could protect neurones from Aβ25-35 mediated toxicity, a protocol was developed in which neurones were treated with Aβ25-35 either in non-conditioned medium or control ACM (ACM from astrocytes that have not received Aβ25-35 treatment). Aβ25-35 was added to non-conditioned medium or control ACM, and placed immediately on neurones, see Figure 5.5. The neurones were incubated with either 1) non-conditioned medium + vehicle, 2) control ACM + vehicle, 3) non-conditioned medium + Aβ25-35, or 4) control ACM + Aβ25-35 for 24 hours. After 24 hours the viability or GSH levels of the neurones were measured.

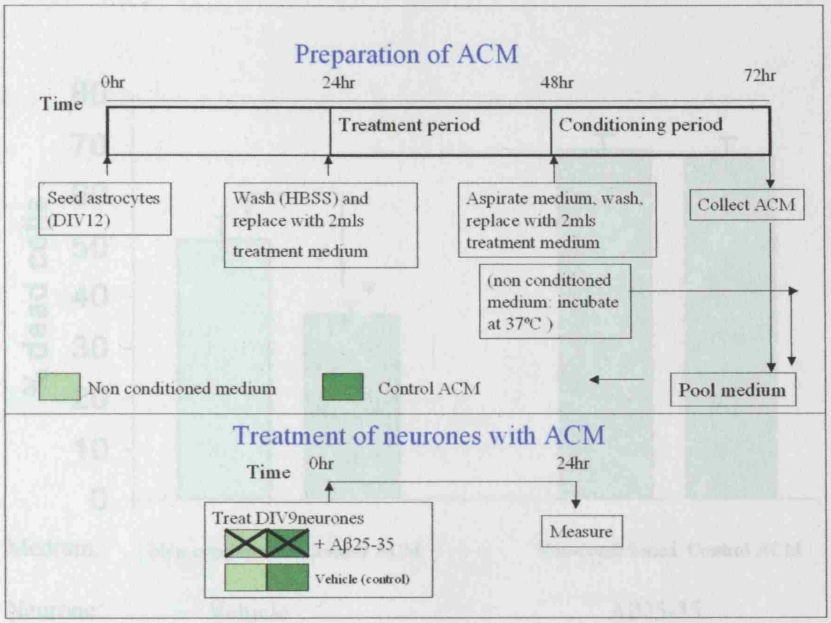

Figure 5.5. Treatment of neurones with Aβ25-35 or control ACM. Astrocyte conditioned medium was prepared by incubating astrocytes (seeded in 6 well plates) with Neurobasal medium for 24 hours, at which time the media was removed, the cells were washed and fresh Neurobasal medium was added for a further 24 hours. The conditioned media form the second 24-hour period was removed and added to the neurones. Non-conditioned medium, was aged for 24 hours at 37°C, before being added to neurones. Control ACM = conditioned medium from astrocytes that have not received Aβ25-35 treatment.

As previously observed there was a decrease in the amount of cell death when neurones were incubated in control ACM compared to non-conditioned medium (Non conditioned + vehicle = 51.4 ± 4.4, control ACM + vehicle = 36.1 ± 3.1%), Figure 5.6. However there was no difference between the amount of cell death of neurones treated with Aβ25-35 in non-conditioned medium or control ACM (Non-conditioned + Aβ25-35 = 69.0 ± 3.2 %, control ACM = 67.8 ± 3.5%. N=7 non significant at 5% level paired t test).

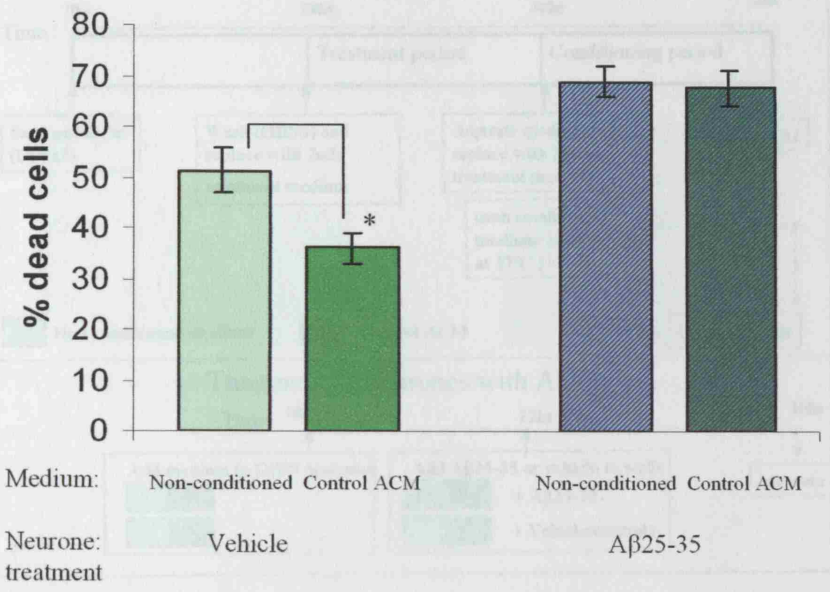

Figure 5.6: Viability of neurones treated with Aβ25-35 in non-conditioned medium or control ACM. Vehicle treated neurones; Non-conditioned = 51.4 ± 4.4 % dead cells, control ACM = 36.1 ± 3.1 % dead cells. Aβ25-35 treated neurones = 69.0 ± 3.2 % dead cells, control ACM= 67.8 ± 3.5 % dead cells n=7. $p<0.05$ paired t test. Error bars =SEM.

One possibility was that the astrocyte derived GSH was not able to protect the neurones when presented at the same time as the Aβ25-35 insult because of the time needed for neuronal intracellular GSH synthesis. The conditioned medium protocol was adapted so that neurones received a 12-hour pre-incubation in which they could take up GSH precursors from the control ACM and upregulate their GSH levels. After a 12-hour pre-incubation, 500µl of medium were removed from each well and supplemented with Aβ25-35 or vehicle, vortexed and then returned to the well. This was done, rather than removing the entire medium from the well, to limit the stress on the neurones. The neurones were then incubated for a further 24 hours with Aβ25-35 or vehicle, and the amount of cell death measured at the end of this period. See Figure 5.7.

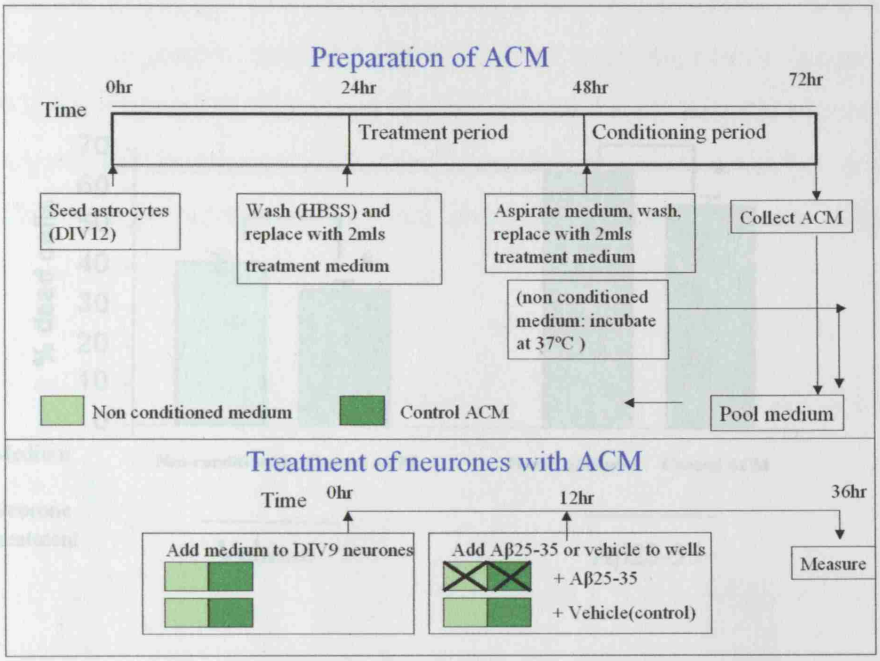

Figure 5.7: Conditioned medium protocol to include a 12-hour pre-incubation period. Control astrocyte conditioned medium was prepared from vehicle treated astrocytes as before. Neurones were incubated in non-conditioned medium or control ACM for 12 hours, at which point Aβ25-35 or vehicle (H_2O) was added to the neurones. After a further 24 hours cell viability was measured by assessing nuclear morphology and membrane permeability.

Figure 5.8 shows that neurones that were treated with Aβ25-35 after a pre-incubation in control ACM showed a small but significant decrease in cell death compared with neurones treated after pre-incubation in non-conditioned medium (non-conditioned + Aβ25-35 = 65.1 ± 2.4%, control ACM + Aβ25-35 = 57.0 ± 1.9% n=10 $P< 0.05$ paired t test). As with previous experiments, there was significantly less cell death in vehicle treated neurones pre-incubated in control ACM compared to those in non-conditioned medium (Non-conditioned medium + vehicle = 41.3 ± 2.2, control ACM + vehicle = 34.9 ± 1.9 $P< 0.05$ paired t test)).

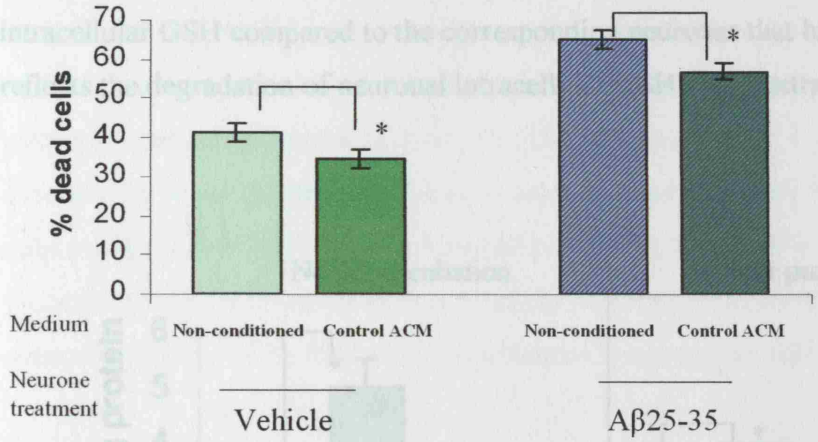

Figure 5.8: Viability of neurones pre-incubated with non-conditioned medium or control ACM for 12 hours prior to vehicle or Aβ25-35 treatment. Vehicle treated neurones; non-conditioned medium = 41.3 ± 2.2%, Control ACM = 34.9 ± 1.9%. Aβ25-35 treated neurones; non-conditioned medium = 64.1 ± 2.5, Control ACM =57.0 ± 1.3%. n=10 p <0.05 paired t test. Error bars = SEM

5.3.5. Neurone intracellular GSH levels after treatment with Aβ25-35 in control ACM or non-conditioned medium

The rationale for including a pre-incubation period in this study was based on the arguement that control ACM did not protect neurones that were treated with Aβ25-35 without a pre-incubation period, as the neurones had not built up their intracellular GSH levels before being subjected to Aβ25-35- generated ROS. The intracellular GSH concentration was measured in neurones treated with Aβ25-35 with and without a pre-incubation period and compared to neurones treated with Aβ25-35 in non-conditioned medium. It was observed both with and without a pre-incubation period that neurones treated with Aβ25-35 in control ACM had greater intracellular GSH levels than corresponding neurones treated in non-conditioned medium (No pre-incubation + Aβ25-35; non-conditioned medium = 0.5 ± 0.03 nmol/mg protein, control ACM = 1.5 ±

0.4nmol/mg protein. Pre-incubation + Aβ25-35; non-conditioned medium = 0.5 ± 0.2nmol/mg protein, control ACM = 0.9 ± 0.2 nmol/mg protein (paired t test $P < 0.05$, n=3) See Figure 5.9. Neurones that had received a 12-hour pre-incubation had lower intracellular GSH compared to the corresponding neurones that had not. This probably reflects the degradation of neuronal intracellular GSH in the extra 12-hour period.

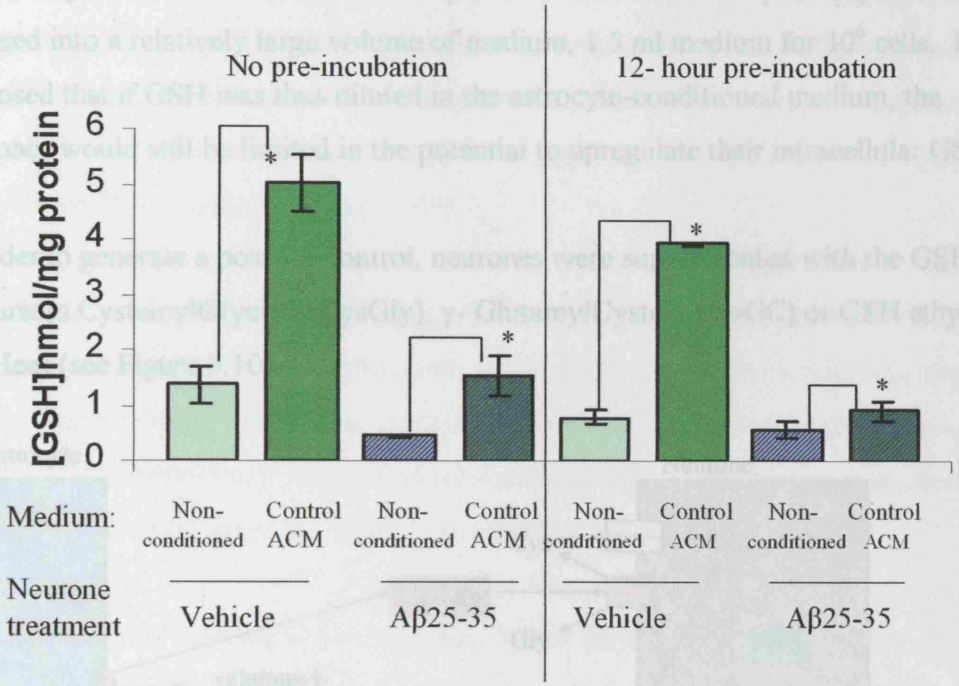

Figure 5.9 Intracellular GSH concentration of neurones treated with Aβ25-35 in non-conditioned medium or control ACM. No pre-incubation, vehicle treated neurones; Non-conditioned medium = 1.4 ± 0.3, control ACM = 5.0 ± 0.5. No pre-incubation, Aβ25-35- treated neurones; non-conditioned medium = 0.5 ± 0.03, control ACM = 1.5 ± 0.4. 12-hour pre-incubation, vehicle treated neurones; non-conditioned medium = 0.8 ± 0.1, control ACM = 3.9 ± 0.03. 12 hour pre-incubation Aβ25-35-treated neurones; non-conditioned medium = 0.5 ± 0.2, control ACM = 0.9 ± 0.2 nmol/mg protein. n= 3. Error bars = SEM.

5.3.6. Supplementation of neurones with GSH precursors: Generation of a positive control.

Control ACM partially protected neurones from Aβ25-35 toxicity. The cytoarchitecture of the brain is organised so that in the small extracellular space between neurones and astrocytes the concentration of extracellular signalling factors is not diluted. Conversely, in the conditioned medium protocol used in this study astrocyte GSH was released into a relatively large volume of medium, 1.5 ml medium for 10^6 cells. It was proposed that if GSH was thus diluted in the astrocyte-conditioned medium, the neurones would still be limited in the potential to upregulate their intracellular GSH.

In order to generate a positive control, neurones were supplemented with the GSH precursors CysteinylGlycine (CysGly), γ- GlutamylCysteine (γ-GC) or GSH ethyl ester (GSHee) (see Figure 5.10).

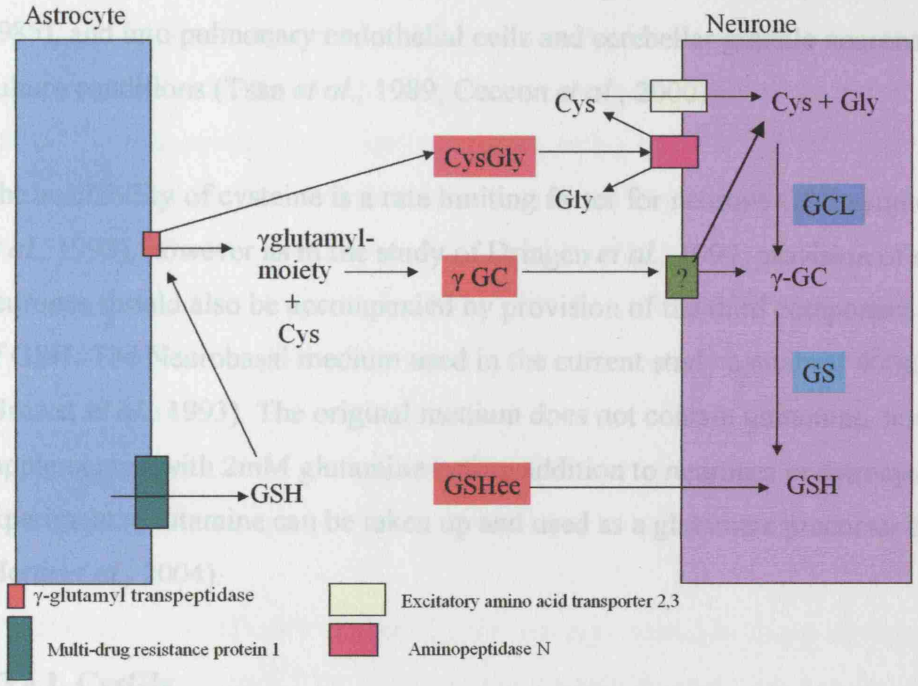

Figure 5.10 Supplementation of neurones with glutathione precursors.

As discussed in section 1.3.4.5, on release from astrocytes GSH is cleaved by γ-glutamyl transpeptidase to produce CysGly, which can be cleaved and the constituent

amino acids taken up by neurones (Dringen *et al.*, 1997; Dringen and Hamprecht, 1998).

The breakdown of GSH catalysed by γ glutamyl transpeptidase generates a γ-glutamyl moiety, which can form bonds with a number of acceptors, including cysteine to form γ-glutamylcysteine (γGC) (Allison and Meister, 1980). Supplementation with γGC is thought to bypass the GCL step of GSH synthesis (see Figure 1.7) in astrocytes and kidney cells, as up-regulation of GSH occurs in the presence of the GCL inhibitor L-BSO (Anderson and Meister, 1983; Dringen *et al.*, 1997). However, in neurones GSH upregulation by γ GC is inhibited by L-BSO suggesting that γGC is cleaved before use for GSH synthesis (Dringen *et al.*, 1997).

Neurones were also supplemented with GSH ethyl ester (GSHee). GSH is not readily transported into cells but GSHee has been shown to be taken into various tissues (liver, kidney, heart) when given in an intraperitoneal injection to mice (Anderson *et al.*, 1985), and into pulmonary endothelial cells and cerebellar granule neurones grown in culture conditions (Tsan *et al.*, 1989; Ceccon *et al.*, 2000).

The availability of cysteine is a rate limiting factor for neurone GSH synthesis (Sagara *et al.*, 1993), however as in the study of Dringen *et al.*, 1999, provision of di-peptides to neurones should also be accompanied by provision of the third component amino acid of GSH. The Neurobasal medium used in the current study contained 400μM glycine (Brewer *et al.*, 1993). The original medium does not contain glutamine, however it was supplemented with 2mM glutamine before addition to neurones or astrocytes in every experiment. Glutamine can be taken up and used as a glutamate precursor by neurones (Hertz *et al.*, 2004).

5.3.6.1. CysGly

CysGly was presented to neurone cultures in concentrations in the range 5 to 100μM in Neurobasal medium supplemented with 2mM glutamine. This was based on the concentration used in Dringen and colleagues (1997) who had found maximal increase in neurone GSH at 30μM CysGly supplementation.

Although it was not possible to use HPLC to accurately measure CysGly in ACM, as the CysGly peak was too close to the solvent front (see Section 2.9.3.4), inhibition of γ GT with 10μM Acivicin preserved extracellular GSH concentrations to levels approximately 2 times higher than in controls at 24 hours (Control = 0.8 μM ± 0.48, Acivicin 1.9 ± 0.8). Dringen and colleagues (1997b) showed that astrocytes incubated with 10μM acivicin for 10 hours had 3 times the extracellular GSH as control astrocytes. As the average extracellular GSH concentration in this study was found to be 1.7 ± 0.3 μM, it would therefore be estimated that the [CysGly] generated from these cells should be around 1-2μM over a 24 hour period

When the intracellular GSH was measured in neurones incubated with 5-100μM CysGly there was no increase in intra-neuronal GSH (Vehicle only = 1.19 ± 0.45; 5μM CysGly = 1.57 ± 1.1 nmol/mg protein; 10μM CysGly = 0.89 ± 0.59 nmol/mg protein; 50μM CysGly = 1.56 ± 1.0 nmol/mg protein; 100μM CysGly = 1.16 ± 0.58 nmol/mg protein, n=3). In addition, it was observed that at concentrations of 10μM or greater, CysGly caused extensive morphological damage to the neurites of neurones. However, a trend for an increase in cell death as measured by Hoechst and propidium iodide staining was apparent only at concentrations above 50μM CysGly (Vehicle only = 41.61 ± 3.9%, 5μM CysGly = 38.26 ± 6.5%, 10μM CysGly = 39.28 ± 4.0%, 50 μM CysGly = 52.80 ± 10.5%, 100μM CysGly = 58 ± 11.5% (% cell death)). The lack of an increase in the neuronal GSH levels in the presence of CysGly could be attributed to the cell damage observed.

5.3.6.2. GSH ethyl ester

The concentration of GSH released by the astrocytes used in this study was typically from 1-3μM (see Figure 5.2). Neurones were supplemented with a range of concentrations of 5μM to 100μM GSHee in Neurobasal medium supplemented with 2mM glutamine. Care was taken in the preparation and storage of GSHee to limit oxidation in solution. This range of GSHee concentrations did not appear to reliably increase neurone intracellular GSH suggesting that GSHee has low efficacy of uptake in primary cortical neurones (Vehicle = 2.92 ± 2.72 nmol/mg protein; 2μM = 1.88 ± 1.55

nmol/mg protein; 5μM = 1.56 ± 0.9 nmol/mg protein; 50μM = 3.24 ± 2.35 nmol/mg protein; 100μM = 2.68 ± 1.78 nmol/mg protein, n=3).

5.3.6.3. γ GC

γ-GC was added to neurones in the range 500μM to 1.5mM in Neurobasal medium supplemented with 2mM glutamine, this was based on the concentration of γGC ethyl ester used in the study of Boyd-Kimball *et al.*, 2005. There was no cellular damage as assessed by morphological inspection over this concentration range. There was a trend for an increase in neurone GSH compared with controls (vehicle) after treatment with 500μM- 1.5mM γ-GC. However, the upregulation of neuronal GSH appeared to plateau rather than increase with higher concentrations of γ-GC, (Figure 5.11). For subsequent experiments a concentration of 1mM γ-GC was used.

The intracellular [GSH] in neurones incubated in non-conditioned medium, control ACM and non-conditioned medium supplemented with γ-GC was compared, (Figure 5.12). There were higher levels of GSH in neurones incubated with control ACM and γ-GC supplemented medium compared to neurones incubated in non-conditioned medium. Control ACM and γ-GC induced an increase in neurone GSH levels to the same degree (One way ANOVA followed by Tukey post hoc test $p < 0.05$) (Non-conditioned medium = 2.2 ± 0.5, Control ACM = 7.2 ± 0.7, γ-GC = 6.6 ± 0.9 nmol/mg protein. N=4).

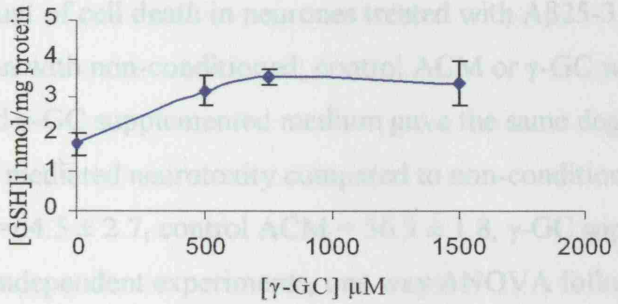

Figure 5.11. Neurone intracellular [GSH] after incubation with a range of concentrations of γ-glutamylcysteine in Neurobasal medium. Control (vehicle) = 1.7 ± 0.3 nmol/mg protein, 0.5mM γGC = 3.2 ± 0.4 nmol/mg protein, 0.75 mM γGC = 3.5 ± 0.2 nmol/mg protein, 1.5mM γGC = 3.4 ± 0.6 nmol/mg protein. n=3. Error bars= SEM.

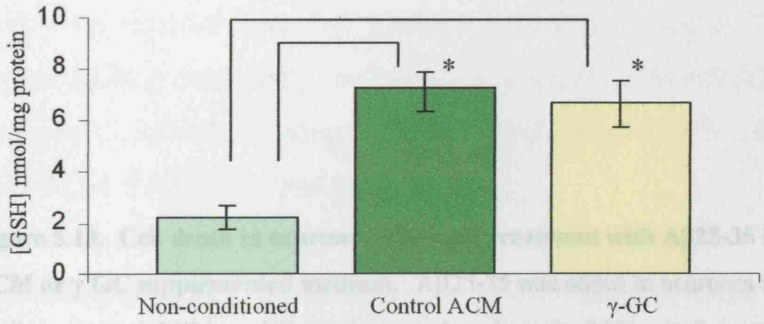

Figure 5.12: Neurone intracellular GSH after supplementation with 1mM γ-GC a comparison with control ACM. Non-conditioned medium = 2.2 ± 0.5, Control ACM = 7.2 ± 0.7, γ-GC = 6.64± 0.9 nmol/mg protein. $p < 0.05$ one way ANOVA followed by Tukey test, n=4. Error bars = SEM

The amount of cell death in neurones treated with Aβ25-35 after a 12-hour pre-incubation with non-conditioned, control ACM or γ-GC was measured. Both control ACM and γ-GC supplemented medium gave the same degree of protection against Aβ25-35 mediated neurotoxity compared to non-conditioned medium (Non conditioned medium =64.5 ± 2.7, control ACM = 56.3 ± 1.8, γ-GC supplemented medium = 51.7 ± 2.5, 4-9 independent experiments, one way ANOVA followed by Tukey test $P<0.05$).

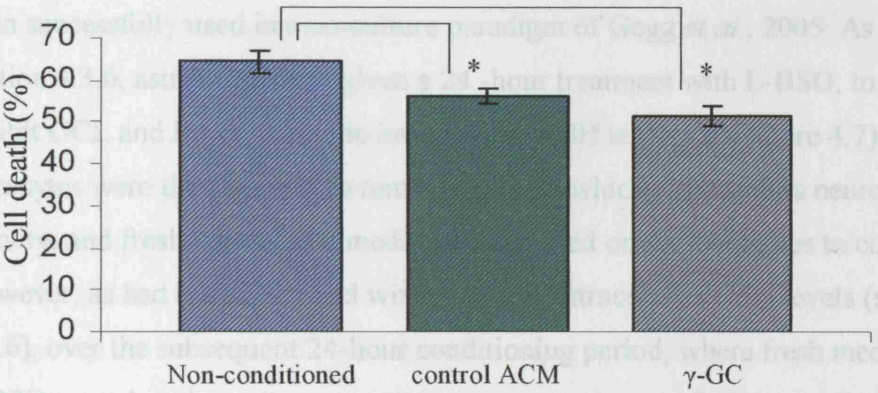

Figure 5.13. Cell death in neurones following treatment with Aβ25-35 in non-conditioned, control ACM or γ GC supplemented medium. Aβ25-35 was added to neurones incubated in non-conditioned medium, control ACM or γGC supplemented medium for 24 hours after neurones had received a 12 hour pre-incubation in these media. Non-conditioned medium = 64.5 ± 2.7, Control ACM = 56.3 ± 1.8, γ- GC supplemented medium = 51.7 ± 2.5. n=4-9 independent experiments. $p<0.05$ paired t test. Error bars = SEM.

5.3.7. Generation of a negative control

1mM γ-GC supplementation was considered an appropriate positive control, as intra-neuronal GSH levels were raised to the same levels as neurones incubated in control ACM. It was also attempted to produce a negative control which would be control ACM without the astrocyte derived GSH.

The first approach was to inhibit GSH synthesis and lower astrocyte intracellular GSH levels using L-BSO to inhibit glutamate cysteine ligase (GCL). It hads been suggested (Sagara *et al.*, 1996) that GSH efflux positively correlates with intracellular GSH levels, therefore extracellular GSH would be lowered by L-BSO treatment. This approach had been successfully used in a co-culture paradigm of Gegg *et al.*, 2005. As described in section 4.3.6, astrocytes were given a 24 -hour treatment with L-BSO, to selectively inhibit GCL and lower astrocyte intracellular GSH levels (see figure 4.7). The astrocytes were then washed to remove L-BSO, which also inhibits neurone GCL activity, and fresh Neurobasal medium was placed on the astrocytes to condition. However, as had been observed with astrocyte intracellular GSH levels (see Section 4.3.6), over the subsequent 24-hour conditioning period, where fresh medium without L-BSO was placed on astrocytes, the astrocyte – neurone GSH upregulation was completely restored (One way ANOVA $P< 0.05$ followed by Tukey post hoc test control ACM > non conditioned medium, control ACM = BSO ACM. Non-conditioned medium = 2.5 ± 0.8 nmol/mg protein, control ACM = 6.9 ± 0.9 nmol/mg protein, L-BSO ACM = 6.0 ± 1.1 nmol/mg protein).

The second approach was to inhibit γ- glutamyl transpeptidase using the specific inhibitor acivicin (see Section 2.4.5). Neurones can utilise CysGly but not GSH for uptake of GSH precursors. γ- glutamyl transpeptidase is responsible for cleaving GSH to CysGly. It had been shown that concentrations greater than 5μM acivicin approximately doubled the amount of GSH in the astrocyte extracellular medium (see Figure 2.5). The concentration of extracellular GSH did not increase with increasing concentrations of acivicin; therefore it was proposed that maximal inhibition of γ

glutamyl transpeptidase of the astrocytes occurred after supplementation with 5μM acivicin. In a preliminary study 10μM acivicin was added to the astrocytes for the 24-hour conditioning period. This medium was then transferred to neurones for 24 hours.

It had been shown by Dringen *et al.*, 1999 in a co-culture paradigm, using cystine/cysteine free medium that inhibition of γ glutamyl transpeptidase, using acivicin, prevented an up regulation of neurone intracellular GSH levels. However a preliminary experiment in this study showed that acivicin treated astrocytes appeared to up-regulate neurone GSH but less so than control ACM (non-conditioned medium = 1.7 nmol/mg protein, control ACM = 8.0 nmol/mg protein, Acivicin ACM = 4.8 nmol/mg protein, γ –GC supplemented medium = 6.9 nmol/mg protein. n=1, conducted in duplicate). It was however shown by Deneke *et al.*, (1995) that GSH in the presence of cystine, that would be present in the media used in the current study, but not used by Dringen *et al.*, (1999), could undergo a reaction to liberate cysteine that could be taken up by neurones.

Based on the experiments conducted in this study, it is proposed that to generate a negative control of astrocyte conditioned medium, using the same media conditions as used throughout this study, would require inhibition of γ-glutamyl transpeptidase along with the specific removal of GSH by immunoprecipitation.

5.3.8. Comparison of the protection of control ACM and Aβ25-35 ACM against Aβ25-35 neurotoxicity

To test whether Aβ25-35 ACM would exhibit the same level of neuroprotection against Aβ25-35 treated neurones as control ACM, neurones were pre-incubated for 12 hours in non-conditioned medium, control ACM and Aβ25-35 ACM and the amount of cell death after Aβ25-35 treatment in these media was compared (Figure 5.13). A one-way ANOVA showed that there was a significant difference between the three groups, Tukey post hoc analysis showed a significant difference between control ACM and non-conditioned medium. There was no difference between the amount of cell death in control ACM and Aβ25-35 ACM but the amount of cell death in Aβ25-35 ACM also

did not differ to a significant degree from the amount observed in neurones incubated in non-conditioned medium (Non-conditioned = 64.3 ± 2.9%, Control ACM = 55.6 ± 1.5%, Aβ25-35 ACM = 58.4 ± 1.4% n=6-9 independent experiments). For paired experiments there was a significant difference between the ability of Aβ25-35 ACM and control ACM to protect neurones from Aβ25-35 mediated toxicity (paired t test $p< 0.05$) Figure 5.13.

In this study the neurone viability was assessed after treatment with Aβ25-35 in all three media and was compared in neurones that had not been pre-incubated prior to treatment. There was no difference in the degree of cell death in each medium (non-conditioned = 70.3 ± 3.2%, Control ACM = 70.8 ± 4.2%, Aβ25-35ACM= 75.9 ± 5.1% n=5).

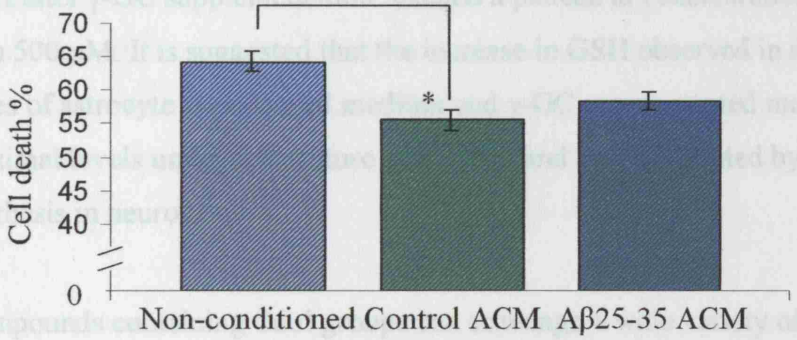

Figure 5.14: Neurone death after 24hr (with 12hr preincubation) treatment with Aβ25-35 in non-conditioned medium, control ACM or Aβ25-35 ACM. Non-conditioned = 64.3± 3.0%, control ACM = 55.6 ± 1.5 %, Aβ25-35 ACM = 58.4 ± 1.4% n=6-9 independent experiments. ANOVA followed by Tukey test, $p< 0.05$. Error bars = SEM.

5.4. Discussion

5.4.1. Upregulation of neurone intracellular GSH by control and Aβ25-35 ACM

The experiments described in this chapter show that the intracellular GSH content of neurones grown under culture conditions in the absence of astrocytes may be upregulated by conditioned medium from both control astrocytes and Aβ25-35 treated astrocytes to the same degree despite Aβ25-35 ACM containing higher GSH. This suggests that the GSH present in control ACM already upregulates neurone GSH maximally. Supplementation of neurones with γ-GC also increased neurone GSH. γ-GC has been proposed by some research groups to by-pass the rate-limiting step of GSH synthesis in some cell types (Anderson and Meister, 1983). However, in neurones γ- GC appears to require functional GCL in order to upregulate neuronal GSH levels (Dringen *et al.*, 1999). In the present study it was found that the increase in the levels of neurone GSH after γ-GC supplementation reached a plateau at concentrations of γ-GC greater than 500 μM. It is suggested that the increase in GSH observed in neurones in both types of astrocyte conditioned medium and γ-GC supplemented medium is at the maximal levels under cell culture conditions and may be limited by the rate of GSH synthesis in neurones.

Compounds containing thiol groups can scavenge a wide variety of ROS and RNS, therefore thiols are considered to be antioxidants. It was interesting to observe that cysteinylglycine (CysGly) damaged neurones in relatively low concentrations, whereas, γ-GC was non-toxic even at concentrations 100 times higher. The concentrations of CysGly used were based on the range approximated from astrocyte-conditioned medium and on the concentration used by Dringen *et al.*, 1999. In their study, however, Dringen's group had treated the neurones with CysGly for 6 hours in minimal medium. Minimal medium has a base of Hanks buffered saline solution to which sodium, chloride, calcium and potassium ions are added in addition to glucose. Importantly this medium should not contain transition metal ions. Most commercial cell culture media, including the Neurobasal medium used in the present study, contain trace levels of ferrous ions. It was demonstrated by Hua Long and Halliwell (2001), that a wide range of thiols including cysteine, cysteinylglycine, γ-glutamylcysteine and even GSH can

interact with commonly used cell culture media to produce hydrogen peroxide. However, it was demonstrated by Enoiu *et al.*, 2000 that CysGly and Cys in the presence of ferrous ions generate ROS, whereas GSH does not.

In the present study it has been shown that when equimolar solutions of CysGly and GSH were run on a HPLC coupled to an electrochemical detection system (detecting the oxidation of these thiols), CysGly generated a greater signal than GSH (see Figure 2.15C). Using the same HPLC set-up as used in this thesis, Gegg *et al.*, 2002 showed that equimolar standards of cysteine γ-glutamylcysteine, GSH, and CysGly oxidised at the same electrode potential generated a current that was greater in cysteine > CysGly > GSH> γ-GluCys. The propensity for the H^+ ion to dissociate from its sulphydryl bond may reflect the charge distribution throughout the peptide. The charge distribution may be dependent on amino acid side groups. Hua Long and Halliwell, 2001 demonstrated that the levels of detectable thiols (detected with Ellman's reagent), decreased over time in media containing cysteine or CysGly. There was a greater loss in detectable thiol groups in cysteine-supplemented medium compared to CysGly-supplemented medium. GSH supplemented medium also showed a loss in detectable thiols, but less than cysteinylglycine or cysteine, suggesting that CysGly and cysteine are more readily oxidised.

CysGly is cleaved by the neurone membrane bound enzyme aminopeptidase N (Dringen *et al.*, 2001). A vital function of astrocyte-derived antioxidants may be to maintain CysGly and cysteine in their reduced form in the extracellular environment so that they can be utilised by neurones, and to protect neurones from potentially neurotoxic ROS generated by the interactions of CysGly and cysteine with the extracellular environment.

5.4.2. Effect of Aβ25-35 ACM, control ACM and γ-GC supplementation on neurone viability

The neurones used in this study are grown under particularly challenging conditions. In addition to being deprived of astrocyte support from DIV3 to achieve purity (see Section 2.2.2), they are also maintained and treated after a relatively long period in

culture conditions compared to primary neurones used in many Aβ25-35 toxicity models. Supplementation with γ-GC or ACM increased neurone viability to a similar degree suggesting that the normal degree of basal neurone cell death in primary neurone cultures may be related to ROS production under these conditions. Aβ25-35 ACM and control ACM increased basal neurone viability to a similar degree, suggesting that Aβ25-35 ACM was not directly toxic to neurones or that supplementary factors were sufficient to completely prevent the toxic insult.

Two of the potentially neurotoxic factors proposed to be released by Aβ25-35 treated astrocytes, nitric oxide and the superoxide radical ($O_2^{\cdot-}$) have an exceedingly short half-life. It is important to consider that the conditioned medium protocol presented in this study has a degree of temporal selectivity of the astrocyte-derived factors presented to neurones. Of the cytokines released by astrocytes in the presence of Aβ25-35, there is no evidence in the literature to suggest that these would be directly toxic to neurones. However, TNFα does impair neurite outgrowth (Neumann *et al.*, 2002). In the present study long-lasting, soluble factors released by Aβ25-35 treated astrocytes did not appear to be directly toxic to neurones.

Using this conditioned medium protocol it was shown that control astrocyte conditioned medium only offered protection against Aβ25-35 toxicity if neurones had received a pre-incubation period in this medium. Butterfield and Kanski, 2001 reviewed the evidence that the methionine in position 35 of Aβ25-35 and Aβ1-42, is implicated in ROS production in the presence of Aβ. Methionine is readily oxidised. It is proposed to generate free radicals either by a reaction between its sulphur group and molecular O_2 to form a sulfuramyl free radical or through interactions with iron or copper ions to produce H_2O_2, which can undergo further reactions to produce $OH^{\cdot}$.
It would be expected that if Aβ25-35 toxicity arises in the first instance from generation of extracellular ROS, such as could happen by a methionine 35-mediated mechanism, which leads to cell damage and further ROS formation, that treatment of neurones with Aβ25-35 in astrocyte conditioned medium containing GSH may offer some protection to neurones, even if neurones could not increase their intracellular GSH stores during this time. In the present study simultaneous treatment of Aβ25-35 in ACM did not appear to protect against Aβ25-35 mediated toxicity, suggesting that the protection seen

when neurones were incubated with ACM is unlikely be due to a simple extracellular ROS scavenging mechanism.

Aβ appears to generate ROS by several primary and secondary mechanisms (see Section 1.2.4). After pre-incubation with control ACM or γ-GC, neurones showed a similar decrease in the degree of cell death in the presence of Aβ25-35. γ-GC and control ACM raised neurone intracellular GSH to the same extent, which suggests that the comparable amount of protection could be due to the GSH in ACM. However, in the absence of an appropriate negative control (see Section 5.3.7), it is not possible to discount the protective potential of other astrocyte-derived factors.

Intracellular GSH was measured in neurones after Aβ25-35 treatment in non-conditioned medium and in control ACM. Neurones that were treated with Aβ25-35 in ACM without a pre-incubation, showed higher GSH levels than neurones treated in non-conditioned medium. This could demonstrate that neurones were capable of synthesising GSH even in the presence of Aβ25-35. However, as it had been shown in chapter 4 that Aβ25-35 can generate intracellular ROS within an hour of application to neurones it might be the case that the neurones that survive Aβ25-35 treatment could upregulate their GSH contents but the neurones that have died, did so before GSH upregulation occurred.

5.4.3. Modelling aggregated Aβ cell death and testing potential neuroprotective factors: An appraisal of the method used in this study

The degree of protection against Aβ25-35 neurotoxicity afforded by control ACM compared to non-conditioned medium was small but the trend was maintained in each repeat of the experiments. Each cell viability experiment was conducted in duplicate and 10 regions of the coverslips were assessed for their viability in each duplicate. It was observed that Aβ25-35 ACM did not give a significant protection against Aβ25-35 mediated neurotoxicity, compared to non-conditioned medium, and neurones in Aβ25-35 ACM treated with Aβ25-35 always showed more cell death than neurones treated in control ACM in paired experiments. The differences observed in the present study were very modest, however, it is interesting to note that the subtle difference found here is

comparable to data presented by Paradisi *et al.*, 2004, who found that untreated astrocytes were neuroprotective, but Aβ treated astrocytes were not.

Modelling astrocyte to neurone communication during a neurotoxic insult under culture conditions is a highly challenging task, however it is important to appraise the model used to assess means by which it could be improved to increase the sensitivity to detect potential differential effects such as in this case between control and Aβ25-35 -activated astrocytes.

It was observed presently that although ACM could protect neurones in this model the degree of protection was relatively small. This may be due to two reasons:

1) The concentration of Aβ25-35 was too large for neurones to defend themselves against ROS generated in its presence even with increased antioxidant defences.
2) Aβ25-35 mediated neurone cell death by ROS- dependent and independent mechanisms.

Estimations of Aβ load in the AD brain difficult due to the uneven distribution of the peptide. Naslund and colleagues (2000) estimated 2-3 nM per mg of brain tissue (Naslund *et al.*, 2000) and the plasma concentrations have been estimated as ~20nM (Mayeaux *et al.*, 2003). However, local concentrations of Aβ1-40/42 aggregates are likely to be much higher in the extracellular space affecting local neurones, but an estimation has not been reported to date. It should also be noted that extracellular concentrations of Aβ will build up over an as yet unknown period of time, but a critical concentration for fibrillogenesis has been estimated at 10-40μM (Harper and Lansbury, 1997). As discussed in Chapter 3 models of Aβ toxicity use concentrations of Aβ that produce the same outcome (neurone death) as observed in the AD brain, but over a 24-hour period. The concentration of Aβ25-35 used in the present study is at the higher end of the concentrations of Aβ25-35 used in 24-hour toxicity models, which had been determined by different measures of cell death.

In the current study cell death was measured by examining the nuclear morphology and assessing membrane permeability. It is a characteristic feature of apoptosis that the membrane remains intact so that potentially toxic intracellular factors are not released before the apoptotic cell is phagocytosed and digested (Raff, 1998). However in late stage apoptosis secondary necrosis can occur (Cotman *et al.*, 1994; Smoleski *et al.*, 2002). Most dead cells had condensed nuclei but were also positive for propidium iodide indicating damaged membranes, suggesting that these cells were at a late stage along the cell death pathway. However, as some apoptotic pathways such as apoptosome activation are ATP dependant and ATP levels have been suggested to be lowered in Aβ25-35 treated neurones (Casley *et al.*, 2002). An alternative explanation is that ATP levels in neurones may be sufficient to initially drive apoptotic processes but Aβ25-35 mediated ATP depletion may force neurones into necrosis (Saito *et al.*, 2006).

Research groups that have used the MTT assay as a measure of cell death have used lower concentrations of Aβ in their treatment models. Boyd Kimball *et al.*, 2005 who treated cells with Aβ concentrations of 10μM (Aβ1-42) found complete protection by 1mM γGC (in ethyl ester form, γGCee) by measuring cell death by the MTT assay (Boyd Kimball *et al.*, 2005). The use of the MTT assay as a measure of cell death in Aβ toxicity is contentious as MTT exocytotosis may be enhanced in both astrocytes and neurones, rather than MTT reduction decreased, in the presence of Aβ (Liu and Schubert, 1997; Kerokoski *et al.*, 2002). Although the MTT assay can reliably show an effect of Aβ on neurones and astrocytes, the cell death assay used in this study gives a less ambiguous indication of cell death. The disadvantage is that higher concentrations of Aβ25-35, which are causing membrane damage to neurones, were used. As a result it is likely that in this model the astrocytes can only give partial protection, as the Aβ25-35 insult is likely to outweigh their protective potential. However, despite the relatively small amount of protection (around 10%) the trend was very consistent. Neurones in ACM showed less cell death than neurones in non-conditioned medium in all repeats of the experiment.

It is proposed that the next step in modelling Aβ toxicity should be to try to elucidate and use reliable measurements of early "points of no return" in the Aβ toxicity

pathways, in order to be able to lower the concentration of Aβ, yet still have a reliable outcome measure.

In their study in which γ-GCee could completely protect against 10μM Aβ1-42 toxicity Boyd Kimball *et al.*, (2005) showed protection from neurite damage. In the present study there was extensive damage to neurites treated with Aβ25-35 with no observable difference between treatment in non-conditioned medium and control ACM. Neurite damage appears to be an early indicator of Aβ damage to neurones. Ivins *et al.*, (1998) demonstrated that apoptotic processes such as membrane blebbing and externalisation of phosphatidyl serine could be observed in neurites 8 hours after their Aβ treatment, however, apoptotic processes in the soma using the same concentration of Aβ was not evident until 24 hours. In Aβ toxicity paradigms, typically the Aβ peptide is added to a layer of cells. The consequence of this is that both neurites and neuronal cell bodies are exposed to Aβ. In the brain however it may be the case that Aβ aggregates may be in contact with distal neurites but not the soma . This is the case for basal forebrain cholinergic neurones, which are particularly vulnerable in AD. These populations differ from other neuronal populations as their neurites, but not their soma, are located at the principal sites of Aβ aggregation (Song *et al.*, 2006). In two studies it has been shown that selective application of Aβ to neurites but not soma can induce local apoptotic processes in the neurites (Ivins *et al.*, 1998). Importantly Aβ-mediated neurite degeneration can lead to apoptotic processes in the soma (Song *et al.*, 2006). Understanding the response of the soma to early neurite damage may be key to producing therapies to attempt to save neurones from Aβ before the point of no return. It is proposed that early apoptotic cascade events in neurites could be measured using Annexin V, a probe that binds to phoshatidylserine, which is translocated from the inner leaflet of the plasma membrane to be exposed to the external surface of the cell in the early stages of apoptosis and may give a better outcome measure for use in modelling neuroprotection against Aβ mediated toxicity in cell culture models.

5.5. Conclusions

The work presented in this chapter shows that astrocyte-conditioned medium can improve basal neurone viability and partially protect neurones from the concentration of Aβ25-35 used in this study. There is strong evidence to suggest that one of the protective factors in ACM may be GSH. ACM raises neurone intracellular GSH, and shows comparable protection to the glutathione precursor γ-GC at a concentration which raises neurone intracellular GSH to the same level as ACM. Conditioned medium from Aβ25-35 treated astrocytes does not appear to be neurotoxic, and raises neurone intracellular GSH to the same level as control ACM. However tentative interpretation of the data suggests that there may be a difference in the ability of control ACM and Aβ25-35 ACM to protect against Aβ25-35 neurotoxicity, although this work requires follow up experiments, at lower concentrations of Aβ25-35 with an earlier indicator of cell death.

Chapter 6: Astrocyte response to Aβ25-35 treated neurones

6: Astrocyte response to Aβ25-35 treated neurones

6.1. Introduction

It has been shown in the work presented in this thesis (section 4.3.3) and in work by other groups (Gegg *et al.*, 2003; Sagara *et al.*, 1999; Watts *et al.*, 2005) that astrocytes can respond to an oxidative insult by releasing more GSH. However, in addition to responding to environmental factors, astrocytes may also respond to a direct "alarm" signal from injured neurones. It has been noted that in the AD brain astrocytes migrate to the site of plaques and damaged neurones and that astrocyte migration in AD is mediated by the monocyte chemoattractant protein 1 (MCP-1) (Wyss Coray *et al.*, 2003). MCP-1 is expressed by both neurones and astrocytes. Astrocytes release MCP-1 in response to NMDA mediated neurotoxicity in cortico-striatal slice cultures (Katayama *et al.*, 2002). Panenka *et al.*, (2001) investigated ATP stimulation of the astrocyte purinergic receptor PX27 as neurones release high levels of ATP in response to brain injury. Stimulation of the PX27 receptor caused an increase in MCP-1 mRNA levels in astrocytes. This would suggest that astrocytes may be able to respond to neurone injury and recruit more astrocytes to the site of injury.

In addition to investigating astrocyte GSH levels after Aβ25-35 treatment in cortical monocultures, as described in section 4.4.1, Abramov *et al.*,(2003) also measured GSH levels in hippocampal astrocyte-neurone mixed cultures after a 24-hour treatment with Aβ25-35. Using the monochlorobimane method (discussed in section 4.4.1.) to measure GSH they showed that astrocyte GSH was lowered by 44% in cultures treated with Aβ25-35 compared to control cultures. In these experiments Abramov *et al.*, (2003) had used the same treatment medium as used in the present study. It was shown by Griffin *et al.*, (2005) that astrocytes co-cultured with neurones for 24 hours had significantly less intracellular GSH than astrocytes in the absence of neurones. It was therefore postulated in the present study that the presence of neurones may have an effect of the astrocyte ability to maintain their GSH in response to Aβ25-35.

In the experiments described in this chapter, the aim was to test whether the presence of Aβ25-35 treated neurones would have a different effect on astrocyte intracellular GSH,

compared to the presence of control neurones. The effect of neurone conditioned medium, with or without Aβ25-35 treatment was also tested on GSH release from astrocytes.

6.2. Methods

Neurones and astrocyte cultures were prepared as described in Section 2.2. Neurones were grown on glass coverslips in Neurobasal medium and were treated with Aβ25-35 on DIV9. Astrocytes were maintained in minimal essential medium (MEM) containing 10% FBS for 12 days, at which time they were seeded onto poly-L-ornithine coated 6 well plates, in MEM + FBS to attach and recover for 24 hours. The two cell types were co-cultured as described in section 6.3.1. Cells were co-cultured on astrocyte DIV13/neurone DIV10, after being washed with HBSS to remove any dead cells and debris.

GSH was measured using HPLC coupled to electrochemical detection in lysed cell pellets as described in Section 2.9.3.2, and in medium samples as in Section 2.9.3.4.

6.3. Results

6.3.1. Development of a protocol to co-culture Aβ25-35 treated neurones with astrocytes

To test the response of astrocytes to Aβ25-35 treated neurones, the co-culture method developed in this laboratory by Griffin *et al.*, 2005 was employed. Neurones were seeded onto glass coverslips, which were later placed cell-side down on a layer of astrocytes on the bottom of a 6 well plate. Four glass beads had previously been soldered through the bottom of each well of the plate to create four raised points inside the well on which the coverslip was rested. The neurones were therefore not in direct contact with the astrocytes, and were separated by a constant distance of 0.6mm (Griffin *et al.*, 2005). See Figure 6.1

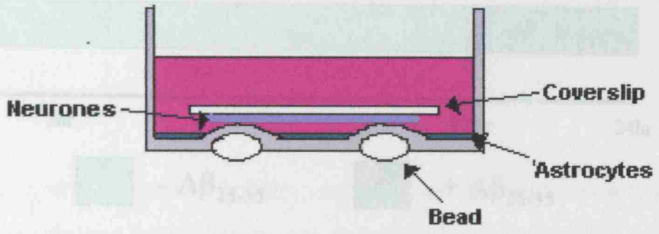

Figure 6.1: Diagram of co-culture apparatus.

Neurones were treated with Aβ25-35 and then transferred to astrocytes, which had not been treated to test the response of non-treated astrocytes to Aβ25-35 treated neurones. Therefore before co-culturing the two cell types it was necessary to assess whether it was possible to treat neurones for a short amount of time, which was too short a treatment for Aβ25-35 mediated neurone death to have occurred, but long enough for Aβ25-35 either to have permanently associated with the neurones or initiated Aβ25-35 mediated death cascades, so that free Aβ25-35 would not come into direct contact with astrocytes.

As illustrated in figure 6.2, neurones were treated for two hours and then transferred to fresh medium for the remaining 22 hours of a 24-hour treatment period (2hr start (b)). The amount of cell death in these neurones was compared to neurones treated with vehicle (control (a)), neurones treated with Aβ25-35 for 24 hours (24 hour (c)) or neurones incubated in control media for 22 hours and then transferred to fresh medium containing Aβ25-35 for 2 hours prior to assessing cell viability (2hr end (d)).

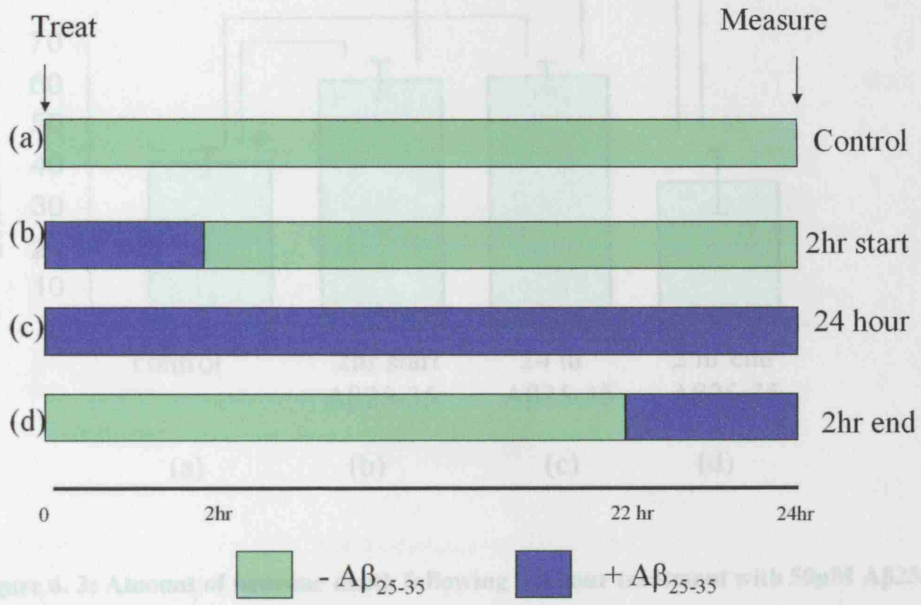

Figure 6.2: Determination of the length of time to treat neurones with Aβ25-35 before transferring the neurones to be co-cultured with astrocytes. (a) 24 hour treatment with vehicle (control), (b) 2 hour treatment with Aβ25-35 before transfer to fresh medium (2 hr start), (c) 24 hour treatment with Aβ25-35 (24 hour), (d) incubation of neurones in medium + vehicle for 22 hours followed by treatment with Aβ25-35 for 2 hours (2hr end).

It was determined that a 2 hour treatment with Aβ25-35 before transferring to fresh medium (b) was sufficient to cause the same degree of cell death 24h later as neurones treated in media containing Aβ25-35 continually for the full 24 hours (c). After 2 hours treatment it was noted that there was no observable damage to the neurone's neurites. Similarly, neurones that had been treated with Aβ25-35 for 2 hours immediately prior to measurement of cell viability showed the same amount of cell death as controls (Control = 40.95 ± 3.3%, 2hr treatment at start = 61.26 ± 4.3%, 24 hour treatment = 61.80 ± 3.7%, 2 hour treatment at end = 35.5 ± 7.8%) $p < 0.05$ one way ANOVA followed by

Tukey post hoc test n=3-6. See Figure 6.3. These results suggested that Aβ25-35 could be washed out of the neuronal extracellular medium, but its effects on neurones could still last for the following 24 hours at least i.e. the period planned for the co-culture experiments.

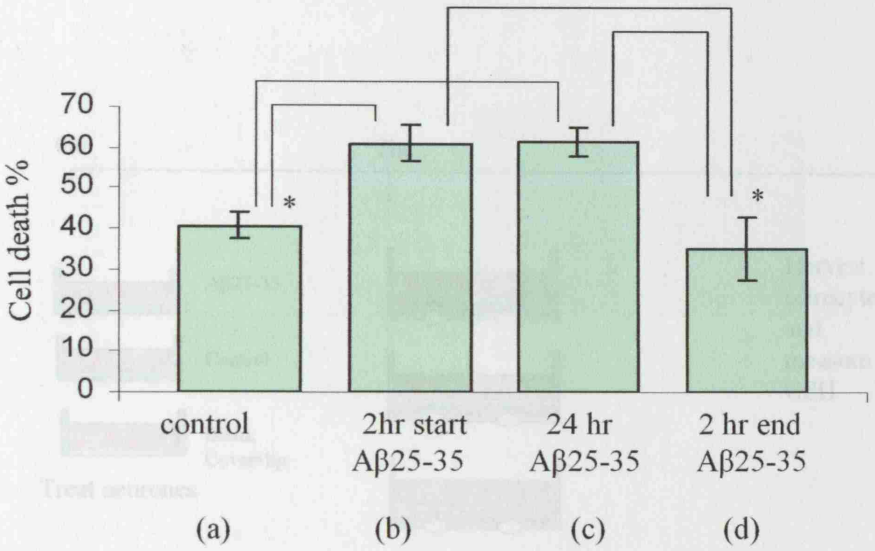

Figure 6. 3: Amount of neurone death following a 2-hour treatment with 50μM Aβ25-35 followed by transfer to fresh medium for 22 hours, compared with continuous treatment with 50μM Aβ25-35 for 24 hours. (a) Control = 40.95 ± 3.38%, (b) 2hr treatment at start = 61.26 ± 4.31%, (c) 24 hour treatment = 61.80 ± 3.65%, (d) 2 hour treatment at end = 35.5 ± 7.79%. n=3-6 independent experiments * = $P<0.05$ one way ANOVA followed by Tukey post hoc test. Error bars = SEM

6.3.2. Co-culture of astrocytes with Aβ25-35 treated neurones

Based on the experiments described in the previous section a co-culture paradigm was designed in which neurones were treated with Aβ25-35 for 2 hours and then transferred to astrocytes for a further 24 hours. Similarly control neurones or a blank cover slip were transferred to astrocytes after 2 hours. The astrocytes were then harvested and the astrocyte intracellular GSH was measured. See Figure 6.4.

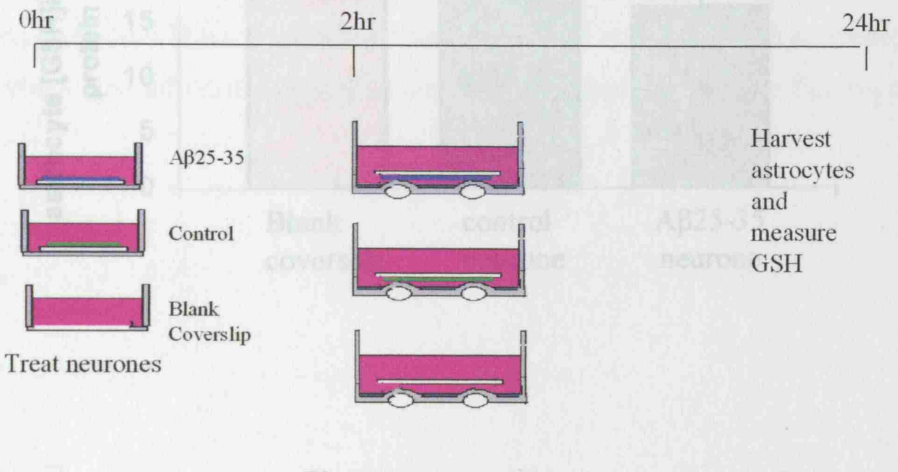

Figure 6.4: Co-culture paradigm.

Neurones were treated with 50μM Aβ25-35, vehicle (control) for 2 hours before transfer to co-culture with astrocytes for 24 hours

There appeared to be variations between each independent astrocyte preparation with regards to astrocyte GSH levels. The astrocytes co-cultured with Aβ25-35 treated neurones, however, always had lower GSH than astrocytes co-cultured with control neurones. Perhaps owing to the variability between trials in basal astrocyte GSH levels a one way ANOVA did not reveal significant differences. However when a t test was applied to paired data in each experiment there was a significant difference between astrocytes in the presence of control neurones compared to the presence of Aβ25-35 treated neurones (Blank coverslip = 21.13 ± 1.3 nmol/mg protein, Control neurone =

18.67 ±1.7 nmol/mg protein, Aβ25-35 neurone = 16.58 ± 1.4 nmol/mg protein, paired t test P<0.05 n=5) See Figure 6.5.

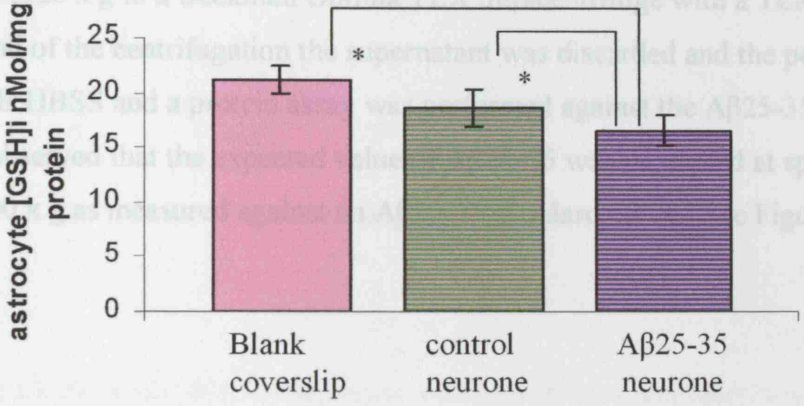

Figure 6.5: Astrocyte GSH in the presence of control neurones or Aβ25-35 treated neurones. (Blank coverslip = 21.13 ± 1.3 nmol/mg protein, Control neurone = 18.67 ±1.7 nmol/mg protein, Aβ25-35 neurone = 16.58 ± 1.4 nmol/mg protein). P<0.05 paired t-test. n=5. Error bars =SEM.

6.3.3. Preparation of neurone conditioned medium

Neurones were seeded at 100,000 neurones per coverslip, astrocytes were at 750,000 astrocytes per well and the medium volume was 2ml. In such a large extracellular volume compared to what might be found *in vivo*, any factor released by neurones may have been exceedingly diluted. A conditioned medium protocol was established in which neurones, seeded at 10^6 cells / well in 1.5 ml Neurobasal medium were treated for 24 hours. Unlike the astrocyte conditioned medium protocol, as it was known that extensive neurone death would have occurred during the 24 hour treatment period, neurone conditioned medium (NCM) was not generated during a second 24 hour conditioning period. Instead, the NCM was collected at the end of the treatment period and centrifuged at 17,000 x g at 4°C to pellet dead cells and Aβ25-35 aggregates. To

assess whether the Aβ25-35 had been removed through this process, a protein assay was conducted using the Lowry method, which had previously been shown to detect Aβ25-35 (see Section 3.3.7). Normally the standard curve would be generated from a BSA standard. In this case a standard curve of Aβ25-35 was used, see Figure 6.6. 50µl of Aβ25-35 solutions were made in HBSS and aged for 24 hours as would occur during the treatment period. These solutions were centrifuged at increasing speeds, from 1,033 x g to 103,320 x g in a Beckman Optima TLX ultracentrifuge with a TLA 100.3 rotor. At the end of the centrifugation the supernatant was discarded and the pellet resuspended in 100µls HBSS and a protein assay was performed against the Aβ25-35 standard curve. It was observed that the expected value of Aβ25-35 was recovered at speeds greater than 17,000 x g as measured against an Aβ25-35 standard curve. See Figures 6.6 & 6.7.

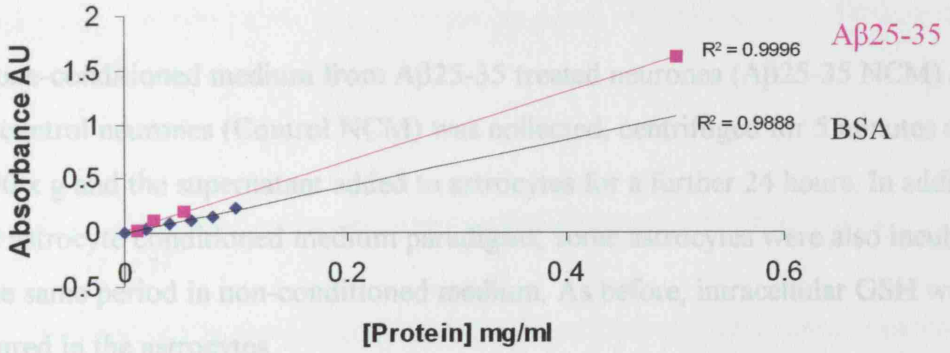

Figure 6.6: Standard curves of Aβ25-35 (pink) and BSA (black) measured by the Lowry assay. The Aβ25-35 standard curve was obtained with concentrations from 10µM to 500µM

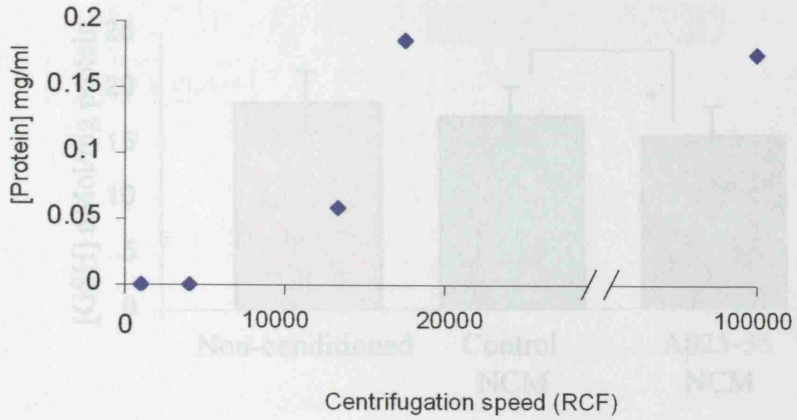

Figure 6.7: Amount of Aβ25-35 aggregates pelleted with increasing centrifugation speed

6.3.4 Effect of NCM on astrocyte glutathione levels

Neurone-conditioned medium from Aβ25-35 treated neurones (Aβ25-35 NCM) and from control neurones (Control NCM) was collected, centrifuged for 5 minutes at 17,000 x g and the supernatant added to astrocytes for a further 24 hours. In addition, as in the astrocyte conditioned medium paradigms, some astrocytes were also incubated for the same period in non-conditioned medium. As before, intracellular GSH was then measured in the astrocytes.

It was observed that there was a similar trend as in co-culture experiments. Astrocytes incubated in non-conditioned medium appeared to contain greater GSH than astrocytes incubated in control NCM or Aβ25-35 NCM. As the main objective was to find out whether there was a difference between the effect on GSH levels of astrocytes incubated in control NCM or Aβ25-35 NCM a paired t test was performed between these two groups. Astrocytes incubated in Aβ25-35 NCM had significantly lower intracellular [GSH] than astrocytes incubated in control NCM. Non-conditioned = 18.8 ± 2.9 nmol/mg protein, control NCM = 17.5 ± 2.6 nmol/mg protein, Aβ25-35 NCM = 15.6 ± 2.7 nmol/mg protein. n=6. Figure 6.8.

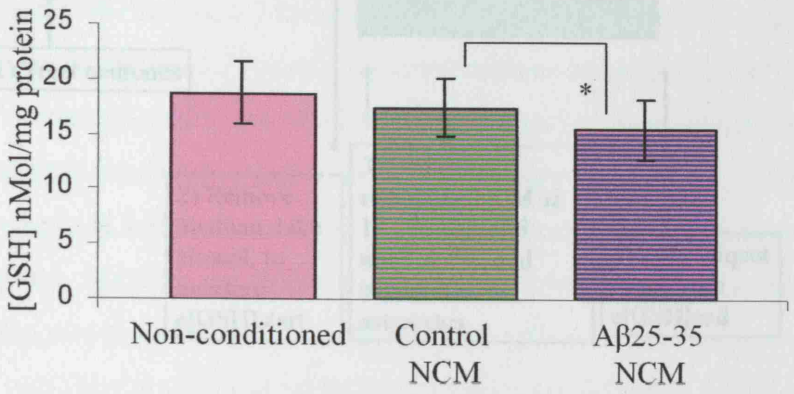

Figure 6.8: Astrocyte intracellular GSH levels following incubation for 24 hours in neurone conditioned medium. Non-conditioned = 18.8 ± 2.9 nmol/mg protein, control NCM = 17.5 ± 2.6 nmol/mg protein, Aβ25-35 NCM = 15.6 ± 2.7 nmol/mg protein. n=6 .Paired t test $p<0.05$ Error bars = SEM.

6.3.5. Effect of incubation in neurone conditioned medium on astrocyte extracellular GSH

It was proposed that in the presence of Aβ25-35 treated neurones, astrocytes may increase the extracellular GSH and derivatives available to neurones. To investigate whether neurone treatment with Aβ25-35 would affect the GSH released from astrocytes extracellular GSH levels released in the NCM were measured at the start and at the end of the astrocyte incubation period, see Figure 6.9.

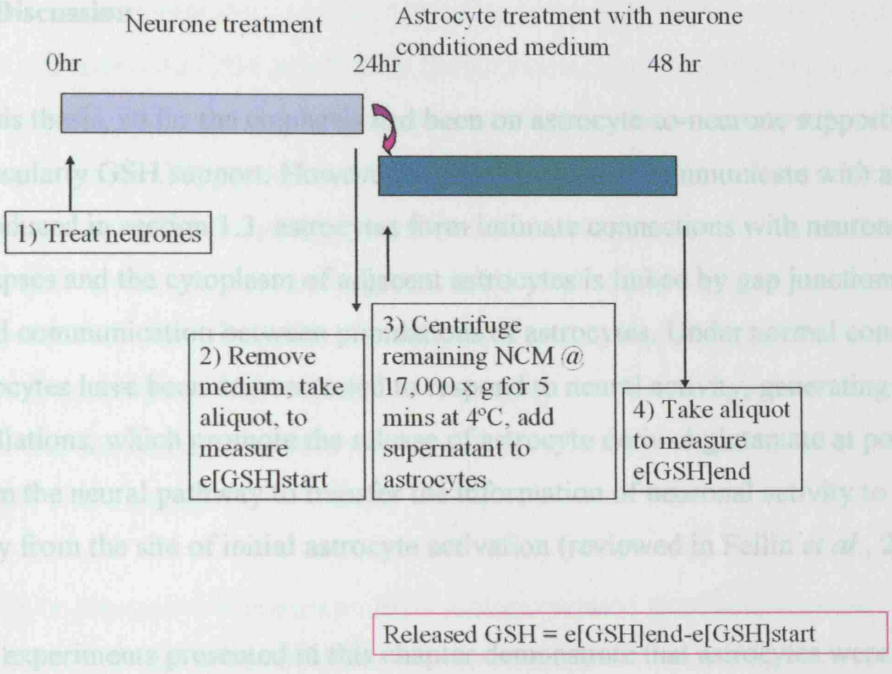

Figure 6.9: Neurone conditioned medium protocol.

There was no detectable difference between the GSH released from astrocytes in non-conditioned medium, control NCM or Aβ25-35 NCM during a 24 hour incubation (Non-conditioned = 2.65 ± 0.53 μM, control NCM = 2.59 ± 0.6, Aβ25-35 NCM = 2.62 ± 0.74 μM. n=3). Figure 6.10.

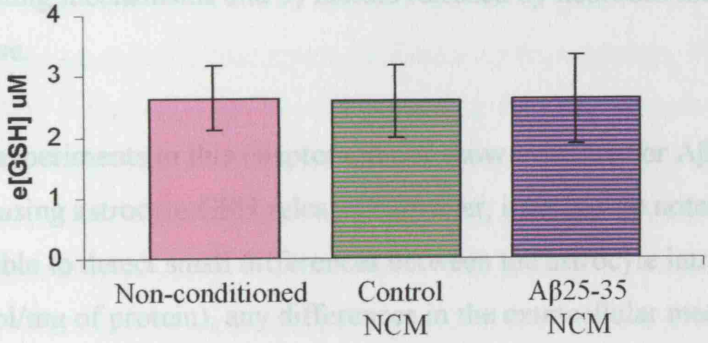

Figure 6.10: Astrocyte released GSH after incubation in NCM. Non-conditioned = 2.65 ± 0.53 μM, control NCM = 2.59 ± 0.6, Aβ25-35 NCM = 2.62 ± 0.74 μM. n=3

6.4 Discussion

In this thesis, so far the emphasis had been on astrocyte-to-neurone supportive functions particularly GSH support. However, neurones can also communicate with astrocytes. As introduced in section 1.3, astrocytes form intimate connections with neurones at synapses and the cytoplasm of adjacent astrocytes is linked by gap junctions, allowing rapid communication between populations of astrocytes. Under normal conditions, astrocytes have been demonstrated to respond to neural activity, generating Ca^{2+} oscillations, which promote the release of astrocyte derived glutamate at points further down the neural pathway to transfer the information of neuronal activity to neurones away from the site of initial astrocyte activation (reviewed in Fellin *et al.*, 2004).

The experiments presented in this chapter demonstrate that astrocytes were affected by the presence of injured neurones and that neurones treated with Aβ25-35 caused a lowering of astrocyte intracellular GSH levels. This effect was observed in the presence of neurones and with neurone-conditioned medium.

There are three possible reasons underlying the depletion of astrocyte GSH; 1) dying neurones release factors that deplete astrocyte GSH supplies, either by direct oxidation of GSH, through conjugation with GSH via a glutathione transferase mediated reaction or in the enzymic detoxification of H_2O_2 as a cofactor for glutathione peroxidase (see Section 1.3.4.1), 2) factors released by neurones affect astrocyte glutathione synthesis or recycling mechanisms and 3) factors released by neurones increase astrocyte GSH release.

The experiments in this chapter did not show evidence for Aβ25-35 treated neurones increasing astrocyte GSH release. However, it should be noted that although it was possible to detect small differences between the astrocyte intracellular GSH level (~ 2nmol/mg of protein), any differences in the extracellular medium may have been diluted in the relatively large volume of medium (1.5ml).

It would seem likely that factors released by dying or lysed neurones may be actively depleting astrocyte GSH or affecting the pathways employed in astrocyte GSH homeostasis. The experiments presented in this thesis have demonstrated the resilience of the astrocyte GSH system to depletion by ROS generated in the presence of Aβ25-35. Likewise studies by other groups have demonstrated that astrocytes can maintain their GSH levels under a variety of oxidative insults, that are toxic to neurones (See Figure (4.14)) which suggests that this effect is unlikely to be due to neurone derived ROS. Support for this hypothesis is provided by the observation that the extracellular GSH was the same from astrocytes incrubated in control NCM, Aβ25-35 NCM and non conditioned medium.

It may be the case that other non-ROS factors released from neurones may be responsible for the observed effect. To date limited work has been done on how astrocytes respond to damaged neurones in isolation of the noxious insult. However, studies carried out on spinal cord astrocyte and neurone cultures have implicated fibroblast growth factor (FGF-1) as a potential neurone to astrocyte signalling factor associated with neurone death (Cassina *et al.*, 2005).

FGF-1 is expressed in neurones and its expression is Ca^{2+} dependent (Kinukawa *et al.*, 2004). FGF-1 is not normally released from healthy neurones, but has been suggested to be released from damaged neurones (Cassina *et al.*, 2005). Fibroblasts transfected with FGF-1 have lowered GSH levels, even though GSH synthesis appears to be increased (Choi *et al.*, 2000). However, Cassina and colleagues (2005) have shown that FGF-1 activated spinal cord astrocytes. In follow up experiments, Vargas *et al.*, (2006), showed that FGF-1 activated spinal cord astrocytes showed increased NO release. Similar to the work of Gegg *et al.*, 2002, activation was also associated with increased intracellular GSH levels and GSH release. In the light of the work presented in this chapter, it would be interesting to assess whether FGF-1 was present in the extracellular medium of Aβ25-35 treated neurones and, as the glutathione system of astrocyte populations from different CNS areas may respond differently. The effect of FGF-1 on cortical astrocyte GSH levels needs further investigation.

An alternative explanation of the decrease in astrocyte GSH would be that lysed neurones release noxious substances that the astrocytes detoxify using their Glutathione-S-transferase system therefore lowering their GSH levels, by its utilisation for conjugation. Whatever the mechanism underlying the lowering of GSH observed in this chapter, it seems that although astrocytes are capable of maintaining their GSH to a greater extent than neurones in the presence of Aβ25-35, concomittent lowering of astrocyte GSH in the presence of damaged neurones may limit the astrocyte's ability to provide neurones with GSH support over a long time period.

6.5 Conclusions

In this chapter astrocytes were co-cultured with Aβ25-35 treated neurones or incubated in conditioned medium from Aβ25-35 treated neurones. It was observed in both cases that this caused a small decrease in the astrocyte GSH levels. It is suggested that a factor either released from neurones whilst they are under stress or an intracellular factor released when the neurone membrane is disrupted in the presence of Aβ25-35 may cause this effect. The lowering of astrocyte glutathione levels did not appear to be due to increased GSH release, and therefore might be due to modulation of astrocyte GSH homeostasis pathways or through utilisation of GSH in its role as an antioxidant, and a co-factor.

Chapter 7: General discussion and suggested future work

7. General discussion and suggested future work

7.1 Antioxidant therapies; a plausible treatment strategy for AD?

Aβ is strongly implicated in the pathogenesis of AD. Aggregated Aβ has been shown to generate ROS and the neurone death in AD is considered to be due to increased oxidative stress. Antioxidant supplementation has been shown to reduce neurone death in *in vitro* (Behl *et al.*, 1992; Behl *et al.*, 1994; Abramov *et al.*, 2004; Boyd Kimball *et al.*, 2005). Besides direct Aβ-mediated toxicity through the generation of ROS, several groups have demonstrated that ROS may actually promote Aβ fibrillisation, and that antioxidants added to solutions might inhibit Aβ fibril formation (Reviewed in Ono *et al.*, 2006) or that Aβ fibril formation is promoted by impaired antioxidant systems (Woltjer *et al.*, 2005). Therefore the use of antioxidant therapies as a possible protective strategy or to slow down progression of AD have been investigated.

However previous studies have shown that dietary vitamin E and C antioxidant supplementation does not seem to improve cognition in elderly people (Jama *et al.*, 1996) nor to have a significant effect on slowing Alzheimer's disease progression (Peterson *et al.*, 2005). Likewise treatment with polyphenols only had an exceedingly modest effect (Truelsen *et al.*, 2002). However, the problem might be that, when delivered through the diet, these antioxidants might have a systemic effect and are not targeted directly to the site in which they are needed.

As the brain is a very metabolically active organ, it generates comparatively higher levels of ROS compared to other tissues. Therefore it posesses a strong battery of antioxidant defences. However, the brain's antioxidant defences appear to become less efficient with age (Smith *et al.*, 1991; Yoritaka *et al.*, 1996; Reich *et al.*, 2001; Lu *et al.*, 2004), and are less capable to detoxify Aβ generated ROS as evidenced by an increased level of oxidative stress markers in the AD brains (Vitek *et al.*, 1994; Markesbery and Lovell, 1998; Butterfield and Lauderback, 2002; Wang *et al.*, 2005). It is important therefore, to delineate how the brain's antioxidant systems mechanisms and pathways operate in the aging

brain and in the presence of Aβ in order to develop future therapeutic strategies that target these intrinsic systems.

7.2 Astrocyte and neurone glutathione in the presence of Aβ

In the present work, the focus had been on the antioxidant glutathione (GSH) and the effect of Aβ on astrocyte and neurone GSH homeostasis. Neurones rely on astrocytes for their GSH synthesis, and in culture conditions, where they are cultured in the absence of astrocytes, neurones have much lower GSH than astrocytes.

In the present study, neurone GSH was upregulated by astrocyte conditioned medium (ACM) and by the glutathione precursor γ glutamylcysteine (γGC) to the same degree. GSH and γGC provided neurones similar protection against Aβ25-35 toxicity suggesting that GSH may be an important factor released by astrocytes for neuronal protection. It has been proposed by other groups, who have shown that under their experimental conditions that Aβ25-35 lowered astrocyte GSH, and that in the presence of Aβ astrocyte to neurone GSH support may be compromised (Abramov *et al.*, 2003). However, in the present study, it was demonstrated that there was an increase in the GSH released from Aβ25-35 treated astrocytes compared to control astrocytes, demonstrating that astrocyte to neurone GSH support was not only maintained, but also may be elevated in the presence of Aβ25-35.

Although an increase in extracellular intact GSH (i.e. GSH which had not been cleaved to CysGly to be taken up by neurones) would protect neurones from ROS generated in the extracellular environment, there seemed to be an upper limit to the up-regulation of the intracellular GSH in cultured neurones incubated in control ACM, Aβ25-35 ACM or supplemented with γ-GC in the 24 hour time period. In addition, the neurone intracellular GSH levels remained much lower compared to the astrocytes even after supplementation with GSH precursors or ACM. In the brain, it has been observed that cortical neurones have less GSH than cortical astrocytes despite having a constant supply of GSH precursors. This was determined by measuring GSH in neurones and astrocytes immediately after

isolation from the adult rat brain (Langeveld *et al.*, 1996). Although neurone GSH levels are limited by the availability of cysteine (Sagara *et al.*, 1993), the GSH levels are also regulated by the activity of glutamate cysteine ligase (GCL), the rate-limiting enzyme in glutathione synthesis. GSH itself may have a feedback inhibiting effect on its own synthesis, by inhibiting GCL activity (Huang *et al.*, 1993).

If it were a therapeutic strategy to increase the ability of neurones to defend against ROS generated in the presence of Aβ using their GSH systems, clearly it would be useful to understand mechanisms by which neurone GCL activity can be modulated.

It has been shown that GCL activity can be upregulated in astrocytes by a NO mediated mechanism, but this does not seem to occur in neurones (Gegg *et al.*, 2002). Neurone GCL activity was increased, however, when neurones were co-cultured with GSH deficient astrocytes, compared with non-conditioned medium or GSH releasing astrocytes suggesting that other astrocyte derived signals might increase neurone GSH synthesis capabilities (Gegg *et al.*, 2005). Iwata-Ichikawa *et al.*, (1999) showed that an oxidative treatment with (6hydroxydopamine (6-OHDA), or H_2O_2) presented in astrocyte conditioned medium (ACM) increased neurone GCL mRNA levels. This effect was not observed when the neurones were treated with ACM alone or with 6-OHDA or H_2O_2 in non-conditioned medium. In the present study it was demonstrated that supplementation of neurones with γ-glutamylcysteine or ACM increased the basal viability of neurone cultures suggesting that a proportion of the normal basal neurone death in primary culture might be due to the ROS generated under these cell culture conditions where cells did not receive antioxidant support. It is tempting to speculate that in the study of Gegg *et al.*, (2005) a response to basal ROS production in the neurones (which are deprived of astrocyte antioxidant support) coupled with astrocyte derived factors, might have been responsible for the observed up-regulation of GCL. To test the hypothesis that neurone GCL activity or expression may be upregulated by an astrocyte derived factor coupled with the presence of ROS, a suggested follow on experiment would be to measure the rate of activity of GCL directly by measuring its product, γ-GC by the HPLC method

described in Gegg *et al.*, (2002) and GCL mRNA levels in neurones treated with Aβ25-35 in non-conditioned medium compared to neurones treated with Aβ25-35 in ACM.

In this thesis the responses of neurones and astrocytes to Aβ25-35 in separate cultures, but treated under the same medium conditions, were investigated and compared. It was shown that astrocytes could maintain their GSH levels in the presence of Aβ25-35 whereas neurones could not. The ability of astrocytes to maintain their GSH levels appeared to correspond to their ability to up-regulate the activity of the enzyme glutathione reductase, needed to recycle GSH from the oxidised disulphide form (GSSG). The activity of glutathione reductase depends on the availability of its co-factor NADPH. The main source of NADPH is the pentose phosphate pathway (PPP) (Palmer *et al.*, 1999). Lovel *et al.*, (1995) and Palmer *et al.*, (1999) have shown that there is increased activity of one of the enzymes of this pathway glucose-6-phosphate dehydrogenase (G6PD) in the AD brain. Therefore it would be worthwhile to measure the activity of G6PD in the presence of Aβ35-35. However, it might be the case that glutathione reductase expression is increased, this possibility should be also assessed.

The ability of astrocytes to maintain their GSH levels in the presence of Aβ25-35 seems to fit a pattern in which astrocytes keep functioning when treated with oxidative insults that are toxic to neurones, whilst increasing their GSH release.

Neurones did not appear to be able to upregulate their glutathione reductase (GR) activity or glutathione levels in the response to Aβ25-35. As neurones have much lower GSH levels than astrocytes under culture conditions, they may have a lower critical threshold for oxidative damage, and GSH maintenance mechanisms may not be able to operate in damaged cells. Studies in which neurones were treated with sub-lethal doses of Aβ25-35 (treatment with 10μM Aβ25-35 on DIV2 neurones) had shown that neurones were capable of upregulating their GR activity under milder oxidative conditions (White *et al.*, 1999). Garcia Nogales *et al.*, (2003) have also shown that neurones treated with sub-lethal doses of peroxynitrite could upregulate their PPP activity and NADPH production. In future studies it would be, therefore, interesting to gradually

decrease the amount of Aβ25-35 as well as the treatment period to see the points at which these potential protective mechanisms are lost in neurones, and the emergence of other cellular processes that occur at these points.

Aβ25-35 ACM contained more GSH than control ACM but was also likely to have contained numerous releasable factors upregulated in stellate astrocytes in response to Aβ25-35 (see Figure 1.9). Conditioned medium from Aβ25-35 treated astrocytes did not appear to be directly toxic to neurones; however therewas a trend for Aβ25-35 ACM to be less protective than control ACM when neurones were treated with Aβ25-35. Paradisi *et al.*, (2004) had previously shown that control astrocytes were protective to neurones but Aβ treated astrocytes were not. This suggests that the potential for protection of the astrocyte derived GSH may be outbalanced or modulated by other factors released by astrocytes. To unequivocally test that astrocyte derived GSH is a factor in ACM that is protective to neurones, and to tease out other factors that are released by astrocytes, that have an effect on neurones on exposure to Aβ25-35, that may be masked by the effect of the astrocyte derived antioxidant support it is necessary to find a way to selectively block astrocyte GSH release. Depletion of astrocyte GSH by selective inhibition of GSH was not sufficient owing to the quick recovery of astrocyte GSH levels on the removal of the GCL inhibitor L-BSO. Although inhibition of astrocyte γ-glutamyl transpeptidase, the enzyme that cleaves GSH to CysGly, which can be utilised by neurones to up-regulate their GSH levels was shown by Dringen *et al.*,(1999), to prevent neurone GSH upregulation in the presence of astrocytes. However, in the culture conditions used in the present this did not seem sufficient to completely abrogate GSH upregulation in neurones. It is therefore proposed that inhibition of γ-glutamyl transpeptidase coupled with immunoprecipitation of GSH is a possible strategy to remove astrocyte derived GSH to further resolve the role of astrocyte derived GSH in the support to neurones.

The neuroprotective potential of astrocyte glutathione may also be influenced by the neurones themselves. The treatment protocol used in the present study resulted in extensive neurone death and neuronal membrane lysis. Astrocytes

cultured in the presence of Aβ25-35 treated neurones had lower GSH than those grown in control conditions, the mechanisms for this decrease were not elucidated in the current study. However, this demonstrates that in the brain, astrocytes might react to neurone death as well as Aβ (Katayama *et al.*, 2002; Cassina *et al.*, 2005). Astrocyte support may not be maintained in the presence of dying neurones even though it is maintained in the presence of Aβ. As neurone death persists over the course of AD chronic exposure to Aβ treated neurones may diminish the astrocyte ability to provide GSH and its associated protection to neurones in the long term. The observations presented in this thesis show an interesting effect but further investigation into the factors released from neurones responsible for this effect would be worthwhile.

As both astrocyte and conditioned media contain a cocktail of unknown factors. A practical approach would be to do an initial screen of the conditioned medium from Aβ25-35 treated neurones and astrocytes compared to their controls using 2D gel electrophoresis followed by mass spectrometric analysis, to find candidate factors that could be involved in astrocyte –neuron communication in the presence of Aβ25-35.

7.3 Neurones are more vulnerable to Aβ toxicity than astrocytes: Additional differences between the two cell types

It is a useful approach to compare the properties of astrocytes and neurones to try to elucidate why neurones are particularly vulnerable to Aβ mediated toxicity. It was striking that although the neurones treated with Aβ25-35 in this study appeared to undergo apoptotic nuclear condensation, the majority of dead cells also had permeable membranes at the time of examination. Apoptotic cells are usually defined as having intact membranes; this is one feature of the controlled nature of this death pathway allowing apoptotic cells to be phagocytised without releasing their contents, which could be potentially neurotoxic to other cells (Raff, 1998). Nevertheless it has also been observed that late stage apoptotic cells can have permeable membranes (Smolewski *et al.*, 2002). Aβ can generate ROS and reactive nitrogen species (RNS) by a variety of mechanisms both intracellularly and extracellularly. One target of oxidative damage is the lipid

components of the plasma membrane, which when disrupted may then lead to the membrane becoming permeable.

Another particularly interesting finding was that neurite degeneration occurred before apoptotic cascade activation in the soma when Aβ was added to neurones in culture (Ivins *et al.*, 1998). Bedlack *et al.*, (1994) had previously shown that there was a difference in the intramembrane electric field between soma and neurites that was independent of ion channel distribution. The authors attributed the difference to a difference in membrane composition between neurite and the soma membranes of the cell. Although similar data were not available for cortical neurones, Calderon *et al.*, 1995 had shown a higher proportion of cholesterol in the neurites compared to the soma for dorsal root ganglia. Cholesterol has been implicated in learning and memory mechanisms (Nelson and Alkon, 2005a), as well as in Alzheimer's disease as therapy with statins which lower plasma cholesterol levels can lower the risk for AD (Jick *et al.*, 2003). Cholesterol is found in plasma membranes and is important for determining the fluidity of the membrane. However cholesterol can be oxidised by Aβ to generate 7-beta hydroxyl cholesterol, which is a pro-apoptotic signalling molecule (Nelson and Alkon, 2005b). It has also been observed that if the membrane cholesterol contents of rat pheochromocytoma (PC12) cells were lowered the cells were less vulnerable to Aβ toxicity (Wang *et al.*, 2005).

These observations of the differences between soma and neurites and their differential vulnerability to Aβ provide impetus to compare the membrane characteristics of neurones and astrocytes. Although it was not possible to find data in the literature to compare the membrane composition of neurone and astrocytes, Tabernero *et al.*, (1993), have reported a difference in the rate of lipogenesis from lactate in rat primary neurone and astrocyte cultures which might lead to differential lipid composition of adult neurones and astrocytes. The distribution of cholesterol in different membrane structures may also differ. Astrocytes have a higher proportion of cholesterol in their intracellular membranes, whereas neurones have a higher proportion of cholesterol in their plasma membrane (Rapp *et al.*, 2006).

To address why neurites are particularly vulnerable to Aβ mediated damage, and to investigate a potential difference between neurones and astrocytes besides their intracellular GSH levels which render neurones more susceptible to Aβ than astrocytes, it is proposed that the membranes lipid composition of neurone and astrocytes under the culture conditions employed in this study should be assessed.

7.4 Conclusions.

In conclusion, the experiments presented in this thesis have used primary cortical neurone and astrocyte cultures, co-cultures and conditioned medium paradigms to investigate the toxic mechanisms of Aβ and the response of the astrocyte and neurone GSH systems to Aβ25-35. The work presented has demonstrated that primary cortical astrocytes are particularly resistant to Aβ25-35 toxicity compared with neurones. It is proposed that at least one of the mechanisms involved may be that in addition to having greater glutathione levels, astrocytes unlike neurones are able to upregulate GSSG to GSH recycling in response to the concentration of Aβ25-35 used in this study, by upregulating the activity of glutathione reductase. Astrocytes, in this way, are able to maintain their GSH levels to defend against ROS generated in the presence of Aβ. Furthermore, astrocytes treated with Aβ25-35 release more GSH into the extracellular medium than control astrocytes, which suggests that astrocyte to neurone GSH support is enhanced in the presence of Aβ25-35. The response of the astrocyte GSH system to Aβ25-35 demonstrated in this project seems to parallel the response of astrocytes to other oxidative insults.

Neurones in pure culture conditions may have limited availability of GSH substrates than they would receive *in vivo*. Astrocyte conditioned medium can upregulate neuronal GSH and give partial protection against Aβ25-35 mediated toxicity. However, neurone GSH levels are not only limited by the availability of substrates but also the rate of glutamate cysteine ligase. Possible routes to further enhance neuronal GSH levels in culture conditions in addition to providing astrocyte support may be to further investigate factors regulating the activities of neurone glutamate cysteine ligase and glutathione reductase.

Although astrocyte GSH release is increased in the presence of Aβ25-35, other factors released by astrocytes that may have an effect on neurones should be determined. In addition astrocyte GSH levels seem to be lowered by factors released from Aβ25-35 treated neurones. Chronic exposure to such neurone-derived factors may further limit astrocyte GSH neuroprotective potential in Alzheimer's Disease.

REFERENCES

Abe K. and Misawa M. (2003) Amyloid beta protein enhances the clearance of extracellular L-glutamate by cultured rat cortical astrocytes. *Neurosci Res* **45,** 25-31.

Abramov A. Y., Canevari L., and Duchen M. R. (2003) Changes in intracellular calcium and glutathione in astrocytes as the primary mechanism of amyloid neurotoxicity. *J Neurosci* **23,** 5088-5095.

Abramov A. Y., Canevari L., and Duchen M. R. (2004) beta-amyloid peptides induce mitochondrial dysfunction and oxidative stress in astrocytes and death of neurons through activation of NADPH oxidase. *J Neurosci* **24,** 565-575.

Abramov A. Y., Canevari L., and Duchen M. R. (2004) Amyloid beta peptides induce mitochondrial dysfunction and oxidative stress in astrocytes and death of neurons through activation of NADPH oxidase. *Biophysical Journal* **86,** 469A.

Abramov A. Y., Jacobson J., Wientjes F., Hothersall J., Canevari L., and Duchen M. R. (2005) Expression and modulation of an NADPH oxidase in mammalian astrocytes. *J Neurosci* **25,** 9176-9184.

Adachi T., Satoh M., Pramanik R., Kuroda S., Ishido M., and Kunimoto M. (2006) Region-dependent differences and alterations of protective thiol compound levels in cultured astrocytes and brain tissues. *Biol Pharm Bull* **29,** 1466-1469.

Akama K. T. and Van Eldik L. J. (2000) beta-amyloid stimulation of inducible nitric-oxide synthase in astrocytes is interleukin-1 beta- and tumor necrosis factor-alpha (TNF alpha)-dependent, and involves a TNF alpha receptor-associated factor- and NF kappa B-inducing kinase-dependent signaling mechanism. *Journal of Biological Chemistry* **275,** 7918-7924.

Aksenov M. Y., Aksenova M. V., Carney J. M., and Butterfield D. A. (1997) Oxidative modification of glutamine synthetase by amyloid beta peptide. *Free Radical Research* **27,** 267-281.

Alarcon R., Fuenzalida C., Santibanez M., and von Bernhardi R. (2005) Expression of scavenger receptors in glial cells - Comparing the adhesion of astrocytes and microglia from neonatal rats to surface-bound beta-amyloid. *J Biol Chem* **280,** 30406-30415.

Alexander G. E., Chen K., Pietrini P., Rapoport S. I., and Reiman E. M. (2002) Longitudinal PET Evaluation of Cerebral Metabolic Decline in Dementia: A Potential Outcome Measure in Alzheimer's Disease Treatment Studies. *Am J Psychiatry* **159,** 738-745.

Ali-Osman F., Antoun G., Wang H., Rajagopal S., and Gagucas E. (1996) Buthionine sulfoximine induction of gamma-L-glutamyl-L-cysteine synthetase gene expression, kinetics of glutathione depletion and resynthesis, and modulation of carmustine-induced DNA-DNA cross-linking and cytotoxicity in human glioma cells. *Mol Pharmacol* **49,** 1012-1020.

Allison R. D. and Meister A. (1981) Evidence that transpeptidation is a significant function of gamma-glutamyl transpeptidase. *J Biol Chem* **256,** 2988-2992.

Alvarez G., Ramos M., Ruiz F., Satrustegui J., and Bogonez E. (2003) Pyruvate protection against beta-amyloid-induced neuronal death: role of mitochondrial redox state. *J Neurosci Res* **73,** 260-269.

Alzheimer A (1907) Über eine eigenartige Erkrankung der Hirnrinde. *Allg. Zeitschr Psychiatr Psychiatr-Gerichtl Med 109, 146-148.*

Alzheimer A., Stelzmann R. A., Schnitzlein H. N., and Murtagh F. R. (1995) An English translation of Alzheimer's 1907 paper, "Uber eine eigenartige Erkankung der Hirnrinde". *Clin Anat* **8,** 429-431.

Anderson M. E. and Meister A. (1983) Transport and direct utilization of gamma-glutamylcyst(e)ine for glutathione synthesis. *Proc Natl Acad Sci U S A* **80,** 707-711.

Anderson M. E., Powrie F., Puri R. N., and Meister A. (1985) Glutathione monoethyl ester: preparation, uptake by tissues, and conversion to glutathione. *Arch Biochem Biophys* **239,** 538-548.

Apelt J., Ach K., and Schliebs R. (2003) Aging-related down-regulation of neprilysin, a putative beta-amyloid-degrading enzyme, in transgenic Tg2576 Alzheimer-like mouse brain is accompanied by an astroglial upregulation in the vicinity of beta-amyloid plaques. *Neurosci Lett* **339,** 183-186.

Araki N., Higashi T., Mori T., Shibayama R., Kawabe Y., Kodama T., Takahashi K., Shichiri M., and Horiuchi S. (1995) Macrophage scavenger receptor mediates the endocytic uptake and degradation of advanced glycation end products of the Maillard reaction. *Eur J Biochem* **230,** 408-415.

Araujo D. M. and Cotman C. W. (1992) Beta-Amyloid Stimulates Glial-Cells Invitro to Produce Growth-Factors That Accumulate in Senile Plaques in Alzheimers-Disease. *Brain Research* **569,** 141-145.

Araujo D. M. and Cotman C. W. (1992) Basic Fgf in Astroglial, Microglial, and Neuronal Cultures - Characterization of Binding-Sites and Modulation of Release by Lymphokines and Trophic Factors. *J Neurosce* **12,** 1668-1678.

Arispe N., Rojas E., and Pollard H. B. (1993) Alzheimer disease amyloid beta protein forms calcium channels in bilayer membranes: blockade by tromethamine and aluminum. *Proc Natl Acad Sci U S A* **90,** 567-571.

Attwell D. and Laughlin S. B. (2001) An energy budget for signaling in the grey matter of the brain. *Journal of Cerebral Blood Flow and Metabolism* **21,** 1133-1145.

Aylward E. H., Li Q., Honeycutt N. A., Warren A. C., Pulsifer M. B., Barta P. E., Chan M. D., Smith P. D., Jerram M., and Pearlson G. D. (1999) MRI volumes of the hippocampus and amygdala in adults with Down's syndrome with and without dementia. *Am J Psychiatry* **156,** 564-568.

Bains J. S. and Shaw C. A. (1997) Neurodegenerative disorders in humans: the role of glutathione in oxidative stress-mediated neuronal death. *Brain Res Brain Res Rev* **25,** 335-358.

Balazs and Leon (1994) Evidence of an oxidative challenge to Alzheimer's brain. *Neurochemical research* 19 (9)1131-7.

Bal-Price A., Moneer Z., and Brown G. C. (2002) Nitric oxide induces rapid, calcium-dependent release of vesicular glutamate and ATP from cultured rat astrocytes. *Glia* **40,** 312-323.

Banker G. A. (1980) Trophic interactions between astroglial cells and hippocampal neurons in culture. *Science* **209,** 809-810.

Barnham K. J., McKinstry W. J., Multhaup G., Galatis D., Morton C. J., Curtain C. C., Williamson N. A., White A. R., Hinds M. G., Norton R. S., Beyreuther K., Masters C. L., Parker M. W., and Cappai R. (2003) Structure of the Alzheimer's disease amyloid precursor protein copper binding domain. A regulator of neuronal copper homeostasis. *J Biol Chem* **278,** 17401-17407.

Bedlack R. S., Jr., Wei M. D., Fox S. H., Gross E., and Loew L. M. (1994) Distinct electric potentials in soma and neurite membranes. *Neuron* **13,** 1187-1193.

Beffert U., Aumont N., Dea D., Lussier-Cacan S., Davignon J., and Poirier J. (1998) Beta-amyloid peptides increase the binding and internalization of apolipoprotein E to hippocampal neurons. *J Neurochem* **70,** 1458-1466.

Behl C., Davis J., Cole G. M., and Schubert D. (1992) Vitamin-e Protects Nerve-Cells from Amyloid Beta-Protein Toxicity. *Biochemical and Biophysical Research Communications* **186,** 944-950.

Behl C., Davis J. B., Lesley R., and Schubert D. (1994) Hydrogen-Peroxide Mediates Amyloid-Beta Protein Toxicity. *Cell* **77,** 817-827.

Behl C., Davis J. B., Klier F. G., and Schubert D. (1994) Amyloid-Beta Peptide Induces Necrosis Rather Than Apoptosis. *Brain Research* **645,** 253-264.

Benarroch E (2005) Neuron-astrocyte interactions: Partnership for normal function and disease in the central nervous system. *Mayo Clin proceedings 80(10): 1326-1338.*

Ben Yoseph O., Camp D. M., Robinson T. E., and Ross B. D. (1995) Dynamic measurements of cerebral pentose phosphate pathway activity in vivo using [1,6-13C2,6,6-2H2]glucose and microdialysis. *J Neurochem* **64,** 1336-1342.

Benveniste H., Einstein G., Kim K. R., Hulette C., and Johnson G. A. (1999) Detection of neuritic plaques in Alzheimer's disease by magnetic resonance microscopy. *Proc Natl Acad Sci U S A* **96,** 14079-14084.

BenYoseph O., Boxer P. A., and Ross B. D. (1996) Assessment of the role of the glutathione and pentose phosphate pathways in the protection of primary cerebrocortical cultures from oxidative stress. *J Neurochem* **66,** 2329-2337.

Benzi G. and Moretti A. (1995) Age- and peroxidative stress-related modifications of the cerebral enzymatic activities linked to mitochondria and the glutathione system. *Free Radic Biol Med* **19,** 77-101.

Beyreuther K.L and Masters C.L (1991) Amyloid precursor protein (APP) and beta A4 in the aetiology of Alzheimer's disease: Precursor product relationships in the development of neuronal function. *Brain Pathology* 1:241-251.

Bianca V. D., Dusi S., Bianchini E., Dal P., I, and Rossi F. (1999) beta-amyloid activates the O-2 forming NADPH oxidase in microglia, monocytes, and neutrophils. A possible inflammatory mechanism of neuronal damage in Alzheimer's disease. *J Biol Chem* **274,** 15493-15499.

Bieschke J., Zhang Q., Powers E. T., Lerner R. A., and Kelly J. W. (2005) Oxidative metabolites accelerate Alzheimer's amyloidogenesis by a two-step mechanism, eliminating the requirement for nucleation. *Biochemistry* **44,** 4977-4983.

Billingsley M. L. and Kincaid R. L. (1997) Regulated phosphorylation and dephosphorylation of tau protein: effects on microtubule interaction, intracellular trafficking and neurodegeneration. *Biochem J* **323 (Pt 3),** 577-591.

Blanchard B. J., Konopka G., Russell M., and Ingram V. M. (1997) Mechanism and prevention of neurotoxicity caused by beta-amyloid peptides: relation to Alzheimer's disease. *Brain Res* **776,** 40-50.

Bolanos J. P., Peuchen S., Heales S. J., Land J. M., and Clark J. B. (1994) Nitric oxide-mediated inhibition of the mitochondrial respiratory chain in cultured astrocytes. *J Neurochem* **63,** 910-916.

Bolanos J. P., Heales S. J. R., Land J. M., and Clark J. B. (1995) Effect of Peroxynitrite on the Mitochondrial Respiratory-Chain - Differential Susceptibility of Neurons and Astrocytes in Primary Culture. *J Neurochem* **64,** 1965-1972.

Bouzier-Sore A. K., Voisin P., Canioni P., Magistretti T. J., and Pellerin T. (2003) Lactate is a preferential oxidative energy substrate over glucose for neurons in culture. *Journal of Cerebral Blood Flow and Metabolism* **23,** 1298-1306.

Boyd-Kimball D., Sultana R., Abdul H. M., and Butterfield D. A. (2005) gamma-glutamylcysteine ethyl ester-induced up-regulation of glutathione protects neurons against A beta(1-42)-mediated oxidative stress and neurotoxicity: Implications for Alzheimer's disease. *Journal of Neuroscience Research* **79,** 700-706.

Braak H. and Braak E. (1991) Neuropathological stageing of Alzheimer-related changes. *Acta Neuropathol (Berl)* **82,** 239-259.

Bradford M. M. (1976) A rapid and sensitive method for the quantitation of microgram quantities of protein utilizing the principle of protein-dye binding. *Anal Biochem* **72,** 248-254.

Bramblett G. T., Goedert M., Jakes R., Merrick S. E., Trojanowski J. Q., and Lee V. M. (1993) Abnormal tau phosphorylation at Ser396 in Alzheimer's disease recapitulates development and contributes to reduced microtubule binding. *Neuron* **10,** 1089-1099.

Breen K. C., Bruce M., and Anderton B. H. (1991) Beta amyloid precursor protein mediates neuronal cell-cell and cell-surface adhesion. *J Neurosci Res* **28,** 90-100.

Brewer G. J., Torricelli J. R., Evege E. K., and Price P. J. (1993) Optimized Survival of Hippocampal-Neurons in B27-Supplemented Neurobasal(Tm), A New Serum-Free Medium Combination. *J Neurosci Res* **35,** 567-576.

Butterfield D. A. and Lauderback C. M. (2002) Lipid peroxidation and protein oxidation in Alzheimer's disease brain: Potential causes and consequences involving amyloid beta-peptide-associated free radical oxidative stress. *Free Radical Biology and Medicine* **32,** 1050-1060.

Butterfield D. A. and Kanski J. (2002) Methionine residue 35 is critical for the oxidative stress and neurotoxic properties of Alzheimer's amyloid beta-peptide 1-42. *Peptides* **23,** 1299-1309.

Caccamo A., Oddo S., Sugarman M. C., Akbari Y., and LaFerla F. M. (2005) Age- and region-dependent alterations in Abeta-degrading enzymes: implications for Abeta-induced disorders. *Neurobiol Aging* **26,** 645-654.

Calderon R. O., Attema B., and DeVries G. H. (1995) Lipid composition of neuronal cell bodies and neurites from cultured dorsal root ganglia. *J Neurochem* **64,** 424-429.

Callahan L. M. and Coleman P. D. (1995) Neurons bearing neurofibrillary tangles are responsible for selected synaptic deficits in Alzheimer's disease. *Neurobiol Aging* **16,** 311-314.

Canevari L., Clark J. B., and Bates T. E. (1999) beta-amyloid fragment 25-35 selectively decreases complex IV activity in isolated mitochondria. *Febs Letters* **457,** 131-134.

Canevari L., Abramov A. Y., and Duchen M. R. (2004) Toxicity of amyloid beta peptide: Tales of calcium, mitochondria, and oxidative stress. *Neurochemical Research* **29,** 637-650.

Caricasole A., Copani A., Caruso A., Caraci F., Iacovelli L., Sortino M. A., Terstappen G. C., and Nicoletti F. (2003) The Wnt pathway, cell-cycle activation and beta-amyloid: novel therapeutic strategies in Alzheimer's disease? *Trends in Pharmacological Sciences* **24,** 233-238.

Carson J. A. and Turner A. J. (2002) Beta-amyloid catabolism: roles for neprilysin (NEP) and other metallopeptidases? *J Neurochem* **81,** 1-8.

Casley C. S., Land J. M., Sharpe M. A., Clark J. B., Duchen M. R., and Canevari L. (2002) beta-amyloid fragment 25-35 causes mitochondrial dysfunction in primary cortical neurons. *Neurobiology of Disease* **10,** 258-267.

Casley C. S., Canevari L., Land J. M., Clark J. B., and Sharpe M. A. (2002) beta-amyloid inhibits integrated mitochondrial respiration and key enzyme activities. *J Neurochem* **80,** 91-100.

Cassina P., Pehar M., Vargas M. R., Castellanos R., Barbeito A. G., Estevez A. G., Thompson J. A., Beckman J. S., and Barbeito L. (2005) Astrocyte activation by fibroblast growth factor-1 and motor neuron apoptosis: implications for amyotrophic lateral sclerosis. *J Neurochem* **93,** 38-46.

Castegna A., Aksenov M., Aksenova M., Thongboonkerd V., Klein J. B., Pierce W. M., Booze R., Markesbery W. R., and Butterfield D. A. (2002) Proteomic identification of oxidatively modified proteins in Alzheimer's disease brain. Part 1: Creatine kinase bb, glutamine synthase, and ubiquitin carboxy-terminal hydrolase L-1. *Free Radical Biology and Medicine* **33,** 562-571.

Cecchi C., Latorraca S., Sorbi S., Iantomasi T., Favilli F., Vincenzini M. T., and Liguri G. (1999) Gluthatione level is altered in lymphoblasts from patients with familial Alzheimer's disease. *Neurosci Lett* **275,** 152-154.

Ceccon M., Giusti P., Facci L., Borin G., Imbesi M., Floreani M., and Skaper S. D. (2000) Intracellular glutathione levels determine cerebellar granule neuron sensitivity to excitotoxic injury by kainic acid. *Brain Res* **862,** 83-89.

Chen Y. and Swanson R. A. (2003) The glutamate transporters EAAT2 and EAAT3 mediate cysteine uptake in cortical neuron cultures. *J Neurochem* **84,** 1332-1339.

Cherny R. A., Atwood C. S., Xilinas M. E., Gray D. N., Jones W. D., McLean C. A., Barnham K. J., Volitakis I., Fraser F. W., Kim Y., Huang X., Goldstein L. E., Moir R. D., Lim J. T., Beyreuther K.,

Zheng H., Tanzi R. E., Masters C. L., and Bush A. I. (2001) Treatment with a copper-zinc chelator markedly and rapidly inhibits beta-amyloid accumulation in Alzheimer's disease transgenic mice. *Neuron* **30,** 665-676.

Choi J., Opalenik S. R., Wu W., Thompson J. A., and Forman H. J. (2000) Modulation of glutathione synthetic enzymes by acidic fibroblast growth factor. *Arch Biochem Biophys* **375,** 201-209.

Chou S.A. and Goldstein A. (1960) Chromogenic groupings in the Lowry protein determination. *Biochem J* **75,** 109-115.

Chung H., Brazil M. I., Soe T. T., and Maxfield F. R. (1999) Uptake, degradation, and release of fibrillar and soluble forms of Alzheimer's amyloid beta-peptide by microglial cells. *J Biol Chem* **274,** 32301-32308.

Clementi M. E., Martorana G. E., Pezzotti M., Giardina B., and Misiti F. (2004) Methionine 35 oxidation reduces toxic effects of the amyloid beta-protein fragment (31-35) on human red blood cell. *International Journal of Biochemistry & Cell Biology* **36,** 2066-2076.

Combs C. K., Karlo J. C., Kao S. C., and Landreth G. E. (2001) beta-Amyloid stimulation of microglia and monocytes results in TNF alpha-dependent expression of inducible nitric oxide synthase and neuronal apoptosis. *J Neurosci* **21,** 1179-1188.

Cooper AJL (1998) Role of astrocytes in maintaining cerebral glutathione homeostasis and protecting the brain against xenobiotics. In Glutathione in the nervous system ed Shaw CA; Taylor and Francis.

Corder E. H., Saunders A. M., Strittmatter W. J., Schmechel D. E., Gaskell P. C., Small G. W., Roses A. D., Haines J. L., and Pericakvance M. A. (1993) Gene Dose of Apolipoprotein-e Type-4 Allele and the Risk of Alzheimers-Disease in Late-Onset Families. *Science* **261,** 921-923.

Cotman C. W., Whittemore E. R., Watt J. A., Anderson A. J., and Loo D. T. (1994) Possible role of apoptosis in Alzheimer's disease. *Ann N Y Acad Sci* **747,** 36-49.

Dante S., Hauss T., and Dencher N. A. (2003) Insertion of externally administered amyloid beta peptide 25-35 and perturbation of lipid bilayers. *Biochemistry* **42,** 13667-13672.

Dawson T. M. and Snyder S. H. (1994) Gases as biological messengers: nitric oxide and carbon monoxide in the brain. *J Neurosci* **14,** 5147-5159.

de Ceballos M. L., Brera B., and Fernandez-Tome M. P. (2001) beta-Amyloid-induced cytotoxicity, peroxide generation and blockade of glutamate uptake in cultured astrocytes. *Clin Chem Lab Med* **39,** 317-318.

De Jonghe C., Esselens C., Kumar-Singh S., Craessaerts K., Serneels S., Checler F., Annaert W., Van Broeckhoven C., and De Strooper B. (2001) Pathogenic APP mutations near the gamma-secretase cleavage site differentially affect Abeta secretion and APP C-terminal fragment stability. *Hum Mol Genet* **10,** 1665-1671.

Deane R., Wu Z., Sagare A., Davis J., Du Y. S., Hamm K., Xu F., Parisi M., LaRue B., Hu H. W., Spijkers P., Guo H., Song X., Lenting P. J., Van Nostrand W. E., and Zlokovic B. V. (2004) LRP/amyloid beta-peptide interaction mediates differential brain efflux of Abeta isoforms. *Neuron* **43,** 333-344.

Deane R., Sagare A., Hamm K., Parisi M., LaRue B., Guo H., Wu Z., Holtzman D. M., and Zlokovic B. V. (2005) IgG-assisted age-dependent clearance of Alzheimer's amyloid beta peptide by the blood-brain barrier neonatal Fc receptor. *J Neurosci* **25,** 11495-11503.

Deneke S. M., Susanto I., Vogel K. A., Williams C. E., and Lawrence R. A. (1995) Mechanisms of use of extracellular glutathione by lung epithelial cells and pulmonary artery endothelial cells. *Am J Respir Cell Mol Biol* **12,** 662-668.

Dikalov S. I., Vitek M. P., Maples K. R., and Mason R. P. (1999) Amyloid beta peptides do not form peptide-derived free radicals spontaneously, but can enhance metal-catalyzed oxidation of hydroxylamines to nitroxides. *J Biol Chem* **274,** 9392-9399.

Domenici M. R., Paradisi S., Sacchetti B., Gaudi S., Balduzzi M., Bernardo A., Ajmone-Cat M. A., Minghetti L., and Malchiodi-Albedi F. (2002) The presence of astrocytes enhances beta amyloid-induced neurotoxicity in hippocampal cell cultures. *J Physiol Paris* **96,** 313-316.

Dong J., Atwood C. S., Anderson V. E., Siedlak S. L., Smith M. A., Perry G., and Carey P. R. (2003) Metal binding and oxidation of amyloid-beta within isolated senile plaque cores: Raman microscopic evidence. *Biochemistry* **42,** 2768-2773.

Double K. L., Halliday G. M., Kril J. J., Harasty J. A., Cullen K., Brooks W. S., Creasey H., and Broe G. A. (1996) Topography of brain atrophy during normal aging and Alzheimer's disease. *Neurobiology of Aging* **17,** 513-521.

Dringen R., Kranich O., Loschmann P. A., and Hamprecht B. (1997) Use of dipeptides for the synthesis of glutathione by astroglia-rich primary cultures. *J Neurochem* **69,** 868-874.

Dringen R., Hamprecht B., and Broer S. (1998) The peptide transporter PepT2 mediates the uptake of the glutathione precursor CysGly in astroglia-rich primary cultures. *J Neurochem* **71,** 388-393.

Dringen R., Kussmaul L., Gutterer J. M., Hirrlinger J., and Hamprecht B. (1999) The glutathione system of peroxide detoxification is less efficient in neurons than in astroglial cells. *J Neurochem* **72,** 2523-2530.

Dringen R. (2000) Metabolism and functions of glutathione in brain. *Progress in Neurobiology* **62,** 649-671.

Dringen R., Gutterer J. M., Gros C., and Hirrlinger J. (2001) Aminopeptidase N mediates the utilization of the GSH precursor CysGly by cultured neurons. *J Neurosci Res* **66,** 1003-1008.

Duara R., Grady C., Haxby J., Sundaram M., Cutler N. R., Heston L., Moore A., Schlageter N., Larson S., and Rapoport S. I. (1986) Positron Emission Tomography in Alzheimers-Disease. *Neurology* **36,** 879-887.

Edbauer D., Winkler E., Regula J. T., Pesold B., Steiner H., and Haass C. (2003) Reconstitution of gamma-secretase activity. *Nat Cell Biol* **5,** 486-488.

Eddleston M. and Mucke L. (1993) Molecular Profile of Reactive Astrocytes - Implications for Their Role in Neurologic Disease. *Neuroscience* **54,** 15-36.

Enoiu M., Aberkane H., Salazar J. F., Leroy P., Groffen J., Siest G., and Wellman M. (2000) Evidence for the pro-oxidant effect of gamma-glutamyltranspeptidase-related enzyme. *Free Radic Biol Med* **29,** 825-833.

Farrer L. A., Cupples L. A., Haines J. L., Hyman B., Kukull W. A., Mayeux R., Myers R. H., Pericak-Vance M. A., Risch N., and van Duijn C. M. (1997) Effects of age, sex, and ethnicity on the association between apolipoprotein E genotype and Alzheimer disease. A meta-analysis. APOE and Alzheimer Disease Meta Analysis Consortium. *JAMA* **278,** 1349-1356.

Fellin T. and Carmignoto G. (2004) Neurone-to-astrocyte signalling in the brain represents a distinct multifunctional unit. *J Physiol* **559,** 3-15.

Fellin T., Sul J. Y., D'Ascenzo M., Takano H., Pascual O., and Haydon P. G. (2006) Bidirectional astrocyte-neuron communication: the many roles of glutamate and ATP. *Novartis Found Symp* **276,** 208-217.

Fernandez-Tome P., Brera B., Arevalo M. A., and de Ceballos M. L. (2004) Beta-amyloid25-35 inhibits glutamate uptake in cultured neurons and astrocytes: modulation of uptake as a survival mechanism. *Neurobiol Dis* **15,** 580-589.

Floyd R. A. (1999) Antioxidants, oxidative stress, and degenerative neurological disorders. *Proceedings of the Society for Experimental Biology and Medicine* **222,** 236-245.

Fox N. C., Scahill R. I., Crum W. R., and Rossor M. N. (1999) Correlation between rates of brain atrophy and cognitive decline in AD. *Neurology* **52,** 1687-1689.

Francis R., McGrath G., Zhang J., Ruddy D. A., Sym M., Apfeld J., Nicoll M., Maxwell M., Hai B., Ellis M. C., Parks A. L., Xu W., Li J., Gurney M., Myers R. L., Himes C. S., Hiebsch R., Ruble C., Nye J. S., and Curtis D. (2002) aph-1 and pen-2 are required for Notch pathway signaling, gamma-secretase cleavage of betaAPP, and presenilin protein accumulation. *Dev Cell* **3,** 85-97.

Franks A. S. and Rawls W. N. (1998) Alzheimer's disease: Clinical features and pharmacologic management. *American Journal of Managed Care* **4,** 595-604.

Garcia-Nogales P., Almeida A., Fernandez E., Medina J. M., and Bolanos J. P. (1999) Induction of glucose-6-phosphate dehydrogenase by lipopolysaccharide contributes to preventing nitric oxide-mediated glutathione depletion in cultured rat astrocytes. *J Neurochem* **72,** 1750-1758.

Garcia-Nogales P., Almeida A., and Bolanos J. P. (2003) Peroxynitrite protects neurons against nitric oxide-mediated apoptosis - A key role for glucose-6-phosphate dehydrogenase activity in neuroprotection. *J Biol Chem* **278,** 864-874.

Gegg M. E., Clark J. B., and Heales S. J. (2002) Determination of glutamate-cysteine ligase (gamma-glutamylcysteine synthetase) activity by high-performance liquid chromatography and electrochemical detection. *Anal Biochem* **304,** 26-32.

Gegg M. E., Beltran B., Salas-Pino S., Bolanos J. P., Clark J. B., Moncada S., and Heales S. J. R. (2003) Differential effect of nitric oxide on glutathione metabolism and mitochondrial function in astrocytes and neurones: implications for neuroprotection/neurodegeneration? *J of Neurochem* **86,** 228-237.

Gegg M. E., Clark J. B., and Heales S. J. R. (2005) Co-culture of neurones with glutathione deficient astrocytes leads to increased neuronal susceptibility to nitric oxide and increased glutamate-cysteine ligase activity. *Brain Research* **1036,** 1-6.

Giaccone G., Tagliavini F., Linoli G., Bouras C., Frigerio L., Frangione B., and Bugiani O. (1989) Down Patients - Extracellular Preamyloid Deposits Precede Neuritic Degeneration and Senile Plaques. *Neuroscience Letters* **97,** 232-238.

Gibson G. E., Sheu K. F., and Blass J. P. (1998) Abnormalities of mitochondrial enzymes in Alzheimer disease. *J Neural Transm* **105,** 855-870.

Ginsberg S. D., Galvin J. E., Chiu T. S., Lee V. M., Masliah E., and Trojanowski J. Q. (1998) RNA sequestration to pathological lesions of neurodegenerative diseases. *Acta Neuropathol (Berl)* **96,** 487-494.

Glenner G. G. and Wong C. W. (1984) Alzheimer's disease: initial report of the purification and characterization of a novel cerebrovascular amyloid protein. *Biochem Biophys Res Commun* **120,** 885-890.

Golde T. E. and Younkin S. G. (2001) Presenilins as therapeutic targets for the treatment of Alzheimer's disease. *Trends Mol Med* **7,** 264-269.

Good P. F., Werner P., Hsu A., Olanow C. W., and Perl D. P. (1996) Evidence for neuronal oxidative damage in Alzheimer's disease. *American Journal of Pathology* **149,** 21-28.

Gouras G. K., Tsai J., Naslund J., Vincent B., Edgar M., Checler F., Greenfield J. P., Haroutunian V., Buxbaum J. D., Xu H. X., Greengard P., and Relkin N. R. (2000) Intraneuronal A beta 42 accumulation in human brain. *American Journal of Pathology* **156,** 15-20.

Griffin S., Clark J. B., and Canevari L. (2005) Astrocyte-neurone communication following oxygen-glucose deprivation. *J Neurochem* **95,** 1015-1022.

Griffin W. S. T., Stanley L. C., Ling C., White L., Macleod V., Perrot L. J., White C. L., and Araoz C. (1989) Brain Interleukin-1 and S-100 Immunoreactivity Are Elevated in Down Syndrome and Alzheimer-Disease. *Pro Nat Acad Sci* **86,** 7611-7615.

Grundke-Iqbal I., Iqbal K., Quinlan M., Tung Y. C., Zaidi M. S., and Wisniewski H. M. (1986) Microtubule-associated protein tau. A component of Alzheimer paired helical filaments. *J Biol Chem* **261,** 6084-6089.

Gu Y., Misonou H., Sato T., Dohmae N., Takio K., and Ihara Y. (2001) Distinct intramembrane cleavage of the beta-amyloid precursor protein family resembling gamma-secretase-like cleavage of Notch. *J Biol Chem* **276,** 35235-35238.

Gutterer J. M., Dringen R., Hirrlinger J., and Hamprecht B. (1999) Purification of glutathione reductase from bovine brain, generation of an antiserum, and immunocytochemical localization of the enzyme in neural cells. *J Neurochem* **73,** 1422-1430.

Gylys K. H., Fein J. A., Tan A. M., and Cole G. M. (2003) Apolipoprotein E enhances uptake of soluble but not aggregated amyloid-beta protein into synaptic terminals. *J Neurochem* **84,** 1442-1451.

Haass C., Schlossmacher M. G., Hung A. Y., Vigo-Pelfrey C., Mellon A., Ostaszewski B. L., Lieberburg I., Koo E. H., Schenk D., Teplow D. B., and . (1992) Amyloid beta-peptide is produced by cultured cells during normal metabolism. *Nature* **359,** 322-325.

Harper J. D. and Lansbury P. T., Jr. (1997) Models of amyloid seeding in Alzheimer's disease and scrapie: mechanistic truths and physiological consequences of the time-dependent solubility of amyloid proteins. *Annu Rev Biochem* **66,** 385-407.

Harris M. E., Wang Y. N., Pedigo N. W., Hensley K., Butterfield D. A., and Carney J. M. (1996) Amyloid beta peptide (25-35) inhibits Na+-dependent glutamate uptake in rat hippocampal astrocyte cultures. *J Neurochem* **67,** 277-286.

Hartley D. M., Walsh D. M., Ye C. P. P., Diehl T., Vasquez S., Vassilev P. M., Teplow D. B., and Selkoe D. J. (1999) Protofibrillar intermediates of amyloid beta-protein induce acute electrophysiological changes and progressive neurotoxicity in cortical neurons. *J Neurosci* **19,** 8876-8884.

Heales S. J., Davies S. E., Bates T. E., and Clark J. B. (1995) Depletion of brain glutathione is accompanied by impaired mitochondrial function and decreased N-acetyl aspartate concentration. *Neurochem Res* **20,** 31-38.

Hertel C., Hauser N., Schubenel R., Seilheimer B., and Kemp J. A. (1996) Beta-amyloid-induced cell toxicity: enhancement of 3-(4,5-dimethylthiazol-2-yl)-2,5-diphenyltetrazolium bromide-dependent cell death. *J Neurochem* **67,** 272-276.

Hertz L., Dringen R., Schousboe A., and Robinson S. R. (1999) Astrocytes: glutamate producers for neurons. *J Neurosci Res* **57,** 417-428.

Hirakura Y., Satoh Y., Hirashima N., Suzuki T., Kagan B. L., and Kirino Y. (1998) Membrane perturbation by the neurotoxic Alzheimer amyloid fragment beta 25-35 requires aggregation and beta-sheet formation. *Biochem Mol Biol Int* **46,** 787-794.

Hirakura Y., Lin M. C., and Kagan B. L. (1999) Alzheimer amyloid abeta1-42 channels: effects of solvent, pH, and Congo Red. *J Neurosci Res* **57,** 458-466.

Hirrlinger J., Konig J., Keppler D., Lindenau J., Schulz J. B., and Dringen R. (2001) The multidrug resistance protein MRP1 mediates the release of glutathione disulfide from rat astrocytes during oxidative stress. *J Neurochem* **76,** 627-636.

Hirrlinger J., Resch A., Gutterer J. M., and Dringen R. (2002) Oligodendroglial cells in culture effectively dispose of exogenous hydrogen peroxide: comparison with cultured neurones, astroglial and microglial cells. *J Neurochem* **82,** 635-644.

Hirrlinger J., Schulz J. B., and Dringen R. (2002) Glutathione release from cultured brain cells: multidrug resistance protein 1 mediates the release of GSH from rat astroglial cells. *J Neurosci Res* **69,** 318-326.

Hu J., Ferreira A., and Van Eldik L. J. (1997) S100beta induces neuronal cell death through nitric oxide release from astrocytes. *J Neurochem* **69,** 2294-2301.

Hu J., Akama K. T., Krafft G. A., Chromy B. A., and Van Eldik L. J. (1998) Amyloid-beta peptide activates cultured astrocytes: morphological alterations, cytokine induction and nitric oxide release. *Brain Res* **785,** 195-206.

Hu J. G., Akama K. T., Krafft G. A., Chromy B. A., and Van Eldik L. J. (1998) Amyloid-beta peptide activates cultured astrocytes: morphological alterations, cytokine induction and nitric oxide release. *Brain Research* **785,** 195-206.

Hua L. L. and Halliwell B. (2001) Oxidation and generation of hydrogen peroxide by thiol compounds in commonly used cell culture media. *Biochem Biophys Res Commun* **286,** 991-994.

Huang C. S., Chang L. S., Anderson M. E., and Meister A. (1993) Catalytic and regulatory properties of the heavy subunit of rat kidney gamma-glutamylcysteine synthetase. *J Biol Chem* **268,** 19675-19680.

Huang J. and Philbert M. A. (1996) Cellular responses of cultured cerebellar astrocytes to ethacrynic acid-induced perturbation of subcellular glutathione homeostasis. *Brain Res* **711,** 184-192.

Hussain S., Slikker W., Jr., and Ali S. F. (1995) Age-related changes in antioxidant enzymes, superoxide dismutase, catalase, glutathione peroxidase and glutathione in different regions of mouse brain. *Int J Dev Neurosci* **13,** 811-817.

Hynd M. R., Scott H. L., and Dodd P. R. (2004) Glutamate-mediated excitotoxicity and neurodegeneration in Alzheimer's disease. *Neurochem Int* **45,** 583-595.

Ibanez V., Pietrini P., Alexander G. E., Furey M. L., Teichberg D., Rajapakse J. C., Rapoport S. I., Schapiro M. B., and Horwitz B. (1998) Regional glucose metabolic abnormalities are not the result of atrophy in Alzheimer's disease. *Neurology* **50,** 1585-1593.

Ii M., Sunamoto M., Ohnishi K., and Ichimori Y. (1996) beta-Amyloid protein-dependent nitric oxide production from microglial cells and neurotoxicity. *Brain Research* **720,** 93-100.

Ikegaya Y., Matsuura S., Ueno S., Baba A., Yamada M. K., Nishiyama N., and Matsuki N. (2002) Beta-amyloid enhances glial glutamate uptake activity and attenuates synaptic efficacy. *J Biol Chem* **277,** 32180-32186.

Ivins K. J., Bui E. T., and Cotman C. W. (1998) Beta-amyloid induces local neurite degeneration in cultured hippocampal neurons: evidence for neuritic apoptosis. *Neurobiol Dis* **5,** 365-378.

Iwata-Ichikawa E., Kondo Y., Miyazaki I., Asanuma M., and Ogawa N. (1999) Glial cells protect neurons against oxidative stress via transcriptional up-regulation of the glutathione synthesis. *J Neurochem* **72,** 2334-2344.

Iwata N., Tsubuki S., Takaki Y., Watanabe K., Sekiguchi M., Hosoki E., Kawashima-Morishima M., Lee H. J., Hama E., Sekine-Aizawa Y., and Saido T. C. (2000) Identification of the major Abeta1-42-degrading catabolic pathway in brain parenchyma: suppression leads to biochemical and pathological deposition. *Nat Med* **6,** 143-150.

Jama J. W., Launer L. J., Witteman J. C., den Breeijen J. H., Breteler M. M., Grobbee D. E., and Hofman A. (1996) Dietary antioxidants and cognitive function in a population-based sample of older persons. The Rotterdam Study. *Am J Epidemiol* **144,** 275-280.

Janssens N. and Lesage A. S. J. (2001) Glutamate receptor subunit expression in primary neuronal and secondary glial cultures. *J Neurochem* **77,** 1457-1474.

Janus C., Chishti M. A., and Westaway D. (2000) Transgenic mouse models of Alzheimer's disease. *Biochimica et Biophysica Acta-Molecular Basis of Disease* **1502,** 63-75.

Jarrett J. T. and Lansbury P. T. (1993) Seeding One-Dimensional Crystallization of Amyloid - A Pathogenic Mechanism in Alzheimers-Disease and Scrapie. *Cell* **73,** 1055-1058.

Jarrett J. T., Berger E. P., and Lansbury P. T., Jr. (1993) The carboxy terminus of the beta amyloid protein is critical for the seeding of amyloid formation: implications for the pathogenesis of Alzheimer's disease. *Biochemistry* **32,** 4693-4697.

Jick H., Zornberg G. L., Jick S. S., Seshadri S., and Drachman D. A. (2000) Statins and the risk of dementia. *Lancet* **356,** 1627-1631.

Kagan B. L., Hirakura Y., Azimov R., Azimova R., and Lin M. C. (2002) The channel hypothesis of Alzheimer's disease: current status. *Peptides* **23,** 1311-1315.

Kaneko I., Yamada N., Sakuraba Y., Kamenosono M., and Tutumi S. (1995) Suppression of mitochondrial succinate dehydrogenase, a primary target of beta-amyloid, and its derivative racemized at Ser residue. *J Neurochem* **65,** 2585-2593.

Kaneko I., Morimoto K., and Kubo T. (2001) Drastic neuronal loss in vivo by beta-amyloid racemized at Ser(26) residue: conversion of non-toxic [D-Ser(26)]beta-amyloid 1-40 to toxic and proteinase-resistant fragments. *Neuroscience* **104,** 1003-1011.

Kang D. E., Pietrzik C. U., Baum L., Chevallier N., Merriam D. E., Kounnas M. Z., Wagner S. L., Troncoso J. C., Kawas C. H., Katzman R., and Koo E. H. (2000) Modulation of amyloid beta-protein clearance and Alzheimer's disease susceptibility by the LDL receptor-related protein pathway. *J Clin Invest* **106,** 1159-1166.

Kang J., Lemaire H. G., Unterbeck A., Salbaum J. M., Masters C. L., Grzeschik K. H., Multhaup G., Beyreuther K., and Muller-Hill B. (1987) The precursor of Alzheimer's disease amyloid A4 protein resembles a cell-surface receptor. *Nature* **325,** 733-736.

Kang Y., Viswanath V., Jha N., Qiao X., Mo J. Q., and Andersen J. K. (1999) Brain gamma-glutamyl cysteine synthetase (GCS) mRNA expression patterns correlate with regional-specific enzyme activities and glutathione levels. *J Neurosci Res* **58,** 436-441.

Katayama T., Minami M., Nakamura M., Ito M., Katsuki H., Akaike A., and Satoh M. (2002) Excitotoxic injury induces production of monocyte chemoattractant protein-1 in rat cortico-striatal slice cultures. *Neurosci Lett* **328,** 277-280.

Kawahara M. and Kuroda Y. (2000) Molecular mechanism of neurodegeneration induced by Alzheimer's beta-amyloid protein: channel formation and disruption of calcium homeostasis. *Brain Res Bull* **53,** 389-397.

Keelan J., Allen N. J., Antcliffe D., Pal S., and Duchen M. R. (2001) Quantitative imaging of glutathione in hippocampal neurons and glia in culture using monochlorobimane. *J Neurosci Res* **66,** 873-884.

Kerokoski P., Soininen H., and Pirttila T. (2001) Beta-amyloid (1-42) affects MTT reduction in astrocytes: implications for vesicular trafficking and cell functionality. *Neurochem Int* **38,** 127-134.

Kinukawa H., Jikou T., Nitta A., Furukawa Y., Hashimoto M., Fukumitsu H., Nomoto H., and Furukawa S. (2004) Cyclic AMP/protein kinase a signal attenuates Ca(2+)-induced fibroblast growth factor-1 synthesis in rat cortical neurons. *J Neurosci Res* **77,** 487-497.

Kish S. J., Bergeron C., Rajput A., Dozic S., Mastrogiacomo F., Chang L. J., Wilson J. M., Distefano L. M., and Nobrega J. N. (1992) Brain Cytochrome-Oxidase in Alzheimers-Disease. *J Neurochem* **59,** 776-779.

Kitaguchi N., Takahashi Y., Tokushima Y., Shiojiri S., and Ito H. (1988) Novel precursor of Alzheimer's disease amyloid protein shows protease inhibitory activity. *Nature* **331,** 530-532.

Koike H., Tomioka S., Sorimachi H., Saido T. C., Maruyama K., Okuyama A., Fujisawa-Sehara A., Ohno S., Suzuki K., and Ishiura S. (1999) Membrane-anchored metalloprotease MDC9 has an alpha-secretase activity responsible for processing the amyloid precursor protein. *Biochem J* **343 Pt 2,** 371-375.

Koistinaho M., Lin S., Wu X., Esterman M., Koger D., Hanson J., Higgs R., Liu F., Malkani S., Bales K. R., and Paul S. M. (2004) Apolipoprotein E promotes astrocyte colocalization and degradation of deposited amyloid-beta peptides. *Nat Med* **10,** 719-726.

Kontush A. (2001) Alzheimer's amyloid-beta as a preventive antioxidant for brain lipoproteins. *Cell Mol Neurobiol* **21,** 299-315.

Kranich O., Hamprecht B., and Dringen R. (1996) Different preferences in the utilization of amino acids for glutathione synthesis in cultured neurons and astroglial cells derived from rat brain. *Neuroscience Letters* **219,** 211-214.

Kranich O., Dringen R., Sandberg M., and Hamprecht B. (1998) Utilization of cysteine and cysteine precursors for the synthesis of glutathione in astroglial cultures: preference for cystine. *Glia* **22,** 11-18.

Kubo T., Nishimura S., Kumagae Y., and Kaneko I. (2002) In vivo conversion of racemized beta-amyloid ([D-Ser 26]A beta 1-40) to truncated and toxic fragments ([D-Ser 26]A beta 25-35/40) and fragment presence in the brains of Alzheimer's patients. *J Neurosci Res* **70,** 474-483.

LaFerla F. M., Troncoso J. C., Strickland D. K., Kawas C. H., and Jay G. (1997) Neuronal cell death in Alzheimer's disease correlates with apoE uptake and intracellular Abeta stabilization. *J Clin Invest* **100,** 310-320.

Lammich S., Kojro E., Postina R., Gilbert S., Pfeiffer R., Jasionowski M., Haass C., and Fahrenholz F. (1999) Constitutive and regulated alpha-secretase cleavage of Alzheimer's amyloid precursor protein by a disintegrin metalloprotease. *Proc Natl Acad Sci U S A* **96,** 3922-3927.

Langeveld C. H., Schepens E., Jongenelen C. A. M., Stoof J. C., Hjelle O. P., Ottersen O. P., and Drukarch B. (1996) Presence of glutathione immunoreactivity in cultured neurones and astrocytes. *Neuroreport* **7,** 1833-1836.

Lauderback C. M., Kanski J., Hackett J. M., Maeda N., Kindy M. S., and Butterfield D. A. (2002) Apolipoprotein E modulates Alzheimer's Abeta(1-42)-induced oxidative damage to synaptosomes in an allele-specific manner. *Brain Res* **924,** 90-97.

Lesne S., Ali C., Gabriel C., Croci N., MacKenzie E. T., Glabe C. G., Plotkine M., Marchand-Verrecchia C., Vivien D., and Buisson A. (2005) NMDA receptor activation inhibits alpha-secretase and promotes neuronal amyloid-beta production. *J Neurosci* **25,** 9367-9377.

Leverenz J. B. and Raskind M. A. (1998) Early amyloid deposition in the medial temporal lobe of young Down syndrome patients: a regional quantitative analysis. *Exp Neurol* **150,** 296-304.

LeVine H., III (1993) Thioflavine T interaction with synthetic Alzheimer's disease beta-amyloid peptides: detection of amyloid aggregation in solution. *Protein Sci* **2,** 404-410.

Lewis J., Dickson D. W., Lin W. L., Chisholm L., Corral A., Jones G., Yen S. H., Sahara N., Skipper L., Yager D., Eckman C., Hardy J., Hutton M., and McGowan E. (2001) Enhanced neurofibrillary degeneration in transgenic mice expressing mutant tau and APP. *Science* **293,** 1487-1491.

Litersky J. M., Johnson G. V., Jakes R., Goedert M., Lee M., and Seubert P. (1996) Tau protein is phosphorylated by cyclic AMP-dependent protein kinase and calcium/calmodulin-dependent protein kinase II within its microtubule-binding domains at Ser-262 and Ser-356. *Biochem J* **316 (Pt 2),** 655-660.

Liu R., McAllister C., Lyubchenko Y., and Sierks M. R. (2004) Residues 17-20 and 30-35 of beta-amyloid play critical roles in aggregation. *J Neurosci Res* **75,** 162-171.

Liu Y, Peterson D.A., Kimura M., Schubert D. (1997) Mechanism of cellular 2-(4,5-dimethylthiazol-2-yl)-2,5-diphenyltetrazolium bromide (MTT) reduction *J Neurochem* **69**(2) 581-93.

Liu Y. and Schubert D. (1997) Cytotoxic amyloid peptides inhibit cellular 3-(4,5-dimethylthiazol-2-yl)-2,5-diphenyltetrazolium bromide (MTT) reduction by enhancing MTT formazan exocytosis. *J Neurochem* **69,** 2285-2293.

Loe D. W., Deeley R. G., and Cole S. P. (2000) Verapamil stimulates glutathione transport by the 190-kDa multidrug resistance protein 1 (MRP1). *J Pharmacol Exp Ther* **293,** 530-538.

Lovell M. A., Ehmann W. D., Butler S. M., and Markesbery W. R. (1995) Elevated thiobarbituric acid-reactive substances and antioxidant enzyme activity in the brain in Alzheimer's disease. *Neurology* **45,** 1594-1601.

Lowry O. H., Rosebrough N. J., Farr A. L., and Randall R. J. (1951) Protein measurement with the Folin phenol reagent. *J Biol Chem* **193,** 265-275.

Lu T., Pan Y., Kao S. Y., Li C., Kohane I., Chan J., and Yankner B. A. (2004) Gene regulation and DNA damage in the ageing human brain. *Nature* **429,** 883-891.

Luhrs T., Ritter C., Adrian M., Riek-Loher D., Bohrmann B., Dobeli H., Schubert D., and Riek R. (2005) 3D structure of Alzheimer's amyloid-beta(1-42) fibrils. *Proc Natl Acad Sci U S A* **102,** 17342-17347.

Luo Y., Bolon B., Kahn S., Bennett B. D., Babu-Khan S., Denis P., Fan W., Kha H., Zhang J., Gong Y., Martin L., Louis J. C., Yan Q., Richards W. G., Citron M., and Vassar R. (2001) Mice deficient in BACE1, the Alzheimer's beta-secretase, have normal phenotype and abolished beta-amyloid generation. *Nat Neurosci* **4,** 231-232.

Maher P (2005) The effects of stress and aging on glutathione metabolism. *Aging Res Rev 4(2):288-314.*

Mahley R. W. (1988) Apolipoprotein-e - Cholesterol Transport Protein with Expanding Role in Cell Biology. *Science* **240,** 622-630.

Mahley R. W., Weisgraber K. H., and Huang Y. (2006) Apolipoprotein E4: a causative factor and therapeutic target in neuropathology, including Alzheimer's disease. *Proc Natl Acad Sci U S A* **103,** 5644-5651.

Makar T. K., Cooper A. J. L., Tofelgrehl B., Thaler H. T., and Blass J. P. (1995) Carnitine, Carnitine Acetyltransferase, and Glutathione in Alzheimer Brain. *Neurochemical Research* **20,** 705-711.

Malchiodi-Albedi F., Domenici M. R., Paradisi S., Bernardo A., Ajmone-Cat M. A., and Minghetti L. (2001) Astrocytes contribute to neuronal impairment in beta A toxicity increasing apoptosis in rat hippocampal neurons. *Glia* **34,** 68-72.

Mandelkow E. M., Stamer K., Vogel R., Thies E., and Mandelkow E. (2003) Clogging of axons by tau, inhibition of axonal traffic and starvation of synapses. *Neurobiol Aging* **24,** 1079-1085.

Marchetti P., Decaudin D., Macho A., Zamzami N., Hirsch T., Susin S. A., and Kroemer G. (1997) Redox regulation of apoptosis: impact of thiol oxidation status on mitochondrial function. *Eur J Immunol* **27,** 289-296.

Marcus D. L., Thomas C., Rodriguez C., Simberkoff K., Tsai J. S., Strafaci J. A., and Freedman M. L. (1998) Increased peroxidation and reduced antioxidant enzyme activity in Alzheimer's disease. *Experimental Neurology* **150,** 40-44.

Mark R. J., Lovell M. A., Markesbery W. R., Uchida K., and Mattson M. P. (1997) A role for 4-hydroxynonenal, an aldehydic product of lipid peroxidation, in disruption of ion homeostasis and neuronal death induced by amyloid beta-peptide. *J Neurochem* **68,** 255-264.

Markesbery W. R. and Lovell M. A. (1998) Four-hydroxynonenal, a product of lipid peroxidation, is increased in the brain in Alzheimer's disease. *Neurobiol Aging* **19,** 33-36.

Martensson J., Lai J. C., and Meister A. (1990) High-affinity transport of glutathione is part of a multicomponent system essential for mitochondrial function. *Proc Natl Acad Sci U S A* **87,** 7185-7189.

Martins R. N., Harper C. G., Stokes G. B., and Masters C. L. (1986) Increased cerebral glucose-6-phosphate dehydrogenase activity in Alzheimer's disease may reflect oxidative stress. *J Neurochem* **46,** 1042-1045.

Masters C. L., Simms G., Weinman N. A., Multhaup G., McDonald B. L., and Beyreuther K. (1985) Amyloid plaque core protein in Alzheimer disease and Down syndrome. *Proc Natl Acad Sci U S A* **82,** 4245-4249.

Mattson M. P., Cheng B., Davis D., Bryant K., Lieberburg I., and Rydel R. E. (1992) Beta-Amyloid Peptides Destabilize Calcium Homeostasis and Render Human Cortical-Neurons Vulnerable to Excitotoxicity. *J Neurosci* **12,** 376-389.

Mattson M. P. (1997) Cellular actions of beta-amyloid precursor protein and its soluble and fibrillogenic derivatives. *Physiol Rev* **77,** 1081-1132.

Mattson M. P., Pedersen W. A., Duan W., Culmsee C., and Camandola S. (1999) Cellular and molecular mechanisms underlying perturbed energy metabolism and neuronal degeneration in Alzheimer's and Parkinson's diseases. *Ann N Y Acad Sci* **893,** 154-175.

Mattson M. P. and Chan S. L. (2003) Neuronal and glial calcium signaling in Alzheimer's disease. *Cell Calcium* **34,** 385-397.

Mavis R. D. and Stellwagen E. (1968) Purification and subunit structure of glutathione reductase from bakers' yeast. *J Biol Chem* **243,** 809-814.

Mayeux R., Honig L. S., Tang M. X., Manly J., Stern Y., Schupf N., and Mehta P. D. (2003) Plasma A[beta]40 and A[beta]42 and Alzheimer's disease: relation to age, mortality, and risk. *Neurology* **61,** 1185-1190.

McGeer P. L., Schulzer M., and McGeer E. G. (1996) Arthritis and anti-inflammatory agents as possible protective factors for Alzheimer's disease: a review of 17 epidemiologic studies. *Neurology* **47,** 425-432.

McGowan E., Eriksen J., and Hutton M. (2006) A decade of modeling Alzheimer's disease in transgenic mice. *Trends Genet* **22,** 281-289.

McKee A. C., Kosik K. S., Kennedy M. B., and Kowall N. W. (1990) Hippocampal neurons predisposed to neurofibrillary tangle formation are enriched in type II calcium/calmodulin-dependent protein kinase. *J Neuropathol Exp Neurol* **49,** 49-63.

Meda L., Baron P., and Scarlato G. (2001) Glial activation in Alzheimer's disease: the role of Abeta and its associated proteins. *Neurobiol Aging* **22,** 885-893.

Meister A. and Anderson M. E. (1983) Glutathione. *Annu Rev Biochem* **52,** 711-760.

Meister A. (1994) Glutathione-ascorbic acid antioxidant system in animals. *J Biol Chem* **269,** 9397-9400.

Miller B. C., Eckman E. A., Sambamurti K., Dobbs N., Chow K. M., Eckman C. B., Hersh L. B., and Thiele D. L. (2003) Amyloid-beta peptide levels in brain are inversely correlated with insulysin activity levels in vivo. *Proc Natl Acad Sci U S A* **100,** 6221-6226.

Milstein S., Sakai N., Brew B.J., Kreiger C., Vickers J.H., Saito K., Heyes M.P. (1994) Cerebral spinal fluid nitrite/nitrate levels in neurologic diseases. *J Neurochem* ***63(3), 1178-80.***

Mirzabekov T., Lin M. C., Yuan W. L., Marshall P. J., Carman M., Tomaselli K., Lieberburg I., and Kagan B. L. (1994) Channel formation in planar lipid bilayers by a neurotoxic fragment of the beta-amyloid peptide. *Biochem Biophys Res Commun* **202,** 1142-1148.

Morrison R. S. and de Vellis J. (1983) Differentiation of purified astrocytes in a chemically defined medium. *Brain Res* **285,** 337-345.

Mrak R. E. and Griffin W. S. (2001) The role of activated astrocytes and of the neurotrophic cytokine S100B in the pathogenesis of Alzheimer's disease. *Neurobiol Aging* **22,** 915-922.

Multhaup G., Schlicksupp A., Hesse L., Beher D., Ruppert T., Masters C. L., and Beyreuther K. (1996) The amyloid precursor protein of Alzheimer's disease in the reduction of copper(II) to copper(I). *Science* **271,** 1406-1409.

Muyderman H., Nilsson M., and Sims N. R. (2004) Highly selective and prolonged depletion of mitochondrial glutathione in astrocytes markedly increases sensitivity to peroxynitrite. *J Neurosci* **24,** 8019-8028.

Nagele R. G., Wegiel J., Venkataraman V., Imaki H., Wang K. C., and Wegiel J. (2004) Contribution of glial cells to the development of amyloid plaques in Alzheimer's disease. *Neurobiol Aging* **25,** 663-674.

Naiki H., Hasegawa K., Yamaguchi I., Nakamura H., Gejyo F., and Nakakuki K. (1998) Apolipoprotein E and antioxidants have different mechanisms of inhibiting Alzheimer's beta-amyloid fibril formation in vitro. *Biochemistry* **37,** 17882-17889.

Naslund J., Schierhorn A., Hellman U., Lannfelt L., Roses A. D., Tjernberg L. O., Silberring J., Gandy S. E., Winblad B., Greengard P., and . (1994) Relative abundance of Alzheimer A beta amyloid peptide variants in Alzheimer disease and normal aging. *Proc Natl Acad Sci U S A* **91,** 8378-8382.

Naslund J., Haroutunian V., Mohs R., Davis K. L., Davies P., Greengard P., and Buxbaum J. D. (2000) Correlation between elevated levels of amyloid beta-peptide in the brain and cognitive decline. *Jama-Journal of the American Medical Association* **283,** 1571-1577.

Nedergaard M., Ransom B., and Goldman S. A. (2003) New roles for astrocytes: redefining the functional architecture of the brain. *Trends Neurosci* **26,** 523-530.

Nelson T. J. and Alkon D. L. (2005) Oxidation of cholesterol by amyloid precursor protein and beta-amyloid peptide. *J Biol Chem* **280,** 7377-7387.

Nelson T. J. and Alkon D. L. (2005) Insulin and cholesterol pathways in neuronal function, memory and neurodegeneration. *Biochem Soc Trans* **33,** 1033-1036.

Neumann H., Schweigreiter R., Yamashita T., Rosenkranz K., Wekerle H., and Barde Y. A. (2002) Tumor necrosis factor inhibits neurite outgrowth and branching of hippocampal neurons by a rho-dependent mechanism. *J Neurosci* **22,** 854-862.

Oddo S., Caccamo A., Shepherd J. D., Murphy M. P., Golde T. E., Kayed R., Metherate R., Mattson M. P., Akbari Y., and LaFerla F. M. (2003) Triple-transgenic model of Alzheimer's disease with plaques and tangles: intracellular Abeta and synaptic dysfunction. *Neuron* **39,** 409-421.

Ogino Y. and Costa T. (1992) Thrombin is the major serum factor stimulating phosphoinositide turnover, but not DNA synthesis in human neuroblastoma SH-EP cells. *Eur J Pharmacol* **225,** 299-303.

Olichney J. M., Hansen L. A., Galasko D., Saitoh T., Hofstetter C. R., Katzman R., and Thal L. J. (1996) The apolipoprotein E epsilon 4 allele is associated with increased neuritic plaques and cerebral amyloid angiopathy in Alzheimer's disease and Lewy body variant. *Neurology* **47,** 190-196.

Olivieri G., Baysang G., Meier F., Muller-Spahn F., Stahelin H.B., Brockhaus M., Brack C. (2001) N-acetyl-L-cysteine protects SHSY5Y neuroblastoma cells from oxidative stress and cell toxicity: effects on beta amyloid secretion and tau phosphorylation. *J Neurochem* ***76****(1), 224-33.*

Ono K., Hamaguchi T., Naiki H., and Yamada M. (2006) Anti-amyloidogenic effects of antioxidants: implications for the prevention and therapeutics of Alzheimer's disease. *Biochim Biophys Acta* **1762,** 575-586.

Ott A., Breteler M. M., van Harskamp F., Claus J. J., van der Cammen T. J., Grobbee D. E., and Hofman A. (1995) Prevalence of Alzheimer's disease and vascular dementia: association with education. The Rotterdam study. *BMJ* **310,** 970-973.

Ozmen L., Woolley M., Albientz A., Miss M. T., Nelboeck P., Malherbe P., Czech C., Gruninger-Leitch F., Brockhaus M., Ballard T., and Jacobsen H. (2005) BACE/APPV717F double-transgenic mice develop cerebral amyloidosis and inflammation. *Neurodegener Dis* **2,** 284-298.

Palmer A. M. (1999) The activity of the pentose phosphate pathway is increased in response to oxidative stress in Alzheimer's disease. *Journal of Neural Transmission* **106,** 317-328.

Panenka W., Jijon H., Herx L. M., Armstrong J. N., Feighan D., Wei T., Yong V. W., Ransohoff R. M., and MacVicar B. A. (2001) P2X7-like receptor activation in astrocytes increases chemokine monocyte chemoattractant protein-1 expression via mitogen-activated protein kinase. *J Neurosci* **21,** 7135-7142.

Paradies G., Ruggiero F. M., Petrosillo G., and Quagliariello E. (1998) Peroxidative damage to cardiac mitochondria: cytochrome oxidase and cardiolipin alterations. *FEBS Lett* **424,** 155-158.

Paradisi S., Sacchetti B., Balduzzi M., Gaudi S., and Malchiodi-Albedi F. (2004) Astrocyte modulation of in vitro beta-amyloid neurotoxicity. *Glia* **46,** 252-260.

Parker W. D., Jr., Filley C. M., and Parks J. K. (1990) Cytochrome oxidase deficiency in Alzheimer's disease. *Neurology* **40,** 1302-1303.

Parpura-Gill A., Beitz D., and Uemura E. (1997) The inhibitory effects of beta-amyloid on glutamate and glucose uptakes by cultured astrocytes. *Brain Res* **754,** 65-71.

Patel A. J., Gunasekera S., Jen A., and deSilva H. A. R. (1996) beta-amyloid-mediated inhibition of redox activity (MTT reduction) is not an indicator of astroglial degeneration. *Neuroreport* **7,** 2026-2030.

Pearson H. A. and Peers C. (2006) Physiological roles for amyloid {beta} peptides. *J Physiol* **575,** 5-10.

Pellerin L. and Magistretti P. J. (2004) Neuroenergetics: Calling upon astrocytes to satisfy hungry neurons. *Neuroscientist* **10,** 53-62.

Pena L. A., Brecher C. W., and Marshak D. R. (1995) beta-Amyloid regulates gene expression of glial trophic substance S100 beta in C6 glioma and primary astrocyte cultures. *Brain Res Mol Brain Res* **34,** 118-126.

Pereira C., Santos M. S., and Oliveira C. (1998) Mitochondrial function impairment induced by amyloid beta-peptide on PC12 cells. *Neuroreport* **9,** 1749-1755.

Petersen R. C., Thomas R. G., Grundman M., Bennett D., Doody R., Ferris S., Galasko D., Jin S., Kaye J., Levey A., Pfeiffer E., Sano M., van Dyck C. H., and Thal L. J. (2005) Vitamin E and donepezil for the treatment of mild cognitive impairment. *N Engl J Med* **352,** 2379-2388.

Pike C. J., Walencewicz A. J., Glabe C. G., and Cotman C. W. (1991) In vitro aging of beta-amyloid protein causes peptide aggregation and neurotoxicity. *Brain Res* **563,** 311-314.

Pike C. J., Burdick D., Walencewicz A. J., Glabe C. G., and Cotman C. W. (1993) Neurodegeneration Induced by Beta-Amyloid Peptides Invitro - the Role of Peptide Assembly State. *J Neurosci* **13,** 1676-1687.

Pike C. J., Cummings B. J., Monzavi R., and Cotman C. W. (1994) Beta-Amyloid-Induced Changes in Cultured Astrocytes Parallel Reactive Astrocytosis Associated with Senile Plaques in Alzheimers-Disease. *Neuroscience* **63,** 517-531.

Pike C. J., Walencewiczwasserman A. J., Kosmoski J., Cribbs D. H., Glabe C. G., and Cotman C. W. (1995) Structure-Activity Analyses of Beta-Amyloid Peptides - Contributions of the Beta-25-35 Region to Aggregation and Neurotoxicity. *J Neurochem* **64,** 253-265.

Pike C. J., Vaughan P. J., Cunningham D. D., and Cotman C. W. (1996) Thrombin attenuates neuronal cell death and modulates astrocyte reactivity induced by beta-amyloid in vitro. *J Neurochem* **66,** 1374-1382.

Pike C. J., RamezanArab N., and Cotman C. W. (1997) beta-amyloid neurotoxicity in vitro: Evidence of oxidative stress but not protection by antioxidants. *J Neurochem* **69,** 1601-1611.

Plant L. D., Boyle J. P., Smith I. F., Peers C., and Pearson H. A. (2003) The production of amyloid beta peptide is a critical requirement for the viability of central neurons. *J Neurosci* **23,** 5531-5535.

Podlisny M. B., Walsh D. M., Amarante P., Ostaszewski B. L., Stimson E. R., Maggio J. E., Teplow D. B., and Selkoe D. J. (1998) Oligomerization of endogenous and synthetic amyloid beta-protein at nanomolar levels in cell culture and stabilization of monomer by Congo red. *Biochemistry* **37,** 3602-3611.

Poirier J. (2005) Apolipoprotein E, cholesterol transport and synthesis in sporadic Alzheimer's disease. *Neurobiol Aging* **26,** 355-361.

Ponte P., Gonzalez-DeWhitt P., Schilling J., Miller J., Hsu D., Greenberg B., Davis K., Wallace W., Lieberburg I., and Fuller F. (1988) A new A4 amyloid mRNA contains a domain homologous to serine proteinase inhibitors. *Nature* **331,** 525-527.

Price S. A., Held B., and Pearson H. A. (1998) Amyloid beta protein increases Ca2+ currents in rat cerebellar granule neurones. *Neuroreport* **9,** 539-545.

Puglielli L., Tanzi R. E., and Kovacs D. M. (2003) Alzheimer's disease: the cholesterol connection. *Nat Neurosci* **6,** 345-351.

Qiu W. Q., Ferreira A., Miller C., Koo E. H., and Selkoe D. J. (1995) Cell-surface beta-amyloid precursor protein stimulates neurite outgrowth of hippocampal neurons in an isoform-dependent manner. *J Neurosci* **15,** 2157-2167.

Qiu Z., Naten D. L., Liston J. C., Yess J., and Rebeck G. W. (2001) A novel approach for studying endogenous abeta processing using cultured primary neurons isolated from APP transgenic mice. *Exp Neurol* **170,** 186-194.

Raff M. (1998) Cell suicide for beginners. *Nature* **396,** 119-122.

Rapp A., Gmeiner B., and Huttinger M. (2006) Implication of apoE isoforms in cholesterol metabolism by primary rat hippocampal neurons and astrocytes. *Biochimie* **88,** 473-483.

Rathinam M. L., Watts L. T., Stark A. A., Mahimainathan L., Stewart J., Schenker S., and Henderson G. I. (2006) Astrocyte control of fetal cortical neuron glutathione homeostasis: up-regulation by ethanol. *J Neurochem* **96,** 1289-1300.

Reich E. E., Zackert W. E., Brame C. J., Chen Y., Roberts L. J., Hachey D. L., Montine T. J., and Morrow J. D. (2000) Formation of novel D-ring and E-ring isoprostane-like compounds (D4/E4-neuroprostanes) in vivo from docosahexaenoic acid. *Biochemistry* **39,** 2376-2383.

Reich E. E., Markesbery W. R., Roberts L. J., Swift L. L., Morrow J. D., and Montine T. J. (2001) Brain regional quantification of F-ring and D-/E-ring isoprostanes and neuroprostanes in Alzheimer's disease. *Am J Pathol* **158,** 293-297.

Richardson J. S., Zhou Y., and Kumar U. (1996) Free radicals in the neurotoxic actions of beta-amyloid. *Ann N Y Acad Sci* **777,** 362-367.

Rocchi A., Pellegrini S., Siciliano G., and Murri L. (2003) Causative and susceptibility genes for Alzheimer's disease: a review. *Brain Research Bulletin* **61,** 1-24.

Rottkamp C. A., Raina A. K., Zhu X., Gaier E., Bush A. I., Atwood C. S., Chevion M., Perry G., and Smith M. A. (2001) Redox-active iron mediates amyloid-beta toxicity. *Free Radic Biol Med* **30,** 447-450.

Sagara J. I., Miura K., and Bannai S. (1993) Maintenance of neuronal glutathione by glial cells. *J Neurochem* **61,** 1672-1676.

Sagara J. I., Makino N., and Bannai S. (1996) Glutathione efflux from cultured astrocytes. *J Neurochem* **66,** 1876-1881.

Saito Y., Nishio K., Ogawa Y., Kimata J., Kinumi T., Yoshida Y., Noguchi N., and Niki E. (2006) Turning point in apoptosis/necrosis induced by hydrogen peroxide. *Free Radic Res* **40,** 619-630.

Sandbrink R., Masters C. L., and Beyreuther K. (1994) APP gene family: unique age-associated changes in splicing of Alzheimer's betaA4-amyloid protein precursor. *Neurobiol Dis* **1,** 13-24.

Sasaki N., Toki S., Chowei H., Saito T., Nakano N., Hayashi Y., Takeuchi M., and Makita Z. (2001) Immunohistochemical distribution of the receptor for advanced glycation end products in neurons and astrocytes in Alzheimer's disease. *Brain Res* **888,** 256-262.

Sastre M., Klockgether T., and Heneka M. T. (2006) Contribution of inflammatory processes to Alzheimer's disease: molecular mechanisms. *Int J Dev Neurosci* **24,** 167-176.

Scheff S. W., Price D. A., Schmitt F. A., and Mufson E. J. (2006) Hippocampal synaptic loss in early Alzheimer's disease and mild cognitive impairment. *Neurobiol Aging* **27,** 1372-1384.

Schenk D., Barbour R., Dunn W., Gordon G., Grajeda H., Guido T., Hu K., Huang J., Johnson-Wood K., Khan K., Kholodenko D., Lee M., Liao Z., Lieberburg I., Motter R., Mutter L., Soriano F., Shopp G., Vasquez N., Vandevert C., Walker S., Wogulis M., Yednock T., Games D., and Seubert P. (1999) Immunization with amyloid-beta attenuates Alzheimer-disease-like pathology in the PDAPP mouse. *Nature* **400,** 173-177.

Scheuner D., Eckman C., Jensen M., Song X., Citron M., Suzuki N., Bird T. D., Hardy J., Hutton M., Kukull W., Larson E., Levy-Lahad E., Viitanen M., Peskind E., Poorkaj P., Schellenberg G., Tanzi R., Wasco W., Lannfelt L., Selkoe D., and Younkin S. (1996) Secreted amyloid beta-protein similar to that in the senile plaques of Alzheimer's disease is increased in vivo by the presenilin 1 and 2 and APP mutations linked to familial Alzheimer's disease. *Nat Med* **2,** 864-870.

Schmitz C., Rutten B. P., Pielen A., Schafer S., Wirths O., Tremp G., Czech C., Blanchard V., Multhaup G., Rezaie P., Korr H., Steinbusch H. W., Pradier L., and Bayer T. A. (2004) Hippocampal neuron loss exceeds amyloid plaque load in a transgenic mouse model of Alzheimer's disease. *Am J Pathol* **164,** 1495-1502.

Schwab C., Hosokawa M., and McGeer P. L. (2004) Transgenic mice overexpressing amyloid beta protein are an incomplete model of Alzheimer disease. *Exp Neurol* **188,** 52-64.

Selak I., Skaper S. D., and Varon S. (1985) Pyruvate participation in the low molecular weight trophic activity for central nervous system neurons in glia-conditioned media. *J Neurosci* **5,** 23-28.

Selkoe D. J. (1993) Physiological Production of the Beta-Amyloid Protein and the Mechanism of Alzheimers-Disease. *Trends in Neurosciences* **16,** 403-409.

Selkoe D. J. and Podlisny M. B. (2002) Deciphering the genetic basis of Alzheimer's disease. *Annu Rev Genomics Hum Genet* **3,** 67-99.

Seubert P., Vigo-Pelfrey C., Esch F., Lee M., Dovey H., Davis D., Sinha S., Schlossmacher M., Whaley J., Swindlehurst C., Wolfer R., Selkoe D., Lieberberg I. and Schenk D . (1992) Isolation and quantification of soluble Alzheimer's beta-peptide from biological fluids. *Nature* **359,** 325-327.

Shao Y., Gearing M., and Mirra S. S. (1997) Astrocyte-apolipoprotein E associations in senile plaques in Alzheimer disease and vascular lesions: a regional immunohistochemical study. *J Neuropathol Exp Neurol* **56,** 376-381.

Sharpe M. A. and Cooper C. E. (1998) Interaction of peroxynitrite with mitochondrial cytochrome oxidase. Catalytic production of nitric oxide and irreversible inhibition of enzyme activity. *J Biol Chem* **273,** 30961-30972.

Shaw CA (1998) Multiple functions of glutathione in the nervous system. In Glutathione in the nervous system ed. Shaw CA,;Taylor and Francis.

Shearman M.S, Ragan C.L, Iversen L.L. (1994) Inhibition of PC12 cell redox activity is a specific early indicator of the mechanism of beta amyloid mediated cell death. *ProcNatl Acad Sci USA* **91** (4) 1470-4

Shearman M. S., Hawtin S. R., and Tailor V. J. (1995) The intracellular component of cellular 3-(4,5-dimethylthiazol-2-yl)-2, 5-diphenyltetrazolium bromide (MTT) reduction is specifically inhibited by beta-amyloid peptides. *J Neurochem* **65,** 218-227.

Sheehan J. P., Swerdlow R. H., Miller S. W., Davis R. E., Parks J. K., Parker W. D., and Tuttle J. B. (1997) Calcium homeostasis and reactive oxygen species production in cells transformed by mitochondria from individuals with sporadic Alzheimer's disease. *J Neurosci* **17,** 4612-4622.

Shibata M., Yamada S., Kumar S. R., Calero M., Bading J., Frangione B., Holtzman D. M., Miller C. A., Strickland D. K., Ghiso J., and Zlokovic B. V. (2000) Clearance of Alzheimer's amyloid-ss(1-40) peptide from brain by LDL receptor-related protein-1 at the blood-brain barrier. *J Clin Invest* **106,** 1489-1499.

Sies H. (1999) Glutathione and its role in cellular functions. *Free Radic Biol Med* **27,** 916-921.

Sinha S., Anderson J. P., Barbour R., Basi G. S., Caccavello R., Davis D., Doan M., Dovey H. F., Frigon N., Hong J., Jacobson-Croak K., Jewett N., Keim P., Knops J., Lieberburg I., Power M., Tan H., Tatsuno G., Tung J., Schenk D., Seubert P., Suomensaari S. M., Wang S., Walker D., Zhao J., McConlogue L., and John V. (1999) Purification and cloning of amyloid precursor protein beta-secretase from human brain. *Nature* **402,** 537-540.

Sjogren M., Mielke M., Gustafson D., Zandi P., and Skoog I. (2006) Cholesterol and Alzheimer's disease--is there a relation? *Mech Ageing Dev* **127,** 138-147.

Slack B. E., Ma L. K., and Seah C. C. (2001) Constitutive shedding of the amyloid precursor protein ectodomain is up-regulated by tumour necrosis factor-alpha converting enzyme. *Biochem J* **357,** 787-794.

Smith C. D., Carney J. M., Starke-Reed P. E., Oliver C. N., Stadtman E. R., Floyd R. A., and Markesbery W. R. (1991) Excess brain protein oxidation and enzyme dysfunction in normal aging and in Alzheimer disease. *Proc Natl Acad Sci U S A* **88,** 10540-10543.

Smith M. A., Richey Harris P. L., Sayre L. M., Beckman J. S., and Perry G. (1997) Widespread peroxynitrite-mediated damage in Alzheimer's disease. *J Neurosci* **17,** 2653-2657.

Smith M. A., Rottkamp C. A., Nunomura A., Raina A. K., and Perry G. (2000) Oxidative stress in Alzheimer's disease. *Biochimica et Biophysica Acta-Molecular Basis of Disease* **1502,** 139-144.

Smolewski P., Grabarek J., Halicka H. D., and Darzynkiewicz Z. (2002) Assay of caspase activation in situ combined with probing plasma membrane integrity to detect three distinct stages of apoptosis. *Journal of Immunological Methods* **265,** 111-121.

Song M. S., Saavedra L., and de Chaves E. I. (2006) Apoptosis is secondary to non-apoptotic axonal degeneration in neurons exposed to Abeta in distal axons. *Neurobiol Aging* **27,** 1224-1238.

Sortino M. A., Chisari M., Merlo S., Vancheri C., Caruso M., Nicoletti F., Canonico P. L., and Copani A. (2004) Glia mediates the neuroprotective action of estradiol on beta-amyloid-induced neuronal death. *Endocrinology* **145,** 5080-5086.

Spanopoulou E., Giguere V., and Grosveld F. (1991) The functional domains of the murine Thy-1 gene promoter. *Mol Cell Biol* **11,** 2216-2228.

Stanton R. C., Seifter J. L., Boxer D. C., Zimmerman E., and Cantley L. C. (1991) Rapid Release of Bound Glucose-6-Phosphate-Dehydrogenase by Growth-Factors - Correlation with Increased Enzymatic-Activity. *J Biol Chem* **266,** 12442-12448.

Stewart V. C., Sharpe M. A., Clark J. B., and Heales S. J. R. (2000) Astrocyte-derived nitric oxide causes both reversible and irreversible damage to the neuronal mitochondrial respiratory chain. *J Neurochem* **75,** 694-700.

Stewart V. C., Stone R., Gegg M. E., Sharpe M. A., Hurst R. D., Clark J. B., and Heales S. J. R. (2002) Preservation of extracellular glutathione by an astrocyte derived factor with properties comparable to extracellular superoxide dismutase. *J Neurochem* **83,** 984-991.

Stine W. B., Dahlgren K. N., Krafft G. A., and Ladu M. J. (2003) In vitro characterization of conditions for amyloid-beta peptide oligomerization and fibrillogenesis. *J Biol Chem* **278,** 11612-11622.

Strittmatter W. J., Saunders A. M., Schmechel D., Pericak-Vance M., Enghild J., Salvesen G. S., and Roses A. D. (1993) Apolipoprotein E: high-avidity binding to beta-amyloid and increased frequency of type 4 allele in late-onset familial Alzheimer disease. *Proc Natl Acad Sci U S A* **90,** 1977-1981.

Strittmatter W. J., Weisgraber K. H., Huang D. Y., Dong L. M., Salvesen G. S., Pericak-Vance M., Schmechel D., Saunders A. M., Goldgaber D., and Roses A. D. (1993) Binding of human apolipoprotein E to synthetic amyloid beta peptide: isoform-specific effects and implications for late-onset Alzheimer disease. *Proc Natl Acad Sci U S A* **90,** 8098-8102.

Styren S. D., Kamboh M. I., and DeKosky S. T. (1998) Expression of differential immune factors in temporal cortex and cerebellum: The role of alpha-1-antichymotrypsin, apolipoprotein E, and reactive glia in the progression of Alzheimer's disease. *Journal of Comparative Neurology* **396,** 511-520.

Su J. H., Cummings B. J., and Cotman C. W. (1992) Localization of heparan sulfate glycosaminoglycan and proteoglycan core protein in aged brain and Alzheimer's disease. *Neuroscience* **51,** 801-813.

Sultana R. and Butterfield D. A. (2004) Oxidatively modified GST and MRP1 in Alzheimer's disease brain: implications for accumulation of reactive lipid peroxidation products. *Neurochem Res* **29,** 2215-2220.

Sun W. M., Huang Z. Z., and Lu S. C. (1996) Regulation of gamma-glutamylcysteine synthetase by protein phosphorylation. *Biochem J* **320 (Pt 1),** 321-328.

Suzuki N., Cheung T. T., Cai X. D., Odaka A., Otvos L., Jr., Eckman C., Golde T. E., and Younkin S. G. (1994) An increased percentage of long amyloid beta protein secreted by familial amyloid beta protein precursor (beta APP717) mutants. *Science* **264,** 1336-1340.

Tabernero A., Bolanos J. P., and Medina J. M. (1993) Lipogenesis from lactate in rat neurons and astrocytes in primary culture. *Biochem J* **294 (Pt 3),** 635-638.

Tamaoka A., Sawamura N., Fukushima T., Shoji S., Matsubara E., Shoji M., Hirai S., Furiya Y., Endoh R., and Mori H. (1997) Amyloid beta protein 42(43) in cerebrospinal fluid of patients with Alzheimer's disease. *J Neurol Sci* **148,** 41-45.

Terai K., Iwai A., Kawabata S., Sasamata M., Miyata K., and Yamaguchi T. (2001) Apolipoprotein E deposition and astrogliosis are associated with maturation of beta-amyloid plaques in betaAPPswe transgenic mouse: Implications for the pathogenesis of Alzheimer's disease. *Brain Res* **900,** 48-56.

Thinakaran G., Teplow D. B., Siman R., Greenberg B., and Sisodia S. S. (1996) Metabolism of the "Swedish" amyloid precursor protein variant in neuro2a (N2a) cells. Evidence that cleavage at the "beta-secretase" site occurs in the golgi apparatus. *J Biol Chem* **271,** 9390-9397.

Tretter L. and Adam-Vizi V. (2004) Generation of reactive oxygen species in the reaction catalyzed by alpha-ketoglutarate dehydrogenase. *J Neurosci* **24,** 7771-7778.

Tsan M. F., White J. E., and Rosano C. L. (1989) Modulation of endothelial GSH concentrations: effect of exogenous GSH and GSH monoethyl ester. *J Appl Physiol* **66,** 1029-1034.

Tuppo E. E. and Arias H. R. (2005) The role of inflammation in Alzheimer's disease. *Int J Biochem Cell Biol* **37,** 289-305.

Van Everbroeck B., Dobbeleir I., De Waele M., De Leenheir E., Lubke U., Martin J. J., and Cras P. (2004) Extracellular protein deposition correlates with glial activation and oxidative stress in Creutzfeldt-Jakob and Alzheimer's disease. *Acta Neuropathol (Berl)* **108,** 194-200.

Varadarajan S., Yatin S., Kanski J., Jahanshahi F., and Butterfield D. A. (1999) Methionine residue 35 is important in amyloid beta-peptide-associated free radical oxidative stress. *Brain Res Bull* **50,** 133-141.

Varadarajan S., Kanski J., Aksenova M., Lauderback C., and Butterfield D. A. (2001) Different mechanisms of oxidative stress and neurotoxicity for Alzheimer's A beta(1--42) and A beta(25--35). *J Am Chem Soc* **123,** 5625-5631.

Vargas M. R., Pehar M., Cassina P., Beckman J. S., and Barbeito L. (2006) Increased glutathione biosynthesis by Nrf2 activation in astrocytes prevents p75NTR-dependent motor neuron apoptosis. *J Neurochem* **97,** 687-696.

Vassar R., Bennett B. D., Babu-Khan S., Kahn S., Mendiaz E. A., Denis P., Teplow D. B., Ross S., Amarante P., Loeloff R., Luo Y., Fisher S., Fuller J., Edenson S., Lile J., Jarosinski M. A., Biere A. L., Curran E., Burgess T., Louis J. C., Collins F., Treanor J., Rogers G., and Citron M. (1999) Beta-secretase cleavage of Alzheimer's amyloid precursor protein by the transmembrane aspartic protease BACE. *Science* **286,** 735-741.

Vassault A (1983) Lactate Dehydrogenase. *Methods of Enzymic Analysis, 3:118-126.*

Venkov L., Rosental L., and Manolova M. (1976) Subcellular-Distribution of Ldh Isoenzymes in Neuronal and Glial-Enriched Fractions. *Brain Research* **109,** 323-333.

Vitek M. P., Bhattacharya K., Glendening J. M., Stopa E., Vlassara H., Bucala R., Manogue K., and Cerami A. (1994) Advanced glycation end products contribute to amyloidosis in Alzheimer disease. *Proc Natl Acad Sci U S A* **91,** 4766-4770.

von Bernhardi R. and Eugenin J. (2004) Microglial reactivity to beta-amyloid is modulated by astrocytes and proinflammatory factors. *Brain Research* **1025,** 186-193.

Walsh D. M., Lomakin A., Benedek G. B., Condron M. M., and Teplow D. B. (1997) Amyloid beta-protein fibrillogenesis. Detection of a protofibrillar intermediate. *J Biol Chem* **272,** 22364-22372.

Walsh D. M., Klyubin I., Fadeeva J. V., Cullen W. K., Anwyl R., Wolfe M. S., Rowan M. J., and Selkoe D. J. (2002) Naturally secreted oligomers of amyloid beta protein potently inhibit hippocampal long-term potentiation in vivo. *Nature* **416,** 535-539.

Walsh D. M., Klyubin I., Shankar G. M., Townsend M., Fadeeva J. V., Betts V., Podlisny M. B., Cleary J. P., Ashe K. H., Rowan M. J., and Selkoe D. J. (2005) The role of cell-derived oligomers of Abeta in Alzheimer's disease and avenues for therapeutic intervention. *Biochem Soc Trans* **33,** 1087-1090.

Wang J., Xiong S., Xie C., Markesbery W. R., and Lovell M. A. (2005) Increased oxidative damage in nuclear and mitochondrial DNA in Alzheimer's disease. *J Neurochem* **93,** 953-962.

Wang X. F. and Cynader M. S. (2001) Pyruvate released by astrocytes protects neurons from copper-catalyzed cysteine neurotoxicity. *J Neurosci* **21,** 3322-3331.

Watts L. T., Rathinam M. L., Schenker S., and Henderson G. I. (2005) Astrocytes protect neurons from ethanol-induced oxidative stress and apoptotic death. *J Neurosci Res* **80,** 655-666.

Weidemann A., Konig G., Bunke D., Fischer P., Salbaum J. M., Masters C. L., and Beyreuther K. (1989) Identification, biogenesis, and localization of precursors of Alzheimer's disease A4 amyloid protein. *Cell* **57,** 115-126.

Weiss J. H., Pike C. J., and Cotman C. W. (1994) Ca2+ channel blockers attenuate beta-amyloid peptide toxicity to cortical neurons in culture. *J Neurochem* **62,** 372-375.

Werb Z. and Yan Y. (1998) A cellular striptease act. *Science* **282,** 1279-1280.

White A. R., Bush A. I., Beyreuther K., Masters C. L., and Cappai R. (1999) Exacerbation of copper toxicity in primary neuronal cultures depleted of cellular glutathione. *J Neurochem* **72,** 2092-2098.

White A. R., Du T., Laughton K. M., Volitakis I., Sharples R. A., Xilinas M. E., Hoke D. E., Holsinger R. M., Evin G., Cherny R. A., Hill A. F., Barnham K. J., Li Q. X., Bush A. I., and Masters C. L. (2006)

Degradation of the Alzheimer disease amyloid beta-peptide by metal-dependent up-regulation of metalloprotease activity. *J Biol Chem* **281,** 17670-17680.

Wiesinger H., Hamprecht B., and Dringen R. (1997) Metabolic pathways for glucose in astrocytes. *Glia* **21,** 22-34.

Woltjer R. L., Nghiem W., Maezawa I., Milatovic D., Vaisar T., Montine K. S., and Montine T. J. (2005) Role of glutathione in intracellular amyloid-alpha precursor protein/carboxy-terminal fragment aggregation and associated cytotoxicity. *J Neurochem* **93,** 1047-1056.

Wyss-Coray T., Loike J. D., Brionne T. C., Lu E., Anankov R., Yan F., Silverstein S. C., and Husemann J. (2003) Adult mouse astrocytes degrade amyloid-beta in vitro and in situ. *Nat Med* **9,** 453-457.

Yamaguchi H., Nakazato Y., Shoji M., Ihara Y., and Hirai S. (1990) Ultrastructure of the neuropil threads in the Alzheimer brain: their dendritic origin and accumulation in the senile plaques. *Acta Neuropathol (Berl)* **80,** 368-374.

Yan R., Bienkowski M. J., Shuck M. E., Miao H., Tory M. C., Pauley A. M., Brashier J. R., Stratman N. C., Mathews W. R., Buhl A. E., Carter D. B., Tomasselli A. G., Parodi L. A., Heinrikson R. L., and Gurney M. E. (1999) Membrane-anchored aspartyl protease with Alzheimer's disease beta-secretase activity. *Nature* **402,** 533-537.

Yan S. D., Chen X., Fu J., Chen M., Zhu H. J., Roher A., Slattery T., Zhao L., Nagashima M., Morser J., Migheli A., Nawroth P., Stern D., and Schmidt A. M. (1996) RAGE and amyloid-beta peptide neurotoxicity in Alzheimer's disease. *Nature* **382,** 685-691.

Yankner B. A., Dawes L. R., Fisher S., Villakomaroff L., Ostergranite M. L., and Neve R. L. (1989) Neurotoxicity of A Fragment of the Amyloid Precursor Associated with Alzheimers-Disease. *Science* **245,** 417-420.

Yankner B. A., Duffy L. K., and Kirschner D. A. (1990) Neurotrophic and Neurotoxic Effects of Amyloid Beta-Protein - Reversal by Tachykinin Neuropeptides. *Science* **250,** 279-282.

Yoritaka A., Hattori N., Uchida K., Tanaka M., Stadtman E. R., and Mizuno Y. (1996) Immunohistochemical detection of 4-hydroxynonenal protein adducts in Parkinson disease. *Proc Natl Acad Sci U S A* **93,** 2696-2701.

Yu G., Nishimura M., Arawaka S., Levitan D., Zhang L., Tandon A., Song Y. Q., Rogaeva E., Chen F., Kawarai T., Supala A., Levesque L., Yu H., Yang D. S., Holmes E., Milman P., Liang Y., Zhang D. M., Xu D. H., Sato C., Rogaev E., Smith M., Janus C., Zhang Y., Aebersold R., Farrer L. S., Sorbi S., Bruni A., Fraser P., and George-Hyslop P. (2000) Nicastrin modulates presenilin-mediated notch/glp-1 signal transduction and betaAPP processing. *Nature* **407,** 48-54.

Zhu X., Raina A. K., Lee H. G., Casadesus G., Smith M. A., and Perry G. (2004) Oxidative stress signalling in Alzheimer's disease. *Brain Res* **1000,** 32-39.

Zhu Y., Carvey P. M., and Ling Z. (2006) Age-related changes in glutathione and glutathione-related enzymes in rat brain. *Brain Res* **1090,** 35-44.